

Electronic Thesis and Dissertation Repository

8-20-2015 12:00 AM

Design, Synthesis and Study of Novel Nucleobase Analogs

Augusto Matarazzo

The University of Western Ontario

Supervisor

Dr. Hudson

The University of Western Ontario

Graduate Program in Chemistry

A thesis submitted in partial fulfillment of the requirements for the degree in Doctor of Philosophy

© Augusto Matarazzo 2015

Follow this and additional works at: <https://ir.lib.uwo.ca/etd>

Recommended Citation

Matarazzo, Augusto, "Design, Synthesis and Study of Novel Nucleobase Analogs" (2015). *Electronic Thesis and Dissertation Repository*. 3128.

<https://ir.lib.uwo.ca/etd/3128>

This Dissertation/Thesis is brought to you for free and open access by Scholarship@Western. It has been accepted for inclusion in Electronic Thesis and Dissertation Repository by an authorized administrator of Scholarship@Western. For more information, please contact wlsadmin@uwo.ca.

DESIGN, SYNTHESIS AND STUDY OF NOVEL NUCLEOBASE ANALOGS

(Thesis format: Monograph)

by

Augusto Matarazzo

Graduate Program in Chemistry

A thesis submitted in partial fulfillment
of the requirements for the degree of
Doctor of Philosophy

The School of Graduate and Postdoctoral Studies
The University of Western Ontario
London, Ontario, Canada

© Augusto Matarazzo 2015

Abstract

This thesis focused on nucleobase modified peptide nucleic acid (PNA) and DNA to expand the repertoire of available nucleobase analogs used in the study of nucleic acids. More specifically, we are interested in modification of the nucleobases such that they retain their ability to undergo Watson-Crick base pairing. Moreover, our goal is to modify the nucleobases in order to engender them with useful photophysical properties such that they may be used as biomolecular tools to investigate nucleic acid structure and dynamics.

To that end, a derivative of 5-aminouracil (5-AU) labelled with the amine-reactive chromophore 9-chloroacridine was prepared for the purpose of investigating its potential as a base-discriminating fluorophore. This modified nucleobase was incorporated into PNA by fluorenylmethyloxycarbonyl (Fmoc)-based oligomerization chemistry. During study of its hybridization to complementary DNA (cDNA), the 5-substitution was found to be thermally labile and hydrolyzed to a small degree in neutral aqueous solution, thus liberating the highly fluorescent acridone moiety.

Moreover, three novel fluorescent 7-deaza-2'-deoxyadenosine analogs were successfully synthesized via the Sonogashira cross-coupling reaction of 7-iodo-7-deaza-2'-deoxyadenosine with 1-ethynylpyrene, 2-ethynyl-6-methoxynaphthalene, and 9-ethynylphenanthrene. These analogs were photophysically characterized in dioxane, EtOH, and H₂O to evaluate their potential for use as environmentally sensitive fluorescent probes. All three analogs displayed high solvatofluorochromicity in H₂O, relative to their emission wavelengths in dioxane and EtOH. Moreover, all three analogs exhibited moderate to high fluorescence quantum yields in dioxane and EtOH, and significantly lower fluorescence quantum yields in H₂O, indicating that these analogs display microenvironment sensitivity.

Furthermore, the synthesis towards a novel tricyclic adenine analog was attempted by extending the substrate scope of the Sonogashira cross-coupling/heteroannulation chemistry developed in the Hudson group for cytidine analogs to adenine analogs. However, unlike the cytidine scaffold, the 7-deazaadenine substrate did not cyclize under the Sonogashira cross-coupling/heteroannulation reaction conditions to give the tricyclic adenine and the straight cross-coupled product was obtained in moderate yield.

Lastly, an intrinsic nucleobase quencher was synthesized via the azo coupling reaction between 5-diazouracil and *N,N*-dimethylaniline. Fluorescence quenching experiments were performed between the nucleobase quencher and the fluorophores phenylpyrrolocytidine (pC), and pyrene to determine viable FRET pairs for use in molecular beacon constructs.

Keywords

Peptide nucleic acid, PNA, 5-aminouracil, 9-aminoacridine, acridone, fluorescence, environmentally sensitive fluorescence, solvatochromicity, 7-deazaadenine, Sonogashira cross-coupling, intrinsic nucleobase quencher, Stern-Volmer plots.

Co-Authorship Statements

In regard to chapter 2, we report optimized synthetic procedures and corrected photophysical characterization of the 5-(acridin-9-ylamino)uracil moiety. A preliminary report has appeared: Moustafa, M. E. *Design and Synthesis of Novel Quenchers for Fluorescent Hybridization Probes*. Ph.D. Thesis, 2011. In addition, the modified nucleobase was incorporated into PNA and further evaluated for use as a novel probe to detect mismatches in complementary DNA upon hybridization.

In regard to chapter 3, the synthesis and photophysical studies of three novel fluorescent adenosine analogs were carried out in collaboration with a fourth year undergraduate research student, Justin Brow.

In regard to chapter 5, we report optimized synthetic procedures and full spectral characterization of the U^{azo} PNA monomer. A preliminary report has appeared: Moustafa, M. E. *Design and Synthesis of Novel Quenchers for Fluorescent Hybridization Probes*. Ph.D. Thesis, 2011. Moreover, the photophysical properties and energy transfer (quenching) studies of the azo moiety were investigated in collaboration with a previous graduate student in the Hudson group, Christie Ettles.

Acknowledgements

I would like to thank my supervisor Dr. Robert Hudson for his patience, guidance and mentorship during my time here at Western. He has spent countless hours helping me troubleshoot problems arising from chemical research and sharing his knowledge of nucleic acids with me.

I would also like to thank my committee members Dr. James Wisner and Dr. Leonard Luyt for helping me stay on track and providing me with helpful feedback over the years. Moreover, I would like to thank my examiners for taking the time to read my thesis.

I would like to thank all past and present members of the Hudson research group, especially Dr. Mojmir Suchy, Rachel Wang, Dr. Sung Ju Cho, Atifeh, Boyang, Justin, Dan, Dr. Mark Milne, Dr. Melissa Lewis, Dr. Mohamed Moustafa, Christie Ettles, Kelly Firth, Adam Elmeriki, Kirby Chicas, Mchenry Charles and Andre St. Amant.

A big thanks to my volunteers, Joey Lee and Allen Li for helping me set up experiments in the laboratory.

Thanks to Mathew Wilans for his friendship over the years and keeping the NMR facility in tip top shape. I would also like to thank Doug Hairsine for performing HRMS of small molecules.

A special thanks to my fantastic parents, Gianni and Elvira and my fabulous sisters Stefania and Linda for their ongoing support and encouragement during my doctoral studies. I would also like to thank my extended family and friends here in Canada and in Italy for their support and encouragement over the years.

I would like to thank Pierangelo Gobbo and Stephanie Barbon for their friendship over these past four years here at Western. We have had some truly amazing times.

A huge thanks to my soulmate Adriana Cimo for her support and understanding during my graduate studies. I could not have done this without her by my side. I would also like to extend a thank you to her family for their support over these past four years.

Table of Contents

Abstract	ii
Co-Authorship Statement.....	iv
Acknowledgments.....	v
Table of Contents	vi
List of Tables	x
List of Figures	xi
List of Schemes.....	xiv
List of Appendices	xvii
List of Abbreviations	xix
Chapter 1	1
1 Introduction	1
1.1 Nucleic Acids.....	1
1.2 Fluorescence Spectroscopy	5
1.2.1 Fluorescence Quenching and Resonance Energy Transfer	6
1.3 Fluorescent Nucleobase Analogs.....	7
1.3.1 Naturally Occurring Fluorescent Nucleobases.....	7
1.3.2 Expanded Nucleobases.....	10
1.3.3 Extended Nucleobases.....	11
1.3.4 Isomorphous Nucleobases.....	14
1.3.5 Applications of Fluorescent Nucleobase Analogs.....	16
1.3.5.1 Single Nucleotide Polymorphism (SNP) Detection.....	16
1.3.5.2 Nucleic Acid Structure and Function.....	17

1.3.5.3 Nucleic Acid Microenvironment.....	17
1.4 Peptide Nucleic Acid (PNA).....	18
1.5 Rationale.....	19
1.6 Outline of Thesis.....	20
1.7 References.....	20
Chapter 2.....	23
2 5-(Acridin-9-ylamino)uracil a hydrolytically labile nucleobase modification in peptide nucleic acid (PNA).....	23
2.1 Introduction.....	23
2.2 Results and Discussion.....	24
2.2.1 Spectroscopic properties of acridine-labelled nucleobase.....	25
2.2.2 PNA oligomerization.....	26
2.2.3 Hybridization studies.....	26
2.2.4 Chemical behavior of U ^A	27
2.3 Conclusions.....	33
2.4 Future Work.....	33
2.5 Experimental.....	34
2.6 References.....	39
Chapter 3.....	40
3 Fluorescent Adenosine Analogs: Synthesis and Photophysical Evaluation of Novel Fluorescent 7-Substituted 7-Deazaadenosine Analogs.....	40
3.1 Introduction.....	40
3.1.1 Background on Adenosine Analogs Substituted at the 7-Position.....	40

3.2 Results and Discussion.....	48
3.2.1 Photophysical Evaluation.....	49
3.3 Conclusion.....	55
3.4 Future Work.....	56
3.5 Experimental.....	58
3.6 References.....	64
Chapter 4.....	65
4 Fluorescent Adenine Analogs: Efforts Toward the Synthesis of a Novel Tricyclic 7-Deazaadenine	65
4.1 Introduction.....	65
4.2 Results and Discussion.....	68
4.3 Conclusion.....	76
4.4 Future Work.....	77
4.5 Experimental.....	78
4.6 References.....	85
Chapter 5.....	86
5 Synthesis and Study of an Intrinsic Nucleobase Quencher.....	86
5.1 Introduction.....	86
5.2 Results and Discussion.....	89
5.2.1 Spectroscopic Properties of Compound V-2.....	90
5.2.2 Quenching Studies.....	91
5.2.3 Efforts Toward PNA Oligomerization.....	95

5.3 Conclusions.....	102
5.4 Future Work.....	103
5.5 Experimental.....	104
5.6 References.....	109
Chapter 6.....	110
6 Overall Conclusion and Outlook.....	110
Appendices.....	113
Curriculum Vitae	171

List of Tables

Table 1: Summary of the selected naturally occurring fluorescent nucleosides presented and their corresponding photophysical properties.	9
Table 2: Summary of the selected expanded nucleobases presented and their corresponding photophysical properties.	11
Table 3: Summary of the selected extended nucleobases presented and their corresponding photophysical properties.	13
Table 4: Summary of the selected isomorphous nucleobases presented and their corresponding photophysical properties.	15
Table 5: Thermal denaturation transition temperatures (T_m) for PNA–DNA duplexes.	26
Table 6: Photophysical properties of fluorescent 7-deaza-2'-deoxyadenosines.	50
Table 7: Sonogashira/cyclization reaction at elevated temperatures.	70
Table 8: Cyclization reaction attempts with increased amounts of CuI.	71
Table 9: Cyclization reaction attempts with AgNO ₃ and HAuCl ₄	73
Table 10: Attempts at troubleshooting the U ^{azo} coupling reaction.	99
Table 11: Attempts at troubleshooting the coupling reaction between PNA-2 and V-3.	101
Table 12: Fluorescence standards and their corresponding quantum yields.....	116

List of Figures

Figure 1: D-ribose and 2-deoxy-D-ribose.	1
Figure 2: The DNA nucleobases: adenine, guanine, cytosine and thymine.	2
Figure 3: Watson/Crick base pairing for G-C and A-T.	3
Figure 4: Jablonski diagram illustrating fundamental photophysical processes.	5
Figure 5: Selected examples of naturally occurring fluorescent nucleosides (R = 2'-deoxyribose).	8
Figure 6: Selected examples of expanded nucleobases (R = 2'-deoxyribose).	10
Figure 7: Selected examples of extended nucleobases (R = 2'-deoxyribose).	12
Figure 8: Selected examples of isomorphous nucleobases (R = 2'-deoxyribose).	14
Figure 9: Comparison of the structures of DNA and PNA.	19
Figure 10: Acridine-labelled 5-aminouracil PNA monomer U ^A	24
Figure 11: Proposed base pair between U ^A and T.	27
Figure 12: PAGE analysis of unprocessed PNA oligomer (lane 1) and extensively heat-cycled PNA oligomer (lane 2) visualized by UV shadowing over a fluorescent TLC plate illuminated at 260 nm.	29
Figure 13: Excitation emission spectrum of acridone in EtOH.	31
Figure 14: HPLC analysis of 5-aminouracil (top) and co-injection of 5-aminouracil and the hydrolyzed mixture (bottom). Note: Chromatograms were extracted at $\lambda = 252$ nm.	31
Figure 15: HPLC analysis of compound 1 (top), and the hydrolyzed mixture after heating at 90 °C for 24 hours (bottom). Note: Chromatograms were extracted at $\lambda = 252$ nm.	32

Figure 16: Excitation emission profiles of A ^{mon} in dioxane (top left), EtOH (top right) and H ₂ O (bottom left).	51
Figure 17: Excitation emission profiles of A ^{phen} in dioxane (top left), EtOH (top right) and H ₂ O (bottom left).	51
Figure 18: Excitation emission profiles of A ^{pyr} in dioxane (top left), EtOH (top right) and H ₂ O (bottom left).	52
Figure 19: Equilibrium geometries of 7-deazaadenine and cytidine analog substrates for cyclization.	75
Figure 20: Structure and principle of operation of molecular beacons.	87
Figure 21: Structure of PNA-11.	88
Figure 22: Azouridine analog capable of Watson/Crick base pairing.	89
Figure 23: Quenching spectra of pC with azouridine analog V-2.	92
Figure 24: Quenching spectra of pyrene with azouridine analog V-2.	93
Figure 25: Stern-Volmer plot for the quenching of pC in EtOH by compound V-2.	94
Figure 26: Stern-Volmer plot for the quenching of pyrene in EtOH by V-2.	95
Figure 27: Chemical structures of PNA monomers pC and U ^{azo}	96
Figure 28: HPLC chromatograms of PNA-1 at 260 nm (top), 360 nm (middle) and 450 nm (bottom).	97
Figure 29: UV-visible spectrum of peak with 36 minute retention time in HPLC chromatogram.	98
Figure 30: UPLC chromatograms of PNA-2 at 450 nm (top), 360 nm (middle) and 260 nm (bottom).	100

Figure 31: UV-visible spectrum of peak with 3.6 minute retention time in HPLC chromatogram.100

List of Schemes

Scheme 1: Synthesis of the acridine-labelled 5-aminouracil PNA monomer.	25
Scheme 2: Observed hydrolysis of compound 1 under neutral conditions and plausible mechanism for the formation of the observed products.	30
Scheme 3: Proposed synthesis of a 5-aminouracil PNA monomer derivatized with the amine reactive fluorophore NBD chloride.....	33
Scheme 4: Synthesis of 7-substituted-7-deazaa-2'-deoxyadenosine analogs.	41
Scheme 5: Synthesis of 7-deaza-7-(1-pyrenecarboxamido)propyl-2'-deoxyadenosine.	44
Scheme 6: Synthesis of 7-dezaadenosine nucleosides bearing Ru(II) complexes.	45
Scheme 7: Synthesis of ethynylnaphthalene substituted 7-deaza-2'-deoxyadenosine.	47
Scheme 8: Synthesis of novel fluorescent 7-deaza-2'-deoxyadenosine analogs.	49
Scheme 9: Proposed synthesis of A ^{pyf} DNA monomer.....	57
Scheme 10: Expanding the substrate scope of the Sonogashira cross coupling-heteroannulation reaction developed for cytidine analogs to adenine analogs.....	65
Scheme 11: Synthesis of a tetracyclic adenosine analog.....	67
Scheme 12: Sequential Sonogashira/cyclization synthetic strategy toward a tricyclic adenine analog.	68
Scheme 13: Efforts toward the synthesis of a tricyclic adenine analog.	69
Scheme 14: A more efficient route towards a tricyclic adenine analog.	72
Scheme 15: Intramolecular carboalkoxylation catalyzed by PtCl ₂	75
Scheme 16: Post synthetic modification of PNA with fluorescent alkynes via the Sonogashira reaction.	77

Scheme 17: Synthesis of azouridine analog.	90
Scheme 18: Amide coupling between U ^{azo} monomer and benzylamine in solution.	102
Scheme 19: Proposed synthesis of a thymine-U ^{azo} dimer.....	103

List of Appendices

Appendix 1: General Experimental Procedures.....	113
Appendix 2: Temperature Dependent UV melting Studies.....	113
Appendix 3: Methods of Photophysical Analysis.....	114
Appendix 4: Fluorescence Quenching Studies.....	117
Appendix 5: ¹ H-NMR spectrum of compound II-1.....	118
Appendix 6: ¹³ C-NMR spectrum of compound II-1.....	119
Appendix 7: ¹ H-NMR spectrum of compound II-2.....	120
Appendix 8: ¹³ C-NMR spectrum of compound II-2.....	121
Appendix 9: ¹ H-NMR spectrum of compound II-3.....	122
Appendix 10: ¹³ C-NMR spectrum of compound II-3.....	123
Appendix 11: ¹ H-NMR spectrum of compound II-4.....	124
Appendix 12: ¹³ C-NMR spectrum of compound II-4.....	125
Appendix 13: ¹ H-NMR spectrum of compound II-5.....	126
Appendix 14: ¹³ C-NMR spectrum of compound II-5.....	127
Appendix 15: ¹ H-NMR spectrum of compound III-17.....	128
Appendix 16: ¹³ C-NMR spectrum of compound III-17.....	129
Appendix 17: ¹ H-NMR spectrum of compound III-18.....	130
Appendix 18: ¹³ C-NMR spectrum of compound III-18.....	131
Appendix 19: ¹ H-NMR spectrum of compound III-19.....	132

Appendix 20: ^{13}C -NMR spectrum of compound III-19.....	133
Appendix 21: ^1H -NMR spectrum of compound III-20.....	134
Appendix 22: ^{13}C -NMR spectrum of compound III-20.....	135
Appendix 23: ^1H -NMR spectrum of compound III-21.....	136
Appendix 24: ^{13}C -NMR spectrum of compound III-21.....	137
Appendix 25: ^1H -NMR spectrum of compound III-22.....	138
Appendix 26: ^{13}C -NMR spectrum of compound III-22.....	139
Appendix 27: ^1H -NMR spectrum of compound III-23.....	140
Appendix 28: ^{13}C -NMR spectrum of compound III-23.....	141
Appendix 29: ^1H -NMR spectrum of compound IV-7.....	142
Appendix 30: ^{13}C -NMR spectrum of compound IV-7.....	143
Appendix 31: ^1H -NMR spectrum of compound IV-8.....	144
Appendix 32: ^{13}C -NMR spectrum of compound IV-8.....	145
Appendix 33: ^1H -NMR spectrum of compound IV-9.....	146
Appendix 34: ^{13}C -NMR spectrum of compound IV-9.....	147
Appendix 35: ^1H -NMR spectrum of compound IV-10.....	148
Appendix 36: ^{13}C -NMR spectrum of compound IV-10.....	149
Appendix 37: ^1H -NMR spectrum of compound IV-11.....	150
Appendix 38: ^{13}C -NMR spectrum of compound IV-11.....	151
Appendix 39: ^1H -NMR spectrum of compound IV-12.....	152

Appendix 40: ^1H -NMR spectrum of compound IV-13.....	153
Appendix 41: ^{13}C -NMR spectrum of compound IV-13.....	154
Appendix 42: ^1H -NMR spectrum of compound IV-15.....	155
Appendix 43: ^{13}C -NMR spectrum of compound IV-15.....	156
Appendix 44: ^1H -NMR spectrum of compound IV-16.....	157
Appendix 45: ^{13}C -NMR spectrum of compound IV-16.....	158
Appendix 46: ^1H -NMR spectrum of compound V-1.....	159
Appendix 47: ^{13}C -NMR spectrum of compound V-1.....	160
Appendix 48: ^1H -NMR spectrum of compound V-2.....	161
Appendix 49: ^{13}C -NMR spectrum of compound V-2.....	162
Appendix 50: ^1H -NMR spectrum of compound V-3.....	163
Appendix 51: ^{13}C -NMR spectrum of compound V-3.....	164
Appendix 52: ^1H -NMR spectrum of compound V-4.....	165
Appendix 53: ^{13}C -NMR spectrum of compound V-4.....	166
Appendix 54: ^1H -NMR spectrum of compound V-5.....	167
Appendix 55: ^{13}C -NMR spectrum of compound V-5.....	168
Appendix 56: Sample calculation: Determination of molar extinction coefficients for compound III-21 (A^{pyr}) in EtOH at 366 nm (blue), dioxane at 367 nm (green) and H_2O at 364 nm (red).....	169
Appendix 57: Sample calculation: data for the calculation of Φ_{F} for compound III-21 (A^{pyr}) in EtOH. A plot of the integrated fluorescence intensity at different absorbance values for 9,10-diphenylanthracene (blue) and compound III-21 (red).....	170

List of Abbreviations

A	adenine
aq.	aqueous
Bhoc	benzhydryloxycarbonyl
Boc	<i>tert</i> -butyloxycarbonyl
br	broad
Bz	benzoyl
°C	degrees Celsius
C	cytosine
calcd	calculated
CLEAR	cross-linked ethoxylate acrylate resin
cDNA	complementary deoxyribonucleic acid
d	doublet
δ	chemical shift in parts per million downfield from tetramethylsilane
DABCYL	4-[4-(dimethylamino)phenylazo] benzoic acid
DBU	1,8-diazabicyclo[5.4.0]undec-7ene
DFT	density functional theory
DIPEA	diisopropylethylamine
DMAP	4-(<i>N,N</i> -dimethylamino)pyridine
DMF	<i>N,N</i> -dimethylformamide
DMSO	dimethyl sulfoxide
DMT	4,4'-dimethoxytrityl
DMTCI	4,4'-dimethoxytrityl chloride
DNA	deoxyribonucleic acid
EDTA	ethylenediaminetetraacetic acid

EtOAc	ethyl acetate
ESI	electrospray ionization
Et	ethyl
equiv	equivalent
EtOH	ethanol
Fmoc	9-fluorenylmethoxycarbonyl
FCC	flash column chromatography
FRET	Forster resonance energy transfer
g	grams
G	guanine
H	hours
HATU	2-(7-Aza-1H-benzotriazol-1-yl)- <i>N,N,N,N</i> -tetramethyluronium hexafluorophosphate
HBTU	O-benzotriazol-1-yl- <i>N,N,N,N</i> -tetramethyluronium hexafluorophosphate
HOBt	1-hydroxybenzotriazole
HPLC	high-performance liquid chromatography
HRMS	high-resolution mass spectrum
Hz	hertz
<i>i</i> -Pr	isopropyl
<i>J</i>	coupling constant
λ	wavelength
k_q	bimolecular quenching constant
K_{sv}	Stern-Volmer quenching constant
K_{sv}^{-1}	inverse of the Stern-Volmer quenching constant
L	litre
Lys	lysine

μ	micro
MALDI	matrix-assisted laser desorption ionization
m	multiplet
ma	major
MeCN	acetonitrile
MeOH	methanol
mi	minor
min	minutes
NBD chloride	4-chloro-7-nitro-1,2,3-benzoxadiazole
NEt ₃	triethylamine
NIS	<i>N</i> -iodosuccinimide
NMR	nuclear magnetic resonance
ODN	oligodeoxynucleotide
pC	phenylpyrrolocytidine
Ph	phenyl
PNA	peptide nucleic acid
ppm	parts per million
q	quartet
R _f	retention factor
RP-HPLC	Reversed phase high performance liquid chromatography
RNA	ribonucleic acid
rt	room temperature
s	singlet
T	thymine
t	triplet
TFA	trifluoroacetic acid

THF	tetrahydrofuran
TLC	thin layer chromatography
T_m	thermal melt transition temperature (melting temperature for a nucleic acid complex)
TMS	trimethylsilyl
Tol	toluoyl
U	uracil
UV	ultraviolet
vis	visible
Φ_F	fluorescence quantum yield

Chapter 1

1 Introduction

1.1 Nucleic Acids¹

The origins of nucleic acids research dates back to 1868 when the Swiss chemist Friedrich Miescher isolated a phosphorus containing substance from human puss cells which he called nuclein. The nuclein that Miescher isolated was actually a mixture of nucleic acid and protein. In 1889, Richard Altman obtained the first protein-free material which he called nucleic acid.

In 1909, Phoebus Levene began some early structural studies on nucleic acids at the Rockefeller Institute of Medical Research. He discovered that thymus nucleic acid, which was readily available from calf tissue, was resistant to basic hydrolysis but hydrolyzed by acid. He also found that nucleic acids from plants and yeast were hydrolyzed readily by base. In 1911, Levene and coworkers crystallized D-ribose from plant nucleic acid and also went on to isolate 2-deoxy-D-ribose from animal nucleic acid (Figure 1).

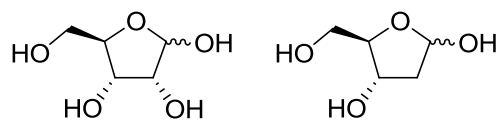


Figure 1: D-ribose and 2-deoxy-D-ribose.

In 1879, Albrecht Kossel isolated and described the heterocyclic components that are present in nucleic acid. These include the purines, adenine and guanine, and the pyrimidines, cytosine and thymine (Figure 2).

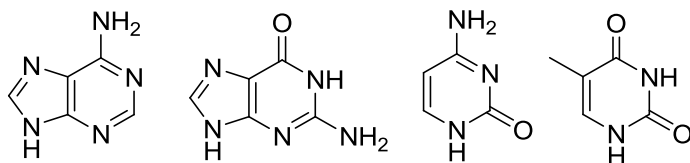


Figure 2: The DNA nucleobases: adenine, guanine, cytosine and thymine.

Up until the 1940s, it was believed that hydrolysis of nucleic acids gave the appropriate bases in equal relative proportions. This misconception led to the general acceptance of a tetranucleotide hypothesis for the structure of both animal and plant nucleic acids. While the tetranucleotide hypothesis was generally accepted among the scientific community it imposed invariance on the structure of nucleic acids which denied them any role in biological diversity. However, in 1944, Oswald Theodore Avery published his ground breaking work on the transforming activity of bacterial DNA, which showed that DNA was responsible for completely transforming the behaviour of bacteria.² This contrasted the tetranucleotide hypothesis and demanded a reinvestigation of nucleic acid structure.

In 1952, Erwin Chargaff studied the base composition of DNA from a variety of sources and showed that the composition of the bases, A, G, T and C varies from one species to another.³ He also found that the number of adenine units equals the number of thymine units and the number of guanine units equals the number of cytosine units.³ This disproved Levene's widely accepted tetranucleotide hypothesis, which called for equal proportions of all four bases in DNA. Although Chargaff did not make the connection himself, his research hinted towards the base pair makeup of DNA. Chargaff's work would later help James Watson and Francis Crick deduce the double helical structure of DNA.

A major piece of the puzzle in determining the structure of DNA came in 1953 from King's College in London England. There, Maurice Wilkins observed the importance of keeping the DNA fibers in a moist state and an X-ray crystallographer named Rosalind Franklin found that the X-ray diffraction pattern obtained from these fibers showed the existence of an A-form of DNA at low humidity and a B-form of DNA at high humidity. Both the A and B-forms of DNA were highly crystalline and helical in structure. This led

Franklin to hypothesize that the phosphate groups were exposed to water on the outside of the helix, while the bases were on the inside of the helix.

Also in 1953, James Watson deduced that the number of nucleotides in the unit crystallographic cell favoured a double stranded helix. Francis Crick recognized the symmetry implications of the monoclinic C^2 space group of the A-form diffraction pattern. He concluded that there had to be local twofold symmetry axes normal to the helix, this called for a double stranded helix whose two chains run in opposite directions.

The last piece of the problem was to figure out how the bases were connected to each other. Some years earlier, Gulland concluded that the DNA bases were joined together by hydrogen bonds. Thus, Watson began to experiment with models using the enol tautomers of the bases and paired like with like. However this structure was rejected because it had the wrong symmetry for B-DNA. Self-pairing was also rejected because it was not in accordance with Chargaff's 1:1 base ratios. Finally Watson experimented with models using the keto tautomers of the bases and paired adenine with thymine and guanine with cytosine. At last he found a simple relation involving two hydrogen bonds for an A-T pair and three hydrogen bonds for a G-C pair (Figure 3). Thus in 1953 the structure of DNA had been solved.⁴ As a result, the Nobel prize for chemistry in 1962 was awarded to Watson, Crick and Wilkins.

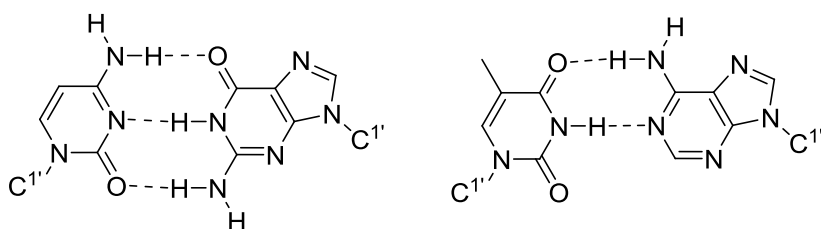


Figure 3: Watson/Crick base pairing for G-C and A-T.

The elucidation of the structure of DNA marked the end of the classical period in the study of nucleic acids and the beginning of molecular biology. It soon became evident that locked into the sequence of nucleotide bases in the DNA of a cell was all the information required to specify the variety of biological molecules needed to carry out

the functions of that cell. For example, from the DNA duplex structure, genetic information is stored, accessed and replicated as a linear nucleotide code. In conjunction with DNA, RNA is the biopolymer which is responsible for the transportation of genetic information from DNA to the ribosome, the site of protein manufacturing. This flow of genetic information, DNA transcribed into RNA which is ultimately translated into protein, constitutes the central dogma of molecular biology set forth by Francis Crick in 1970.⁵

During this period, scientists have devoted much time and effort toward exploring nucleic acid structure and function. Fluorescence spectroscopy is a very attractive technique for studying nucleic acids, as it is easily accessible, versatile and provides real time information with excellent sensitivity.⁶ Covalent attachment of traditional fluorophores such as fluorescein or rhodamine to the phosphate backbone, sugar or nucleobase is the most common method to fluorescently label nucleic acids.⁷ However, a major drawback of this method is that these molecules perturb the native structure of nucleic acids.⁶ As a result, traditional fluorophores are often covalently attached to nucleic acids via long linkers in order to minimize structural perturbations.⁶ Since the fluorescent reports are located far away from the site of interest, covalent modification of nucleic acids with traditional fluorophores via long linkers does not paint a clear picture of what is happening at or near the region of interest. To that end, fluorescent nucleosides and analogs have long interested chemists and biochemists involved in the study of nucleic acids.^{8,9} Ideally these analogs are structurally small such that they do not perturb the native structure of nucleic acids.^{8,9} Moreover, they possess ideal photophysical properties for studying nucleic acids such as red-shifted absorption and emission maxima compared to the natural nucleobases and high fluorescence quantum yields and fluorescence lifetimes.^{8,9} Due to the relative scarcity of naturally occurring fluorescent nucleosides, there has been increasing focus on the synthesis of analogs. Before looking at some examples of fluorescent nucleoside analogs in the literature, a brief introduction of fluorescence spectroscopy is warranted.

1.2 Fluorescence Spectroscopy

Fluorescence is a photophysical process that involves emission of a photon from a singlet excited state to the ground state subsequent to absorption of a photon by a chromophore.¹⁰ This process is illustrated in the Jablonski diagram (Figure 1).¹⁰ In the simplified Jablonski diagram below, S_0 represents the ground electronic singlet state of a molecule whereas S_1 and T_1 represent the first excited electronic singlet state and the first excited electronic triplet state. Upon absorption of light by a molecule, a number of pathways are possible for transitions back to the ground electronic singlet state. From the lowest vibrational energy level of S_1 the molecule can undergo internal conversion (IC) to the various vibrational energy levels of S_0 followed by vibrational relaxation (VR).¹¹ Fluorescence is also possible resulting in radiative decay from the lowest vibrational energy level of S_1 to the various vibrational energy levels of S_0 . Intersystem crossing (ISC) from S_1 to T_1 is also possible and from the lowest vibrational energy level of T_1 the molecule can undergo internal conversion and vibrational relaxation back to S_0 . The molecule can also undergo phosphorescence as a result of radiative decay from T_1 to S_0 .

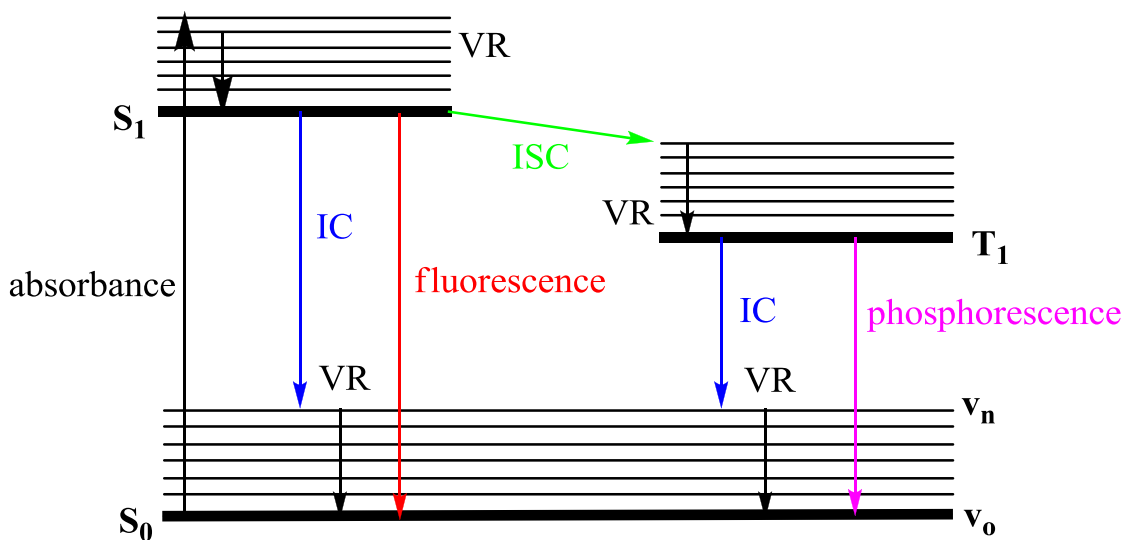


Figure 4: Jablonski diagram illustrating fundamental photophysical processes.

The fluorescence properties of a system are governed by the excitation and emission wavelengths, the fluorescence quantum yield, and lifetime of the excited state.

Fluorescence quantum yield is defined as the ratio of the number of molecules that fluoresce to the total number of excited molecules, or the ratio of photons emitted to photons absorbed (see equation 1 below).¹⁰

$$\phi_f = \frac{k_f}{k_f + k_{nr}} \quad (\text{eq. 1})$$

In equation 1, k_f represents the first order rate constant for fluorescence relaxation and k_{nr} represents the rate constant for radiationless relaxation.

The excited state lifetime, τ_o , represents the sum of radiative and radiationless processes that the excited fluorophore undergoes upon decaying back to the ground state. The fluorescence lifetime, τ , is the portion responsible for emitting a photon and is related to the quantum yield of the fluorophore (see equation 2).¹⁰

$$\phi_f = \frac{\tau}{\tau_o} \quad (\text{eq. 2})$$

For many fluorophores the measurable parameters of fluorescence, i.e. emission maximum, quantum yield and fluorescence lifetime are sensitive to the local environment of the fluorophore. Researchers have exploited the sensitivity of fluorophores to various environmental parameters such as pH, polarity, viscosity, presence of quenchers, and so on. In turn they have also designed fluorescent probes with the appropriate excitation and emission wavelengths that minimize interference by other emissive species. Thus it is this selective excitation as well as the sensitivity of fluorophores to various environmental parameters that makes fluorescence such an effective technique for studying nucleic acids.

1.2.1 Fluorescence Quenching and Resonance Energy Transfer

Two common processes that cause loss of fluorescence intensity are static and dynamic quenching. Static quenching occurs when a non-fluorescent ground state complex is formed.¹⁰ Dynamic quenching is described by the Stern-Volmer equation (see equation 3) and is characterized by a linear relationship between the quenching effect and the

quencher concentration.¹⁰ Deviation from linearity often infers the involvement of static quenching.

$$\frac{I_0}{I} = 1 + K_{sv}[Q] = 1 + k_q\tau_0[Q] \quad (\text{eq. 3})$$

In equation 3, K_{sv} is the Stern-Volmer quenching constant, k_q is the bimolecular quenching constant, τ_0 is the unquenched lifetime and $[Q]$ is the quencher concentration.

A related phenomenon involves resonance energy transfer, a nonradiative transfer of excitation energy between two chromophores, often referred to as donors and acceptors.¹⁰ Different mechanisms can facilitate energy transfer. The Dexter mechanism operates over short distances and requires intermolecular orbital overlap.¹¹ The Förster mechanism (FRET) operates over larger distances (30 – 60 Å) and occurs when the excited state dipole moment of a donor induces electron excitation of an acceptor.¹² FRET efficiency depends on the inverse sixth power of intermolecular separation, thus making it useful for studying distances similar to those of biological macromolecules such as nucleic acids.

1.3 Fluorescent Nucleobase Analogs

The literature shows us that uridine/deoxyuridine and uracil nucleobase analogs are the most abundant due to it offering the simplest chemistry relative to the other nucleobases.^{8,9} However, over the past decade, great strides have been made in the variety of fluorescent cytidines, adenosines and guanosines prepared.^{8,9} Based on their structural features, these fluorescent nucleobase analogs can be divided into four main categories, naturally occurring fluorescent nucleobase analogs, expanded nucleobases, extended nucleobases and isomorphous nucleobases.^{8,9} The purpose of the following sections is not to provide a comprehensive review of fluorescent nucleobase analogs, but to highlight the structural characteristics that improve the photophysical properties compared to the native nucleobases.

1.3.1 Naturally Occurring Fluorescent Nucleobases

Some examples of naturally occurring fluorescent nucleobase analogs include 2-aminopurine (2-AP)¹³ and the pteridine analogs studied by Hawkins and co-workers¹⁴⁻¹⁸ (Figure 5, Table 1). Although these compounds exhibit desirable photophysical properties for studying nucleic acids, i.e. red-shifted absorption and emission maxima compared to the canonical nucleosides, high fluorescence quantum yields and fluorescence lifetimes, due to the relative scarcity of naturally occurring fluorescent nucleosides, researchers have focused on the synthesis of analogs.

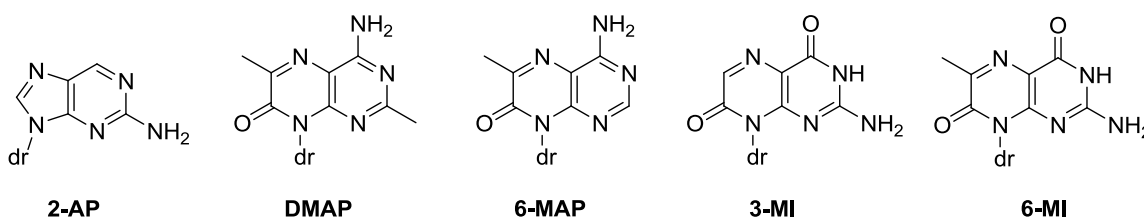


Figure 5: Selected examples of naturally occurring fluorescent nucleosides (dr = 2'-deoxyribose)

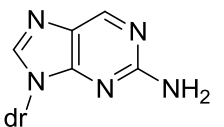
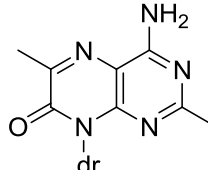
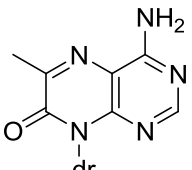
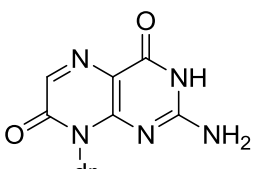
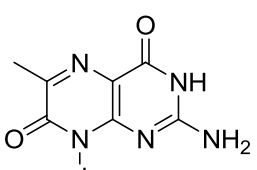
Structure (dr = 2'-deoxyribose)	$\lambda_{\text{absorbance}}$ (nm)	$\lambda_{\text{emission}}$ (nm)	Φ_{F} (solvent)	τ (ns) (solvent)
	303	370	0.68 (H ₂ O)	7.0 (H ₂ O)
	310	430	0.48 (10 mM Tris buffer, pH 7.5)	4.8 (10 mM Tris buffer, pH 7.5)
	320	430	0.39 (10 mM Tris buffer, pH 7.5)	3.8 (10 mM Tris buffer, pH 7.5)
	350	430	0.88 (10 mM Tris buffer, pH 7.5)	6.5 (10 mM Tris buffer, pH 7.5)
	340	431	0.70 (10 mM Tris buffer, pH 7.5)	6.4 (10 mM Tris buffer, pH 7.5)

Table 1: Summary of the selected naturally occurring fluorescent nucleosides presented and their corresponding photophysical properties.

1.3.2 Expanded Nucleobases

The fusion of aromatic rings onto the purine and pyrimidine scaffold results in an extension of conjugation which in turn enhances the photophysical properties compared to the native nucleobases. Some examples of expanded nucleobase analogs include benzoadenosine,¹⁹ naphthothymine,²⁰ methoxybenzodeazaadenosine,²¹⁻²³ and the phenoxazine nucleobase analog tC²⁴⁻²⁶ (Figure 6). All of these compounds exhibit red-shifted absorption and emission maxima and moderate to high fluorescence quantum yields. The photophysical properties of these analogs are summarized in Table 2.

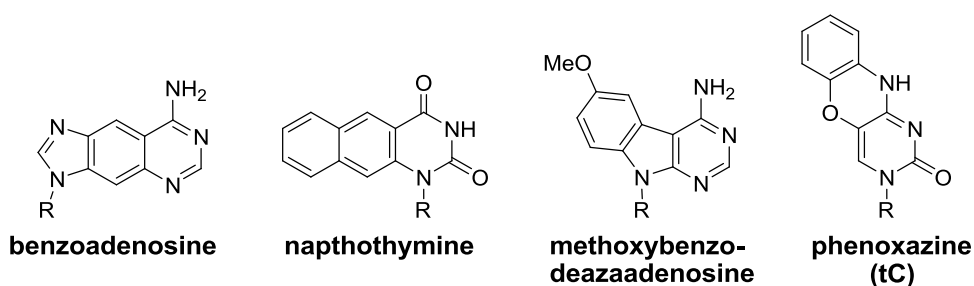


Figure 6: Selected examples of expanded nucleobases (**R** = 2'-deoxyribose).

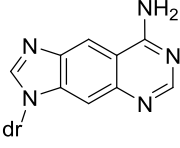
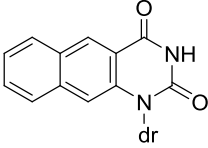
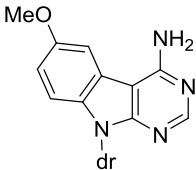
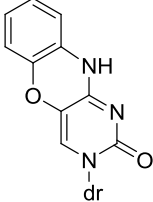
Structure (dr = 2'-deoxyribose)	$\lambda_{\text{absorbance}}$ (nm)	$\lambda_{\text{emission}}$ (nm)	Φ (solvent)	τ (ns) (solvent)
	340	395	0.44 (H ₂ O)	3.7 (H ₂ O)
	360	434	0.82 (aqueous buffer, pH 7)	nr
	327	397, 427	0.118 (50 mM sodium phosphate, 0.1 M sodium chloride, pH 7)	nr
	375	500	0.17 (aqueous buffer, pH 7.5)	3.7

Table 2: Summary of the selected expanded nucleobases presented and their corresponding photophysical properties (nr = not reported).

1.3.3 Extended Nucleobases

Chromophores that are linked or conjugated to the natural nucleobases, via rigid or flexible linkers, result in extended fluorescent nucleobase analogs.^{8,9} The connection of known fluorophores through nonconjugating linkers results in nucleobase analogs with photophysical properties similar to that of the parent fluorophore.^{8,9} In contrast, attachment of known fluorophores via conjugated linkers usually results in a new chromophore with its own unique photophysical properties.^{8,9} Some examples of

extended nucleobase analogs include 2-ethynyl-6-cyanonaphthalene-8-aza-7-deaza-2'-deoxyadenosine (A^{CN}),²⁷ 2-phenylpropyl-2'-deoxyadenosine,²⁸⁻²⁹ pyU^{23} and 5-(1-pyrenyl)-2'-deoxyuridine,³⁰⁻³¹ (Figure 7). Similarly to the expanded nucleobases, these compounds also exhibit red-shifted absorption and emission maxima and moderate to high fluorescence quantum yields. The photophysical properties of these extended nucleobase analogs are summarized in Table 3.

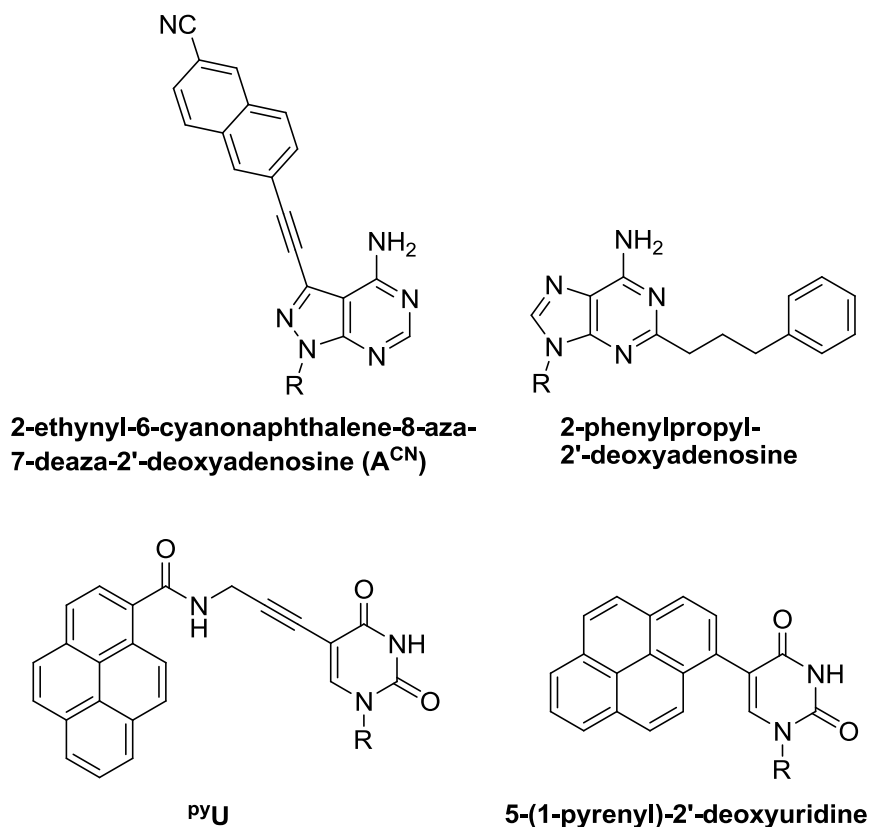


Figure 7: Selected examples of extended nucleobases ($R = 2'$ -deoxyribose or ribose).

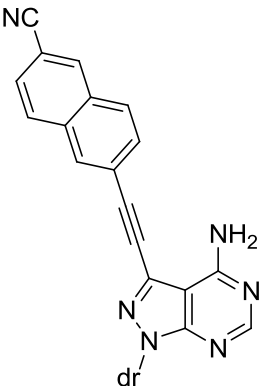
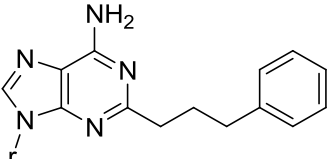
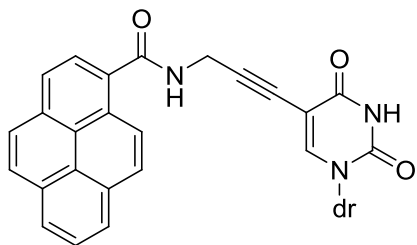
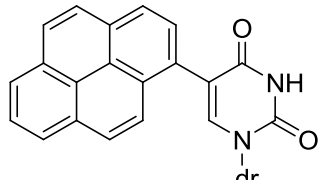
Structure (dr = 2'-deoxyribose r = ribose)	$\lambda_{\text{absorbance}}$ (nm)	$\lambda_{\text{emission}}$ (nm)	Φ (solvent)	τ (ns) (solvent)
	327 323 327	375 399 429	0.29 (1,4-dioxane) 0.37 (ethanol) 0.35 (DMF)	nr nr nr
	292	385	0.011 (H ₂ O)	6.22 (H ₂ O)
	341	397	0.2 (aqueous phosphate buffer, pH 7.0)	nr
	342	474	0.027 (methanol)	nr

Table 3: Summary of the selected extended nucleobases presented and their corresponding photophysical properties (nr = not reported).

1.3.4 Isomorphous Nucleobases

Isomorphous nucleobase analogs are structurally similar to the native nucleobases, however they possess enhanced photophysical properties. Some examples of isomorphous nucleobase analogs are 8-vinyl-6-aminopurine,³²⁻³³ 8-(fur-2-yl)guanosine,³⁴ thieno[3,4-*d*]-uridine,³⁵ and phenylpyrrolocytidine³⁶ (Figure 8). Similarly to the expanded and extended nucleobases, these isomorphous nucleobase analogs also exhibit red-shifted absorption and emission maxima and relatively high fluorescence quantum yields. The photophysical properties of these compounds are summarized in Table 4.

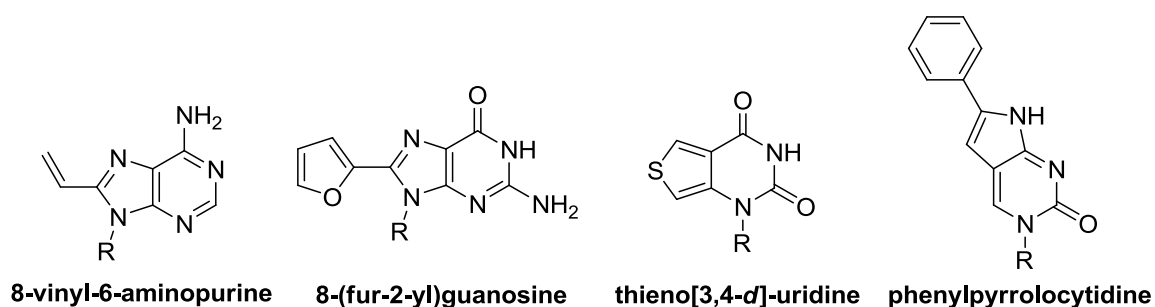


Figure 8: Selected examples of isomorphous nucleobases (R = 2'-deoxyribose or ribose).

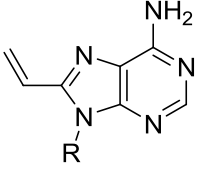
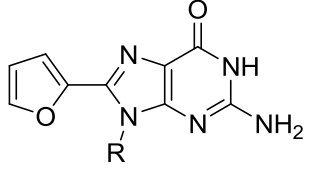
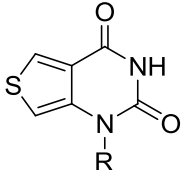
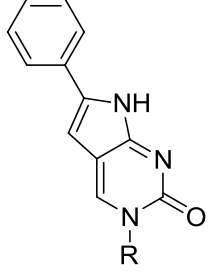
Structure (dr = 2'-deoxyribose, r = ribose)	$\lambda_{\text{absorbance}}$ (nm)	$\lambda_{\text{emission}}$ (nm)	Φ (solvent)	τ (ns) (solvent)
 <p>8-vinyl-6-aminopurine</p>	290	382	0.66 (25mM HEPES buffer, pH 7.5)	4.7
 <p>8-(fur-2-yl)guanosine</p>	294	378	0.57 (H ₂ O)	nr
 <p>thieno[3,4-d]-uridine</p>	304	412	0.48 (H ₂ O)	nr
 <p>phenylpyrrolocytidine</p>	362	454	0.31 (H ₂ O)	nr

Table 4: Summary of the selected isomorphous nucleobases presented and their corresponding photophysical properties (nr = not reported).

1.3.5 Applications of Fluorescent Nucleobase Analogs

1.3.5.1 Single Nucleotide Polymorphism (SNP) Detection

Many diseases arise from variations within the human genome. For instance cystic fibrosis and sickle cell anemia are caused by base sequence changes in a single gene. The most common type of human genetic variation is the single nucleotide polymorphism (SNP).⁹ A useful technique for SNP detection relies on fluorescent nucleoside analogs.⁹ In more detail, a fluorescent oligonucleotide complementary to the region of interest is hybridized to a target DNA sequence.⁹ The emissive nucleoside probe is usually placed across from the base of interest, resulting in either a red-shift or blue-shift in the emission wavelength, an increase or decrease in the fluorescence quantum yield or a change in the length of the excited state lifetime.⁹

In 2003 Saito and co-workers designed methoxybenzodeazaadenosine (^{MD}A) a base-discriminating fluorescent (BDF) nucleoside which is used to detect single nucleotide polymorphisms (SNPs) (figure 5, table 1).²¹⁻²³ Incorporation of ^{MD}A into a single stranded oligodeoxynucleotide, 5'-d(CGCAAT^{MD}AATAACGC)-3', resulted in a massive decrease in fluorescence intensity with a quantum yield value of 0.005.²¹⁻²³ A similar result was observed for double stranded duplexes containing ^{MD}A, quantum yields ranged from <0.0005 in the fully complementary duplex to 0.0006 when the base opposite ^{MD}A was adenine.²¹⁻²³ Interestingly a DNA duplex containing guanine opposite of ^{MD}A exhibited a dramatic increase in fluorescence intensity with a quantum yield of 0.020.²¹⁻²³ More importantly however, a quantum yield of 0.081 was obtained for a DNA duplex with cytidine opposite from ^{MD}A.²¹⁻²³ Although the fluorescence of an ^{MD}A containing duplex was significantly depressed when the flanking base pair was a G/C base pair, thus hampering the general utility of this method, the authors successfully demonstrated SNP detection of the C SNP sequence in the human breast cancer 1 gene (BRCA1) using this "base discriminating fluorophore" (BDF) technology.²¹⁻²³

1.3.5.2 Nucleic Acid Structure and Function

Nucleic acids can be found in various forms and aggregated states, which may be related to a specific cellular function.⁸ Incorporation of emissive nucleosides into nucleic acid strands can fluorometrically report hybridization, folding and conformational changes.⁸ Moreover, fluorescent nucleoside analogs have been used to design assays that monitor enzymes operating on nucleic acids such as RNase H.³⁷

In 2010, Hudson and co-workers demonstrated that 6-phenylpyrrolocytosine (PhpC) (figure 7, table 3), serves as a cytosine mimic in terms of its recognition by enzymes.³⁷ To that end, a DNA – RNA heteroduplex containing a single PhpC insert was used to develop an RNase H assay that fluorometrically reports on the cleavage of the enzyme substrate.³⁷ In more detail, PhpC was incorporated into the RNA single strand PhPC-1 (5'-GAUCUGAGCCUGGGAG**Php**CU-3'), and hybridized with its complementary DNA target. In the DNA – RNA heteroduplex, PhpC exhibited low fluorescence. However, treatment with HIV-1 RT RNase H generated an RNA tetranucleotide bearing PhpC, and rapidly dissociated from its DNA complement resulting in a concomitant drastic increase in fluorescence intensity.³⁷

1.3.5.3 Nucleic Acid Microenvironment

Nucleic acids suffer different types of perturbations such as nucleobase damage, depurination/depyrimidation and base flipping.⁸ Fluorescent nucleoside analogs that are sensitive to their local microenvironment are useful tools for studying these perturbations.⁸ Furthermore, fluorescent nucleosides have been used to assess the polarity of nucleic acid grooves.²⁷

In 2014, Saito and co-workers designed an environmentally sensitive fluorescent 8-aza-7-deaza-2'-deoxyadenosine derivative (A^{CN}), with dual fluorescence for the specific detection of thymine (figure 6, table 2).²⁷ The authors report that the emission of this fluorescent adenosine analog is shifted to longer wavelengths in highly polar solvents and thus exhibits typical solvatofluorochromicity, which can be attributed to intramolecular charge transfer (ICT) fluorescence.²⁷

Measurement of the fluorescence spectra of DNA1 (5'-d(CGCAATA^{CN}TAACGC)-3'), in the absence or presence of complementary strands showed that the fluorescence emission of the single strand was relatively weak.²⁷ However when complementary DNA strands were added the fluorescence intensity of the duplexes was significantly enhanced.²⁷ In more detail, when DNA1 was hybridized with a complementary sequence containing an abasic site across from the fluorescent adenosine analog, a strong broad fluorescence emission band was observed at 417 nm.²⁷ Furthermore when DNA1 was hybridized with complementary sequences containing A or C across from the fluorescent adenosine analog, strong broad emission bands were observed at 409 and 405 nm respectively.²⁷ In contrast, when DNA1 was hybridized with a complementary sequence containing G across from the fluorescent adenosine analog, the fluorescence emission considerably decreased due to quenching by G.²⁷ Interestingly, in the perfectly matched DNA duplex the fluorescence maximum was largely blue shifted at 362 and 381 nm and an enhanced dual fluorescence emission with vibronic structures was observed.²⁷ Thus changing the base across from the surrogate fluorescent adenine caused a change in the fluorescence intensity and emission wavelength of the ODN probe.

1.4 Peptide Nucleic Acid (PNA)

Peptide nucleic acid (PNA) was first reported in 1991 by Nielsen et al.³⁸ and is a DNA mimic comprised of a polyamide backbone (Figure 9).³⁸⁻³⁹ Over the years, PNA has been exploited by researchers due to its ability to form stable base pairs with complementary DNA or complementary RNA sequences with high stability and fidelity.³⁸⁻³⁹ In contrast to DNA and RNA, PNA is more suitable for *in vivo* applications since the nonstandard backbone is not recognized by nucleases, resulting in increased stability of PNA in living cells.³⁹

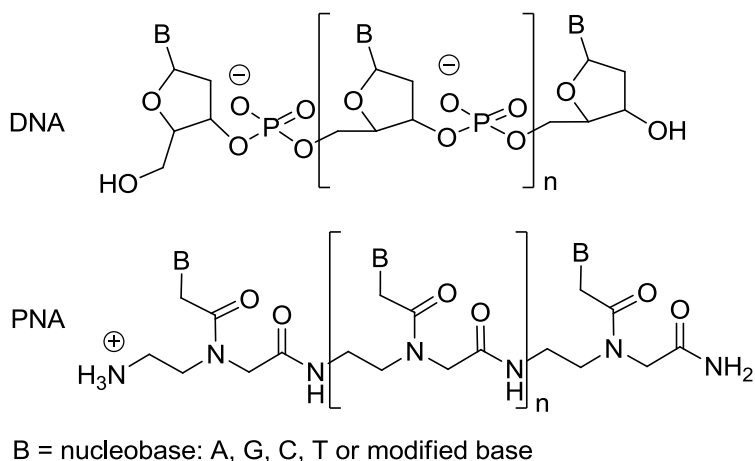


Figure 9: Comparison of the structures of DNA and PNA

1.5 Rationale

The focus of this thesis is on nucleobase modified PNA and DNA to expand the repertoire of available nucleobase analogs used in the study of nucleic acids. Although there exists a wide variety of fluorescent nucleobase analogs, the search for an ideal analog with optimal properties, i.e., high fluorescence quantum yield, red-shifted absorption maxima, not destabilizing to hybridization, ability to provide nucleobase discrimination, and the ability to report differences in the local environment through a change in fluorescence intensity or emission wavelength is very much still a challenge.

The literature also shows us that certain fluorescent nucleobase analogs are underrepresented, especially analogs of adenine and guanine.^{8,9} To that end, this thesis focused on the synthesis of novel fluorescent 7-dezaadenosine analogs and chemistry toward a novel tricyclic 7-dezaadenine analog.

Lastly, the synthesis of an intrinsic nucleobase quencher was also undertaken to overcome some of the limitations associated with traditional FRET based molecular beacons which will be further discussed in chapter 5.

1.6 Outline of Thesis

The focus of this thesis is on nucleobase modified peptide nucleic acid (PNA) and DNA. Chapter 2 describes the synthesis of an acridine-labelled 5-aminouracil PNA monomer, for the purpose of investigating its potential as a base-discriminating fluorophore.

Chapter 3 describes the synthesis and photophysical characterization of novel fluorescent 7-deazaadenosine analogs. The photophysical properties of these 7-deazaadenosine analogs were studied in solvents of different polarity to evaluate their potential for use as environmentally sensitive fluorescent probes in DNA.

Chapter 4 describes efforts toward the synthesis of a novel tricyclic 7-deazaadenine analog. The goal of this research project was to synthesize a novel tricyclic adenine analog by extending the substrate scope of the Sonogashira cross-coupling/heteroannulation chemistry developed in the Hudson group for cytidine analogs to adenine analogs.

Lastly, chapter 5 focuses on the synthesis, fluorescence quenching studies and efforts toward the oligomerization of a novel intrinsic fluorescence quencher, 5-(4-dimethylaminophenyl)azouridine, which incorporates the key structural feature of the universal quencher DABCYL. The goal of this work was to synthesize a base pairing competent quencher for use in novel stemless molecular beacon constructs.

1.7 References

- 1) Blackburn G. M.; Gait, M. J. *Nucleic Acids in Chemistry and Biology*, 2nd ed. Oxford University Press: Oxford, England; New York, **1996**.
- 2) Avery, O. T.; MacLeod, C. M.; McCarty, M. *J. Exp. Med.* **1944**, 79, 137.
- 3) Tamm, C., Chargaff, E. *Congres International de Biochimie, Resumes des Communications.* **1952**, 206.
- 4) Watson, J. D. Crick, F. H. C. **1953**, *Nature*, 171, 737.
- 5) Crick, F. *Nature.* **1970**, 227, 561.

- 6) Tanpure, A. A.; Pawar, M. G.; Srivatsan, S. G. *Isr. J. Chem.* **2013**, 53, 366.
- 7) Marti, A. A.; Jockusch, S.; Stevens, N.; Ju, J.; Turro, N. J. *Acc. Chem. Res.* **2007**, 40, 402.
- 8) Sinkeldam, R. W.; Greco, N. J.; Tor, Y. *Chem. Rev.* **2010**, 110, 2579.
- 9) Dodd, D. W.; Hudson, R.H.E. *Mini. Rev. Org. Chem.* **2009**, 6, 378.
- 10) Lakowicz, J.R. *Principles of Fluorescence Spectroscopy*, 3rd ed. Springer Science + Business Media: New York, NY, **2006**.
- 11) Turro, N.J.; Ramamurthy, V.; Scaiano, J.C. *Modern Molecular Photochemistry of Organic Molecules*, 10th ed. University Science Books: Sausalito, CA, **2010**.
- 12) (a) Förster, T. *Ann. Phys.* **1948**, 6, 55. (b) Michalet, X.; Weiss, S.; Jager, M. *Chem. Rev.* **2006**, 106, 1785.
- 13) Ward, D. C.; Reich, E.; Stryer, L. *J. Biol. Chem.* **1969**, 244, 1228.
- 14) Hawkins, M. E.; Brand, L.; Michael, L. J. *Methods Enzymol.* **2008**, 450, 201.
- 15) Hawkins, M. E. *Cell. Biochem. Biophys.* **2001**, 34, 257.
- 16) Hawkins, M. E.; Pfliederer, W.; Mazumder, A.; Pommier, Y. G.; Falls, F. M.; *Nucleic Acids Res.* **1995**, 23, 2872.
- 17) Hawkins, M. E.; Pfliederer, W.; Jungmann, O.; Balis, F. M. *Anal. Biochem.* **2001**, 298, 231.
- 18) Hawkins, M. E.; Pfliederer, W.; Balis, F. M.; Porter, D.; Knutson, J. R. *Anal. Biochem.* **1997**, 244, 86.
- 19) Scopes, D. I. C.; Barrio, J. R.; Leonard, N. J. *Science* **1977**, 195, 296.
- 20) Godde, F.; Aupeix, K.; Moreau, S.; Toulme, J. J. *Antisense Nucleic Acid Drug Dev.* **1998**, 8, 469.

- 21) Okamoto, A.; Tanaka, K.; Fukuta, T.; Saito, I. *J. Am. Chem. Soc.* **2003**, 125, 9296.
- 22) Okamoto, A.; Tanaka, K.; Saito, I. *J. Am. Chem. Soc.* **2003**, 125, 5066.
- 23) Okamoto, A.; Saito, Y.; Saito, I. *J. Photochem. Photobiol., C.* **2005**, 6, 108.
- 24) Lin, K. Y.; Jones, R. J.; Matteucci, M. *J. Am. Chem. Soc.* **1995**, 117, 3873.
- 25) Wilhelmsson, L. M.; Holmen, A.; Lincoln, P.; Nielsen, P. E.; Norden, B. *J. Am. Chem. Soc.* **2001**, 123, 2434.
- 26) Sandin, P.; Wilhelmsson, L. M.; Lincoln, P.; Powers, V. E.; Brown, T.; Albinsson, B. *Nucleic Acids Res.* **2005**, 33, 5019.
- 27) Suzuki, A.; Nobukatsu, N.; Saito, I.; Saito, Y. *Org. Biomol. Chem.* **2014**, 12, 660.
- 28) Zhao, Y.; Baranger, A. M. *J. Am. Chem. Soc.* **2003**, 125, 2480.
- 29) Zhao, Y.; Knee, J. L.; Baranger, A. M. *Bioorg. Chem.* **2008**, 36, 271.
- 30) Kerr, C. E.; Mitchell, C. D.; Headrick, J.; Eaton, B. E.; Netzel, T. L. *J. Phys. Chem. B* **2000**, 104, 1637.
- 31) Netzel, T. L. *Tetrahedron* **2007**, 63, 3491.
- 32) Gaied, N. B.; Glasser, N.; Ramalanjaona, N.; Beltz, H.; Wolff, P.; Marquet, R.; Burger, A.; Mely, Y. *Nucleic Acids Res.* **2005**, 33, 1031.
- 33) Kenfack, C. A.; Burger, A.; Mely, Y. *J. Phys. Chem. B* **2006**, 110, 26327.
- 34) Greco, N. J.; Tor, Y. *Tetrahedron* **2007**, 63, 3515.
- 35) Srivatsan, S. G.; Weizman, H.; Tor, Y. *Org. Biomol. Chem.* **2008**, 6, 1334.
- 36) Elmehriki, A.; Suchy, M.; Chicas, K.; Wojciechowski, F.; Hudson, R.H.E. *Artif DNA PNA XNA.* **2014**, 5, 29174.
- 37) Wahba, A. S.; Esmaeili, A.; Damha, M. J.; Hudson, R.H.E. *Nucleic Acids Res.* **2010**, 38, 1048.
- 38) Nielsen, P. E.; Egholm, M.; Berg, R. H.; Buchardt, O. *Science* **1991**, 254, 1497.
- 39) Nielsen, P. E. *Peptide Nucleic Acids Methods and Protocols.* Humana Press: Totowa, New Jersey, **2002**.

Chapter 2

2 5-(Acridin-9-ylamino)uracil a hydrolytically labile nucleobase modification in peptide nucleic acid (PNA)

2.1 Introduction

Natural nucleic acids are not appreciably fluorescent,¹ thus engendering them with fluorescence dramatically expands their range of applications.² Nucleobases that are also luminophores may exhibit fluorescence that is dependent on their chemical environment, thus being able to report the difference between the single-stranded state and duplex as well as the difference between a complementary base and a mismatch. Nucleobases that possess this ability have been termed “base-discriminating fluorophores” (BDFs).³ BDFs have uses in fluorimetric sequence detection, the detection of single nucleotide polymorphisms, reporting enzymatic processing of nucleic acids, and the ability to visualize their trafficking within biological systems.^{2,4}

Our approach to modification of the nucleobase is such that it retains Watson–Crick base-pairing yet possesses fluorescent properties. Acridine and 9-aminoacridine are well-known fluorophores,⁵ thus we set out to synthesize the chromophore-labelled nucleobase 5-(acridin-9-ylamino)uracil, U^A , derived from 5-aminouracil, which will be described (Figure 10).⁶ Although the development of fluorescent uridine analogues has been extensively investigated,^{2,7} the derivatization of 5-aminouracil with chromophoric molecules remains relatively unexplored.⁸ The spectroscopic and biophysical properties of this compound will also be described.

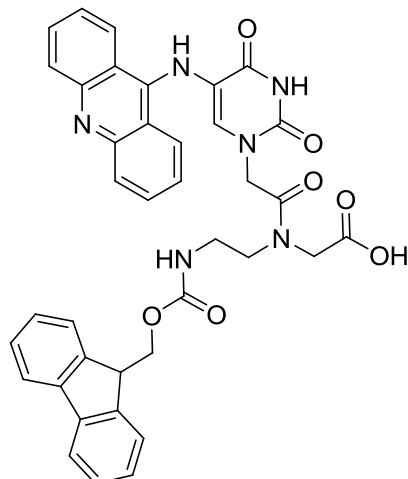
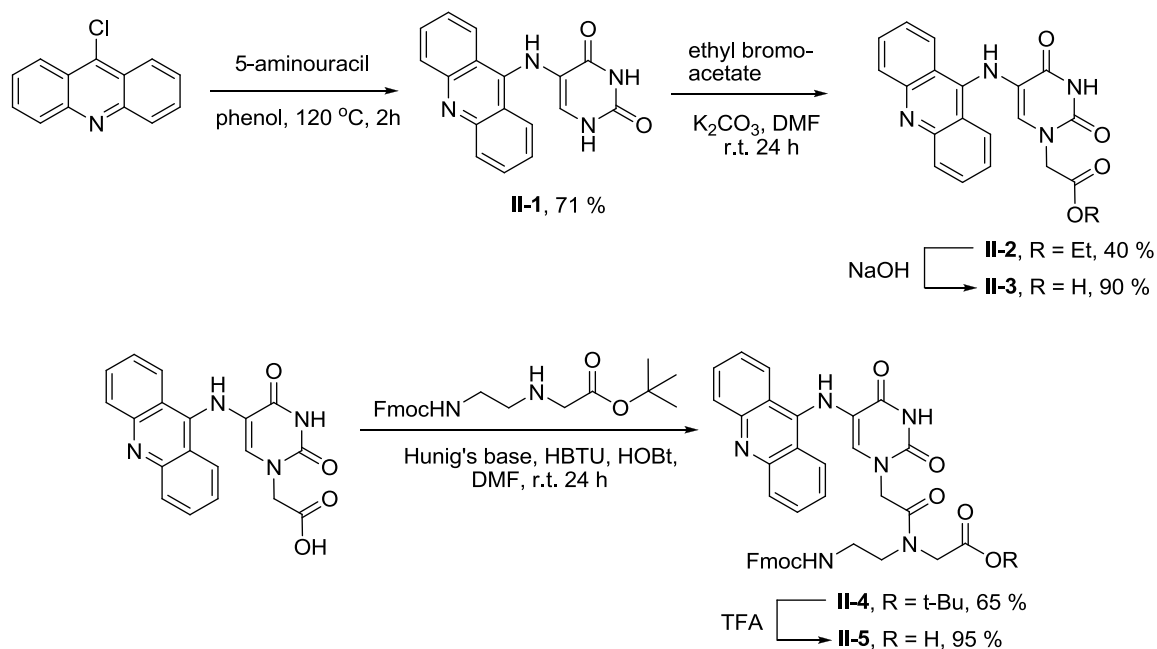


Figure 10: Acridine-labelled 5-aminouracil PNA monomer U^A.

2.2 Results and Discussion

For some time, we have pursued a minimalist approach to the transformation of essentially nonfluorescent natural nucleobases into base-pairing competent intrinsic fluorophores. Approaches for the transformation of uracil to a luminophore have focused predominantly on derivatization at C5.⁷ In this vein, 5-aminouracil represents a convenient starting material for derivatization with small, amine-reactive fluorophores. For example, the acridine-labelled base can be accessed via reaction with 9-chloroacridine. Further standard transformations yield a monomer suitable for peptide nucleic acid oligomer synthesis (Scheme 1). The low yield of compound **II-2** is due to formation of the undesired dialkylated product; however, the mono- and di-alkylated products are easily separated by column chromatography.



Scheme 1: Synthesis of the acridine-labelled 5-aminouracil PNA monomer.

2.2.1 Spectroscopic properties of acridine-labelled nucleobase

Compound **II-2** exhibits strong absorption peaks at 260 and 411 nm in the UV-vis spectrum, which is more similar to 9-aminoacridine than acridine.⁵ The longer wavelength absorption is well separated from the absorption of native nucleic acids and possesses high molar absorptivity ($\epsilon = 11200/(\text{mol/L}) \text{ cm}$, at $\lambda = 411 \text{ nm}$, in EtOH), possibly providing a good route to selective excitation of the modified base. This compound, and its congeners, were also visibly fluorescent under illumination by a handheld UV lamp ($\lambda = 360 \text{ nm}$) while in solution or as a solid adsorbed on to a TLC plate. However, when the fluorescence emission intensity was quantitated, it was found to be rather weak. The relative quantum yield in EtOH was determined to be 0.093% measured against 9,10-diphenylanthracene, whereas the fluorescence quantum yield of 9-aminoacridine in EtOH is 0.61.⁹ It has been argued that 9-aminoacridine possesses a planar conformation with respect to the exocyclic nitrogen, but non-hydrogen substituents on the 9-amino group cause a conformational change preventing effective conjugation of this group to the acridine moiety.⁹ Despite the loss in fluorescence

emission intensity, 9-*N*-substituted aminoacridines have been shown to be responsive to changes in solvent polarity.⁹

2.2.2 PNA Oligomerization

PNA synthesis was accomplished with the assistance of an automated synthesizer on the 5 μ mol scale using manufacturer supplied cycles for fluorenylmethyloxycarbonyl (Fmoc)-based oligomerization with *tert*-butyloxycarbonyl (Boc)-nucleobase protection.¹⁰ The custom monomer, U^A , was successfully incorporated into adjacent central positions in a 14-mer PNA oligomer, *N-terminus*-Lys-C-T-T-T-C-C- U^A - U^A -C-A-C-T-G-T-Lys-C-*terminus*. The peptide was cleaved from the resin, and isolated and purified according to previously reported procedures.¹¹ The reason for incorporation of two contiguous uracil analogues was to investigate the possibility of inducing excimer formation to visualize a fluorescence change upon hybridization to somewhat compensate for the low fluorescence quantum yield of U^A .

2.2.3 Hybridization studies

The stability of complexes formed with cDNA or with sequences possessing a central mismatch was evaluated by temperature dependent UV-vis spectroscopy (Table 5). The fully complementary PNA–DNA duplex has a thermal denaturation transition temperature (T_m) value of 59 °C, which is approximately 15 °C higher than the fully cDNA–DNA duplex reported by Gambari and co-workers¹² in 2001. Single mismatch discrimination across from U^A was also determined and corresponded to the base pairs U^A -G, U^A -C, and U^A -T (Table 5). The T_m values reported in Table 5 suggest that the 14-mer PNA oligomer can effectively discriminate between the fully complementary PNA–DNA duplex and the PNA–DNA duplexes containing a single base pair mismatch. In each case, the T_m values of the mismatched duplexes are all lower than the T_m value of the fully complementary duplex. The duplex containing a U^A -T mismatch is significantly stabilized compared to the C and G mismatched duplexes. It is possible that greater stability is due to a two H-bond pair formed by shearing of the thymine and U^A relative to the helical axis (Figure 11).¹³

PNA-DNA duplex	T_m ($^{\circ}\text{C}$; +/- 1 $^{\circ}\text{C}$)
<i>N-term-Lys-C-T-T-T-C-C-U^A-U^A-C-A-C-T-G-T-Lys-C-term</i> 5'-G-A-A-A-G-G-A-A-G-T-G-A-C-A-3'	59.0
<i>N-term-Lys-C-T-T-T-C-C-U^A-U^A-C-A-C-T-G-T-Lys-C-term</i> 5'-G-A-A-A-G-G-A-C-G-T-G-A-C-A-3'	40.5 ^a
<i>N-term-Lys-C-T-T-T-C-C-U^A-U^A-C-A-C-T-G-T-Lys-C-term</i> 5'-G-A-A-A-G-G-A-G-G-T-G-A-C-A-3'	46.5
<i>N-term-Lys-C-T-T-T-C-C-U^A-U^A-C-A-C-T-G-T-Lys-C-term</i> 5'-G-A-A-A-G-G-A-T-G-T-G-A-C-A-3'	52.5

Table 5: Thermal denaturation transition temperatures (T_m) for PNA–DNA duplexes: Oligonucleotide complexes were 2 $\mu\text{mol/L}$ in a buffer containing 100 mmol/L NaCl, 10 mmol/L Na_2HPO_4 , and 0.1 mmol/L EDTA at pH 7. ^aThe renaturation data was used to extract the T_m value instead of the melt data, which exhibited a larger error (43 ± 2 $^{\circ}\text{C}$).

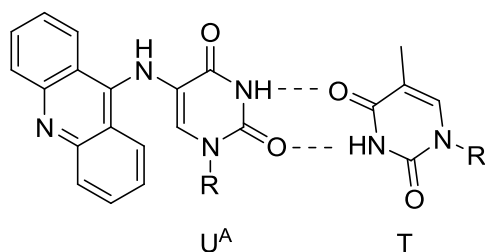


Figure 11: Proposed base pair between U^{A} and T

2.2.4 Chemical behaviour of U^{A}

During the temperature cycling in aqueous buffer for evaluation of the hybridization properties of the PNA, it was noted that the initially pale yellow solutions developed visible blue fluorescence. After a nontrivial amount of investigation, we determined that the fluorescence was due to the presence of acridone. Acridone is highly fluorescent, exhibiting quantum yield values near unity in water and alcoholic solvents,¹⁴ and displays

easily visually observed blue fluorescence emission at low concentrations. Analysis of the PNA oligomer by mass spectrometry after heat cycling showed that the oligomer was still intact; HR-MS (ESI) m/z : calcd. for $C_{185}H_{228}N_{76}O_{50}$: 4314.7713; found: 4314.7284 $[M + H]^+$.

The oligomer was also analyzed using polyacrylamide gel electrophoresis (PAGE) according to a literature procedure.¹⁵ Figure 12 clearly shows two bands for the heat treated oligomer, a slower moving nonfluorescent band possessing a mobility similar to the untreated oligomer and a faster moving (smaller) fluorescent material, while only a single band for the oligomer without heat treatment is observed. The fluorescent band has been identified as acridone, whereas the other band is attributed to the fully intact oligomer. It was not possible to isolate the putative 5-aminouracil containing PNA, nor find evidence for its formation by mass spectrometry studies on the oligomer.

The intended use of the oligomer bearing the modified bases, to potentially fluorimetrically report hybridization and discrimination of perfectly matched sequences to mismatch sequences, is not possible. The intensely fluorescent acridone ($\Phi = 0.83$ in EtOH)¹⁶ produced during the annealing of strands effectively masks any signal from the modified oligomer.

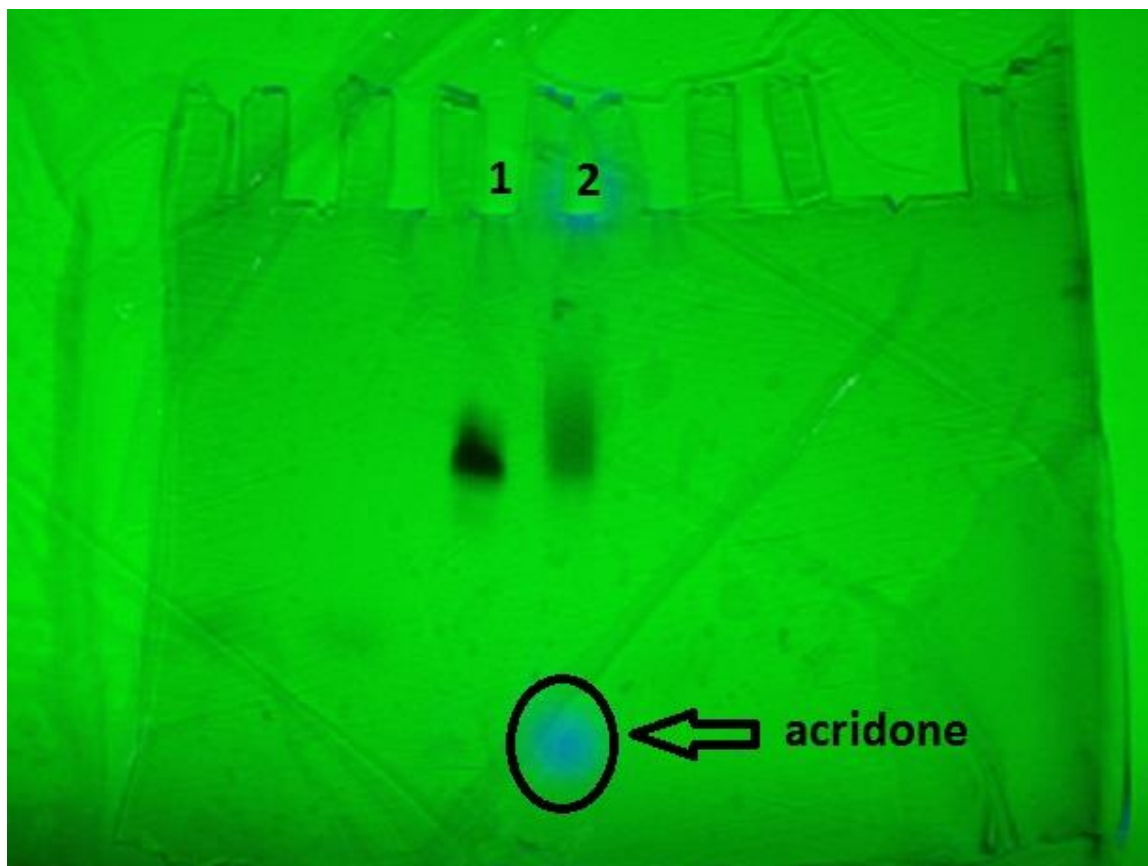
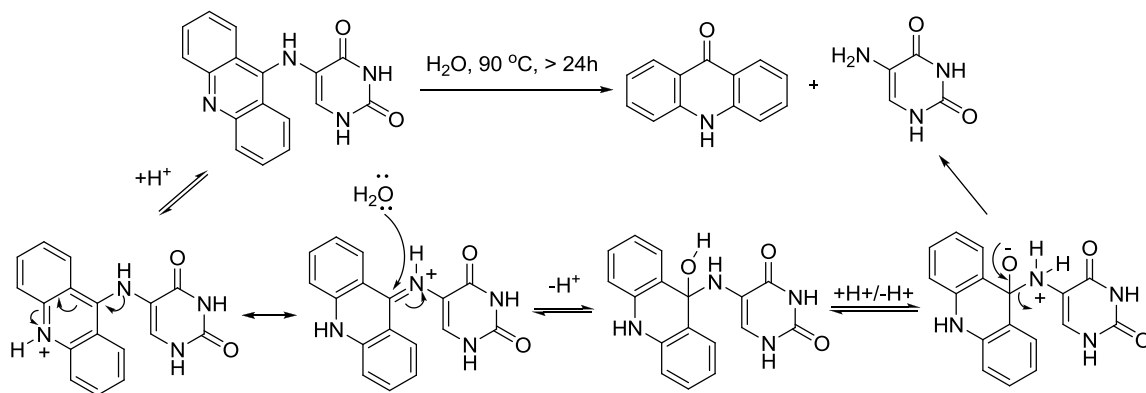


Figure 12: PAGE analysis of unprocessed PNA oligomer (lane 1) and extensively heat-cycled PNA oligomer (lane 2) visualized by UV shadowing over a fluorescent TLC plate illuminated at 260 nm. The arrowhead indicates the presence of acridone displaying its typical blue fluorescence. PAGE conditions: 26% acrylamide, 1.6% bisacrylamide, and 8.2 mol/L urea.

Due to difficulty in analyzing the oligomer and low abundance hydrolysis products, we turned to a model reaction to understand the chemistry (Scheme 2). When compound **II-1** was heated in water at 90 °C for 4 h the appearance of acridone was observed by thin layer chromatography (TLC) ($R_f = 0.5$, EtOAc–hexanes 1:1). The presence of acridone was also confirmed by low resolution mass spectrometry (calcd. for $C_{13}H_9NO$ $[M]^+$: 195.1; found: 195.1) and fluorescence spectroscopy (Figure 13). 5-Aminouracil proved to be more difficult to identify by any of the above techniques; however, the presence of 5-aminouracil was confirmed by HPLC (Figure 14). Upon extended heating, >24 h,

complete hydrolysis could be achieved and the reaction products were characterized by HPLC analysis (Figure 15).



Scheme 2: Observed hydrolysis of compound II-1 under neutral conditions and plausible mechanism for the formation of the observed products.

Excitation Emission Profile of Acridone in EtOH

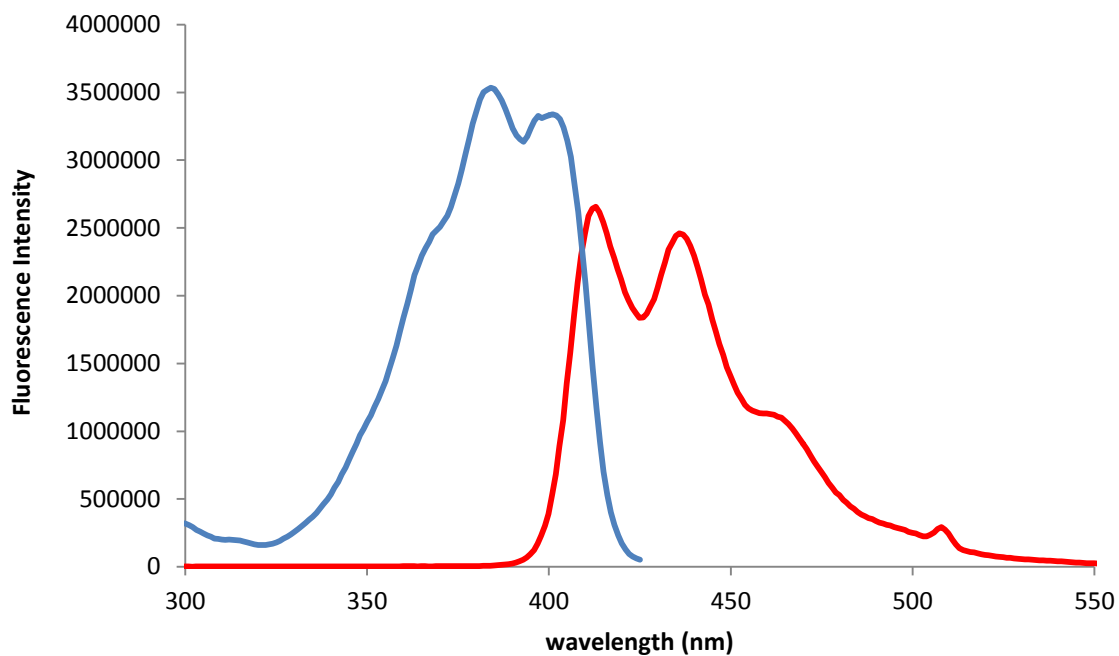


Figure 13: Excitation emission spectrum of acridone in EtOH.

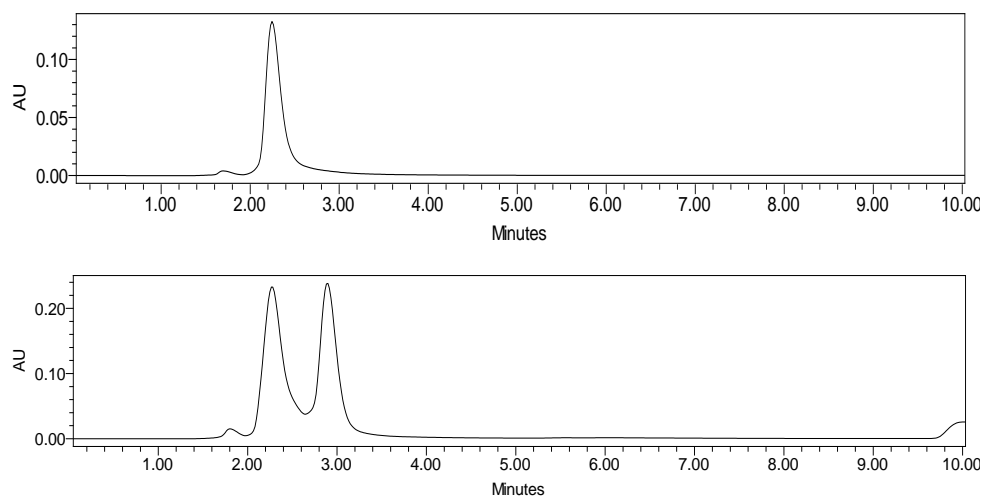


Figure 14: HPLC analysis of 5-aminouracil (top) and co-injection of 5-aminouracil and the hydrolyzed mixture (bottom). Note: Chromatograms were extracted at $\lambda = 252$ nm.

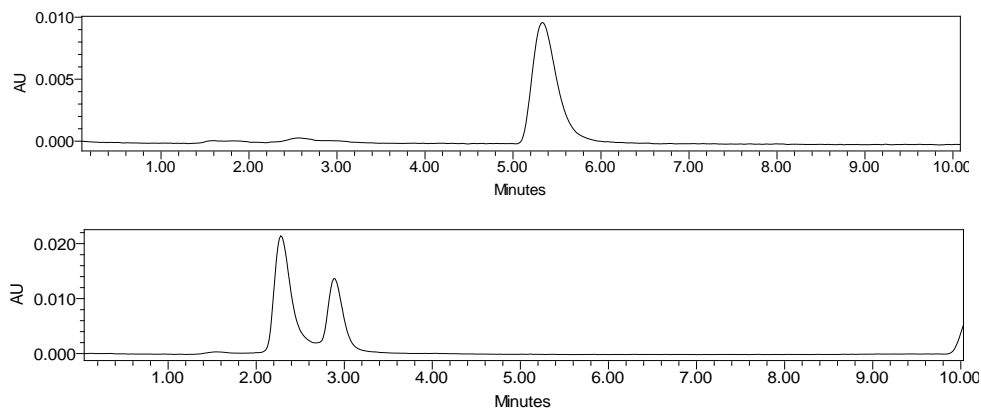


Figure 15: HPLC analysis of compound 1 (top), and the hydrolyzed mixture after heating at 90 °C for 24 hours (bottom). Note: Chromatograms were extracted at $\lambda = 252$ nm.

It has been reported that bulky substituents on the 9-amino group prevents coplanarity of the nitrogen with the acridine nucleus, thus resulting in a decrease in the chemical stability of aminoacridines.¹⁷ For example, in the series 9-aminoacridine, 9-methylaminoacridine, and 9-dimethylaminoacridine, there is a general decline in stability toward alkaline hydrolysis.^{17,18} A similar trend is observed with neutral and acid hydrolysis whereby 9-aminoacridine is more stable than 9-*N*-dialkylaminoacridines.¹⁹

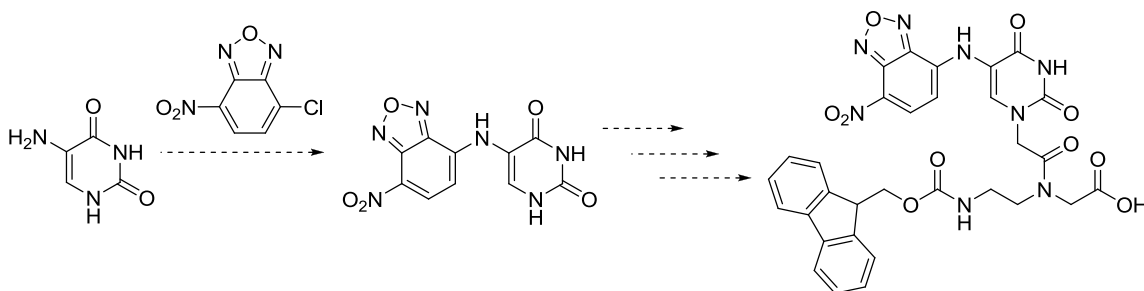
We have noted that the thermal lability of the 5-(acridin-9-ylamino)uracil moiety is affected by N1-substitution. For example, complete hydrolysis of **II-1** was achieved by heating in water at 90 °C for over 24 h, while similar treatment of **II-5** led to much less conversion (<10% by NMR analysis, data not shown). Likewise, our studies indicate that heating of the PNA oligomer containing the modified base under the conditions used to measure the T_m leads to a relatively small amount of conversion, which is estimated to be less than 10% based on the amount of acridone released and our inability to detect the 5-aminouracil containing PNA by HPLC–MS or PAGE analysis. Separate experiments incubating the oligomer for 4 h at 90 °C and analysis of the amount of released acridone versus intact oligomer shows about 15% conversion. Thus, the T_m values reported are valid for the 5-(acridin-9-ylamino)uracil modified PNA. The slow release of acridone from the oligomer argues against its long term storage. As well, the acridinyl moiety would not be a useful thermally labile protecting group as a route to 5-aminouracil modified PNA because of the slow rate of release.

2.3 Conclusions

The optimized synthesis of a weakly fluorescent nucleobase derived from 5-aminouracil was developed. The modified monomer was incorporated into a PNA oligomer. Thermal denaturation studies of DNA complexes with this oligomer illustrated its ability to discriminate between a fully matched complementary strand and the corresponding U-G, U-C, and U-T mismatched strands. The fluorescence of the PNA oligomer could not be used to study hybridization because the 5-(acridin-9-ylamino)uracil modification was thermally labile in aqueous solution and liberated the highly fluorescent acridone moiety obscuring the signal from the PNA. Despite not being an effective BDF, the ease at which the modification was introduced indicates the potential of this chemical route for the introduction of chemically modified nucleobases into PNA.

2.4 Future Work

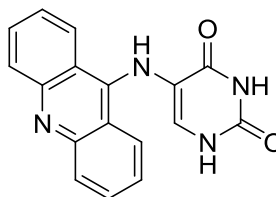
For some time now, we have been interested in the synthesis and photophysical properties of other structurally small, environmentally responsive fluorophores derived from 5-aminouracil. For instance, treatment of 5-aminouracil with the amine reactive fluorophore NBD chloride should produce a novel nucleobase analog with interesting fluorescent properties (Scheme 3). Moreover, further standard transformations would yield a monomer suitable for incorporation into a PNA oligomer. The photophysical properties of the novel PNA oligomer can then be evaluated for use as a potential fluorescent probe to study nucleic acids.



Scheme 3: Proposed synthesis of a 5-aminouracil PNA monomer derivatized with the amine reactive fluorophore NBD chloride.

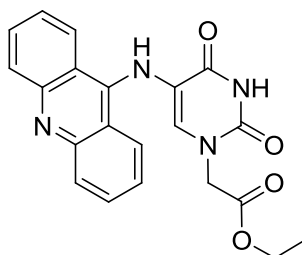
2.5 Experimental

5-(Acridin-9-ylamino)pyrimidine-2,4(1H,3H)-dione (**II-1**):

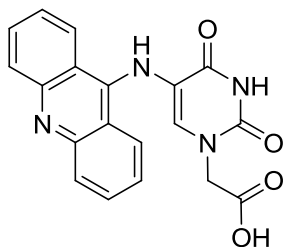


A mixture of 9-chloroacridine (2.15 g, 10.1 mmol) and phenol (11.41 g, 121.2 mmol) was heated to 80 °C. Once the phenol had melted, 5-aminouracil (1.22 g, 9.60 mmol) was added to the stirred solution at 80 °C and the reaction was further heated to 120 °C. The reaction was stirred at 120 °C for 2 h under an atmosphere of nitrogen. The reaction mixture was then cooled to room temperature and treated with 200 mL of 1M NH₄OH to precipitate an orange/brown solid. The crude product was collected by vacuum filtration, triturated in boiling EtOH for 2 h and collected by vacuum filtration again to afford compound **II-1** in 71 % yield. ¹H-NMR (DMSO-d₆, 400 MHz): δ 11.09 (s, 1H) 10.92 (s, 1H), 10.60 (s, 1H), 8.45-7.75 (m, 2H), 7.70-6.80 (m, 7H). ¹³C-NMR (DMSO-d₆, 400 MHz): δ 159.5, 154.6, 150.5, 140.2, 131.3, 127.0, 126.5, 125.0, 120.5, 117.5. HRMS (EI): calcd. For C₁₇H₁₂N₄O₂ [M]⁺ 304.0960, found 304.0959.

Ethyl-2-(5-(acridin-9-ylamino)-2,4-dioxo-3,4-dihydropyrimidin-1(2H)-yl)acetate (II-2):

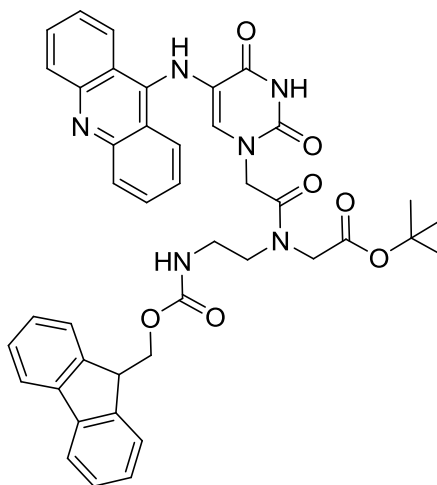


Compound **II-1** (2.00 g, 6.58 mmol) and anhydrous K_2CO_3 (2.73 g, 19.7 mmol) were dissolved in dry DMF (32.1 mL) and cooled to $-10\text{ }^\circ\text{C}$ in an ice-salt bath. Ethylbromoacetate (0.80 mL, 7.24 mmol) was then added dropwise to the reaction mixture at $-10\text{ }^\circ\text{C}$. The reaction was left stirring overnight under an atmosphere of nitrogen, with a gradual increase in temperature due to the melting of the ice-salt bath, and monitored by TLC for completion, approximately 48 h. The solvent was removed under reduced pressure and the crude product was dissolved in dichloromethane (200 mL) and washed with saturated $NaHCO_3$ (2 x 100 mL), water (2 x 100 mL) and brine (2 x 100 mL). The organic phase was collected and dried over anhydrous sodium sulfate, filtered and concentrated under reduced pressure. The crude product was purified via FCC eluting with dichloromethane:hexanes 20:80 to dichloromethane:acetone 50:50, to afford compound **II-2** in 40 % yield. $^1\text{H-NMR}$ (DMSO- d_6 , 400 MHz): δ 11.45 (s, 1H), 11.00 (s, 1H), 8.35-7.90 (m, 2H), 7.60-6.80 (m, 7H), 4.54 (s, 2H), 4.18 (q, $J = 7.0$ Hz, 2H), 1.23 (t, $J = 7.0$ Hz, 3H). $^{13}\text{C-NMR}$ (DMSO- d_6 , 400 MHz): δ 168.6, 159.1, 155.3, 150.2, 140.0, 131.7, 129.4, 127.7, 126.5, 120.6, 117.3, 61.4, 48.8, 14.2. HRMS (ED): calcd. For $C_{21}H_{18}N_4O_4$ $[M]^+$ 390.1328, found 390.1337.

2-(5-(acridin-9-ylamino)-2,4-dioxo-3,4-dihydropyrimidin-1(2H)-yl)acetic acid (II-3):

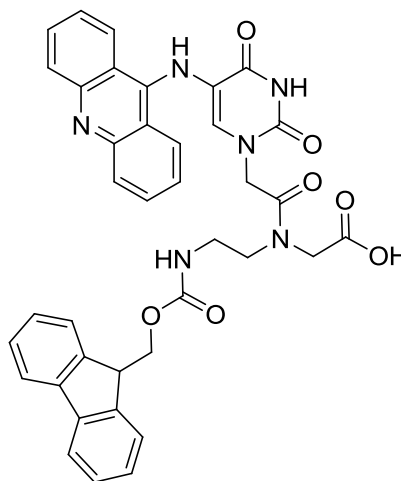
Compound **II-2** (0.20 g, 0.51 mmol) was dissolved in 14.4 mL of THF and kept in an ice bath for 15 minutes followed by the slow drop wise addition of NaOH (2.9 mL, 2.5 M). The reaction mixture was removed from the ice bath and stirred at room temperature until TLC indicated complete consumption of the starting material, approximately 2 hours. A yellow solid had precipitated from the reaction mixture and the remaining liquid was slowly decanted. To the yellow solid was added 40 mL of 1 M HCl. The product was filtered and dried under vacuum to afford compound **II-3** in 90 % yield which was used without further purification. $^1\text{H-NMR}$ (DMSO- d_6 , 600 MHz): δ 13.38 (bs, 1H), 11.93 (s, 1H), 10.99 (bs, 1H), 8.70-7.45 (m, 9H), 4.61 (s, 2H). $^{13}\text{C-NMR}$ (DMSO- d_6 , 400 MHz): δ 169.3, 159.7, 155.9, 150.1, 142.6, 139.5, 135.3, 124.9, 124.2, 119.0, 114.9, 113.7, 49.3. HRMS (EI): calcd. For $\text{C}_{19}\text{H}_{14}\text{N}_4\text{O}_4$ $[\text{M}]^+$ 362.1015, found 362.1003.

tert-butyl-2-(N-(2-(((9H-fluoren-9-yl)methoxy)carbonyl)amino)ethyl)-2-(5-(acridin-9-ylamino)-2,4-dioxo-3,4-dihydropyrimidin-1(2H)-yl)acetamido)acetate (II-4):



Compound **II-3** (0.15 g, 0.41 mmol) was dissolved in 10.3 mL of anhydrous DMF and cooled to 0 °C followed by the addition of a solution of *N*-[2-(Fmoc)aminoethyl]glycine-*t*-butyl ester (0.15 g, 0.39 mmol) in DMF (0.065 M), Hunig's base (0.6 mL, 3.4 mmol), HOBt (53 mg, 0.39 mmol) and HBTU (0.15 g, 0.39 mmol). The reaction was warmed to room temperature and left stirring for 24 h under an atmosphere of nitrogen. The reaction mixture was diluted with 60 mL of EtOAc and washed with 1 M NaHSO₄ (2 x 30 mL), water (2 x 30 mL) and brine (2 x 30 mL). The organic layer was collected, dried over sodium sulfate, filtered and concentrated under reduced pressure. The crude product was purified via FCC eluting with dichloromethane:methanol 100:0 – 90:10 to afford compound **II-4** in 65 % yield. Compound **II-4** exists in solution as a pair of slowly exchanging rotamers; signals attributed to major (ma.) and minor (min.) rotamers are designated. ¹H-NMR (DMSO-d₆, 400 MHz): δ 11.85 (s, 1H), 8.55 (s, 2H), 8.10-7.15 (m, 18H), 4.88 (s, ma., 1.05H), 4.67 (s, min., 0.66H), 4.32 (s, min., 0.66H), 4.02 (s, ma., 1.15 H), 4.39-4.11 (m, 3H), 3.45 (m, 2H), 3.28 (m, 2H), 3.14 (m, 1H), 1.48 (s, min., 3H), 1.41 (s, ma. 6H). ¹³C-NMR (DMSO-d₆, 400 MHz): δ 168.4, 168.0, 167.5, 167.1, 159.6, 156.4, 156.1, 150.1, 143.8, 142.8, 140.7, 139.5, 135.2, 127.8, 127.6, 127.3, 127.0, 125.1, 124.5, 124.0, 120.1, 119.1, 118.9, 114.2, 109.6, 82.1, 81.0, 65.5, 46.7, 27.7. HRMS (EI): calcd. For C₄₂H₄₁N₆O₇ [M + H]⁺ 741.3037, found 741.3038.

2-(N-(2-(((9H-fluoren-9-yl)methoxy)carbonyl)amino)ethyl)-2-(5-(acridin-9-ylamino)-2,4-dioxo-3,4-dihydropyrimidin-1(2H)-yl)acetamido)acetic acid (II-5):



Compound **II-4** (99 mg, 0.13 mmol) was dissolved in 3 mL of anhydrous CH_2Cl_2 and cooled to 0°C followed by the slow dropwise addition of TFA (2 mL). The reaction was stirred for 30 minutes at 0°C and 2 hours at room temperature. The reaction was evaporated to dryness via nitrogen stream and the remaining volatiles were removed by coevaporation with CH_2Cl_2 and diethyl ether. The product was dried under vacuum to afford compound **II-5** in 95 % yield. Compound **II-5** was used without further purification. Compound **II-5** exists in solution as a pair of slowly exchanging rotamers; signals attributed to major (ma.) and minor (min.) rotamers are designated. $^1\text{H-NMR}$ (DMSO- d_6 , 400 MHz): δ 11.91 (s, 1H), 10.84 (s, 1H), 8.62 (d, $J = 6$ Hz, 2H), 8.14 (s, ma., 0.62H), 8.08 (s, min., 0.40H), 8.06-7.25 (m, 16H), 4.92 (s, ma., 1.67H), 4.72 (s, min., 1.33H), 4.32 (s, min., 0.61H), 4.07 (s, ma., 1.02H), 4.35-4.10 (m, 3H, CH_2), 3.48 (m, 1H, CH_2), 3.41 (m, 1H, CH_2), 3.30 (m, 1H, CH_2), 3.15 (m, 1H, CH_2). $^{13}\text{C-NMR}$ (DMSO- d_6 , 400 MHz): δ 170.7, 170.4, 167.4, 167.0, 159.7, 158.5, 156.4, 156.3, 150.1, 143.8, 143.2, 140.7, 139.4, 135.6, 127.6, 127.3, 127.0, 125.1, 124.8, 124.4, 120.1, 119.2, 114.7, 113.6, 109.6, 65.6, 65.4, 48.6, 47.7, 46.7, 37.9, 26.8. HRMS (ED): calcd. For $\text{C}_{38}\text{H}_{33}\text{N}_6\text{O}_7$ [$\text{M} + \text{H}$] $^+$ 685.2411, found 685.2427.

PNA oligomer: HRMS (ESI) m/z ; found 4314.7836 [$\text{M} + \text{H}$] $^+$ (calculated 4314.7713 for $\text{C}_{185}\text{H}_{228}\text{N}_{76}\text{O}_{50}$).

2.6 References

- (1) Daniels, M.; Hauswirth, W. *Science* **1971**, *171*, 675.
- (2) Dodd, D. W.; Hudson, R. H. E. *Mini Rev. Org. Chem.* **2009**, *6*, 378.
- (3) Okamoto, A.; Tanaka, K.; Fukuta, T.; Saito, I. *J. Am. Chem. Soc.* **2003**, *125*, 9296.
- (4) Wahba, A. S.; Fereshteh, A.; Deleavey, G. F.; Brown, C.; Robert, F.; Carrier, M.; Kalota, A.; Gewirtz, A. M.; Pelletier, J.; Hudson, R. H. E.; M. J. Damha, M. J. *ACS Chem. Biol.* **2011**, *6*, 912.
- (5) Aaron, J. J.; Maafi, M. *Spectrochim. Acta* **1995**, *51A*, 603.
- (6) Herein we report optimized synthetic procedures and corrected photophysical characterization of the 5-(acridin-9-ylamino)uracil moiety. A preliminary report has appeared: Moustafa, M. E. *Design and Synthesis of Novel Quenchers for Fluorescent Hybridization Probes*. Ph.D. Thesis, 2011.
- (7) Sinkeldam, R. W.; Greco, N. J.; Tor, Y. *Chem. Rev.* **2010**, *110*, 2579.
- (8) (a) Barawkar, D. A.; Ganesh, K. N. *Nucleic Acids Res.* **1995**, *23*, 159. (b) Gondela, A.; Kumar, T. S.; Walczak, K.; Wengel, J. *Chem. Biodivers.* **2010**, *7*, 350.
- (9) Ya, V.; Artyukhov, T. N.; Kopylova, L. G.; Samsonova., L. *Russ. Phys. J.* **2008**, *51*, 1097.
- (10) Wojciechowski, F.; Hudson, R. H. E. *J. Org. Chem.* **2008**, *73*, 3807.
- (11) Hudson, R. H. E.; Liu, Y.; Wojciechowski, F. *Can. J. Chem.* **2007**, *85* (4), 302.
- (12) Feriotto, G.; Ferlini, A.; Gambari, R. *Hum. Mutat.* **2001**, *18*, 70.
- (13) Dickerson, R. E. *Nucleic Acids Res.* **1989**, *17*, 1797.
- (14) Bowen, E. J.; Sahu, J. *J. Chem. Soc.* **1958**, 3716.
- (15) Dodd, D. W.; Hudson, R. H. E. *Electrophoresis* **2007**, *28*, 3884.
- (16) Strickler, S. J.; Berg, R. A. *J. Chem. Phys.* **1962**, *37*, 814.
- (17) Acheson, R. M.; *Chemistry of Heterocyclic Compounds*, 2nd ed., **1973**; *9*, 878.
- (18) Kalatzis, E. J. *J. Chem. Soc. B* **1969**, *2*, 96.
- (19) Goodall, R. R.; Kermack, W. O. *J. Chem. Soc.* **1936**, 339, 1546.

Chapter 3

3 Fluorescent Adenosine Analogs: Synthesis and Photophysical Evaluation of Novel Fluorescent 7-Substituted 7-Deazaadenosine Analogs

3.1 Introduction

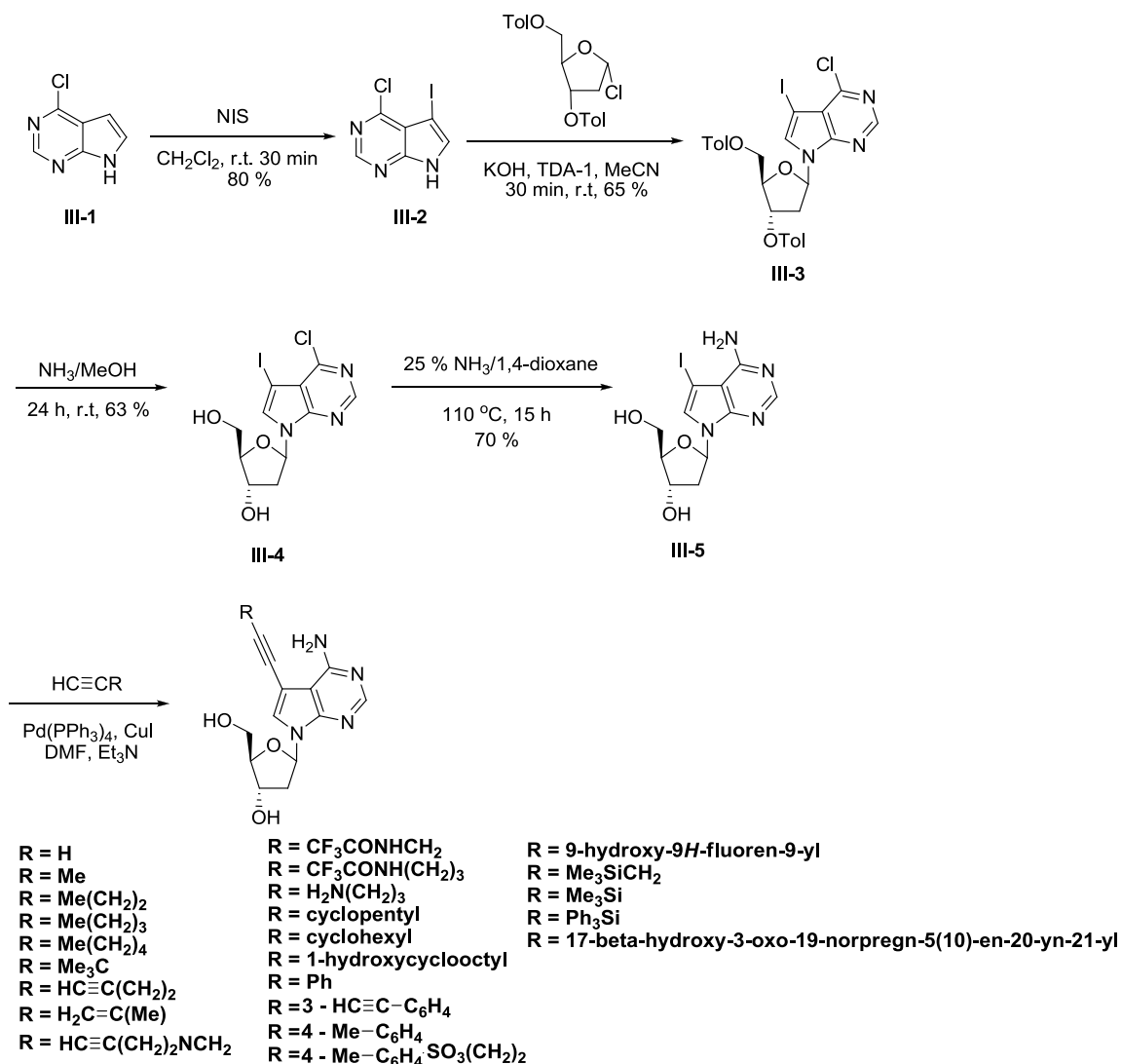
2-Aminopurine nucleoside, a highly fluorescent isomer of adenosine, has been one of the most utilized adenosine analogs for the past forty years.¹ However, this compound does not possess ideal properties for studying nucleic acids. For instance, 2-aminopurine nucleoside (2-AP), suffers dramatically reduced emission once incorporated into single-stranded oligonucleotides and further yet upon duplex formation.¹ This leaves relatively weak emission for studying the structure and dynamics of duplex species. Therefore recent developments have sought to overcome the limitations of 2-AP.

Although adenosine analogs may be substituted at various positions,² this chapter will specifically focus on fluorescent adenosine analogs which are capable of Watson-Crick hydrogen bonding and are substituted at the 7-position with various alkynes. The benefit of substitution at the 7-position of the 7-deazapurine is that large groups can be accommodated in the major groove of resultant duplexes.³

3.1.1 Background on Adenosine Analogs Substituted at the 7-position

Seela and co-workers have synthesized a small library of fluorescent 7-deazaadenosine nucleobase analogs via attachment of various alkynes to the 7-position via the Sonogashira reaction.⁴⁻⁸ Synthesis of the 7-substituted-7-deaza-2'-deoxyadenosines began with the iodination of the commercially available starting material 6-chloro-7-deazapurine **III-1**. Compound **III-1** was suspended in anhydrous dichloromethane, treated with *N*-iodosuccinimide and stirred at room temperature for 30 minutes to afford 6-chloro-7-iodo-7-deazapurine, **III-2**, in 80 % yield (scheme 4). Compound **III-2** was then suspended in acetonitrile and reacted with 1-chloro-3,5-di-*O*-toluoyl-2-deoxy-D-ribofuranose in the presence of KOH and the phase transfer catalyst tris[2-(2-

methoxyethoxy)ethyl]amine (TDA-1) to obtain the glycosylated product **III-3** in 65 % yield. Next compound **III-3** was deprotected by treatment with a saturated solution of NH_3/MeOH to give compound **III-4** in 63 % yield. Installation of the amino group was accomplished by reacting compound **III-4** with a 25 % aqueous $\text{NH}_3/1,4\text{-dioxane}$ solution and heating the mixture to $110\text{ }^\circ\text{C}$ for 15 h (sealed vial) to obtain compound **III-5** in 70 % yield. With compound **III-5** in hand, a variety of 7-substituted 7-deaza-2'-deoxyadenosines were synthesized by reacting compound **III-5** with a range of different alkynes under Sonogashira conditions.



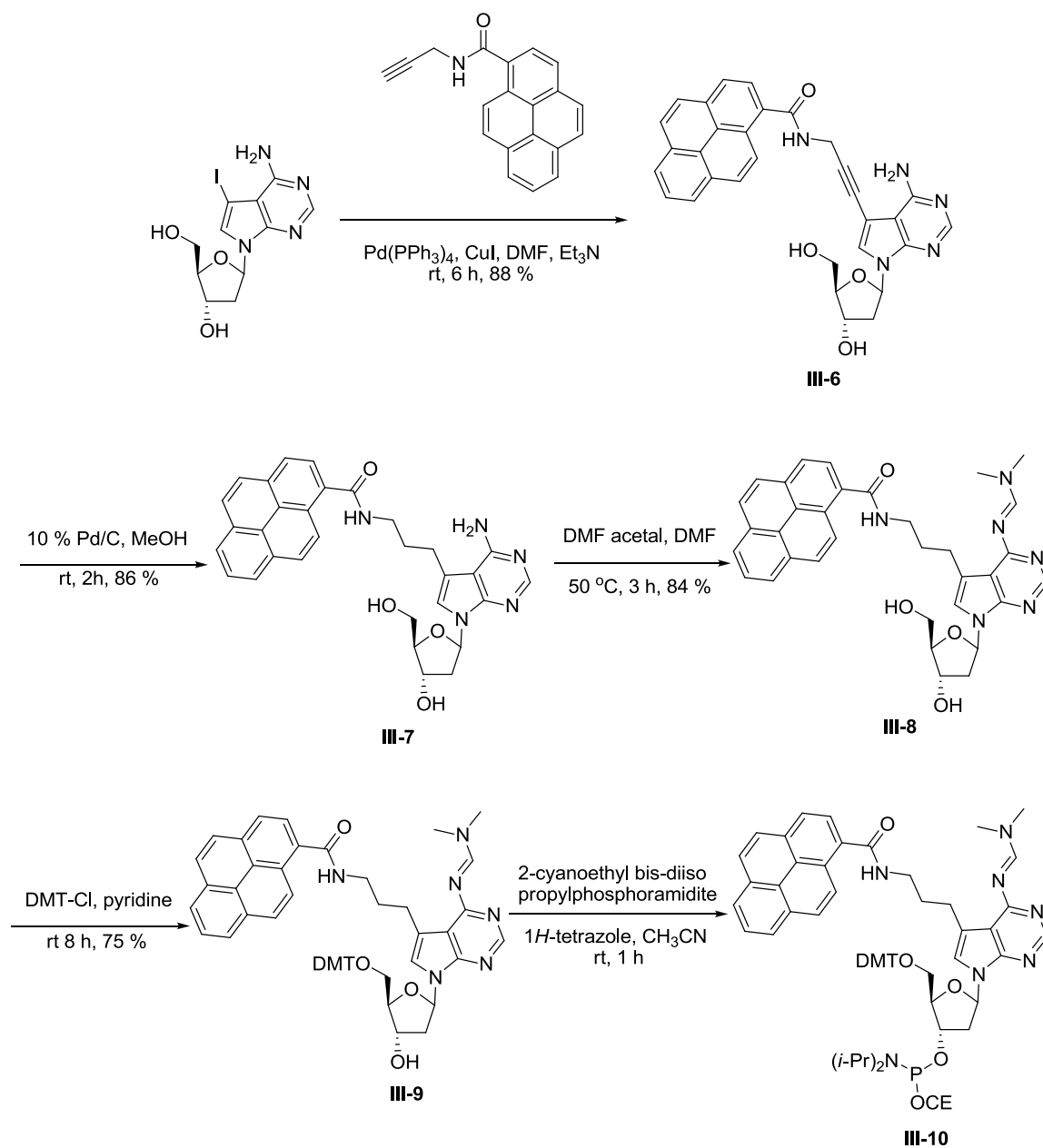
Scheme 4: Synthesis of 7-substituted-7-deaza-2'-deoxyadenosine analogs.

Fluorescence quantum yields in H₂O of the various 7-substituted-7-deazaadenosine analogs reported by Seela *et al.* range from 0.002 – 0.27 and the fluorescence lifetimes range from < 0.2 – 7.98 ns.⁴⁻⁸ Although many of these modified nucleobases exhibit fairly large Stoke shifts, a drawback associated with these fluorescent analogs is that their absorption wavelength maxima range from 270 – 320 nm. The shorter wavelengths substantially overlaps with the excitation wavelength of the natural nucleobases which implies that selective excitation of the modified nucleobases will not be possible in all cases and there exists the hazard of photochemical damage to the nucleic acids.

One particular compound, 7-deaza-7-(hex-1-ynyl)-2'-deoxyadenosine, has been further investigated by Seela *et al.* This modified nucleobase exhibits an absorption maximum at 280 nm and an emission wavelength maximum at 397 nm in H₂O.⁴⁻⁸ Additionally the fluorescence quantum yield and fluorescence lifetime of 7-deaza-7-(hex-1-ynyl)-2'-deoxyadenosine is 0.27 and 5.8 ns respectively.⁴⁻⁸ Furthermore, Seela and co-workers have demonstrated that the lipophilic hexynyl residue of 7-deaza-7-(hex-1-ynyl)-2'-deoxyadenosine stabilizes oligonucleotide duplex structure and that stabilization occurs with both self-complementary and non-self-complementary oligonucleotide duplexes.⁴⁻⁸

In 2004, Saito and co-workers developed a tethered pyrene adenosine analog, 7-deaza-7-(1-pyrenecarboxamido)propyl-2'-deoxyadenosine (**A^{PY}**).⁹ The first step in the synthesis entailed a Sonogashira cross coupling reaction between 7-deaza-7-iodo-2'-deoxyadenosine, which was prepared according to Seela's method, and a pyrene substituted propargyl amine using Pd(PPh₃)₄ as the catalyst to afford compound **III-6** (Scheme 5). Compound **III-6** was then hydrogenated using 10 % Pd/C in MeOH to obtain compound **III-7**. The next steps entailed protection of the exocyclic amino group of compound **III-7** using *N,N*-dimethylformamide dimethylacetal to give compound **III-8** and protection of the 5'-hydroxyl group with 4,4'-dimethoxytrityl to obtain compound **III-9**. Lastly compound **III-9** was converted to phosphoramidite **III-10** using 2-cyanoethyl-bis-diisopropylphosphoramidite. Compound **III-10** was then oligomerized using an automated DNA synthesizer.

The authors did not report the spectroscopic properties of the monomer, rather they showed that this fluorescent modification exhibited a fluorescence quantum yield of 0.064, in the single strand 5'-d(CGCAATA^{py}TAACGC)-3'.⁹ The corresponding A^{py}-C, A^{py}-G and A^{py}-A mismatched duplexes showed fluorescence quantum yields of 0.097, 0.098 and 0.054 respectively.⁹ Interestingly the fluorescence quantum yield of the fully complementary A^{py}-T duplex was significantly lower, 0.006, than the single strand or the mismatched duplexes. The authors hypothesized that the observed fluorescence quenching of the matched duplex was due to intercalation of pyrene into the duplex.⁹ Molecular modelling studies supported this hypothesis that pyrene was intercalated into the duplex, resulting in duplex stabilization.⁹ The authors have thus developed a probe that can clearly distinguish thymine in a DNA-DNA duplex.

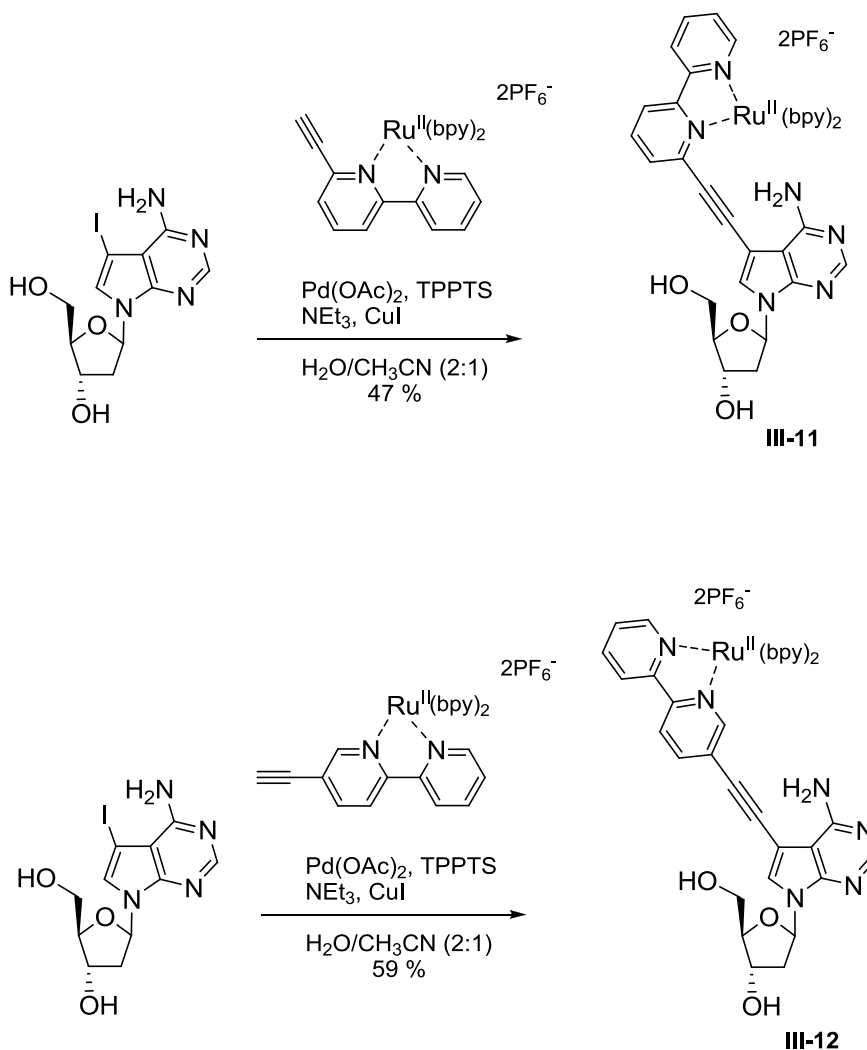


Scheme 5: Synthesis of 7-deaza-7-(1-pyrenecarboxamido)propyl-2'-deoxyadenosine.

In 2008, Hocek and co-workers reported on the synthesis and photophysical properties of 7-deaza-2'-deoxyadenosine derivatives bearing bipyridine ligands and their Ru(II)-complexes.¹⁰⁻¹¹ Synthesis of compounds **III-11** and **III-12** was accomplished via aqueous phase Sonogashira cross-coupling reactions between the corresponding Ru-containing

acetylene and 7-iodo-7-deaza-2'-deoxyadenosine using palladium/triphenylphosphine-3,3',3''-trisulfonic acid trisodium salt (TPPTS) as the catalyst (scheme 6).

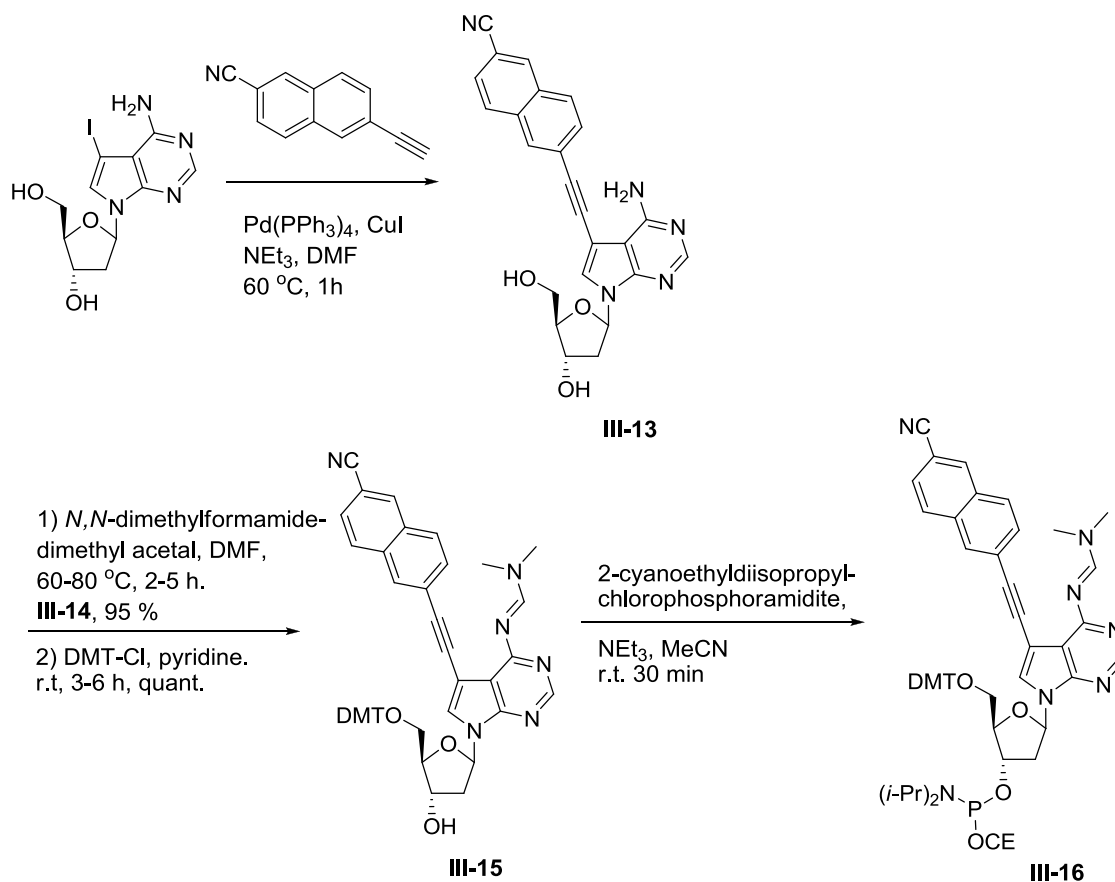
These Ru(II)-complexes showed rather weak red luminescence.¹⁰ The fluorescence quantum yields in acetonitrile ranged from 2.1 to 289×10^{-4} .¹⁰ Although the authors have not yet included compound **III-11** into oligonucleotides, they did prepare the corresponding triphosphate of compound **III-12** and incorporated this modification into oligonucleotides that were used for SNP detection.¹¹



Scheme 6: Synthesis of 7-deazaadenosine nucleosides bearing Ru(II) complexes.

A recent contribution to this class of nucleobases was made by Saito and co-workers where they synthesized fluorescent environmentally sensitive 7-deaza-2'-deoxyadenosine derivatives such as ethynylantracene and ethynynaphthalene substituted derivatives.¹² Synthesis of the ethynyl-cyanonaphthalene substituted derivative was accomplished via a Sonogashira reaction between 7-iodo-7-deaza-2'-deoxyadenosine and 2-ethynyl-cyanonaphthalene to afford compound **III-13** in high yield (scheme 7). Compound **III-13** was then treated with dimethylformamide dimethyl acetal in order to protect the exocyclic amino group on the purine core. The 5'-hydroxyl group of compound **III-14** was then protected using dimethoxytrityl chloride to obtain compound **III-15** in quantitative yield. Lastly compound **III-15** was converted to the phosphoramidite **III-16** using 2-cyanoethyl-diisopropylchlorophosphoramidite and triethylamine. Although scheme 6 specifically shows the synthesis of compound **III-16**, other derivatives were also synthesized using the same protocol.¹²

Interestingly the cyano-naphthylethynylated 7-deaza-2'-deoxyadenosine exhibited remarkable solvatochromatic properties, for instance in chloroform this compound exhibits an absorption maximum at 345 nm and an emission maximum at 423 nm whereas in acetonitrile the emission maximum shifts to 494 nm, $\Delta\lambda = 71$ nm.¹² Furthermore, upon incorporation of this modification into oligodeoxynucleotides, the authors found that this analog forms stable base pairs with both thymine and cytosine which is accompanied by a change in fluorescence intensity.¹² When the opposite base in the complementary strand is thymine, strong fluorescence was observed at 468 nm.¹² When the opposite base in the complementary strand is cytosine, stronger fluorescence intensity was observed and the emission maximum was blue-shifted to 446 nm.¹² Fluorescence emission of the single strand was weak and appeared at 461 nm.¹² The authors do not show the fluorescence emission when adenine or guanine are opposite the modification. The authors proposed that the change in fluorescence intensity and emission wavelength observed with thymine and cytosine opposite the fluorescent adenine moiety was caused by a change in the local environment near the solvatochromatic adenine moiety.¹² Thus these 7-deazaadenosine analogs exhibit desirable photophysical characteristics which bode well for their use in studying nucleic acids.



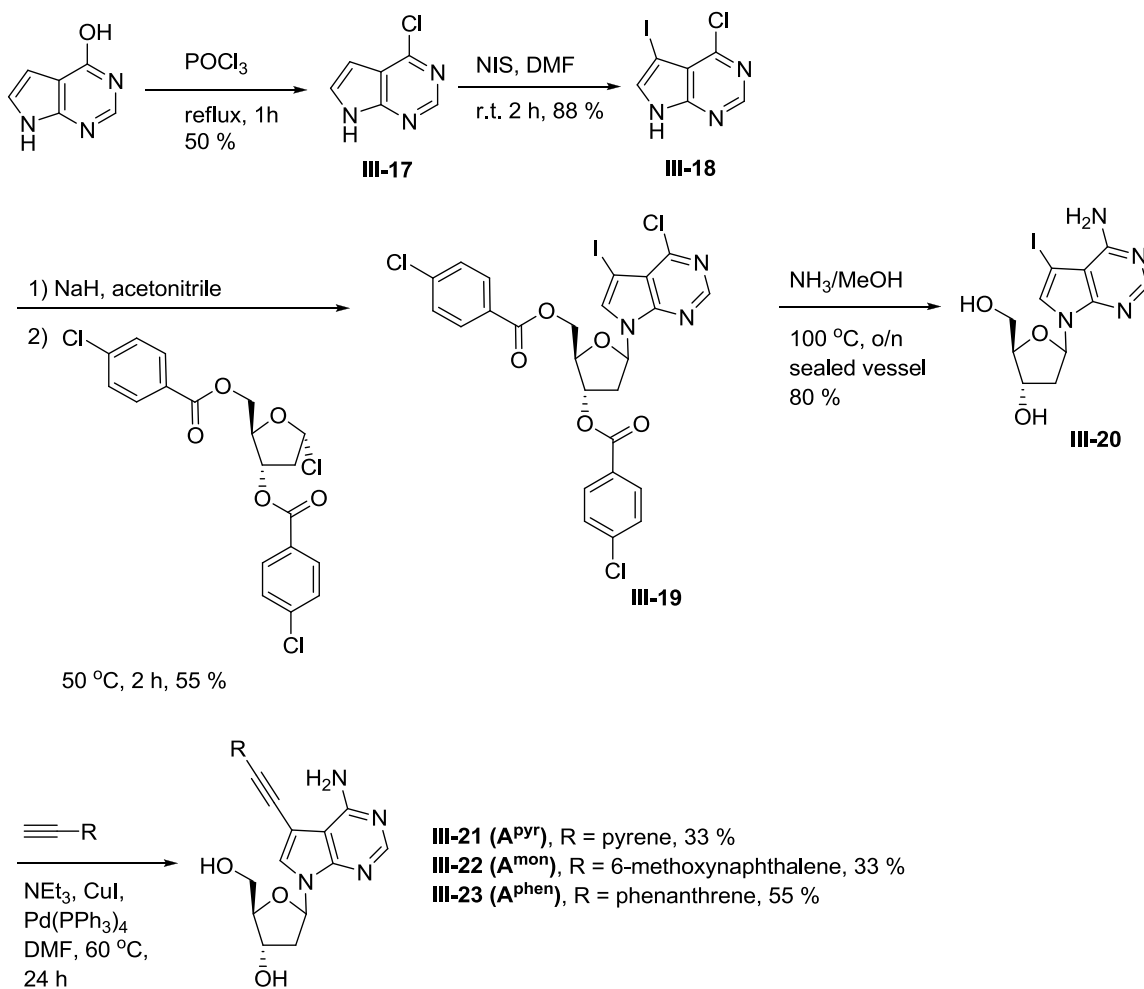
Scheme 7: Synthesis of ethynynaphthalene substituted 7-deaza-2'-deoxyadenosine.

This chapter focuses on the synthesis and photophysical characterization of novel fluorescent 7-deaza-2'-deoxyadenosines analogs, in order to evaluate their potential for use as fluorescent probes in DNA oligonucleotides. The photophysical properties of these analogs were studied in three different solvents, H₂O, EtOH and 1,4-dioxane, to study their microenvironment sensitivity. The photophysical properties that were investigated include the wavelength of absorption (λ_{ab}), the wavelength of fluorescence (λ_{fl}), the molar extinction coefficient (ϵ), the fluorescence quantum yield (Φ_F), and the Stokes shift. Moreover, the brightness values of these fluorophores are also reported. The brightness of a fluorophore is the product of the molar extinction coefficient and the fluorescence quantum yield. Brightness values are useful for comparing the utility of two fluorophores with similar fluorescence quantum yields but strikingly different molar extinction coefficients.

The adenosine analogs were synthesized via the Sonogashira cross-coupling reaction of 9-ethynylphenanthrene, 2-ethynyl-6-methoxynaphthalene, and 1-ethynylpyrene to 7-iodo-7-deaza-2'-deoxyadenosine (**III-20**), in order to produce three fluorescent 7-deaza-2'-deoxyadenosines containing rigid, polyaromatic pendant fluorophores. 9-ethynylphenanthrene and 1-ethynylpyrene were selected as alkynes due to the rigidity and moderate to high fluorescence quantum yields of phenanthrene (0.13 in EtOH)¹³ and pyrene (0.65 in EtOH).¹³ 2-ethynyl-6-methoxynaphthalene was selected in order to investigate the effect of the electron-donating methoxy group on the fluorescence quantum yield.

3.2 Results and Discussion

The synthesis began with chlorination of commercially available 7-deaza-6-hydroxypurine using POCl₃,¹⁴ to afford the desired compound **III-17** in reasonable 50 % yield (scheme 8). Compound **III-17** was then iodinated at the 7 position by treatment with NIS in DMF¹⁵ to obtain compound **III-18** in high yield. Next compound **III-18** was deprotonated with NaH in acetonitrile followed by the addition of 1-chloro-2-deoxy-3,5-di-O-*p*-chlorobenzoyl- α -D-ribose to afford exclusively the β -anomer of the glycosylated product,¹⁶ compound **III-19**, in 60 % yield. Next, installation of the exocyclic amino group and deprotection of the ester protecting groups was accomplished in one step via treatment of compound **III-19** with a saturated NH₃/MeOH solution¹⁷ to afford compound **III-20** in 80 % yield. Lastly compound **III-20** was reacted with various alkynes under Sonogashira conditions¹⁸ to obtain the desired 7-substituted-7-deazaadenosine nucleosides **III-21** – **III-23**.



Scheme 8: Synthesis of novel fluorescent 7-deaza-2'-deoxyadenosine analogs.

3.2.1 Photophysical Evaluation

The photophysical properties of A^{pyr}, A^{mon}, and A^{phen} were evaluated in dioxane, ethanol, and water, in order to study how the fluorescence properties of the products vary across solvents of different polarities. Based on the solvent's dielectric constant (ϵ), dioxane represents a non-polar solvent ($\epsilon = 2$), EtOH represents a polar solvent ($\epsilon = 24$), and water represents a highly polar solvent ($\epsilon = 80$).¹⁹ The results obtained are presented in Table 6 and the excitation-emission profiles are shown in Figures 16-18.

Analog	Solvent	λ_{ab} (nm)	λ_{fl} (nm)	Stokes Shift (nm)	ϵ ($\times 10^3 M^{-1} cm^{-1}$)	Φ_F	Brightness ($\times 10^3 M^{-1} cm^{-1}$)
A^{mon}	dioxane	319	370	51	12.5 ± 0.2	0.15	1.9
	EtOH	318	370	52	8.3 ± 0.4	0.24	2.0
	H ₂ O	317	435	118	2.2 ± 0.2	0.02	0.0
A^{phen}	dioxane	336	390	54	16.1 ± 0.3	0.14	2.3
	EtOH	332	392	60	15.0 ± 0.6	0.08	1.2
	H ₂ O	335	444	109	6.2 ± 0.5	0.02	0.1
A^{pyr}	dioxane	367	429	62	27.1 ± 1.6	0.52	14.1
	EtOH	366	432	66	39.4 ± 1.0	0.43	16.9
	H ₂ O	364	474	110	18.7 ± 0.6	0.01	0.2

Table 6: Photophysical properties of fluorescent 7-deaza-2'-deoxyadenosines.

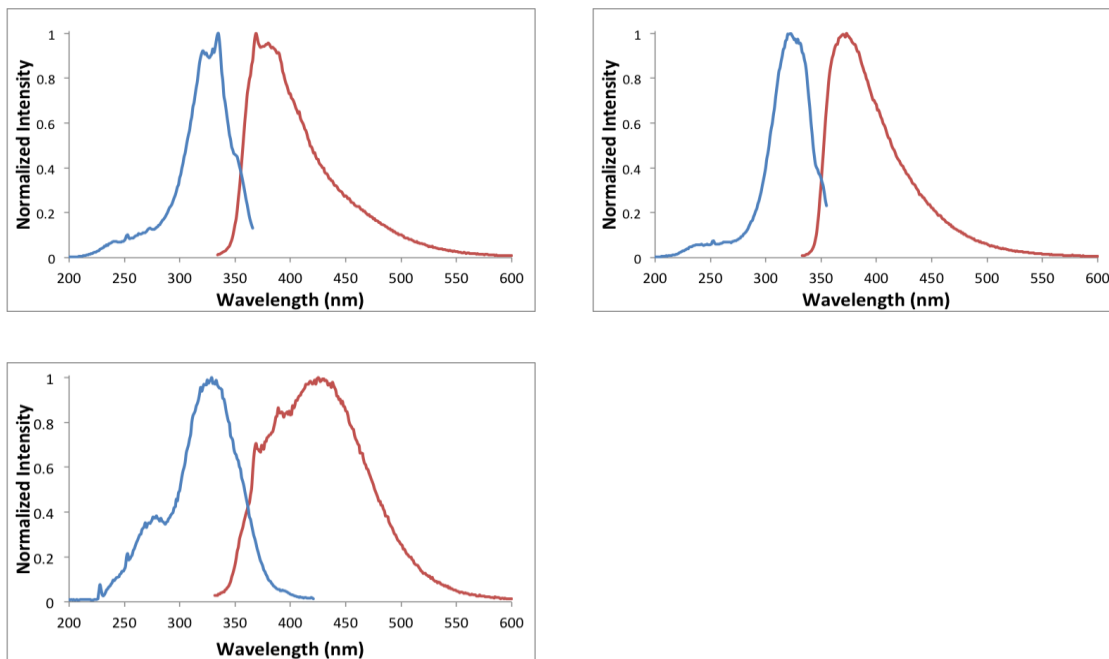


Figure 16: Excitation emission profiles of A^{mon} in dioxane (top left), EtOH (top right) and H₂O (bottom left).

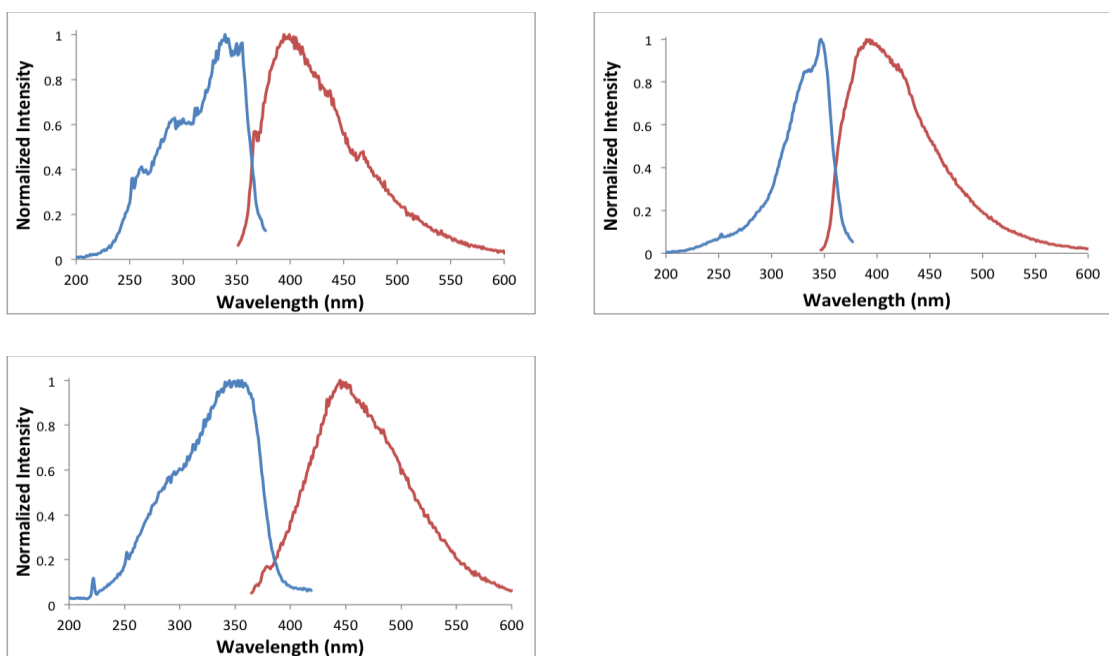


Figure 17: Excitation emission profiles of A^{phen} in dioxane (top left), EtOH (top right) and H₂O (bottom left).

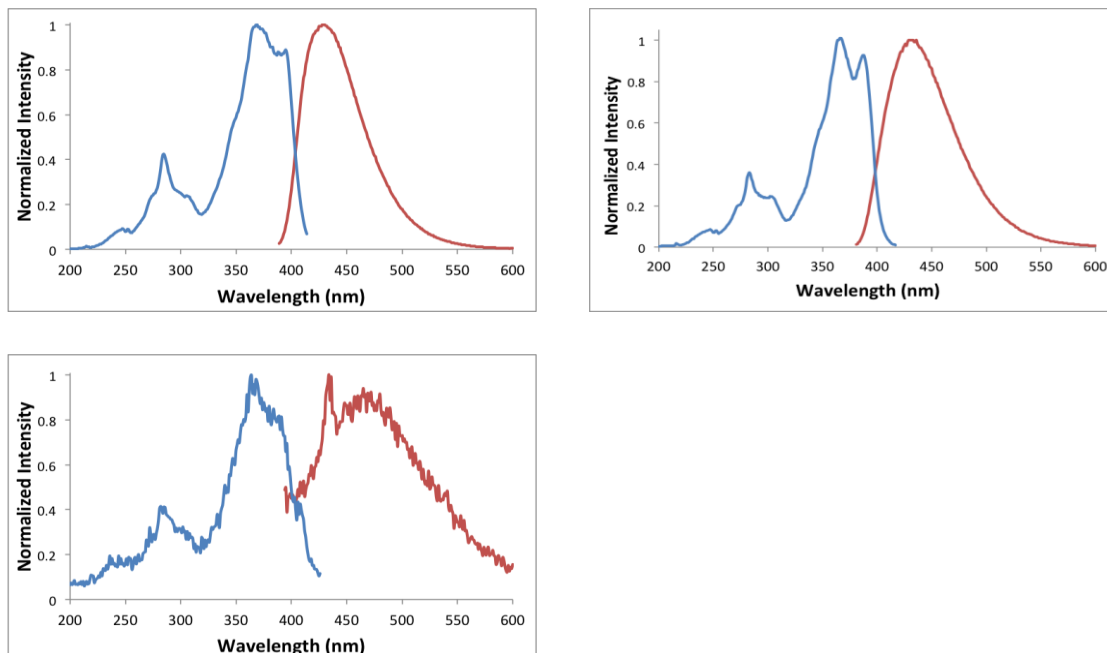


Figure 18: Excitation emission profiles of A^{pyr} in dioxane (top left), EtOH (top right) and H_2O (bottom left).

All three adenosine analogs exhibited red-shifted absorption wavelengths compared to the naturally occurring nucleobases. In addition, the absorption wavelengths were found to increase with the number of polyaromatic rings, such that A^{pyr} had the most red-shifted absorption wavelengths ($\lambda_{\text{ab}} = 364\text{-}367$ nm), followed by A^{phen} ($\lambda_{\text{ab}} = 332\text{-}336$ nm), and A^{mon} ($\lambda_{\text{ab}} = 317\text{-}319$ nm). This trend is a direct consequence of increased conjugation, which decreases the energy gap between the ground state and the excited state, allowing for wavelengths of lower energy to induce electronic transitions.²⁰

Similarly, A^{pyr} exhibited the most red-shifted fluorescence wavelengths ($\lambda_{\text{fl}} = 429, 432, 474$ nm), followed by A^{phen} ($\lambda_{\text{fl}} = 390, 392, 444$ nm), and A^{mon} ($\lambda_{\text{fl}} = 370, 370, 435$ nm). The emission wavelengths in water for all three analogs were significantly red-shifted compared to emission wavelengths in ethanol and dioxane. Thus, all three analogs show solvatofluorochromicity in water, relative to ethanol and dioxane. However, all three analogs did not display significant solvatofluorochromicity with respect to their emission wavelengths in ethanol versus dioxane. Only a slight increase in the emission wavelength was observed for A^{pyr} and A^{phen} in ethanol, relative to dioxane. This result suggests that

highly polar aqueous solvents stabilize the excited states to a greater extent than organic solvents of both high and low polarity. In addition, this result also indicates that polyaromatic substituents containing conjugated electron-donating groups do not enhance the solvatochromicity of 7-deaza-2'-deoxyadenosines, as was found with conjugated electron-withdrawing groups.¹²

Due to the stabilizing effect of solvent polarity on the excited states of fluorophores, all three analogs had Stokes shifts that increased with solvent polarity. In addition, the Stokes shifts were found to increase with the number of aromatic rings present, such that A^{pyr} had the largest Stokes shifts (62, 66, 110 nm), followed by A^{phen} (54, 60, 109 nm), and A^{mon} (51, 52, 118 nm). However, one interesting exception to this trend was that A^{mon} displayed a larger Stokes shift in water than both A^{pyr} and A^{phen} . This effect is believed to be a direct consequence of the presence of the methoxy group, since fluorophores of higher polarity are more sensitive to the stabilizing effects of polar solvents.²⁰

The molar extinction coefficients were also found to increase significantly with the size of the polyaromatic fluorophore. This trend is attributed to the fact that larger polyaromatic substituents provide a greater conjugated surface area for π - π^* transitions to occur.²⁰ Considering the impact of the molar absorption coefficient on fluorophore brightness, larger molar extinction coefficients are desirable. Thus, A^{pyr} ($\epsilon = 18.7, 27.1, 39.4 \times 10^3 \text{ M}^{-1} \text{ cm}^{-1}$) was found to be the most efficient at absorbing light, followed by A^{phen} ($\epsilon = 6.2, 15.0, 16.1 \times 10^3 \text{ M}^{-1} \text{ cm}^{-1}$), and A^{mon} ($\epsilon = 2.2, 8.3, 12.5 \times 10^3 \text{ M}^{-1} \text{ cm}^{-1}$).

Due to the high fluorescence quantum yield of pyrene (Φ_f in ethanol = 0.65),¹² A^{pyr} was expected to display desirable fluorescence properties. These expectations were indeed met, as A^{pyr} displayed high fluorescence quantum yields in dioxane, $\Phi_f = 0.52$, and ethanol, $\Phi_f = 0.43$. Conversely, A^{pyr} had a dramatically reduced fluorescence quantum yield in water, $\Phi_f = 0.01$. These large differences in quantum yield are attractive because they enable A^{pyr} to be used as an environmentally sensitive fluorescent probe across all three solvents. In addition, when the molar extinction coefficients of A^{pyr} are factored

into the equation, its remarkable brightness measurements (16.9, 14.1, 0.2) indicate that A^{pyr} would make a highly efficient and highly sensitive fluorescence probe.

Similarly, due to the moderate fluorescence quantum yield of phenanthrene (Φ_f in ethanol = 0.13),¹³ A^{phen} was expected to display useful fluorescence properties. Overall, A^{phen} displayed modest fluorescence quantum yield differences across dioxane $\Phi_f = 0.14$, ethanol $\Phi_f = 0.08$, and water $\Phi_f = 0.02$. Although it was expected that A^{phen} would display lower quantum yields than A^{pyr} , it was interesting to find that A^{phen} also displayed lower fluorescence quantum yields than A^{mon} , despite the inherent benefit of increased aromaticity. These moderate fluorescence quantum yields significantly impacted the brightness measurements observed for A^{phen} (2.3, 1.2, $0.1 \times 10^3 \text{ M}^{-1} \text{ cm}^{-1}$), despite having high molar absorptivity. Nevertheless, A^{phen} displays fair potential for use as an environmentally sensitive fluorescence probe.

Lastly, due to previous reports that conjugated electron-donating groups can be used to increase fluorescence quantum yields,⁴ A^{mon} was expected to show a marked increase in quantum yields, relative to the 2-ethynylnaphthalene derivative.¹² A^{mon} exhibited its largest fluorescence quantum yield in ethanol $\Phi_f = 0.24$, followed by dioxane $\Phi_f = 0.15$, and water, $\Phi_f = 0.01$. These moderately high fluorescence quantum yields had a positive effect on fluorophore brightness ($2.0, 1.9, 0.0 \times 10^3 \text{ M}^{-1} \text{ cm}^{-1}$), compensating for the compound's relatively low molar absorptivity. Thus, A^{mon} displays fair potential for use as an environmentally sensitive fluorescent probe across all three solvents. In addition, the 2-ethynylnaphthalene derivative was synthesized and photophysically characterized by Saito and co-workers.¹² The authors reported similar spectral characteristics to A^{mon} in ethanol, $\lambda_{\text{ab}} = 318 \text{ nm}$, $\lambda_{\text{fl}} = 371 \text{ nm}$, however the fluorescence quantum yield in ethanol was significantly lower, $\Phi_f = <0.01$.¹² This result confirms the ability of conjugated electron-donating groups to enhance the fluorescence quantum yield of 7-deaza-2'-deoxyadenosines.

3.3 Conclusion

In conclusion, three novel fluorescent 7-deaza-2'-deoxyadenosine derivatives containing rigid, polyaromatic fluorophores were successfully synthesized via the Sonogashira cross-coupling reaction of 7-iodo-7-deaza-2'-deoxyadenosine (**III-20**) with 1-ethynylpyrene, 2-ethynyl-6-methoxynaphthalene, and 9-ethynylphenanthrene. These 7-deaza-2'-deoxyadenosine analogs were photophysically characterized in dioxane, EtOH, and H₂O in order to evaluate their potential for use as environmentally sensitive fluorescent probes.

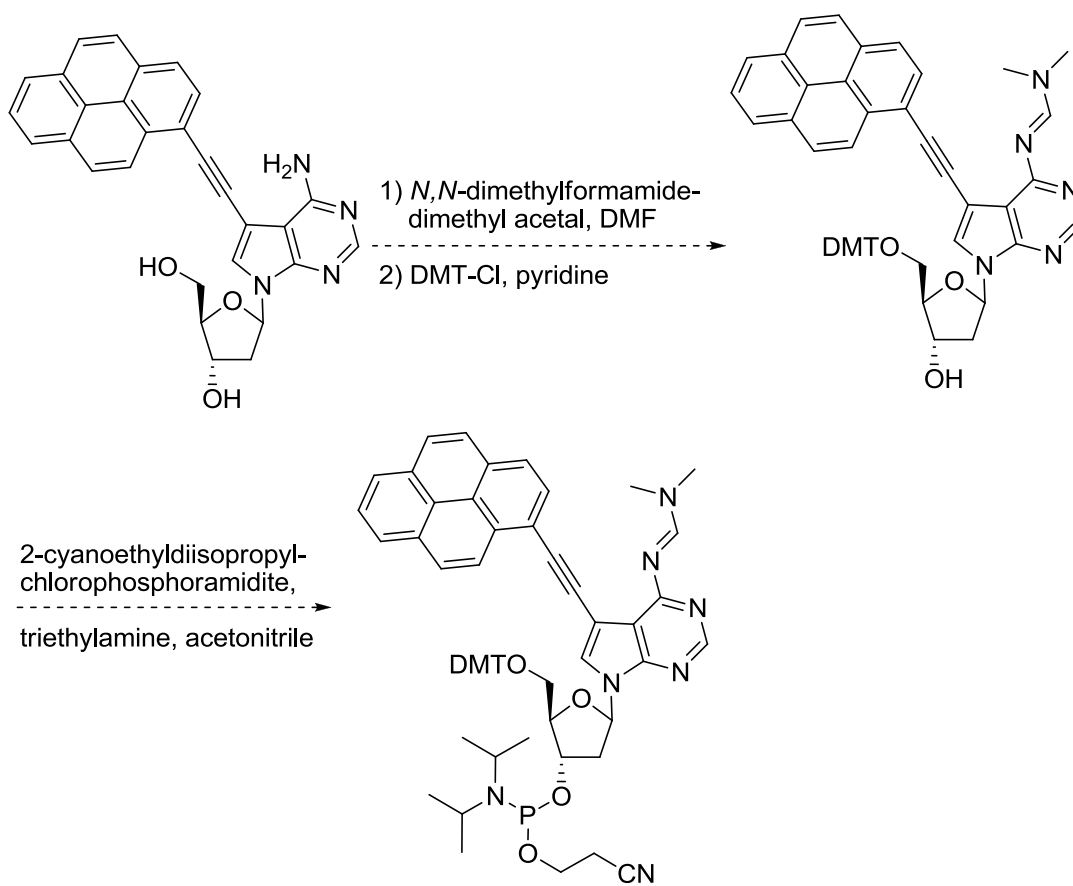
Among them, A^{pyr} showed the most promise, due to its red-shifted absorption wavelengths ($\lambda_{ab} = 364, 366, 367$ nm), red-shifted emission wavelengths ($\lambda_{fl} = 429, 432, 474$ nm), large molar extinction coefficients ($\epsilon = 18.7, 27.1, 39.4 \times 10^3 \text{ M}^{-1} \text{ cm}^{-1}$), high fluorescence quantum yields in dioxane ($\Phi_F = 0.52$) and EtOH ($\Phi_F = 0.43$), and dramatic decrease in fluorescence quantum yield in H₂O ($\Phi_F = 0.01$). Such sizable differences in quantum yields and molar absorption coefficients allow for A^{pyr} to be detected with high sensitivity across all three solvents, as illustrated by its large brightness measurements ($16.9, 14.1, 0.2 \times 10^3 \text{ M}^{-1} \text{ cm}^{-1}$). These characteristics, in conjunction with the benefit that large substituents at the 7-position of the 7-deazapurine can be accommodated in the major groove of resultant duplexes,³ suggests that A^{pyr} has considerable potential for use as an environmentally sensitive fluorescent probe.

In addition, A^{mon} and A^{phen} were found to display modest potential for use as environmentally sensitive fluorescent probes. Both A^{mon} and A^{phen} had red-shifted absorption and emission wavelengths above those of the naturally occurring nucleobases. However, A^{mon} was the least red-shifted of all three analogues. The lower molar absorptivity ($\epsilon = 2.2, 8.3, 12.5 \times 10^3 \text{ M}^{-1} \text{ cm}^{-1}$) but higher quantum yields ($\Phi_F = 0.24, 0.15, 0.01$) of A^{mon}, versus the lower quantum yields ($\Phi_F = 0.14, 0.08, 0.02$) but higher molar absorptivity ($\epsilon = 6.2, 15.0, 16.1 \times 10^3 \text{ M}^{-1} \text{ cm}^{-1}$) of A^{phen}, combined to produce comparable brightness measurements. The relatively low brightness measurements observed for A^{mon} ($2.0, 1.9, 0.0 \times 10^3 \text{ M}^{-1} \text{ cm}^{-1}$) and A^{phen} ($2.3, 1.2, 0.1 \times 10^3 \text{ M}^{-1} \text{ cm}^{-1}$) hamper their ability to be detected with high sensitivity in the applications of interest.

Lastly, the fluorescence quantum yield of the 2-ethynyl-6-methoxynaphthalene derivative (A^{mon}) was found to increase dramatically (EtOH: $\Phi_F = 0.24$) from that of the 2-ethynyl-naphthalene derivative (EtOH: $\Phi_F = <0.01$).¹² This result confirms the ability of polyaromatic substituents containing conjugated electron-donating groups to increase the fluorescence quantum yields of 7-deaza-2'-deoxyadenosines.

3.4 Future Work

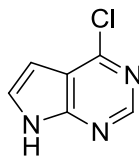
The next phase of this research project would be to incorporate A^{pyr} into an oligonucleotide sequence for use as an environmentally sensitive fluorescent probe. This would entail protection of the exocyclic amino group of A^{pyr} using dimethylformamide dimethyl acetal¹² (Scheme 9). Next the 5'-hydroxyl group will be protected by treatment with dimethoxytrityl chloride and pyridine.¹² Lastly, phosphoramidite synthesis will be accomplished using 2-cyanoethyl-diisopropylchlorophosphoramidite and trimethylamine.¹² This will yield a monomer suitable for incorporation into an oligonucleotide via automated DNA synthesis. Based on the promising photophysical properties of A^{pyr} , we anticipate that this analog will act as a useful fluorescent probe to study nucleic acid microenvironment.



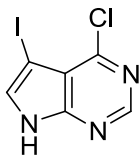
Scheme 9: Proposed synthesis of A^{pyr} DNA monomer.

3.5 Experimental

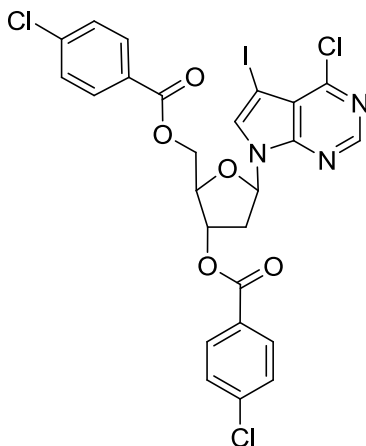
4-chloro-7H-pyrrolo[2,3-d]pyrimidine (III-17):



7H-pyrrolo[2,3-d]pyrimidin-4-ol (4.01 g, 29.7 mmol) was suspended in 45 mL of POCl₃ and refluxed for 1 hour. The solution was cooled to room temperature and excess POCl₃ was removed by rotary evaporation. A mixture of dichloromethane (600 mL) and ice water (200 mL) was then added to the dark-brown residue and stirred for 24 hours, or until the dark-brown residue was completely dissolved. The aqueous layer was then neutralized by adding increments of a saturated sodium bicarbonate solution (3 × 300 mL). The organic layer was collected, dried over MgSO₄, and gravity filtered. The product was dried by rotary evaporation, producing a pale yellow solid (2.35 g, 52%). ¹H-NMR (DMSO-d₆, 400 MHz): δ = 12.57 (br s, 1 H), 8.59 (s, 1 H), 7.69 (d, *J* = 2.3 Hz, 1 H), 6.61 (d, *J* = 2.3 Hz, 1 H); ¹³C-NMR (DMSO-d₆, 400 MHz): δ = 151.75, 150.41, 150.26, 128.35, 116.52, 98.76; HRMS (EI): calcd. for C₆H₃ClN₃[M]⁺ 153.0094, found 153.0090.

4-chloro-5-iodo-7H-pyrrolo[2,3-d]pyrimidine (III-18):

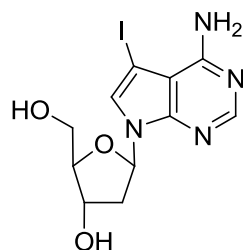
Compound **III-17** (2.33 g, 15.2 mmol) was dissolved in 54 mL of DMF, followed by the addition of NIS (3.58 g, 15.9 mmol). The reaction was stirred at room temperature for 2 hours. The solvent was removed by rotary evaporation and 60 mL of ice water was added to the orange residue. The precipitate was then collected by vacuum filtration, washed with ice water (3 × 15 mL), and concentrated in vacuo. The product was obtained as a pale brown solid (3.75 g, 88%). ¹H-NMR (DMSO-d₆, 400 MHz): δ = 12.94 (br s, 1 H), 8.59 (s, 1 H), 7.93 (s, 1 H). ¹³C-NMR (DMSO-d₆, 400 MHz): δ = 151.95, 151.18, 150.93, 134.31, 116.23, 52.12; HRMS (EI): calcd. for C₆H₃ClIN₃[M]⁺ 278.9060, found 278.9052.

(2R,3S,5R)-5-(4-chloro-5-iodo-7H-pyrrolo[2,3-d]pyrimidin-7-yl)-2-((4-chlorobenzoyloxy)methyl)tetrahydrofuran-3-yl 4-chlorobenzoate (III-19):

Compound **III-18** (1.00 g, 3.60 mmol) was dissolved in 28 mL of anhydrous acetonitrile, followed by the addition of sodium hydride (0.15 g, 6.6 mmol). The reaction was stirred at room temperature under an atmosphere of nitrogen for 30 minutes. Next, 1-chloro-2-deoxy-3,5-di-O-p-chlorobenzoyl- α -D-ribose (1.57 g, 3.6 mmol) was added to the reaction and the mixture was stirred at 50°C for 2 hours. The solvent was removed by rotary

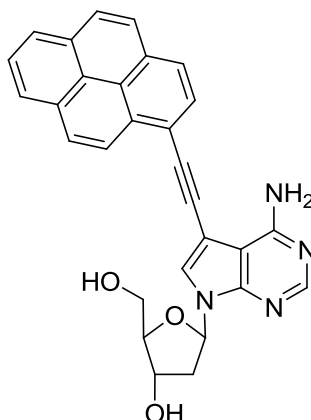
evaporation and the crude product was purified by flash chromatography eluting with 2 % acetone in toluene to afford compound **III-19** as a pale yellow solid (1.36 g, 57%). ¹H-NMR (CDCl₃, 400 MHz): δ = 8.61 (s, 1H), 8.10 – 7.90 (m, 4H), 7.55 (s, 1H), 7.47 (m, 4 H), 6.77 (t, *J* = 4.0 Hz, 1H), 5.76 (m, 1H), 4.80 – 4.50 (m, 3H), 2.90 – 2.70 (m, 2H). ¹³C-NMR (CDCl₃, 400 MHz): δ = 165.0, 164.9, 152.8, 150.9, 150.4, 140.1, 139.9, 131.2, 131.0, 130.5, 128.9, 128.8, 127.5, 127.2, 117.4, 84.3, 82.3, 75.0, 63.9, 52.9, 37.9. HRMS (EI): calcd. for C₂₅H₁₇Cl₃IN₃O₅[M]⁺ 670.9278, found 670.9546.

(2R,3S,5R)-5-(4-amino-5-iodo-7H-pyrrolo[2,3-d]pyrimidin-7-yl)-2-(hydroxymethyl)tetrahydrofuran-3-ol (III-20):



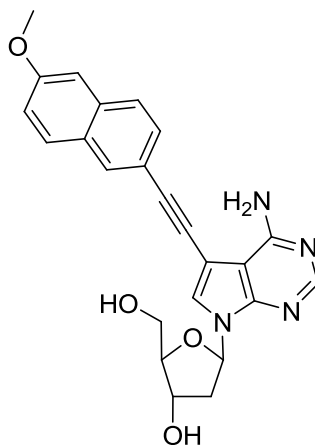
Compound **III-19** (0.55 g, 0.80 mmol) was added to a thick-walled round bottom flask and suspended in 50 mL of methanol. The suspension was cooled to 0 °C followed by the addition of ammonia, which was bubbled into the suspension for 30 minutes. The reaction vessel was tightly sealed and the reaction was stirred at 100 °C for 24 hours. The solvent was removed by rotary evaporation and the crude product was purified by flash chromatography on SiO₂, eluting with 10 % methanol in dichloromethane. The product was obtained as a white solid in 80 % yield. ¹H NMR (DMSO-*d*₆, 400 MHz): δ = 8.09 (s, 1H), 7.65 (s, 1H), 6.48 (m, 1H), 5.25 (d, *J* = 6.0 Hz, 1H), 5.02 (t, *J* = 6.0 Hz, 1H), 4.32 (m, 1H), 3.80 (m, 1H), 3.56 (m, 2H), 2.47 (m, 1H), 2.17 (m, 1H); ¹³C NMR (DMSO-*d*₆, 400 MHz): δ = 157.3, 152.1, 150.0, 126.9, 103.3, 87.5, 83.1, 71.1, 62.0, 52.0, C(2') overlapped with DMSO; HRMS (EI): *m/z* calcd for C₁₁H₁₃ IN₄O₃: 376.0032; found: 376.0025.

7-(1-ethynylpyrene)-7-deaza-2'-deoxyadenosine A^{pyr} (III-21):



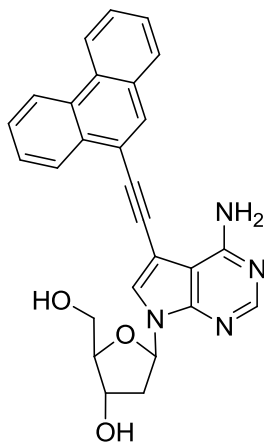
Compound **III-20** (100 mg, 0.26 mmol) was dissolved in dry, deoxygenated DMF (2.0 mL) to which CuI (10 mg, 0.052 mmol), Et₃N (0.075 mL, 0.52 mmol), 1-ethynylpyrene (240 mg, 1.04 mmol) and Pd(PPh₃)₄ (31 mg, 0.026 mmol) were sequentially added. The reaction mixture was stirred in the dark at 60 °C for 24 hours. The solvent was removed in vacuo and the residue diluted with 15 mL of dichloromethane. The organic layer was washed with 3 % EDTA solution (3 x 5 mL) and brine (3 x 5 mL). The organic layer was dried and concentrated in vacuo. The crude product was purified by FCC eluting with 10 % methanol in dichloromethane to afford compound **III-21** in 33 % yield. ¹H-NMR (DMSO-d₆, 600 MHz): δ 8.59 (d, *J* = 12.0 Hz, 1H), 8.49 – 8.00 (m 10H), 6.58 (m, 1H), 5.31 (d, *J* = 6.0 Hz, 1H), 5.11 (t, *J* = 6.0 Hz, 1H), 4.41 (m, 1H), 3.88 (m, 1H), 3.75 - 3.50 (m, 2H), 2.58 (m, 1H), 2.27 (m, 1H). ¹³C-NMR (DMSO-d₆, 400 MHz): δ 157.7, 152.8, 149.5, 131.0, 130.8, 130.7, 130.4, 129.5, 128.7, 128.2, 127.3, 127.2, 126.3, 126.0, 125.9, 125.8, 124.7, 123.6, 123.4, 117.1, 102.1, 94.9, 89.9, 88.9, 87.6, 83.2, 70.9, 61.9, 54.9, C(2') overlapped with DMSO; HRMS (EI): *m/z* calcd for C₂₉H₂₂N₄O₃: 474.1692; found: 474.1697.

7-(2-ethynyl-6-methoxynaphthalene)-7-deaza-2'-deoxyadenosine A^{mon} (III-22):



Compound **III-20** (85 mg, 0.20 mmol) was dissolved in dry, deoxygenated DMF (1.8 mL) to which CuI (8 mg, 0.042 mmol), Et₃N (0.060 mL, 0.43 mmol), 2-ethynyl-6-methoxynaphthalene (163 mg, 0.80 mmol) and Pd(PPh₃)₄ (24 mg, 0.021 mmol) were sequentially added. The reaction mixture was stirred in the dark at 60 °C for 24 hours. The solvent was removed in vacuo and the residue diluted with 15 mL of dichloromethane. The organic layer was washed with 3 % EDTA solution (3 x 5 mL) and brine (3 x 5 mL). The organic layer was dried and concentrated in vacuo. The crude product was purified by FCC eluting with 10 % methanol in dichloromethane to afford compound **III-22** in 33 % yield. ¹H-NMR (DMSO-*d*₆, 600 MHz): δ 8.16 (s, 1H), 8.12 (s, 1H), 7.89 (s, 1H), 7.90 -7.82 (m, 1H), 7.60 (dd, *J*₁ = 12.0 Hz, *J*₂ = 6.0 Hz, 1H), 7.55-7.37 (m, 1H), 7.22 (dd, *J*₁ = 12.0 Hz, *J*₂ = 6.0 Hz, 1H), 6.53 (m, 1H), 5.29 (m, 1H), 5.07 (t, *J* = 6.0 Hz, 1H), 4.37 (m, 1H), 3.88 (s, 3H), 3.83 (m, 1H), 3.59 (m, 1H), 3.57 (m, 1H), 2.23 (m, 1H); ¹³C NMR (DMSO-*d*₆, 400 MHz): δ = 158.2, 157.7, 149.5, 138.5, 133.9, 129.4, 128.2, 119.5, 117.4, 102.2, 95.0, 91.8, 87.9, 82.7, 71.08, 62.0, 51.5, 50.0, C(2') overlapped with DMSO; HRMS (EI): *m/z* calcd for C₂₄H₂₂N₄O₄: 430.1641; found: 430.1636.

7-(9-ethynylphenanthrene)-7-deaza-2'-deoxyadenosine A^{phen} (III-23):



Compound **III-20** (100 mg, 0.27 mmol) was dissolved in dry, deoxygenated DMF (2.0 mL) to which CuI (10 mg, 0.054 mmol), Et₃N (0.075 mL, 0.52 mmol), 9-ethynylphenanthrene (215 mg, 1.08 mmol) and Pd(PPh₃)₄ (31 mg, 0.026 mmol) were sequentially added. The reaction mixture was stirred in the dark at 60 °C for 24 hours. The solvent was removed in vacuo and the residue diluted with 15 mL of dichloromethane. The organic layer was washed with 3 % EDTA solution (3 x 5 mL) and brine (3 x 5 mL). The organic layer was dried and concentrated in vacuo. The crude product was purified by FCC eluting with 10 % methanol in dichloromethane to afford compound **III-23** in 55 % yield. ¹H-NMR (DMSO-*d*₆, 600 MHz): δ 8.93-8.86 (m, 2H), 8.45 (m, 1H), 8.31 (s, 1H), 8.20 (s, 1H), 8.08 (s, 1H), 8.04 (d, *J* = 6.0 Hz, 1H), 7.81-7.70 (m, 4H), 6.56 (m, 1H), 5.30 (d, *J* = 6.0 Hz, 1H), 5.10 (t, *J* = 6.0 Hz, 1H), 4.39 (m, 1H), 3.87 (m, 1H), 3.63 (m, 1H), 3.57 (m, 1H), 2.57 (m, 1H), 2.26 (m, 1H); ¹³C NMR (DMSO-*d*₆, 400 MHz): δ = 157.6, 152.8, 149.5, 132.3, 131.7, 131.4, 130.7, 130.5, 130.2, 129.6, 129.5, 128.5, 127.9, 127.5, 127.3, 122.9, 102.1, 94.6, 89.0, 87.6, 83.2, 70.9, 61.8, 30.7, C(2') overlapped with DMSO; HRMS (EI): *m/z* calcd for C₂₇H₂₂N₄O₃: 450.1692; found: 450.1685.

3.6 References

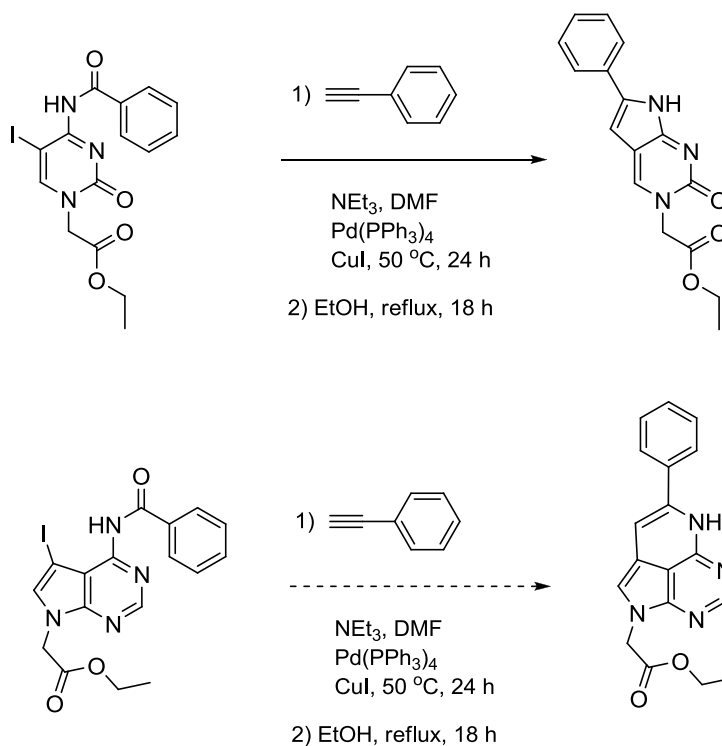
- 1) Sinkeldam, R. W.; Greco, N. J.; Tor, Y. *Chem. Rev.* **2010**, 110, 2579.
- 2) Matarazzo, A.; Hudson, R. H. E. *Tetrahedron*, **2015**, 71, 1627.
- 3) Seela, F.; Shaikh, K. I. *Tetrahedron*. **2005**, 61, 2675.
- 4) Seela, F.; Zulauf, M.; Sauer, M.; Deimel, M. *Helv. Chim. Acta* **2000**, 83, 910.
- 5) Seela, F.; Zulauf, M. *Chem. Eur. J.* **1998**, 4, 1781.
- 6) Seela, F.; Zulauf, M. *Synthesis* **1996**, 726.
- 7) Seela, F.; Zulauf, M. *J. Chem. Soc., Perkin Trans. I* **1998**, 3233.
- 8) Seela, F.; Steker, H.; *Helv. Chim. Acta* **1985**, 68, 563.
- 9) Saito, Y.; Miyauchi, Y.; Okamoto, A.; Saito, I. *Chem. Commun.* **2004**, 1704.
- 10) Vrabel, M.; Pohl, R.; Votruba, I.; Sajadi, M.; Kovalenko, S.A.; Ernsting, N.P.; Hocek, M. *Org. Biomol. Chem.* **2008**, 6, 2852.
- 11) Vrabel, M.; Horakova, P.; Pivonkova, H.; Kalachova, L.; Cernocka, H.; Cahova, H.; Pohl, R.; Sebest, P.; Havran,.; Hocek, M.; Fojta, M. *Chem. Eur. J.* **2009**, 15, 1144.
- 12) Suzuki, A.; Kimura, K.; Ishioroshi, S.; Saito, I.; Nemoto, N.; Saito, Y. *Tetrahedron Lett.* **2013**, 54, 2348.
- 13) Brouwer, A. M. *Pure Appl. Chem.* **2011**, 83, 2213.
- 14) Reigan, P.; Gbaj, A.; Stratford, I. J.; Bryce, R.A.; Freeman, S. *Eur. J. Med. Chem.* **2008**, 43, 1248.
- 15) Song, Y.; Ding, H.; Dou, Y.; Yang, R.; Sun, Q.; Xiao, Q.; Ju, Y. *Synthesis*. **2011**, 9, 1442.
- 16) Dierckx, A.; Miannay, F. A.; Gaied, N. B.; Preus, S.; Björck, M.; Brown, T.; Wilhelmsson, L. M. *Chem. – Eur. J.* **2012**, 18, 5987.
- 17) Seela, F.; Xu, K. *Helv. Chim. Acta.* **2008**, 91, 1083.
- 18) Hudson, R. H. E.; Dambeniaks, A. K.; Viirre, R. D. *Synlett.* **2004**, 13, 2400.
- 19) Maryott, A. A.; Smith, E. R. *Bur. Stand. (U.S.), Circ.* **1951**, 514, 1.
- 20) Saur, M.; Hofkens, J.; Enderlein, J. Wiley-VCH: Weinheim, 2011; 1.

Chapter 4

4 Fluorescent Adenine Analogs: Efforts Toward the Synthesis of a Novel Tricyclic 7-Deazaadenine

4.1 Introduction:

The objective of this research project was to synthesize a novel tricyclic adenine analog by extending the substrate scope of the Sonogashira cross-coupling/heteroannulation chemistry developed in the Hudson group for cytidine analogs¹ to adenine analogs (scheme 10).



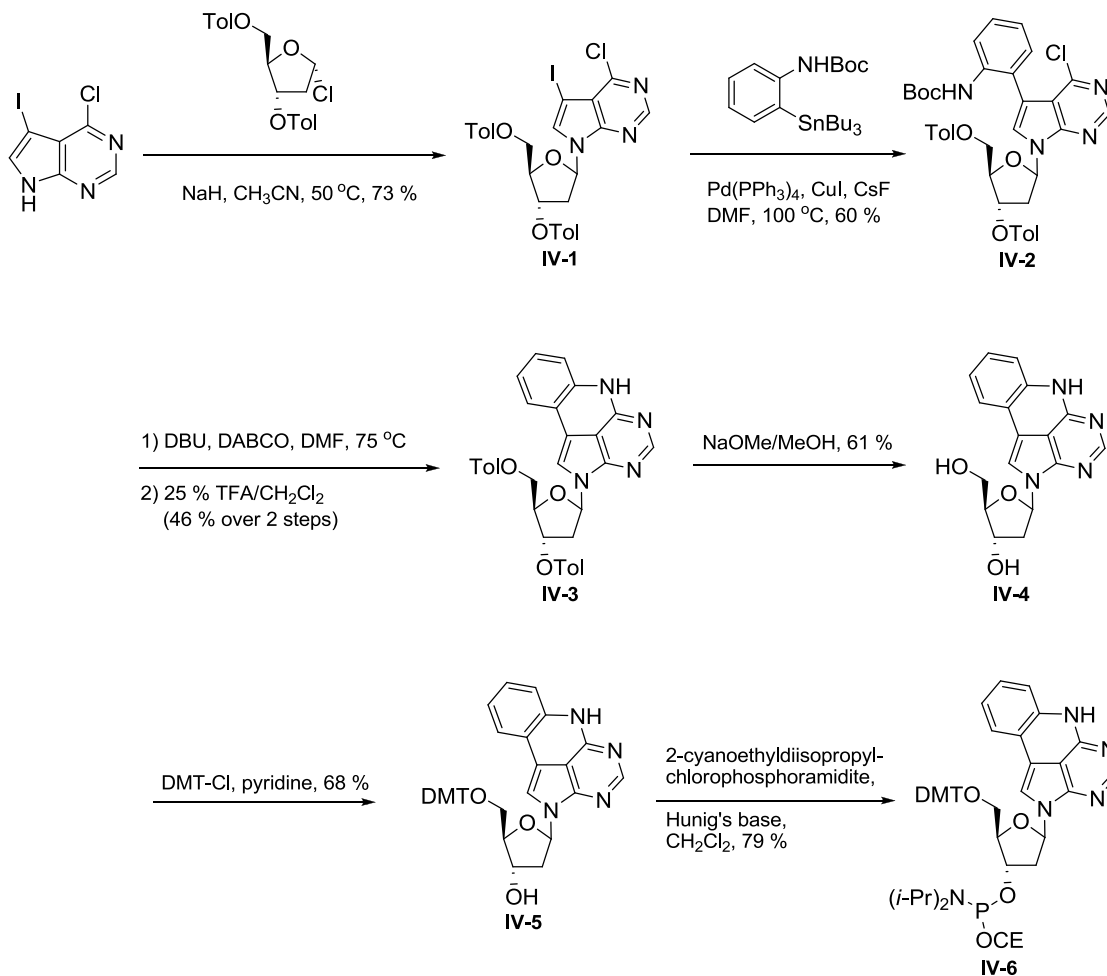
Scheme 10: Expanding the substrate scope of the Sonogashira cross-coupling/heteroannulation reaction developed for cytidine analogs to adenine analogs.

While we were exploring this chemistry for the synthesis of a novel tricyclic adenine analog, Wilhelmsson's group reported the synthesis of a fluorescent, tetracyclic adenine analog.² The synthesis was based on Matteucci's method,³ and began with the condensation of 6-chloro-7-deaza-7-iodopurine with the chloro sugar using sodium hydride to yield the desired compound **IV-1**, predominantly the β anomer (scheme 11). The following step entailed a Stille coupling reaction between compound **IV-1** and tributylstannyl-*N*-(Boc)aniline using Pd(PPh₃)₄, cesium fluoride and copper iodide to enhance the reaction rate.⁴ Ring closure to form compound **IV-3** was achieved using a mixture of DABCO and DBU followed by deprotection of the Boc group using 25 % TFA in dichloromethane. Deprotection of the toluoyl group was then performed using a 0.5 M solution of NaOMe in MeOH to yield the free nucleoside. Compound **IV-4** was then treated with dimethoxytrityl chloride in pyridine to give compound **IV-5**. Lastly compound **IV-5** was converted to the phosphoramidite monomer using Hunig's base and 2-cyanoethyl diisopropylchlorophosphoramidite.

This tetracyclic adenosine analog exhibits an excitation wavelength maximum at 337 nm, which is extremely desirable for selective excitation, and an emission wavelength maximum at 457 nm.² This molecule also displays a modest quantum yield in water of 0.068.² Upon incorporation into DNA this tetracyclic adenosine analog either increases or preserves duplex stability depending on the sequence.² Furthermore this analog does not experience severe quenching upon oligomerization and can reach quantum yield values significantly higher than 2-aminopurine in certain sequences.² Moreover this compound demonstrates highly specific base-pairing with thymine making it a potential probe for mismatch studies.

The authors also examined at the quantum yields of DNA duplexes containing a tetracyclic adenosine mismatch as well as the corresponding matched duplexes. They observed that the quantum yield increased threefold for the mismatched sequences compared to the matched sequences.² They also observed that the average quantum yield of tetracyclic adenine in single strands is higher or equal to their corresponding mismatched duplexes.² Therefore, the authors suggest that the increase in quantum yield may be due to the weaker base pairing between tetracyclic adenine and the mismatched

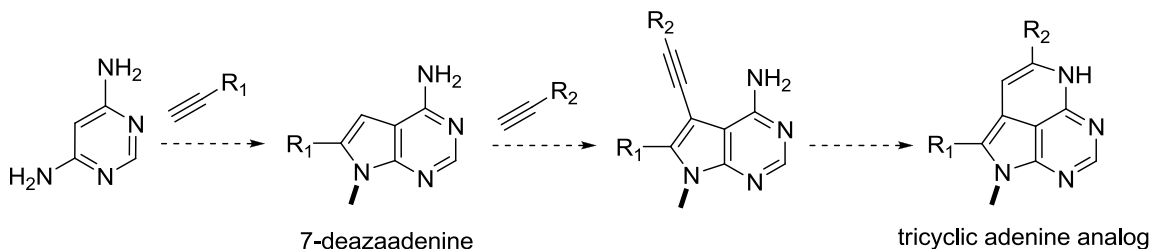
bases.² Thus leading to less extensive base stacking and an increased opening rate for the mismatched tetracyclic adenine base pairs compared to the tetracyclic adenine-thymine base pair.²



Scheme 11: Synthesis of a tetracyclic adenosine analog.

Although the tetracyclic adenine analog and the tricyclic adenine analog have similar structural characteristics, there is a key structural difference between them. The tetracyclic adenine analog possesses a fused aromatic ring whereas the aromatic ring in the tricyclic adenine analog is attached through a carbon-carbon single bond between two sp^2 hybridized carbon atoms. Wilhelmsson's report on the tetracyclic adenine analog gave us confidence that similar types of heterocycles could be accessed, thus we decided to continue to pursue our investigation of the tricyclic adenine analog.

Our approach toward the tricyclic adenine analog is based on a sequential Sonogashira/cyclization methodology (Scheme 12). Matsuda and co-workers have previously reported the synthesis of 7-deazaadenine using this Sonogashira/cyclization reaction sequence.⁵ Thus, by extending this chemistry to the 7-deazaadenine scaffold, we envision the synthesis of a novel tricyclic adenine analog with variable substitution possible at R₁ and R₂ (Scheme 12).

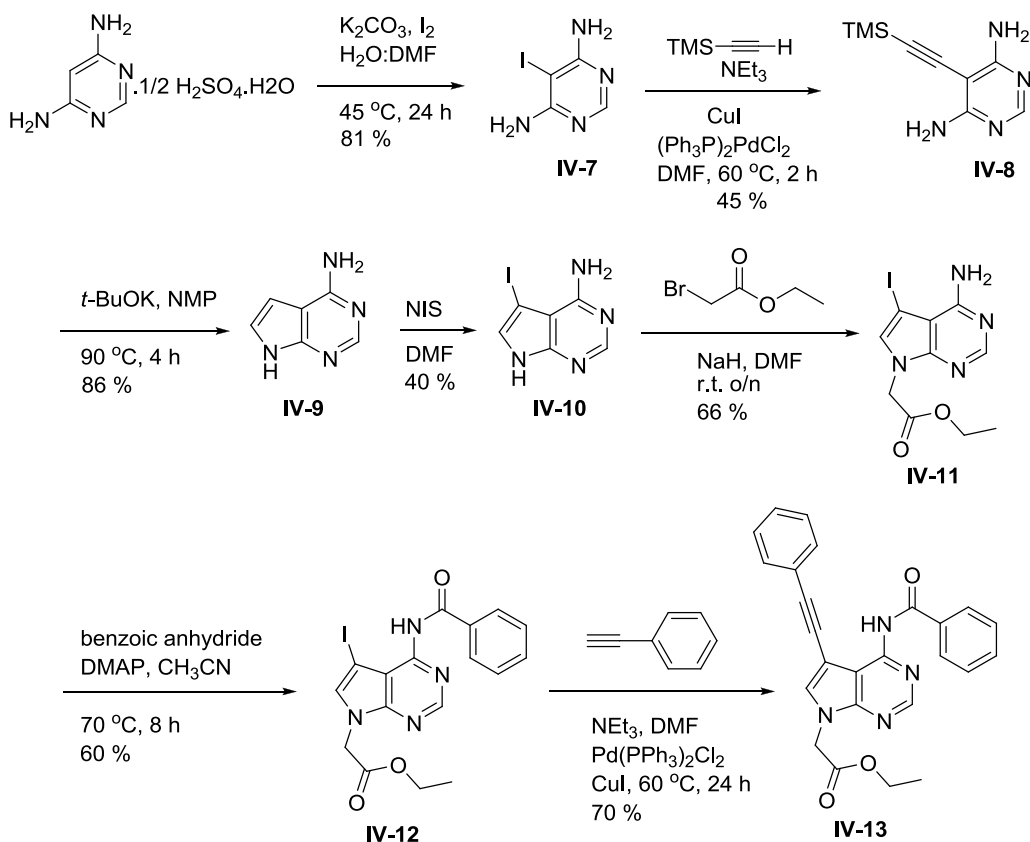


Scheme 12: Sequential Sonogashira/cyclization synthetic strategy toward a tricyclic adenine analog.

4.2 Results and Discussion

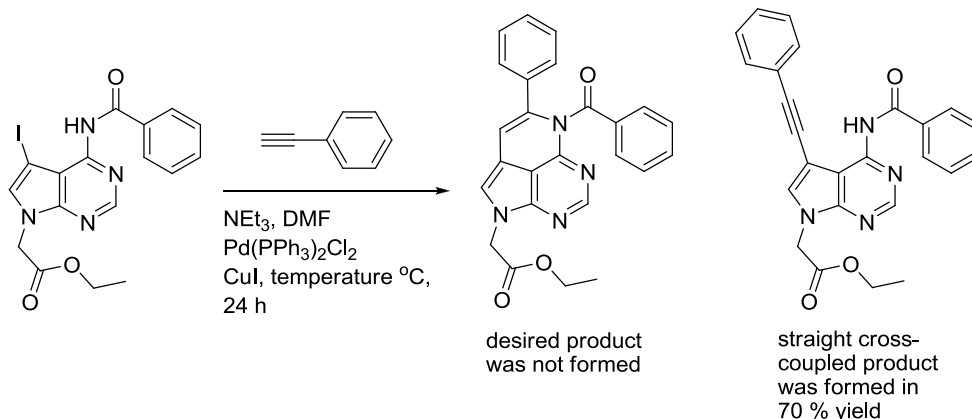
Efforts toward the synthesis of a tricyclic adenine analog began with the iodination of 4,6-diaminopyrimidine hemisulfate monohydrate to afford compound **IV-7** in 81 % yield (scheme 13).⁵ The next step entailed a Sonogashira cross-coupling reaction between compound **IV-7** and TMS acetylene. The catalyst system employed was (Ph₃P)₂PdCl₂ and CuI which gave rise to the cross coupled product compound **IV-8** in 45 % yield.⁵ Compound **IV-8** was then cyclized by treatment with *t*-BuOK in NMP⁵ to afford the 7-deazaadenine heterocycle, compound **IV-9** in 86 % yield. 7-Deazaadenine was then iodinated at the 7-position using NIS in DMF⁶ to afford compound **IV-10** in 40 % yield. Compound **IV-10** was alkylated at N9 by treatment with NaH and ethyl bromoacetate in DMF⁷ to obtain the desired compound **IV-11** in 66 % yield. Installation of the benzoyl group on the exocyclic amine of compound **IV-11** was accomplished using benzoic anhydride and DMAP in acetonitrile⁸ to afford compound **IV-12** in 60 % yield. Lastly, compound **IV-12** was subjected to the Sonogashira cross-coupling/heteroannulation reaction conditions.¹ However, unlike the cytidine scaffold, the 7-deazaadenine substrate

did not cyclize under these conditions to give a tricyclic adenine and the straight cross-coupled product was isolated in 70 % yield.



Scheme 13: Efforts toward the synthesis of a tricyclic adenine analog.

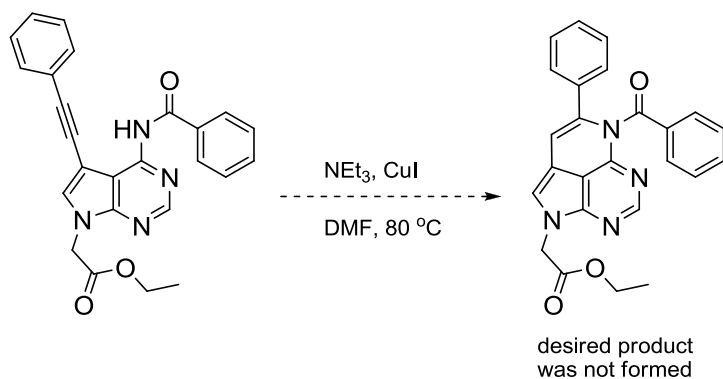
Initial attempts at troubleshooting the Sonogashira/cyclization reaction on the adenine scaffold included carrying out the reaction at higher temperatures while holding all other reaction conditions constant (table 7). However, increased temperatures did not promote the cyclization reaction to occur and only the straight cross-coupled product was formed. The isolated product was analyzed by ^{13}C -NMR and IR spectroscopy to determine the presence of an internal alkyne. The peak at 92.8 ppm in the ^{13}C -NMR spectrum represents the alkyne carbons and the signal at 2150 cm^{-1} in the IR spectrum is indicative of an alkyne stretch.



Trial	Temperature (°C)	¹³ C-NMR signal (ppm)	FTIR signal (cm ⁻¹)
1	60	92.8	2150
2	90	92.8	2150
3	110	92.8	2150

Table 7: Sonogashira/cyclization reaction at elevated temperatures.

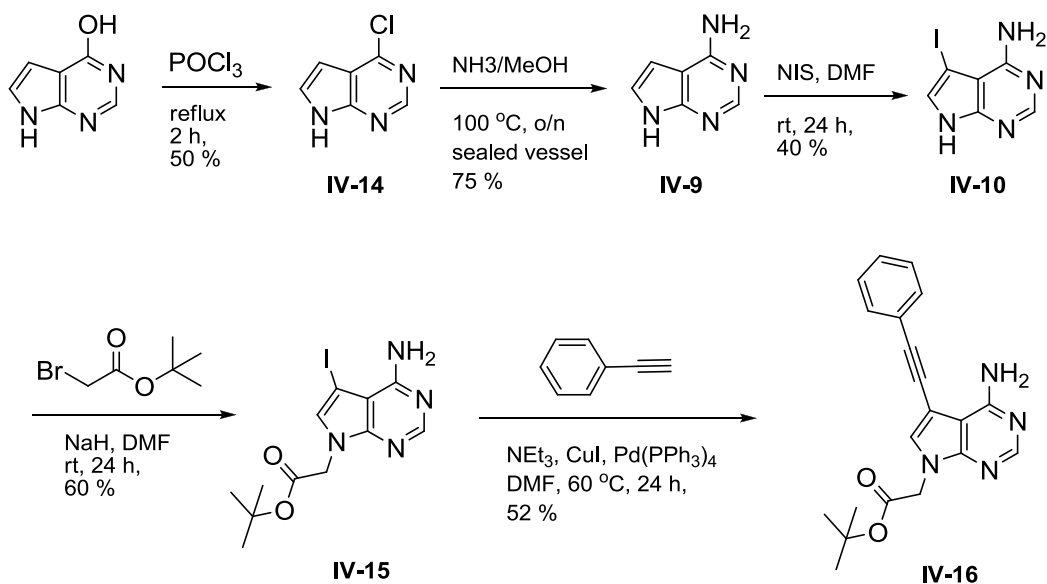
Since the problematic step was the cyclization reaction rather than the Sonogashira reaction, compound **IV-13** was used as the substrate for the cyclization reaction using greater equivalents of CuI (table 8).⁹ Unfortunately, carrying out the cyclization reaction with 30 mol % of CuI resulted in unreacted starting material. Furthermore, increasing the amount of CuI to 50 mol % and allowing the reaction to proceed for 48 hours at 80 °C proved to be detrimental. TLC analysis of the reaction mixture showed many spots including a spot corresponding to the unreacted starting material.



Trial	CuI (mol %)	Reaction time (h)	Result
1	30	24	Unreacted starting material
2	50	48	unreacted starting material + decomposition

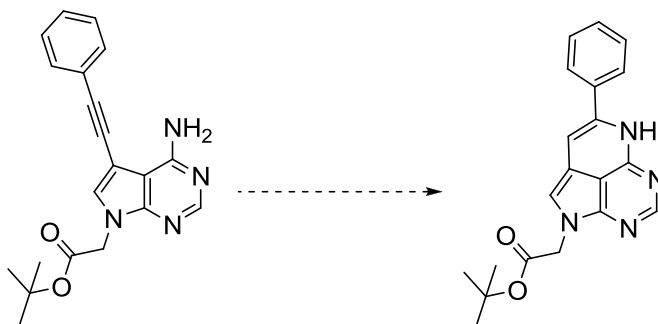
Table 8: Cyclization reaction attempts with increased amounts of CuI.

The initial synthesis towards a tricyclic adenine analog was quite lengthy and some steps proceeded in low yield. This led to the search for a more efficient route to access these compounds. The improved synthesis began with the chlorination of the commercially available starting material, 7-deaza-6-hydroxypurine, using POCl_3 ,¹⁰ which yielded compound **IV-14** in a modest but useful 50 % yield (scheme 14). Next, the exocyclic amino group was installed by treating compound **IV-14** with a saturated solution of ammonia in methanol to afford 7-deazaadenine in 75 % yield.¹¹ 7-deazaadenine was then iodinated at the 7-position by treatment with NIS in DMF ¹² to obtain the iodinated compound **IV-10** in 40 % yield. Compound **IV-10** was alkylated at *N*9 by treatment with NaH and *t*-butyl bromoacetate in DMF ⁷ to afford the desired compound **IV-15** in 60 % yield. Lastly the Sonogashira reaction was performed between compound **IV-15** and phenyl acetylene.¹ The catalyst system employed was $\text{Pd}(\text{PPh}_3)_4$ and CuI which gave rise to the cross coupled product compound **IV-16** in 52 % yield.



Scheme 14: A more efficient route towards a tricyclic adenine analog.

With the desired substrate in hand, the next step was to try the cyclization reaction with other alkynophilic metals such as silver¹³ and gold¹⁴ (table 9). Unfortunately, treating compound **IV-16** with silver nitrate and refluxing the reaction in acetone for eleven days resulted in unreacted starting material. Similarly, treatment of compound **IV-16** with auric acid and heating the reaction at 70 °C in ethanol for four days resulted in nothing more than the transesterification product.



Trial	Catalyst	Solvent	Temperature (°C)	Time (days)	Result
1	AgNO ₃	acetone	reflux	11	unreacted starting material
2	HAuCl ₄	ethanol	70	4	transesterification product was isolated

Table 9: Cyclization reaction attempts with AgNO₃ and HAuCl₄.

In order to explain the difficulty we experienced with this reaction, we turned to Baldwin's "Rules for Ring Closure".¹⁵ Baldwin stated that favored ring closures are expected "when the length and nature of linking chain enables the terminal atoms to achieve the required trajectories" for the final ring bond formation.¹⁵ In contrast, disfavored reactions require severe distortion in order to reach the optimal trajectories.¹⁵ The problematic cyclization step in the formation of the desired tricyclic adenine is hypothesized to proceed via a *6-endo-dig* cyclization. However, the difficulty we experienced with this cyclization suggests that the 7-deazaadenine scaffold does not allow the interacting atoms to achieve the required trajectories for the final ring bond formation to occur. Perhaps severe distortion of the substrate is required to reach these optimal trajectories and this ultimately leads to a disfavored reaction. However, the problem with this hypothesis is that Baldwin's rules are based on molecules with relatively low activation barriers, i.e. more flexible linkers. In our case, the 7-deazaadenine scaffold is quite rigid, thus Baldwin's rules may not be ideal for explaining the lack of reactivity we are experiencing with the 7-deazaadenine substrate.

Transition metal catalysis has become a very useful tool in organic synthesis. It allows for new synthetic transformations which were not previously possible by “classical” organic reactions. The activation of alkynes by late transition metal species toward nucleophilic attack is well known in the literature.¹⁶ In more detail, alkynes possess two orthogonal π -orbitals which can react with electrophilic metal centres.¹⁷ In the interaction with a metal centre, both the π -orbital in the plane of metal co-ordination and the π -orbital perpendicular to it are able to interact with the d-orbitals of the metal.¹⁷ This co-ordination withdraws electron density from the alkyne, thus making it more electrophilic and more susceptible to nucleophilic attack.¹⁷ For example, X-ray crystallographic studies on Cu(1)-alkyne complexes revealed that the π -electrons of the alkyne are strongly involved in the Cu(1) coordination, rendering the secondary carbon with a large partial positive charge.¹⁸ Thus, we hypothesize that the alkyne in our 7-deazaadenine substrate is being activated by the metal, however the exocyclic amino group is too far away to attack the activated alkyne.

In order to gain some insight into the distance between the nucleophile and electrophile, the equilibrium geometries for the 7-deazaadenine and cytidine substrates were studied computationally using DFT methods (B3LYP/6-31+G**) implemented by Spartan14 (Figure 19). The distance between the exocyclic nitrogen and the alkyne carbon in the 7-deazaadenine substrate was calculated to be 3.84 Å, whereas the distance between the exocyclic nitrogen and the alkyne carbon in the cytidine substrate was calculated to be 3.64 Å. Therefore, the nucleophile and electrophile are 0.2 Å further apart in the 7-deazaadenine substrate than in the cytidine substrate. This difference of 0.2 Å may be the reason behind the difficulty we experienced in cyclizing the 7-deazaadenine substrate.

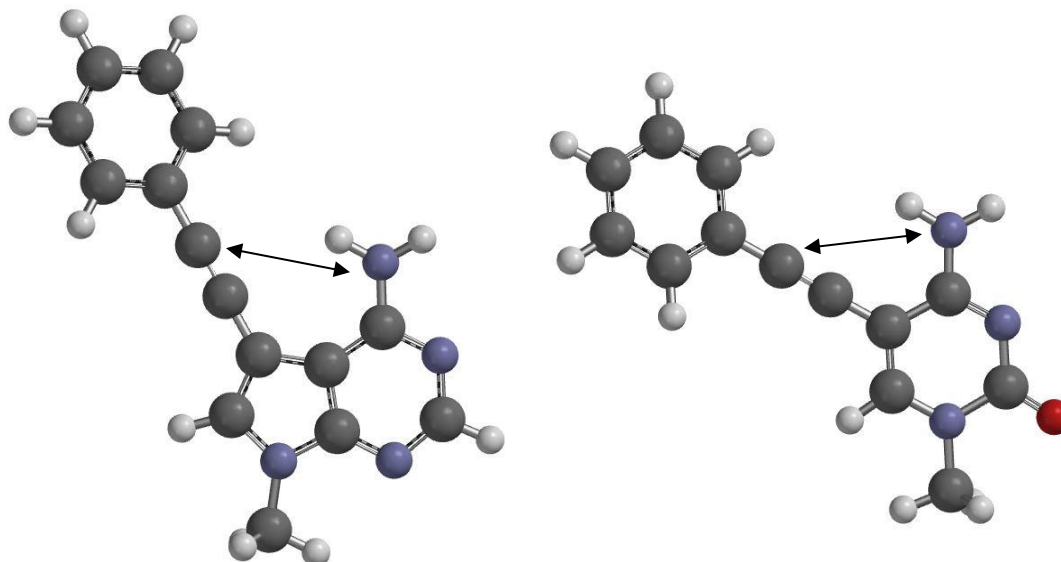
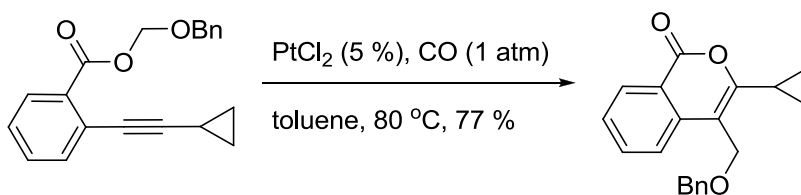


Figure 19: Equilibrium geometries of 7-deazaadenine and cytidine analog substrates for cyclization.

In addition, this type of reaction has not, to our knowledge been reported. However, an example of a slightly different system with similar atom spacing has been described¹⁹ (Scheme 15).



Scheme 15: Intramolecular carboalkoxylation catalyzed by PtCl_2 .

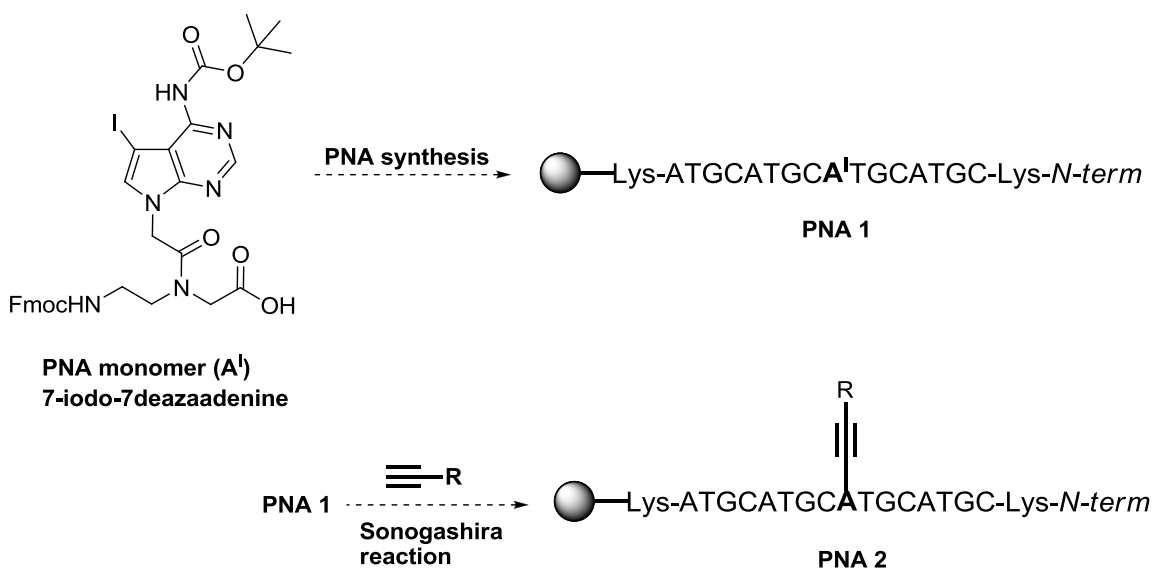
Although the functional groups of the benzoic acid ester starting material in Scheme 15 are different than our 7-deazaadenine substrate, the PtCl_2 catalyzed intramolecular cyclization may be an avenue worth exploring as a final attempt toward the tricyclic adenine analog.

4.3 Conclusion

The synthesis towards a novel tricyclic adenine analog was attempted by extending the substrate scope of the Sonogashira cross-coupling/heteroannulation chemistry developed in the Hudson group for cytidine analogs to adenine analogs. However, it was found that unlike the cytidine scaffold, the 7-deazaadenine substrate did not cyclize under the Sonogashira cross-coupling/heteroannulation reaction conditions to give a tricyclic adenine and the straight cross-coupled product was obtained in moderate yield. Efforts toward troubleshooting the Sonogashira/cyclization reaction on the 7-deazaadenine scaffold included carrying out the reaction at higher temperatures, attempting the cyclization reaction with greater equivalents of CuI and carrying out the cyclization reaction in the presence of other alkynophilic metals such as silver and gold. Unfortunately neither of these attempts produced the desired tricyclic adenine analog. DFT calculations revealed that the nucleophile and electrophile are 0.2 Å further apart in the 7-deazaadenine substrate than in the cytidine substrate. Based on the efficient activation of alkynes by late transition metal species toward nucleophilic attack, we postulate that the exocyclic amino group in our 7-deazaadenine substrate is too far away to attack the activated alkyne.

4.4 Future Work

For some time now, we have been interested in the post synthetic modification of PNA with fluorescent alkynes using the Sonogashira reaction (Scheme 16), to construct novel fluorescent PNAs and evaluate their potential for use as fluorescent probes. However, carrying out the on-resin Sonogashira reaction on the cytidine scaffold is problematic due to the propensity of the substrate toward cyclization. Characterization of the PNA will also be difficult since the molecular mass of the cyclized product and the uncyclized product is the same. In contrast, the 7-deazaadenine substrate is superior to the cytidine substrate for performing the on-resin Sonogashira reaction, since we established that the 7-deazaadenine substrate substituted at the 7-position with phenylacetylene does not undergo cyclization. Thus, using the 7-deazaadenine substrate for the on-resin Sonogashira reaction eliminates the uncertainty associated with whether or not the substrate has cyclized.



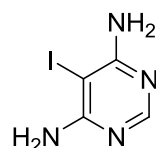
Scheme 16: Post synthetic modification of PNA with fluorescent alkynes via the Sonogashira reaction

There are many advantages associated with the post synthetic modification strategy. For instance, the number of synthetic steps as well as the amount of reagents required for the Sonogashira reaction is reduced. Moreover, upon successful incorporation of an appropriate PNA monomer into a PNA oligomer, the resin may be divided into portions

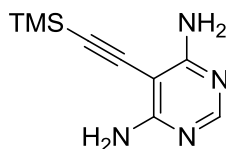
of three, for example, and the Sonogashira reaction can be carried out with three different fluorescent alkynes, thus giving rise to three novel fluorescent PNAs. The photophysical properties of these novel PNAs can then be evaluated for use as potential fluorescent probes to study nucleic acids.

4.5 Experimental

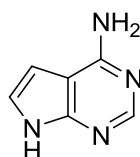
5-iodopyrimidine-4,6-diamine (**IV-7**):



4,6-Diaminopyrimidine hemisulfate monohydrate (3.8 g, 21.45 mmol) and K_2CO_3 (4.45 g, 32.2 mmol) were suspended in 58 mL of water followed by the addition of iodine (6.0 g, 23.6 mmol) and 14.5 mL of DMF. The solution was stirred at 45 °C for 24 hours. After cooling, a 2 M solution of $\text{Na}_2\text{S}_2\text{O}_3$ was added until the solution turned clear. The off-white solid was then collected by vacuum filtration and washed with water (3 x 10 mL). The product was dried under high vacuum to give compound **IV-7** in 81.3 % yield. ^1H -NMR (DMSO- d_6 , 400 MHz): δ 7.71 (s, 1H), 6.32 (bs, 4H). ^{13}C -NMR (DMSO- d_6 , 400 MHz): δ 162.9, 157.1, 55.3. HRMS (EI): calcd. For $\text{C}_4\text{H}_5\text{IN}_4$ $[\text{M}]^+$ 235.9559, found 235.9549.

5-((trimethylsilyl)ethynyl)pyrimidine-4,6-diamine (IV-8):

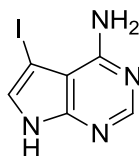
A 200 mL round bottom flask was charged with compound **IV-7** (1.0 g, 4.24 mmol), $(\text{Ph}_3\text{P})_2\text{PdCl}_2$ (89.3 mg, 0.127 mmol) and CuI (146.6 mg, 0.77 mmol) was evacuated and backfilled with nitrogen. Anhydrous DMF (40 mL) was then added to the reaction mixture followed by the addition of TMS-acetylene (1.2 mL, 8.48 mmol) and triethylamine (0.65 mL, 5.05 mmol) via syringe, under nitrogen. The reaction was heated at 60 °C for 2 hours. The solvent was removed in vacuo and the residue diluted with 120 mL of EtOAc. The organic layer was washed with 3 % EDTA solution (3 x 30 mL) and brine (3 x 30 mL). The organic layer was dried and concentrated in vacuo. The crude product was purified by FCC eluting with EtOAc:MeOH 100:0 to 85:15 to afford compound **IV-8** in 45 % yield. $^1\text{H-NMR}$ (DMSO-d_6 , 400 MHz): δ 7.83 (s, 1H), 6.41 (bs, 4H), 0.23 (s, 9H). $^{13}\text{C-NMR}$ (DMSO-d_6 , 400 MHz): δ 163.6, 156.5, 105.1, 97.3, 36.7, 0.1. HRMS (EI): calcd. For $\text{C}_9\text{H}_{14}\text{N}_4\text{Si}[\text{M}]^+$ 206.0988, found 206.0989.

7H-pyrrolo[2,3-d]pyrimidin-4-amine (IV-9):

To a suspension of compound **IV-8** (150 mg, 0.73 mmol) in NMP (1.4 mL), was added a suspension of *t*-BuOK (105.5 mg, 0.94 mmol), in NMP (4.2 mL) drop wise at 90 °C. The reaction mixture was stirred for 4 hours at 90 °C. After being cooled to room temperature the reaction mixture was neutralized with 1 M HCl and the remaining solvent was removed by vacuum distillation. The residue was purified via FCC eluting with CHCl_3 :MeOH 100:0 to 85:15 to give compound **IV-9** in 86 % yield. $^1\text{H-NMR}$ (DMSO-d_6 , 400 MHz): δ 11.44 (bs, 1H), 8.01 (s, 1H), 7.05 (s, 1H), 6.87 (bs, 2H), 6.49 (s, 1H).

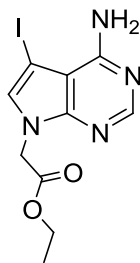
^{13}C -NMR (DMSO- d_6 , 400 MHz): δ 157.4, 151.6, 150.7, 120.8, 102.2, 98.9. HRMS (EI): calcd. For $\text{C}_6\text{H}_6\text{N}_4[\text{M}]^+$ 134.0592, found 134.0589.

5-iodo-7H-pyrrolo[2,3-d]pyrimidin-4-amine (IV-10):



Compound **IV-9** (150 mg, 1.12 mmol) was dissolved in 9.4 mL of DMF followed by the addition of NIS (290.7 mg, 1.12 mmol). The reaction was stirred in the dark, at room temperature overnight. Excess DMF was removed by rotary evaporation and the crude product was co-evaporated with toluene to remove trace amounts of DMF. The crude product was purified via FCC eluting with 5 % MeOH in CH_2Cl_2 to afford the iodinated compound **IV-10** in 40 % yield. ^1H -NMR (DMSO- d_6 , 400 MHz): δ 12.07 (bs, 1H), 8.09 (s, 1H), 7.39 (s, 1H), 6.69 (bs, 2H). ^{13}C -NMR (DMSO- d_6 , 400 MHz): δ 156.4, 150.9, 150.3, 127.1, 102.5, 50.4. HRMS (EI): calcd. For $\text{C}_6\text{H}_5\text{IN}_4[\text{M}]^+$ 259.9559, found 259.9549.

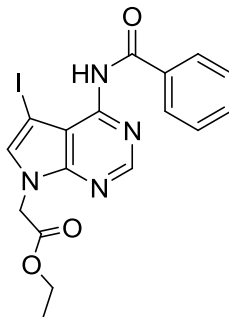
Ethyl 2-(4-amino-5-iodo-7H-pyrrolo[2,3-d]pyrimidin-7-yl)acetate (IV-11):



Under an atmosphere of nitrogen, compound **IV-10** (488 mg, 1.88 mmol) and NaH (60 % dispersion in mineral oil) (98 mg, 2.44 mmol) were suspended in 7.6 mL of DMF. The mixture was stirred for 30 minutes followed by the addition of ethyl bromoacetate. The reaction was left stirring for 24 hours. DMF was then removed by rotary evaporation and the crude product was purified via FCC eluting with EtOAc:Hexanes 50:50 to neat EtOAc to afford the desired compound **IV-11** in 60 % yield. ^1H -NMR (DMSO- d_6 , 600

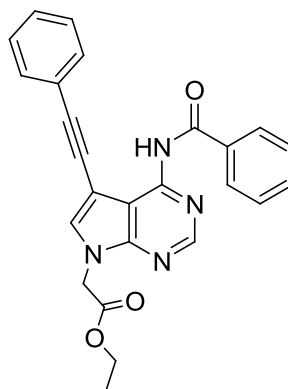
MHz): δ 8.08 (s, 1H), 7.42 (s, 1H), 6.64 (bs, 2H), 4.97 (s, 2H), 4.14 (qt, $J = 12$ Hz, 2H), 1.20 (t, $J = 6$ Hz, 3H). ^{13}C -NMR (DMSO- d_6 , 400 MHz): δ 168.3, 157.1, 152.0, 150.0, 130.2, 102.7, 61.1, 50.3, 45.1, 14.0. HRMS (EI): calcd. for $\text{C}_{10}\text{H}_{11}\text{IN}_4\text{O}_2[\text{M}]^+$ 345.9927, found 345.9924.

Ethyl 2-(4-benzamido-5-iodo-7H-pyrrolo[2,3-d]pyrimidin-7-yl)acetate (IV-12):

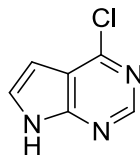


Under an atmosphere of nitrogen, compound **IV-11** (362 mg, 1.05 mmol), benzoic anhydride (950 mg, 4.2 mmol) and DMAP (13 mg, 0.105 mmol) were dissolved in 20 mL of acetonitrile. The reaction mixture was heated to 70 °C and left stirring for 8 hours. Acetonitrile was then removed by rotary evaporation and the crude product was purified via FCC eluting with EtOAc:Hexanes 20:80 to EtOAc:Hexanes 80:20 to afford the desired compound **IV-12** in 60 % yield. ^1H -NMR (DMSO- d_6 , 400 MHz): δ 10.87 (s, 1H), 8.70 (s, 1H), 8.08 (d, $J = 4$ Hz, 2H), 7.83 (s, 1H), 7.70 – 7.53 (m, 3H), 5.16 (s, 2H), 4.18 (m, 2H), 1.23 (m, 3H). HRMS (EI): calcd. for $\text{C}_{17}\text{H}_{15}\text{IN}_4\text{O}_3[\text{M}]^+$ 450.0189, found 450.0172.

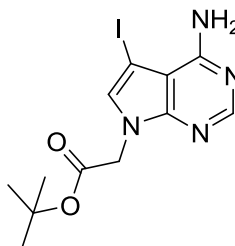
Ethyl 2-(4-benzamido-5-(phenylethynyl)-7H-pyrrolo[2,3-d]pyrimidin-7-yl)acetate (IV-13):



Compound **IV-12** (50 mg, 0.11 mmol) was dissolved in dry, deoxygenated DMF (1 mL) to which CuI (4.2 mg, 0.02 mmol), Et₃N (30 μ L, 0.22 mmol), phenylacetylene (36 μ L, 0.33 mmol) and Pd(PPh₃)₄ (13 mg, 0.01 mmol) were sequentially added. The reaction mixture was stirred in the dark at 60 °C for 24 hours. The solvent was removed in vacuo and the residue diluted with 15 mL of EtOAc. The organic layer was washed with 3 % EDTA solution (3 x 5 mL) and brine (3 x 5 mL). The organic layer was dried and concentrated in vacuo. The crude product was purified by FCC eluting with EtOAc:hexanes 30:70 to 70:30 to afford compound **IV-13** in 70 % yield. ¹H-NMR (CDCl₃, 400 MHz): δ 9.65 (bs, 1H), 8.83 (bs, 1H), 7.96 (m, 2H), 7.50 – 7.20 (m, 10 H), 5.05 (s, 2H), 4.28 (q, J = 8 Hz, 2H), 1.31 (t, J = 8 Hz, 3H). ¹³C-NMR (CDCl₃, 400 MHz): δ 167.4, 132.4, 131.8, 131.4, 128.9, 128.8, 128.5, 127.5, 122.1, 110.0, 92.8, 81.6, 62.2, 45.5, 14.1.

4-chloro-7H-pyrrolo[2,3-d]pyrimidine (IV-14):

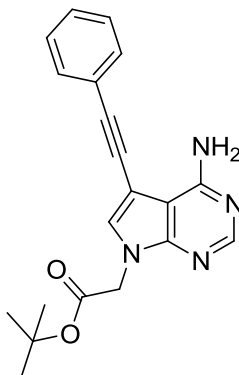
7-deaza-6-hydroxy purine (4.0160 g, 29.7 mmol) was suspended in 45 mL of POCl₃ and refluxed for 2 hours. The solution was cooled to room temperature and excess POCl₃ was removed by rotary evaporation. A mixture of dichloromethane (600 mL) and ice water (200 mL) was then added to the dark-brown residue and stirred for 24 hours, or until the dark-brown residue was completely dissolved. The aqueous layer was then neutralized by adding increments of a saturated sodium bicarbonate solution (3 × 300 mL). The organic layer was collected, dried over MgSO₄, and gravity filtered. The product was dried by rotary evaporation, producing a pale yellow solid (2.35 g, 52%). ¹H-NMR (DMSO-d₆, 400 MHz): δ = 12.57 (br s, 1H), 8.59 (s, 1H), 7.69 (d, *J* = 2.0 Hz, 1H), 6.61 (d, *J* = 2.0 Hz, 1H); ¹³C-NMR (DMSO-d₆, 400 MHz): δ = 151.7, 150.4, 150.3, 128.3, 116.5, 98.7. HRMS (EI): calcd. for C₆H₃ClN₃[M]⁺ 153.0094, found 153.0090.

tert-butyl 2-(4-amino-5-iodo-7H-pyrrolo[2,3-d]pyrimidin-7-yl)acetate (IV-15):

Under an atmosphere of nitrogen, compound **IV-10** (100 mg, 0.365 mmol) and NaH (60 % dispersion in mineral oil) (19 mg, 0.475 mmol) were suspended in 1.6 mL of DMF. The mixture was stirred for 30 minutes followed by the addition of *tert*-butyl bromoacetate. The reaction was left stirring for 21 hours. DMF was then removed by rotary evaporation and the crude product was purified via FCC eluting with EtOAc:Hexanes 10:90 to EtOAc:Hexanes 90:10 to afford the desired compound **IV-15** in 65 % yield. ¹H-NMR (DMSO-d₆, 400 MHz): δ 8.08 (s, 1H), 7.42 (s, 1H), 6.64 (bs, 2H),

4.86 (s, 2H), 1.41 (s, 9H). ^{13}C -NMR (DMSO- d_6 , 400 MHz): δ 167.3, 157.1, 151.9, 149.9, 130.3, 102.7, 81.7, 50.0, 45.7, 27.6.

***tert*-butyl 2-(4-amino-5-(phenylethynyl)-7H-pyrrolo[2,3-d]pyrimidin-7-yl)acetate (IV-16):**



Compound **IV-15** (216.5 mg, 0.58 mmol) was dissolved in dry, deoxygenated DMF (4.1 mL) to which CuI (22.1 mg, 0.12 mmol), Et₃N (0.15 mL, 1.16 mmol), phenylacetylene (0.19 mL, 1.74 mmol) and PdCl₂(PPh₃)₂ (41 mg, 0.058 mmol) were sequentially added. The reaction mixture was stirred in the dark at 60 °C for 24 hours. The solvent was removed in vacuo and the residue diluted with 15 mL of EtOAc. The organic layer was washed with 3 % EDTA solution (3 x 5 mL) and brine (3 x 5 mL). The organic layer was dried and concentrated in vacuo. The crude product was purified by FCC eluting with EtOAc:hexanes 60:40 to afford compound **IV-16** in 52 % yield. ^1H -NMR (CDCl₃, 600 MHz): δ 8.34 (bs, 1H), 7.53 (s, 2H), 7.38 (s, 2H), 5.93 (bs, 2H), 4.89 (s, 2H), 1.51 (s, 9H). ^{13}C -NMR (CDCl₃, 400 MHz): δ 166.9, 157.5, 153.0, 150.1, 131.2, 128.8, 128.5, 128.4, 122.9, 102.9, 95.8, 91.6, 83.0, 82.5, 46.1, 28.0.

4.6 References

- 1) Hudson, R. H. E.; Dambeniaks, A. K.; Viirre, R. D. *Synlett*. **2004**, 13, 2400.
- 2) Dierckx, A.; Miannay, F.A.; Wilhelmsson, L. M. *Chem. Eur. J.* **2012**, 18, 5987.
- 3) Buhr, C. A.; Matteucci, M. D.; Froehler, B. C. *Tetrahedron Lett.* **1999**, 40, 8969.
- 4) Mee, S. P. H.; Lee, V.; Baldwin, J. E. *Angew. Chem. Int. Ed.* **2004**, 43, 1132.
- 5) Minakawa, N.; Kawano, Y.; Murata, S.; Inoue, N.; Matsuda, A. *ChemBioChem*, **2008**, 9, 464.
- 6) Song, Y.; Ding, H.; Dou, Y.; Yang, R.; Sun, Q.; Xiao, Q.; Ju, Y. *Synthesis*. **2011**, 9, 1442.
- 7) Watanabe, T.; Hoshida, T.; Sakyō, J.; Kishi, M.; Tanabe, S.; Matsuura, J.; Akiyama, S.; Nakata, M.; Tanabe, Y.; Suzuki, A.Z.; Watanabe, S.; Furuta, T. *Org. Biomol. Chem.* **2014**, 12, 5089.
- 8) Wojciechowski, F. *Synthesis and Properties of Nucleic Acid Analogues*. Ph.D. Thesis, 2009.
- 9) Robins, M. J.; Barr, P. J. *J. Org. Chem.* **1983**, 48, 1854-1862.
- 10) Reigan, P.; Gbaj, A.; Stratford, I. J.; Bryce, R.A.; Freeman, S. *Eur. J. Med. Chem.* **2008**, 43, 1248.
- 11) Seela, F.; Xu, K. *Helv. Chim. Acta.* **2008**, 91, 1083.
- 12) Song, Y.; Ding, H.; Dou, Y.; Yang, R.; Sun, Q.; Xiao, Q.; Ju, Y. *Synthesis*. **2011**, 9, 1442.
- 13) (a) Aucagne, V.; Amblard, F.; Agrofoglio, L.A.; *Synlett*. **2004**, 13, 2406. (b) Moszynski, J.M.; Hudson, R.H.E. *Synlett*. **2006**, 18, 2997.
- 14) Noe, M.S.; Rios, A.C.; Tor, Y. *Org. Lett.* **2012**, 14, 3150.
- 15) (a) Baldwin, J.E. *J. Chem. Soc. Chem. Commun.* **1976**, 734. (b) Alabugin, I.V.; Gilmore, K.; Manoharan, M. *J. Am. Chem. Soc.* **2011**, 133, 12608.
- 16) Aubert, C.; Buisine, O.; Malacria, M. *Chem. Rev.* **2002**, 102, 813.
- 17) Hashmi, A. S. K. *Gold Bull.* **2003**, 36, 3.
- 18) Meldal, M.; Tornøe, C. W. *Chem. Rev.* **2008**, 108, 2952.
- 19) Furstner, A.; Davies, P. W.; *J. Am. Chem. Soc.* **2005**, 127, 15024.

Chapter 5

5 Synthesis and Study of Intrinsic Nucleobase Quenchers

5.1 Introduction

In 1996 Kramer and Tyagi reported their pioneering work on molecular beacons, which are probes that fluoresce upon hybridization to a target nucleic acid sequence.¹ Molecular beacons are single stranded nucleic acid molecules that possess a stem and loop structure (Figure 20).¹ In more detail, the loop region of the molecule is a probe sequence that is complementary to a predetermined sequence in a target nucleic acid. The stem portion of the molecule is formed by the annealing of two complementary arm sequences that are on either side of the probe sequence. A fluorescent moiety is attached to the end of one arm and a fluorescence quencher is attached to the end of the other arm. The stem region of the molecule keeps these two moieties in close proximity to each other, causing the emission from the fluorophore to be quenched by FRET. Upon hybridization with a target sequence, the probe forms a hybrid that is longer and more stable than the hybrid formed by the arm sequences. This conformational transformation forces the arm sequences apart and causes the fluorophore and quencher to become spatially resolved. Since the fluorophore and quencher are no longer in close proximity to each other, emission from the fluorophore is observed upon irradiation with UV light. Molecular beacons are highly specific, even a single base pair mismatch results in no hybridization to the target sequence and thus no emission from the fluorophore.¹ To that end, molecular beacons are useful probes for the detection of single nucleotide polymorphisms (SNPs).²

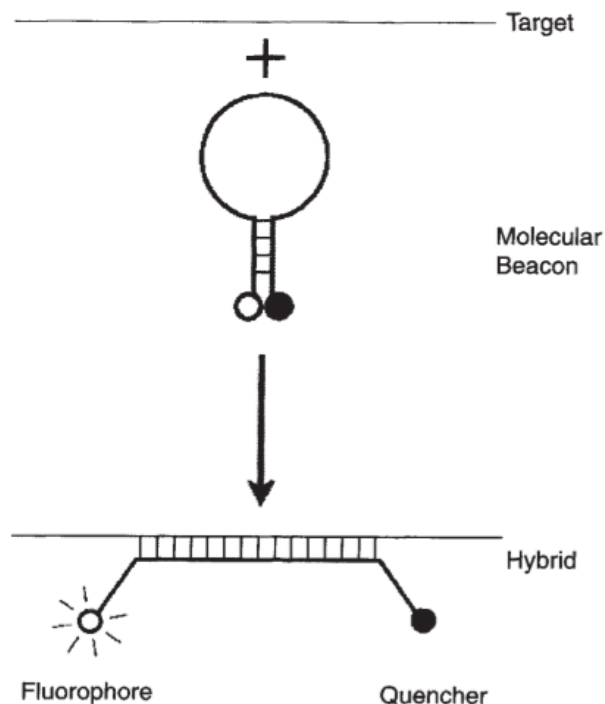


Figure 20: Structure and principle of operation of molecular beacons.

Traditionally, fluorescence quenchers are tethered to the end of an oligonucleotide strand because incorporating them in any other position will interfere with base pairing and thus decrease duplex stability.¹ Moreover, in their seminal publication on molecular beacons, Kramer and Tyagi suggest that the quenching efficiency can be increased by shortening the linkers to which the quencher and fluorophore are attached.¹ Furthermore the authors hinted towards an optimized molecular beacon structure where the fluorophore and quencher are linked to nucleotides that are located within the arm sequences to reduce the effects of unraveling of the stem region.¹

In 2000, Seitz developed a novel stemless PNA molecular beacon to detect the hybridization event.³ The author exploited the fact that unhybridized PNA forms intra- or intermolecular associates of unknown structure due to base stacking.⁴ Moreover, he proposed that a fluorophore and quencher appended to the unhybridized PNA would be positioned in close proximity to each other. In analogy to the DNA-based molecular beacons reported by Kramer and Tyagi, emission from the fluorophore is quenched by

FRET. Hybridization with a complementary nucleic acid sequence should induce a structural rearrangement whereby the fluorophore and quencher are no longer in close proximity to each other and emission from the fluorophore is observed upon irradiation with UV light.

The author synthesized **PNA-11** (Figure 21), via fluorenylmethyloxycarbonyl (Fmoc)-based solid-phase synthesis using benzhydryloxycarbonyl (Bhoc) and *tert*-butyloxycarbonyl (Boc)-nucleobase protection. The on-resin labelling was accomplished by treating the deprotected PNA with DABCYL hydroxysuccinimide ester to attach the DABCYL group to the primary amino group of the *N*⁶-aminoalkyl modified adenine.³ The EDANS group was attached to the thiol group of the cysteine via selective alkylation with 5-(2'-iodoacetamidoethyl)amino-naphthalene sulfonic acid (IEDANS).³



Figure 21: Structure of PNA-11.

Upon treatment with an unrelated DNA sequence containing six mismatches, there was no significant change in the emission spectrum of **PNA-11**.³ However, upon hybridization with a complementary DNA target, the emission of the EDANS group in **PNA-11** was enhanced by a factor of 4.6 at 25 °C and 6.4 at 20 °C respectively.³ Thus, the author developed a novel stemless PNA molecular beacon for detection of the hybridization event. It should be highlighted that target-unrelated arm sequences were not required for maintaining the structural integrity of these probes.

This chapter focuses on the synthesis, quenching studies and attempted oligomerization of a novel intrinsic fluorescence quencher, 5-(4-dimethylaminophenyl)azouridine which incorporates the key structural feature of the universal quencher DABCYL (Figure 22). The advantage of synthesizing a base pairing competent quencher is that it can be incorporated anywhere in an oligonucleotide strand and should not compromise duplex

stability. Moreover, since we can incorporate this intrinsic quencher into the stem region of molecular beacons, more accurate FRET measurements can be obtained compared to traditional molecular beacon constructs where the quencher is attached via a long linker.

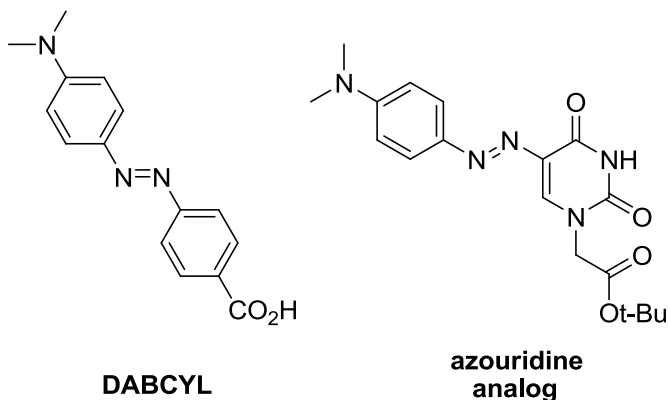
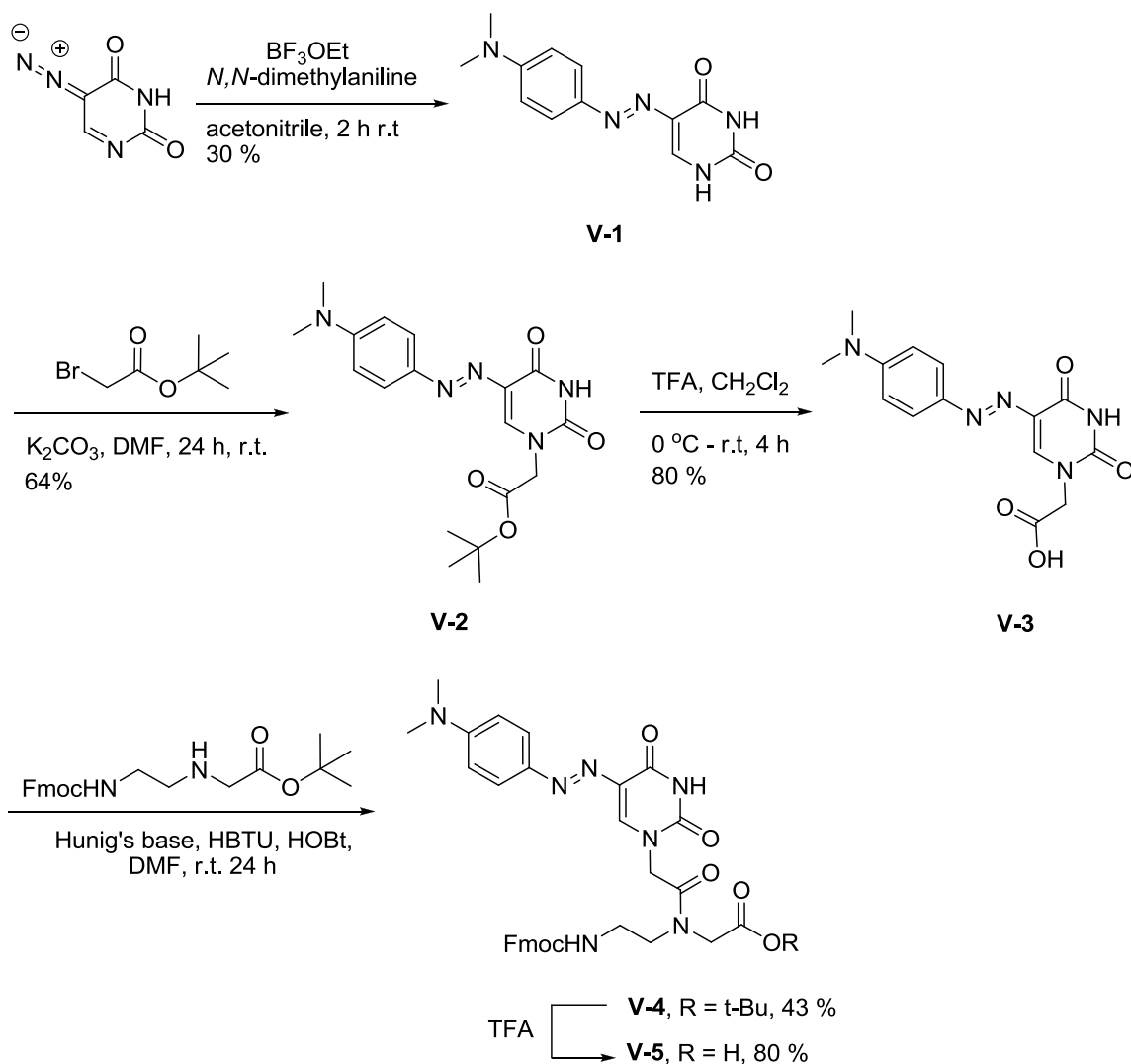


Figure 22: Azouridine analog capable of Watson/Crick base pairing.

5.2 Results and Discussion

Synthesis of 5-(4-dimethylamino-phenyl)azouridine began with an azo coupling reaction between 5-diazouracil⁵ and *N,N*-dimethylaniline in the presence of the Lewis acid boron trifluoride diethyl etherate⁶ to afford compound **V-1** in 30 % yield (Scheme 17). Compound **V-1** was then alkylated at *N1* using potassium carbonate and *t*-butylbromoacetate to obtain compound **V-2** in 64 % yield.⁷ Ester **V-2** was deprotected with TFA to afford the carboxylic acid, compound **V-3** in 80 % yield. Next, compound **V-3** was coupled onto an Fmoc protected peptide nucleic acid (PNA) backbone using HBTU to yield compound **V-4** in 43 % yield. Lastly compound **V-4** was deprotected with TFA to yield compound **V-5**, a monomer suitable for incorporation into a PNA oligomer.



Scheme 17: Synthesis of azouridine analog.

5.2.1 Spectroscopic Properties of Compound V-2

Compound **V-2** exhibits an absorption maximum at 453 nm in EtOH. The molar absorptivity of compound **V-2** in EtOH at 453 nm was calculated to be $27500 \text{ M}^{-1} \text{ cm}^{-1}$. DABCYL exhibits an absorption maximum at 450 nm in EtOH. The molar absorptivity of DABCYL in EtOH at 450 nm is $32000 \text{ M}^{-1} \text{ cm}^{-1}$. Thus compound **V-2** exhibits spectroscopic properties similar to DABCYL and gave us confidence that it will act as an intrinsic fluorescence quencher.

5.2.2 Quenching Studies

In order to determine viable FRET pairs for use in molecular beacon constructs, fluorescence quenching experiments were performed between compound **V-2** and the fluorophores phenylpyrroloctidine (pC), and pyrene. These fluorophores were chosen because their emission spectra overlapped with the absorption spectrum of compound **V-2**.

Thus, a 1 μM solution of the fluorophore phenylpyrroloctidine in EtOH was quenched with varying concentrations of the azouridine analog, compound **V-2**. Figure 23 clearly illustrates a decrease in fluorescence emission from the pC fluorophore with increasing concentrations of quencher. Similarly, a 1 μM solution of pyrene in EtOH was quenched with varying concentrations of azouridine analog **V-2**. Figure 24 also shows a decrease in fluorescence emission from the fluorophore with increasing concentrations of quencher.

Stern-Volmer plots were constructed and the Stern-Volmer quenching constant, K_{sv} , was calculated for each fluorophore quencher pair. The K_{sv} value for the quenching of pC with compound **V-2** was found to be approximately 16000 M^{-1} (Figure 25). The K_{sv} value for the quenching of pyrene with compound **V-2** was found to be approximately 8600 M^{-1} (Figure 26). Fundamentally, the K_{sv} value indicates the sensitivity of a fluorophore to a quencher.⁸ Thus, our K_{sv} values suggest that pC is more sensitive to quenching from compound **V-2** than pyrene. Moreover, the inverse of the Stern-Volmer quenching constant, K_{sv}^{-1} , is the concentration of the quencher at which 50 % of the intensity of the fluorophore is quenched. The K_{sv}^{-1} value for the quenching of pC with compound **V-2** was determined to be $6.25 \times 10^{-5} \text{ M}$. The K_{sv}^{-1} value for the quenching of pyrene with compound **V-2** was determined to be $1.16 \times 10^{-4} \text{ M}$. These values suggest that pC is quenched more efficiently by compound **V-2** than pyrene, since less concentration of the quencher is necessary to obtain the same amount of quenching. Thus compound **V-2** and pC act as a better FRET pair than compound **V-2** and pyrene.

Lastly, K_{sv} is the product of the bimolecular quenching constant, k_q , and the unquenched fluorescence lifetime, τ_0 . Thus, a k_q value for the quenching of pyrene with compound **V-2** was calculated from the K_{sv} value, 8600 M^{-1} , and the unquenched fluorescence lifetime

of pyrene, 410×10^{-9} seconds.⁹ The k_q value for the quenching of pyrene with compound **V-2** was calculated to be approximately $2.10 \times 10^{10} \text{ M}^{-1}\text{s}^{-1}$. Unfortunately, since the fluorescence lifetime of pC is not known, a k_q value for the quenching of pC with compound **V-2** was not calculated.

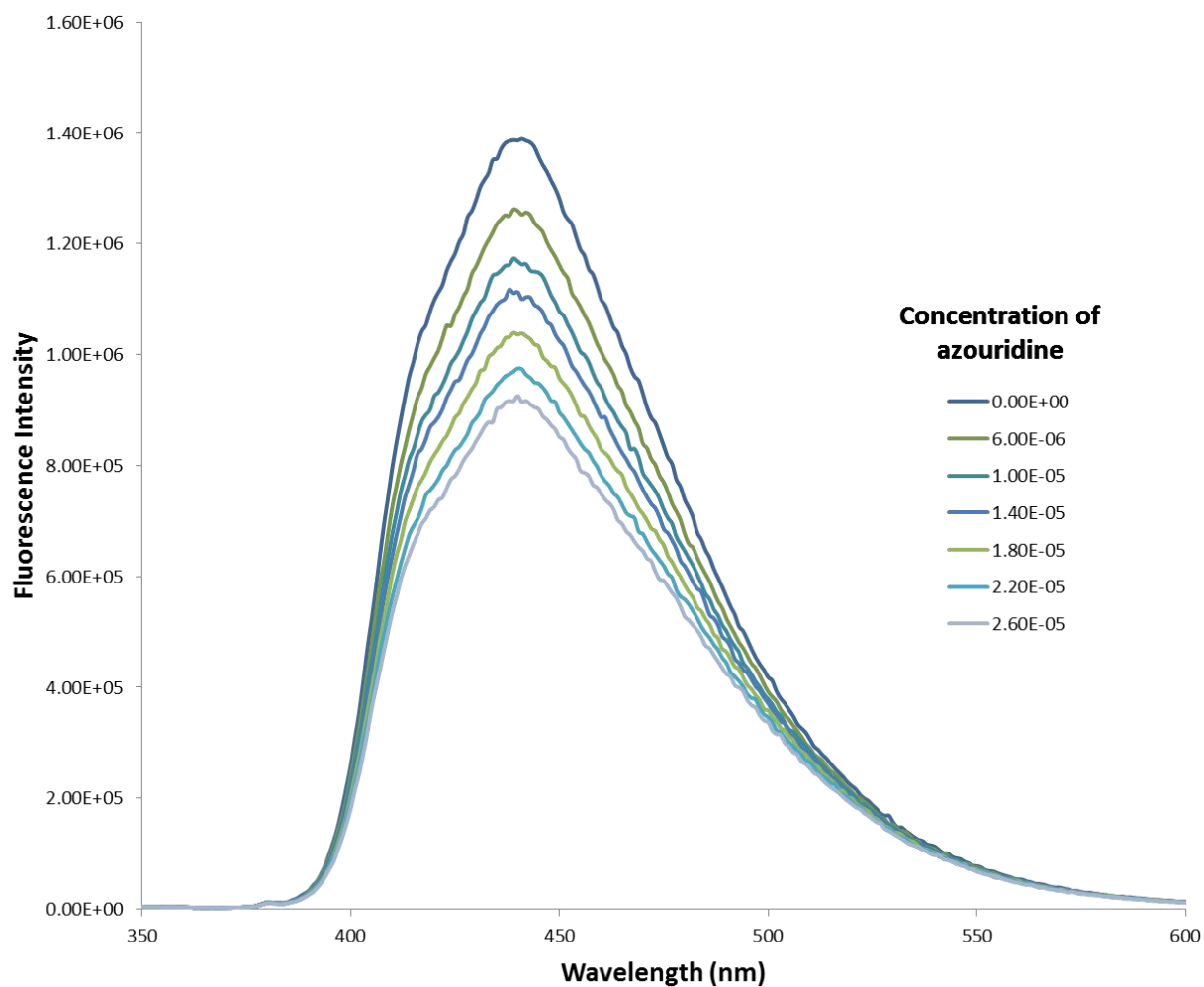


Figure 23: Quenching spectra of pC with azouridine analog V-2.

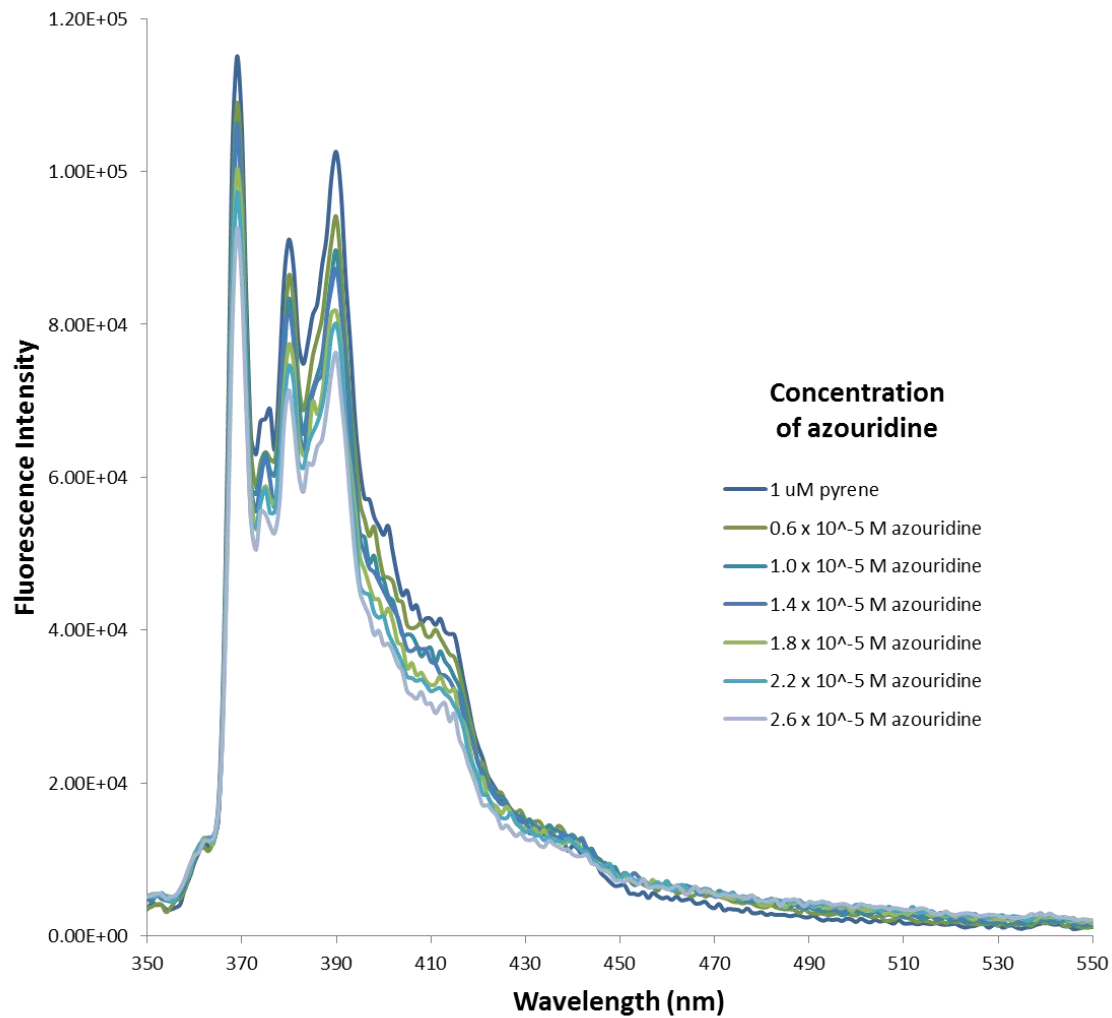


Figure 24: Quenching spectra of pyrene with azouridine analog V-2.

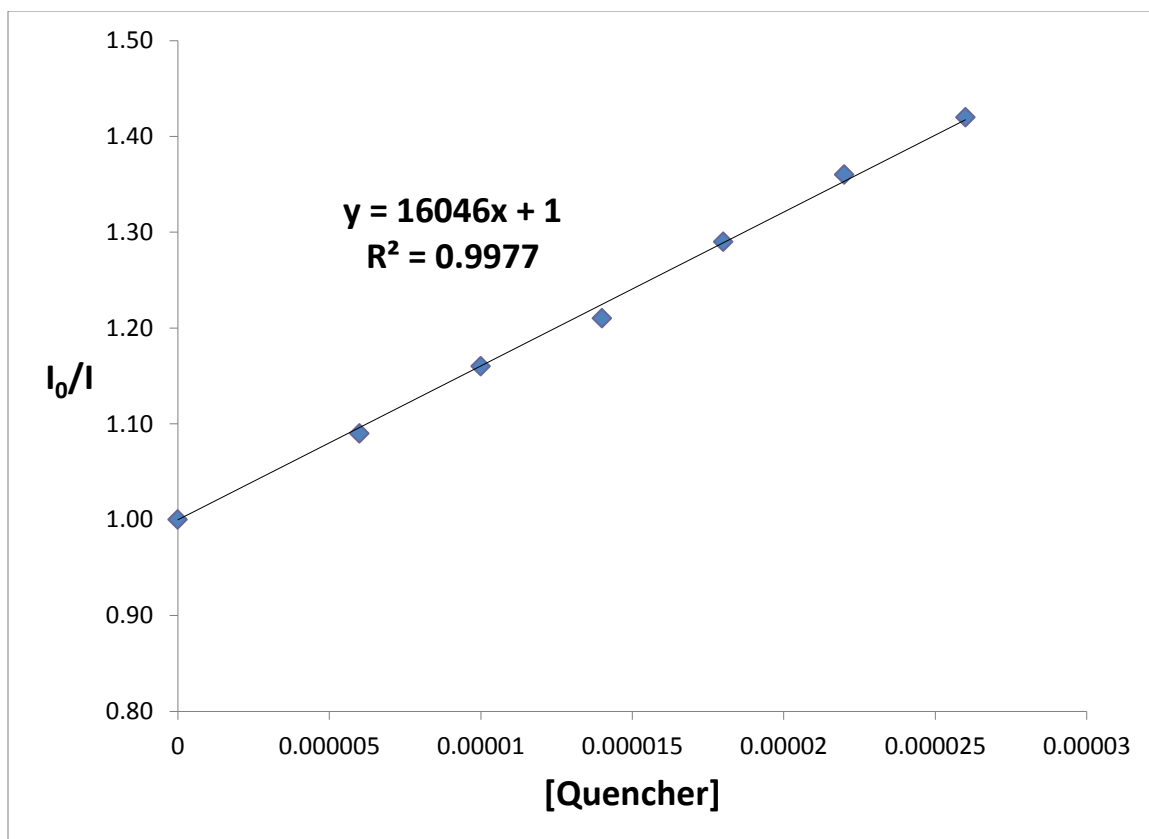


Figure 25: Stern-Volmer plot for the quenching of pC in EtOH by compound V-2.

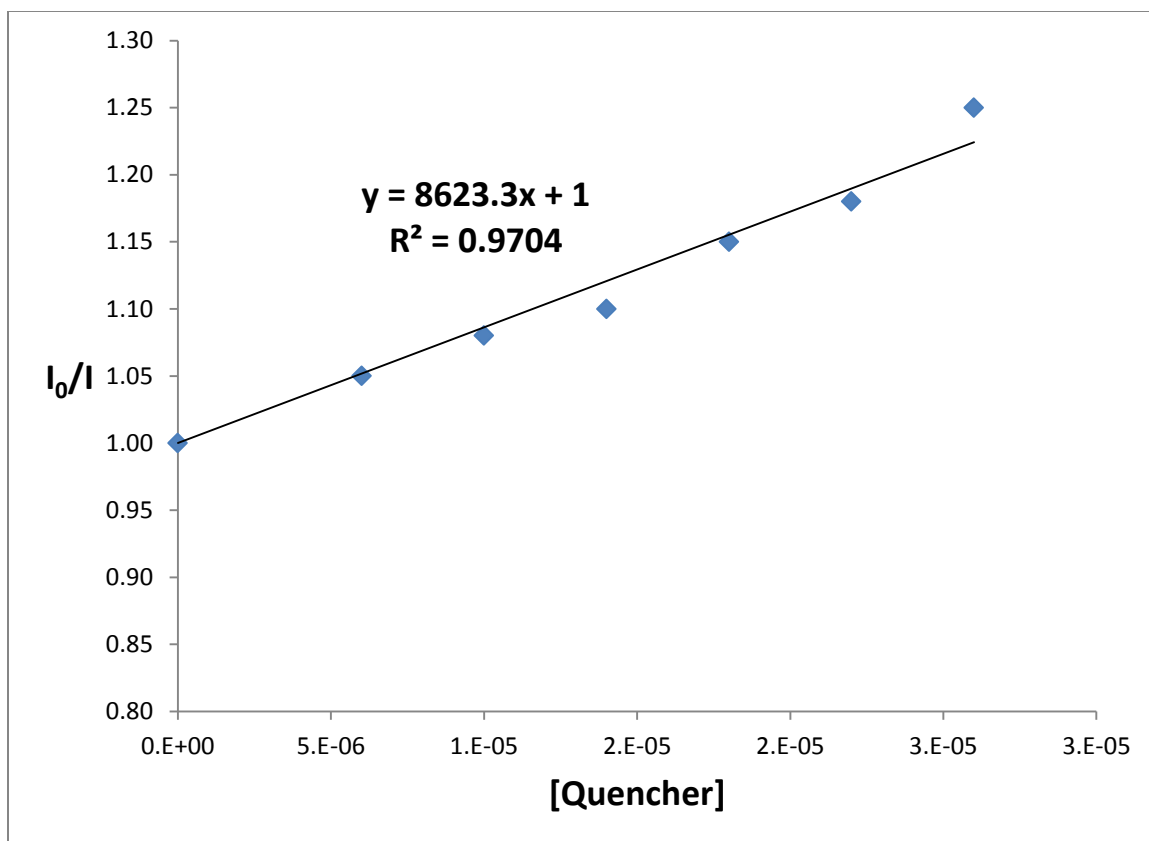


Figure 26: Stern-Volmer plot for the quenching of pyrene in EtOH by V-2.

5.2.3 Efforts Toward PNA Oligomerization

Initially we set out to synthesize the stemless PNA molecular beacon *C-terminus*-Lys-**pC**-TTA-TTA-TTA-TTU^{azo}-Lys-*N-terminus*. The chemical structures of **pC** and **U^{azo}** are shown in Figure 27. PNA synthesis was attempted with the assistance of an automated synthesizer on the 5 μ mol scale using manufacturer supplied cycles for fluorenylmethyloxycarbonyl (Fmoc)-based oligomerization with *tert*-butyloxycarbonyl (Boc)-nucleobase protection.¹⁰ Upon completion of the synthesis, the Fmoc protecting group was removed from the *N*-terminal lysine and the PNA was cleaved from the resin according to previously reported procedures.¹¹ The crude PNA was then subjected to purification by reversed-phase HPLC. Unfortunately, the custom monomer, **U^{azo}**, was not successfully incorporated into **PNA-1** as shown from the HPLC chromatograms in Figure 28. Moreover, the UV-visible spectrum of the peak with a retention time of 36 min in the HPLC chromatograms shows characteristic absorbances at 263.9 and 363.5 nm for the

nucleobases and pC fluorophore respectively, however it lacks the absorbance at 450 nm which is indicative of the azo moiety (figure 29).

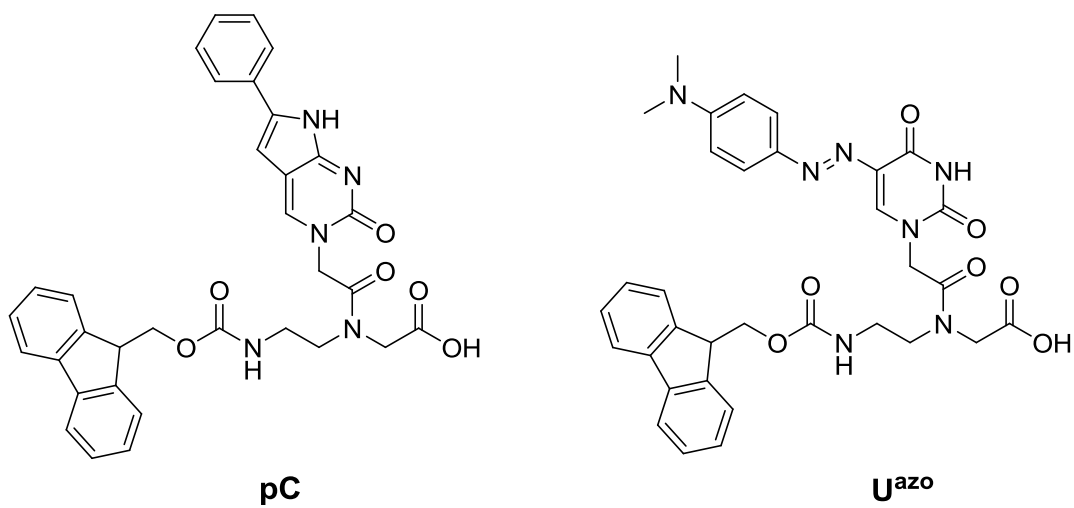


Figure 27: Chemical structures of PNA monomers pC and U^{azo}.

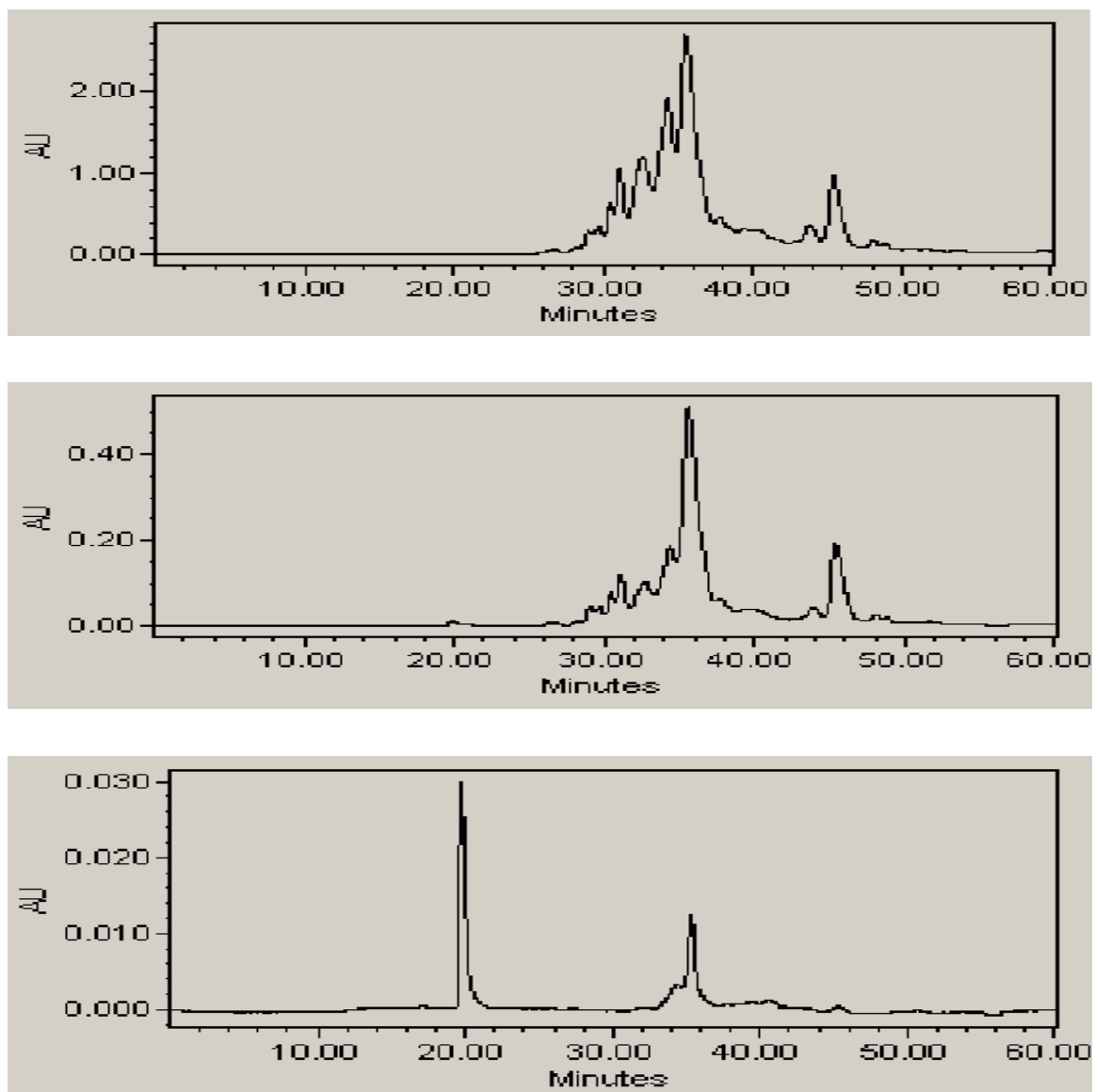


Figure 28: HPLC chromatograms of PNA-1 at 260 nm (top), 360 nm (middle) and 450 nm (bottom).

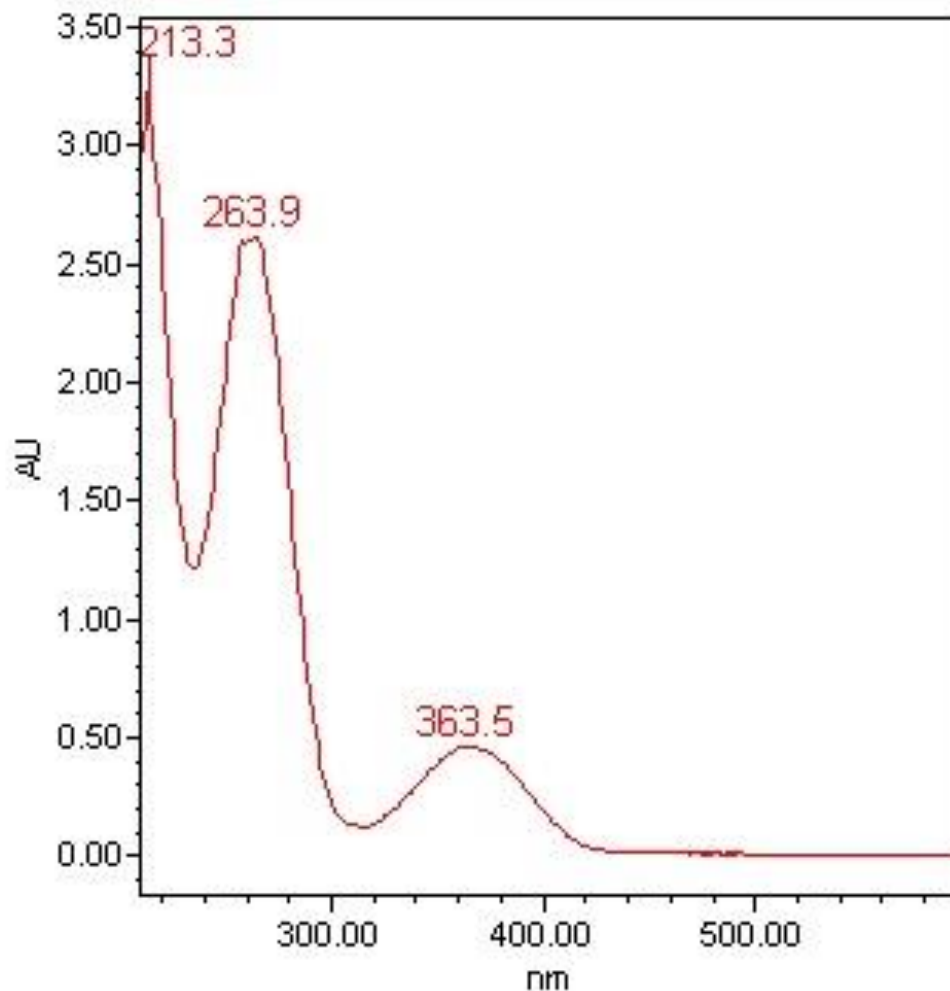


Figure 29: UV-visible spectrum of peak with 36 min retention time in HPLC chromatogram.

Our results suggested that the amide coupling reaction of U^{azo} onto the PNA was the problematic step. Thus, we decided to synthesize a separate PNA sequence on the peptide synthesizer and attempt the coupling reaction of U^{azo} onto the PNA manually in order to troubleshoot the reaction. To that end, PNA-2 (*C-terminus*-Lys-**pC**-TGT-CAC-TTC-CTT-Fmoc-*N-terminus*), was synthesized as described for PNA-1.¹⁰ A small amount of crude PNA-2, approximately 5 mg, was cleaved from the resin and analyzed by mass spectrometry; HR-MS (ESI) m/z : calcd. for $\text{C}_{167}\text{H}_{204}\text{N}_{66}\text{O}_{47}$: 3885.7; found: 3889.8 $[\text{M} + \text{H}]^+$.

Initial attempts at troubleshooting the amide coupling involved carrying out the reaction using a 1:1 mixture of DMF/DMSO as the solvent system (Table 10, trial 1). Our rationale for using DMSO as a co-solvent was based on a report that DMSO is a powerful dissociating solvent which is used to mitigate the potential aggregation of peptides during solid-phase peptide synthesis.¹² After allowing the reaction to proceed for 1.5 h, 5 mg of resin was taken and the PNA was cleaved from the resin according to previously reported procedures.¹¹ The crude PNA was then analyzed by UPLC, UV-visible spectroscopy and mass spectrometry. Unfortunately, the custom monomer, **U^{azo}**, was not successfully incorporated into **PNA-2** as shown from the UPLC traces in Figure 30. Moreover, the UV-visible spectrum of the peak with a retention time of 3.7 min in the UPLC trace shows characteristic absorbances at 260 and 360 nm for the nucleobases and pC fluorophore respectively, however it lacks the absorbance at 450 nm which is indicative of the azo moiety (Figure 31). The reaction was also attempted in neat DMSO at room temperature and at 80 °C (table 10, trials 2 and 3). Similarly, analysis by UPLC, UV-visible spectroscopy and mass spectrometry revealed that the coupling reaction was still not successful.

$$\text{Resin-KCpTGTCACTTCCTT-NH}_2 \xrightarrow[\text{DIPEA (10 eq)}]{\text{U}^{\text{azo}} \text{ (5 eq)}, \text{HATU (5 eq)}} \text{Resin-KCpTGTCACTTCCTT-U}^{\text{azo}}$$

trial	solvent	temperature	time	result
1	DMF/DMSO	rt	1.5 h	U^{azo} not incorporated
2	DMSO	rt	1.5 h	U^{azo} not incorporated
3	DMSO	80 °C	1.5 h	U^{azo} not incorporated

Table 10: Attempts at troubleshooting the **U^{azo} coupling reaction.**

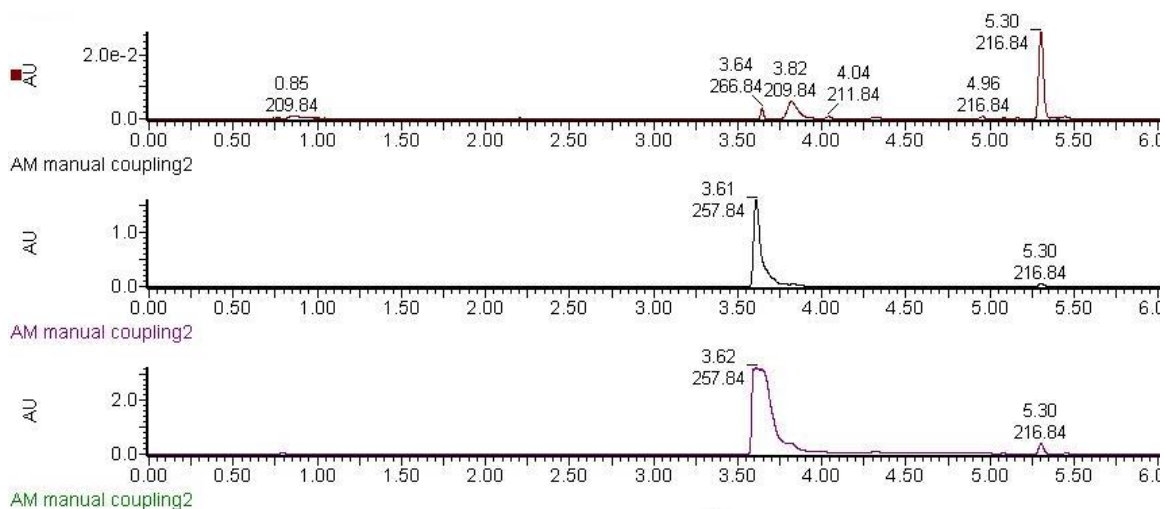


Figure 30: UPLC chromatograms of PNA-2 at 450 nm (top), 360 nm (middle) and 260 nm (bottom).

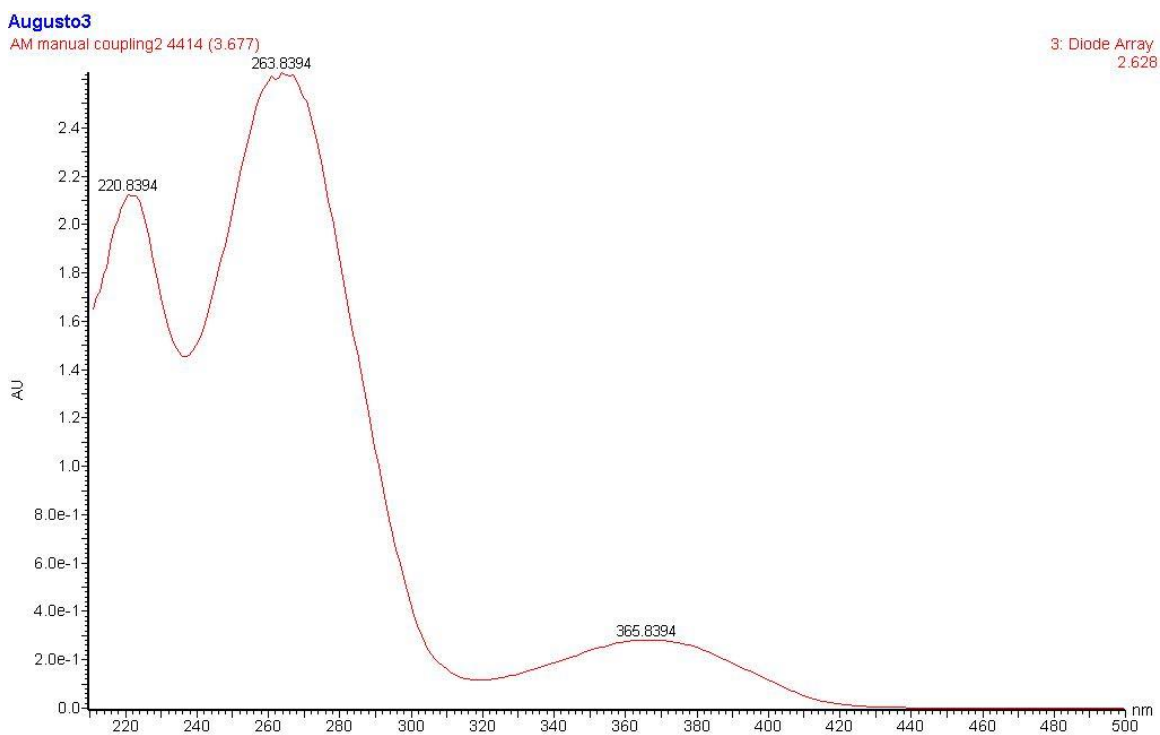
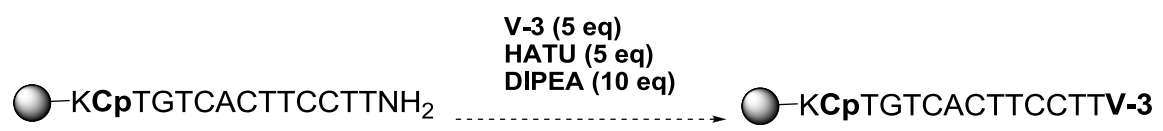


Figure 31: UV-visible spectrum of peak with 3.6 min retention time in UPLC chromatogram.

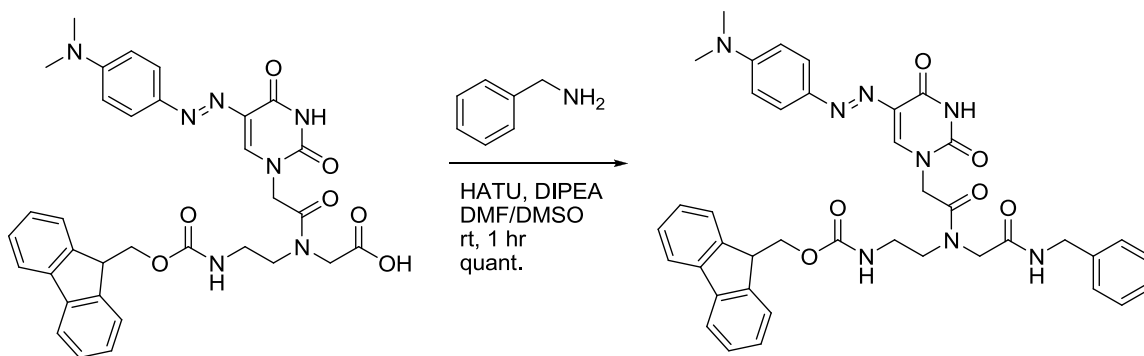
Since the on-resin amide coupling reaction of the U^{azo} PNA monomer onto PNA-2 was problematic, it was thought that perhaps coupling the azo acetic acid derivative, compound **V-3**, onto PNA-2 would be more facile. Unfortunately, carrying out the coupling reaction between the resin-bound PNA-2 and compound **V-3** using HATU, DIPEA and DMF as a solvent, at room temperature for 1.5 hours did not result in incorporation of compound **V-3** (Table 11, trial 1). Similarly, allowing the coupling reaction to proceed for 24 hours while keeping all other reaction conditions constant also resulted in an unsuccessful reaction (Table 11, trial 2). Lastly, the coupling reaction was also attempted using microwave irradiation at 75 °C for 5 minutes,¹³ however compound **V-3** was still not incorporated into PNA-2 (Table 11, trial 3).



trial	solvent	temperature	time	result
1	DMF	rt	1.5 h	V-3 not incorporated
2	DMF	rt	24 h	V-3 not incorporated
3	DMF	MW, 75 °C	5 min	V-3 not incorporated

Table 11: Attempts at troubleshooting the coupling reaction between PNA-2 and compound V-3.

The fact that we can couple compound **V-3** to an Fmoc protected PNA backbone in solution (Scheme 17), suggests that the difficulty we are experiencing is due to the amide coupling reaction being carried out on the resin. Moreover, U^{azo} was successfully coupled with benzylamine in solution (Scheme 18). Thus, the problem seems to arise from the on-resin nature of the reaction.



Scheme 18: Amide coupling between U^{azo} monomer and benzylamine in solution.

Successful solid-phase peptide syntheses are often hampered by aggregation of the growing peptide chain due to secondary structure formation during synthesis, interchain or intrachain association via hydrogen bonding or hydrophobic interactions, and peptide-polymer matrix association.¹⁴ This results in a hindered amino terminus which ultimately results in reduced coupling and deprotection efficiencies.¹⁴ Our rationale for choosing the cross-linked ethoxylate acrylate resin (CLEAR), was to mitigate any peptide-polymer matrix association.¹⁵ Moreover, our relatively low resin loading (0.05 mmol/g) should have ruled out the possibility of interchain aggregation.¹⁴ Initially, we hypothesized that perhaps intrachain aggregation via hydrogen bonding or hydrophobic interactions was responsible for the unsuccessful amide coupling reaction. However, when we attempted to couple U^{azo} onto the *C-terminus* of the PNA rather than the *N-terminus*, the reaction was still not successful. Thus, we can postulate that the difficulty we experienced with this reaction stems from a physical attraction of the U^{azo} monomer to the CLEAR resin, which ultimately hinders its ability to undergo the amide coupling.

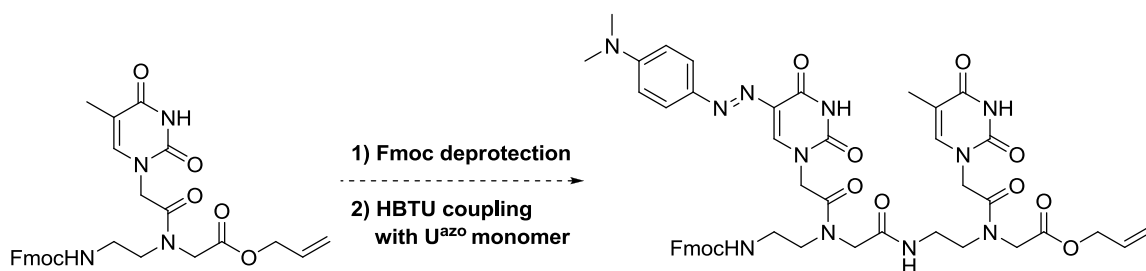
5.3 Conclusions

An intrinsic nucleobase quencher was synthesized via the azo coupling reaction between 5-diazouracil and *N,N*-dimethylaniline. The spectroscopic properties of this compound were found to be similar to those of the universal quencher DABCYL. In order to determine viable FRET pairs for use in molecular beacons, fluorescence quenching experiments were performed between compound **V-2** and the fluorophores

phenylpyrrolocytidine (pC), and pyrene. Stern-Volmer plots were constructed and the Stern-Volmer quenching constant, K_{sv} , was calculated for each fluorophore quencher pair. The K_{sv} values suggest that pC is more sensitive to quenching from compound **V-2** than pyrene. Moreover, the inverse of the Stern-Volmer quenching constant, K_{sv}^{-1} , was calculated for each fluorophore quencher pair. The K_{sv}^{-1} values suggest that pC is quenched more efficiently by compound **V-2** than pyrene. Thus, compound **V-2** and pC act as a better FRET pair than compound **V-2** and pyrene. Lastly, The k_q value for the quenching of pyrene with compound **V-2** was calculated to be approximately $2.10 \times 10^{10} \text{ M}^{-1}\text{s}^{-1}$. Incorporation of the custom monomer U^{azo} into a PNA oligomer proved to be problematic. Our results suggested that the amide coupling reaction of U^{azo} onto the PNA was the problematic step. Unfortunately, various attempts at troubleshooting this reaction were not successful. We postulate that the problematic coupling reaction stems from a physical attraction between the U^{azo} monomer and the CLEAR resin.

5.4 Future Work

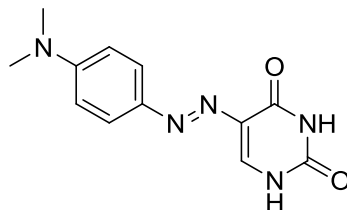
An alternate route to mitigate difficult on resin amide couplings involves carrying out the reaction in solution to form a dimer, followed by on-resin amide coupling of the dimer onto the PNA. Thus, we propose to synthesize a thymine- U^{azo} dimer (Scheme 19) and, upon deprotection of the allyl ester protecting group, attempt the incorporation of this dimer into a PNA oligomer. Upon successful incorporation of the thymine- U^{azo} dimer into a PNA oligomer, the photophysical properties of the PNA can be investigated for potential use as a stemless molecular beacon.



Scheme 19: Proposed synthesis of a thymine- U^{azo} dimer.

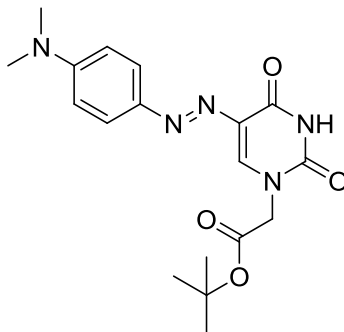
5.5 Experimental

5-((4-(dimethylamino)phenyl)diazenyl)pyrimidine-2,4(1H,3H)-dione (V-1):



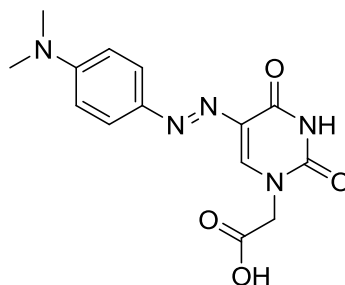
To a cold solution of 5-aminouracil (3.00 g, 23.6 mmol) in 45 mL of 1 M HCl was added a solution of 6.9 % NaNO₂ (26 mL) drop wise over 15 minutes. The reaction mixture was stirred for another 45 minutes on ice, filtered, washed with water and hexanes and dried under vacuum to give 5-diazouracil in 81 % yield, which was used in the next step without further purification. 5-diazouracil (3.00 g, 19.2 mmol) was suspended in 210 mL of anhydrous acetonitrile. The reaction was purged with nitrogen for 5 minutes followed by the slow dropwise addition of borontrifluoride diethyl etherate (2.4 mL, 19.2 mmol). The reaction was stirred for 20 minutes at room temperature followed by the addition of *N,N*-dimethylaniline (2.4 mL, 19.2 mmol). The reaction mixture was stirred at room temperature overnight and the crude product was collected by vacuum filtration. The crude product was triturated in 200 mL of boiling ethanol for 1.5 hours and filtered once again to afford compound **V-1** in 30 % yield. Compound **V-1** was used without further purification. ¹H-NMR (DMSO-d₆, 400 MHz): δ 11.46 (s, 1H), 11.32 (s, 1H), 7.72-7.66 (m, 1H), 7.65-7.59 (m, 2H), 6.83-6.75 (m, 2H), 3.03 (s, 6H). ¹³C-NMR (DMSO-d₆, 400 MHz): δ 161.1, 152.1, 150.6, 142.8, 130.1, 128.8, 124.3, 111.5, 36.7. HRMS (EI): calcd. For C₁₂H₁₃N₅O₂ [M]⁺ 259.1069, found 259.1061.

***tert*-butyl 2-(5-((4-(dimethylamino)phenyl)diazenyl)-2,4-dioxo-3,4-dihydropyrimidin-1(2H)-yl)acetate (V-2):**



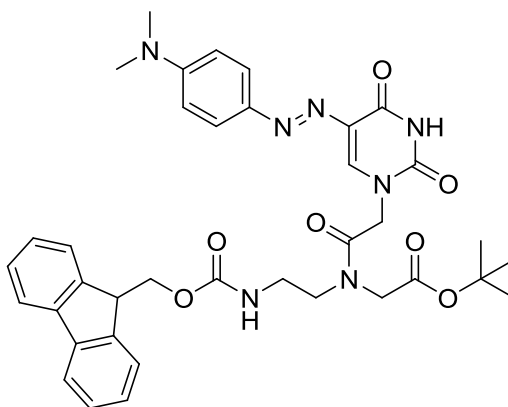
Compound **V-1** (500 mg, 1.93 mmol) and K_2CO_3 (270 mg, 1.95 mmol) were suspended in 8 mL of anhydrous DMF followed by the addition of *tert*-butyl-2-bromoacetate (0.28 mL, 1.93 mmol). The reaction was left stirring at room temperature overnight under an atmosphere of nitrogen. The solvent was removed under reduced pressure and the crude product was dissolved in dichloromethane (50 mL) and washed with saturated $NaHCO_3$ (2 x 25 mL), water (2 x 25 mL) and brine (2 x 25 mL). The organic phase was collected and dried over anhydrous sodium sulfate, filtered and concentrated under reduced pressure. The crude product was purified via FCC eluting with EtOAc:hexanes 10:90 to EtOAc:hexanes 90:10, to afford compound **V-2** in 64 % yield. 1H -NMR (DMSO- d_6 , 600 MHz): δ 11.78 (s, 1H), 8.07 (s, 1H), 7.66 (d, $J = 6$ Hz, 2H), 6.81 (d, $J = 12$ Hz, 2H), 4.54 (s, 2H), 3.05 (s, 6H), 1.43 (s, 9H). ^{13}C -NMR (DMSO- d_6 , 400 MHz): δ 167.0, 160.8, 152.2, 150.2, 142.8, 133.9, 128.9, 124.4, 111.5, 81.9, 49.8, 36.7, 27.7. HRMS (EI): calcd. For $C_{18}H_{23}N_5O_4$ $[M]^+$ 373.1750, found 373.1748.

2-(5-((4-(dimethylamino)phenyl)diazenyl)-2,4-dioxo-3,4-dihydropyrimidin-1(2H)-yl)acetic acid (V-3):



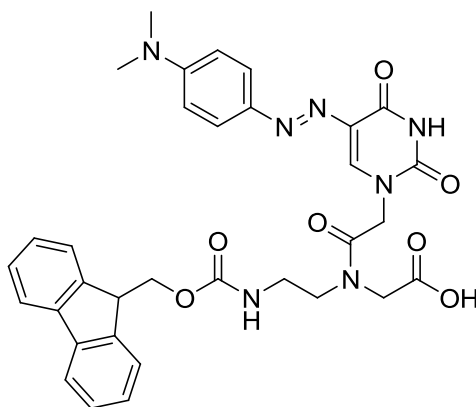
Compound **V-2** (150 mg, 0.40 mmol) was dissolved in 4 mL of anhydrous CH_2Cl_2 and cooled to 0°C followed by the addition of 2 mL of TFA. The reaction was stirred for 10 minutes on ice and a further 3 hours at room temperature. The solvent was then removed by nitrogen stream to give the TFA salt of compound **V-3** in quantitative yield. Compound **V-3** was used without further purification. $^1\text{H-NMR}$ (DMSO- d_6 , 600 MHz): δ 11.74 (s, 1H), 8.05 (s, 1H), 7.65 (d, $J = 12$ Hz, 2H), 6.81 (d, $J = 12$ Hz, 2H), 4.56 (s, 2H), 3.04 (s, 6H). $^{13}\text{C-NMR}$ (DMSO- d_6 , 400 MHz): δ 169.8, 160.9, 152.2, 150.4, 142.9, 134.3, 128.8, 124.4, 111.6, 49.6, 36.6. HRMS (EI): calcd. For $\text{C}_{14}\text{H}_{15}\text{N}_5\text{O}_4$ $[\text{M}]^+$ 317.1124, found 317.1125.

(E)-tert-butyl 2-(N-(2-(((9H-fluoren-9-yl)methoxy)carbonyl)amino)ethyl)-2-(5-((4-(dimethylamino)phenyl)diazenyl)-2,4-dioxo-3,4-dihydropyrimidin-1(2H)-yl)acetamido)acetate (V-4):



Compound **V-3** (150 mg, 0.47 mmol) was dissolved in 3 mL of anhydrous DMF and cooled to 0 °C followed by the addition of a solution of *N*-[2-(Fmoc)aminoethyl]glycine-*t*-butyl ester (178 mg, 0.45 mmol) in DMF (0.225 M), Hunig's base (0.7 mL, 3.95 mmol), HOBT (61 mg, 0.45 mmol) and HBTU (171, 0.45 mmol). The reaction was warmed to room temperature and left stirring for 24 h under an atmosphere of nitrogen. The reaction mixture was diluted with 60 mL of EtOAc and washed with 0.1 M HCl (2 x 30 mL), water (2 x 30 mL) and brine (2 x 30 mL). The organic layer was collected, dried over sodium sulfate, filtered and concentrated under reduced pressure. The crude product was purified via FCC eluting with EtOAc:Hexanes 60:40 – 100:0 to afford compound **V-4** in 43 % yield. Compound **V-4** exists in solution as a pair of slowly exchanging rotamers; signals attributed to major (ma.) and minor (min.) rotamers are designated. ¹H-NMR (DMSO-*d*₆, 400 MHz): δ 11.76 (s, ma., 0.60H), 11.75 (s, min., 0.40H), 8.00 – 6.70 (m, 14 H), 4.86 (s, ma., 1.25H), 4.67 (s, min., 0.81 H), 4.35 (s, min., 0.69 H), 3.95 (s, ma., 1.27 H), 4.34-4.15 (m, 3H), 3.44-3.39 (m, 2H), 3.31-3.24 (m, 2H), 3.15-3.10 (m, 1H), 3.03 (s, 6 H), 1.47 (s, min., 3H), 1.39 (s, ma. 6H). ¹³C-NMR (DMSO-*d*₆, 400 MHz): δ 167.9, 167.0, 160.8, 156.3, 152.1, 150.2, 143.8, 142.8, 140.7, 128.7, 127.6, 127.0, 125.1, 124.3, 120.1, 111.5, 105.2, 82.0, 80.9, 71.5, 65.5, 46.7, 36.2, 27.7, 24.3, 23.6, 20.7, 10.2. HRMS (EI): calcd. For C₃₇H₄₂N₇O₇ [MH]⁺ 696.3146, found 696.3170.

(E)-2-(N-(2-(((9H-fluoren-9-yl)methoxy)carbonyl)amino)ethyl)-2-(5-((4-(dimethylamino)phenyl)diazenyl)-2,4-dioxo-3,4-dihydropyrimidin-1(2H)-yl)acetamido)acetic acid (V-5):



Compound **V-4** (125 mg, 0.18 mmol) was dissolved in 5 mL of CH_2Cl_2 and cooled to 0 °C followed by the slow drop wise addition of TFA (2.5 mL). The reaction was stirred for 4 hours at room temperature. The reaction was evaporated to dryness via nitrogen stream and the remaining volatiles were removed by coevaporation with CH_2Cl_2 and diethyl ether. The product was dried under vacuum to afford the TFA salt of compound **V-5** in 80 % yield. Compound **V-5** exists in solution as a pair of slowly exchanging rotamers; signals attributed to major (ma.) and minor (min.) rotamers are designated. $^1\text{H-NMR}$ (DMSO- d_6 , 600 MHz): δ 11.74 (s, ma., 0.60H), 11.73 (s, min., 0.40H), 8.00 – 6.70 (m, 14 H), 4.87 (s, ma., 1.20H), 4.69 (s, min., 0.80H), 4.35 (s, min., 0.80H), 4.00 (s, ma., 1.20H), 4.34-4.15 (m, 4H), 3.45-3.32 (m, 2H), 3.31-3.09 (m, 2H), 3.03 (s, 6 H). $^{13}\text{C-NMR}$ (DMSO- d_6 , 400 MHz): δ 170.7, 170.4, 167.4, 167.0, 160.8, 158.1, 157.7, 156.3, 152.1, 150.2, 144.8, 143.9, 142.9, 140.7, 134.3, 128.8, 127.6, 127.1, 125.1, 124.3, 120.1, 111.6, 65.5, 46.7. HRMS (EI): calcd. For $\text{C}_{33}\text{H}_{34}\text{N}_7\text{O}_7$ $[\text{MH}]^+$ 640.2520, found 640.2520.

5.6 References

- 1) Kramer, F.; Tyagi, S. *Nat. Biotechnol.* **1996**, 14, 303.
- 2) Dodd, D.W.; Hudson, R.H.E. *Mini Rev. Org. Chem.* **2009**, 6, 378.
- 3) Seitz, O. *Angew. Chem. Int. Ed.* **2000**, 39, 3249.
- 4) Seitz, O.; Bergmann, F.; Heindl, D. *Angew. Chem. Int. Ed.* **1999**, 38, 2203.
- 5) Thurber, T. C.; Townsend, L. B.; *J. Heterocyclic. Chem.* **1972**, 9, 629.
- 6) Tsupak, E. B.; Shevchenko, M. A.; Tkachenko, Y. N.; Nazarov, D. A. *Russ. J. Org. Chem.* **2002**, 38, 923.
- 7) Moustafa, M. E. *Design and Synthesis of Novel Quenchers for Fluorescent Hybridization Probes*. Ph.D. Thesis, 2011.
- 8) Lakowicz, J.R. *Principles of Fluorescence Spectroscopy*, 3rd ed. Springer Science + Business Media: New York, NY, **2006**.
- 9) B. Valeur, *Molecular Fluorescence: Principles and Applications*, Wiley-VCH **2001**.
- 10) Wojciechowski, F.; Hudson, R. H. E. *J. Org. Chem.* **2008**, 73, 3807.
- 11) Hudson, R. H. E.; Liu, Y.; Wojciechowski, F. *Can. J. Chem.* **2007**, 85, 302.
- 12) Hyde, C.; Johnson, T.; Sheppard, R. C. *J. Chem. Soc. Chem. Commun.* **1992**, 1573.
- 13) Yamada, K.; Nagashima, I.; Hachisu, M.; Matsuo, I.; Shimizu, H. *Tetrahedron. Lett.* **2012**, 53, 1066.
- 14) Pennington, M. W.; Dunn, B. M. *Methods in Molecular Biology, Vol. 35: Peptide Synthesis Protocols.* **1994**, Humana Press Inc., Totowa, NJ.
- 15) Kempe, M.; Barany, G. *J. Am. Chem. Soc.* **1996**, 118, 7083.

6 Overall Conclusion and Outlook

This thesis focused on nucleobase modified PNA and DNA to expand the repertoire of available nucleobase analogs used in the study of nucleic acids. Although there are many fluorescent nucleobase analogs to choose from, the search for an ideal analog with optimal photophysical characteristics, i.e., high fluorescence quantum yield, red-shifted absorption maxima, not destabilizing to hybridization, ability to provide nucleobase discrimination, and the ability to report differences in the local environment through a change in fluorescence intensity or emission wavelength is still underway.

Chapter 2 described the synthesis of an acridine labelled nucleobase for the purpose of investigating its potential as a base-discriminating fluorophore. The literature shows us that the development of fluorescent uridine analogs has been extensively investigated, due to it offering the simplest chemistry relative to the other nucleobases. However, the derivatization of 5-aminouracil with chromophoric molecules is an area of research that remains relatively unexplored. Upon successful incorporation of the acridine labelled monomer into a PNA oligomer, thermal denaturation studies of DNA complexes with this oligomer illustrated its ability to discriminate between a fully matched complementary strand and the corresponding mismatched strands. Unfortunately, the fluorescence of the PNA oligomer could not be used to study hybridization because the 5-(acridin-9-ylamino)uracil modification was thermally labile in aqueous solution and liberated the highly fluorescent acridone moiety, thus obscuring the signal from the PNA. Despite not being an effective BDF, the ease at which the modification was introduced indicates the potential of this chemical route for the introduction of chemically modified nucleobases into PNA.

The literature also shows us that certain fluorescent nucleobase analogs are underrepresented, especially analogs of adenine and guanine. To that end, this thesis focused on the synthesis of novel fluorescent 7-deazaadenosine analogs and chemistry toward a novel tricyclic 7-deazaadenine analog. The 7-deazaadenosine analogs, A^{PYR} , A^{mon} and A^{phen} were photophysically characterized in dioxane, EtOH, and H₂O to evaluate their potential for use as environmentally sensitive fluorescent probes. All three

analogs displayed high solvatofluorochromicity in H₂O, relative to their emission wavelengths in dioxane and EtOH. Moreover, all three analogs exhibited moderate to high fluorescence quantum yields in dioxane and EtOH, and significantly lower fluorescence quantum yields in H₂O, indicating that these analogues display microenvironment sensitivity. Among them, A^{pyr} showed the most promise, due to its red-shifted absorption and emission wavelengths, large molar extinction coefficients, high fluorescence quantum yields in dioxane ($\Phi_F = 0.52$) and EtOH ($\Phi_F = 0.43$), and dramatic decrease in fluorescence quantum yield in H₂O ($\Phi_F = 0.01$). These characteristics, in conjunction with the benefit that large substituents at the 7-position of the 7-deazapurine can be accommodated in the major groove of resultant duplexes, suggest that A^{pyr} has considerable potential for use as an environmentally sensitive fluorescent probe and warrants further study in the context of a DNA oligonucleotide.

Unfortunately the tricyclic 7-deazaadenine analog was not accessed. However, the synthesis and photophysical evaluation of novel fluorescent 7-deazaadeine analogs substituted at the 7-position with various fluorescent alkynes is an area of research that is yet to be explored in the context of PNA. The chemistry described in Chapter 4 paves the way for the derivatization of the 7-deazaadenine scaffold with fluorescent alkynes via the Sonogashira reaction. Moreover, the 7-deazaadenine substrate may be useful in the post synthetic modification of PNA with fluorescent alkynes via an on-resin Sonogashira reaction, for the construction of novel fluorescent PNAs which may be used to study nucleic acids.

Lastly, Chapter 5 focused on the synthesis of an intrinsic nucleobase quencher to overcome some of the limitations associated with traditional molecular beacons. PNA monomer U^{azo} was synthesized in 5 steps starting from 5-diazouracil. In order to determine viable FRET pairs, fluorescence quenching experiments were performed between compound V-2 and the fluorophores phenylpyrrolocytidine (pC), and pyrene. Stern-Volmer plots were constructed and the Stern-Volmer quenching constant, K_{sv} , was calculated for each fluorophore quencher pair. The K_{sv} values suggest that pC is more sensitive to quenching from compound V-2 than pyrene. Moreover, the inverse of the Stern-Volmer quenching constant, K_{sv}^{-1} , was calculated for each fluorophore quencher

pair. The K_{sv}^{-1} values suggest that pC is quenched more efficiently by compound **V-2** than pyrene. Thus, compound **V-2** and pC act as a better FRET pair than compound **V-2** and pyrene. Although incorporation of the custom monomer **U^{azo}** into a PNA oligomer proved to be problematic, this work represents a step forward toward the construction of novel stemless PNA molecular beacons which may be used to detect nucleic acids.

Appendices

Appendix 1: General experimental procedures.

Reagents were commercially available and all solvents were HPLC grade except for water (18.2 M Ω cm millipore water) and DMF (dried over Al_2O_3 , in a solvent purification system). Solvents were removed under reduced pressure in a rotary evaporator, aqueous solutions were lyophilised and organic extracts were dried over Na_2SO_4 . Flash column chromatography (FCC) was carried out using silica gel (SiO_2), mesh size 230 - 400 Å. Thin-layer chromatography (TLC) was carried out on Al backed silica gel plate with compounds visualised by UV light. NMR spectra were recorded at room temperature on a 400 or 600 MHz spectrometer for ^1H NMR spectra δ values were recorded as follows: CDCl_3 (7.27 ppm); DMSO-D_6 (2.49 ppm); for ^{13}C (400 MHz) δ CDCl_3 (77.0 ppm); DMSO-D_6 (39.5 ppm). Mass spectra (MS) were obtained using electron impact (EI), or electrospray ionisation (ESI).

Appendix 2: Temperature dependent UV melting studies

Hybridization and UV melting experiments were carried out in aqueous buffer: 100 mmol/L NaCl, 10 mmol/L Na_2HPO_4 , and 0.1 mmol/L EDTA at pH 7. UV melting experiments were performed on a CARY UV-visible spectrophotometer. UV melting experiments were carried out at 2 $\mu\text{mol/L}$ strand concentration. Samples were heated to 90 $^\circ\text{C}$, cooled to room temperature over 3 hours and placed at 10 $^\circ\text{C}$ overnight. Denaturation was performed from 10 $^\circ\text{C}$ to 90 $^\circ\text{C}$ at a scan rate of 0.5 $^\circ\text{C}/\text{min}$. The T_m values are an average of three measurements and are rounded to the nearest 0.5 $^\circ\text{C}$. The error in T_m values was ± 1 $^\circ\text{C}$. The T_m values were extracted from the melt curves using the first derivative method.

Appendix 3: Methods of photophysical analysis

In order to determine the photophysical parameters of A^{pyr} , A^{mon} , and A^{phen} in the various solvents of interest, spectroscopic grade EtOH, spectroscopic grade dioxane, and H_2O (18.2 M Ω cm millipore water) were used for analysis. The samples were analyzed using a 1cm wide four-sided Quartz cuvette for all photophysical analyses. Thus, a light path length (ℓ) of 1 cm was used for all absorption experiments. All absorption experiments were carried out using a CARY UV-Visible spectrophotometer and all fluorescence experiments were carried out using a PTI fluorimeter.

The molar extinction coefficients (ϵ) of A^{pyr} , A^{mon} , and A^{phen} in EtOH, dioxane, and H_2O were calculated using Beer-Lambert's law ($A = \epsilon c \ell$). For each set of analog and solvent, five different solutions of known concentration were prepared by dissolving ~ 0.0010 g of the analogs with 5 mL of solvent, in order to create a stock solution. Then, 50 μL , 100 μL , 150 μL , 200 μL , and 250 μL samples of the stock solution were further diluted with 10 mL of solvent. The resulting samples were then analyzed at the analog's $\lambda_{\text{max}}^{\text{ab}}$ using UV-Vis absorption spectroscopy, in order to generate a plot of sample absorbance (A) against sample concentration (c). The molar extinction coefficient was then determined as the slope of the resulting plot, using a constant light path length (ℓ) of 1 cm. In addition, the error for the molar extinction coefficients were calculated based on a 95% confidence interval. Due to insufficient solubility of A^{pyr} , A^{mon} , and A^{phen} in water, they were first dissolved in 0.20 mL of spectroscopic grade DMSO, prior to dilution with water. However, considering the magnitude of dilution, the final concentration of DMSO in the analyzed samples is considered to be negligible.

The fluorescence quantum yield (Φ_{F}) for A^{pyr} , A^{mon} , and A^{phen} in EtOH, dioxane, and H_2O were calculated. In order to determine the fluorescence quantum yield of an analog, a fluorescence standard that absorbs distinctively at the wavelength of interest must be chosen for co-analysis. For each set of analog and solvent, five solutions of different concentrations were prepared for both the analogue and its corresponding fluorescence

standard. The solutions were then analyzed by UV-Vis absorption spectroscopy, in order to determine the absorbance of each solution at the wavelength of interest. The samples used for analysis were diluted such that their absorbance was below 0.1, in order to minimize re-absorption effects. For this experiment, the wavelength of interest was the wavelength of maximum absorption for each analogue in the corresponding solvent. The samples were then excited at the wavelength of interest and the resulting fluorescence was measured using a PTI fluorimeter. The integrated fluorescence intensity was then plotted against the absorbance for each sample, for both the analog and its corresponding fluorescence standard. The slopes of these two plots were then used in conjunction with the known fluorescence quantum yield of the fluorescence standard (Φ_{STD}), in order to determine the fluorescence quantum yield of the compound of interest. These calculations are based on the following equation:

$$\Phi_F = \Phi_{STD} \left(\frac{Slope_F}{Slope_{STD}} \right) \left(\frac{\eta_F^2}{\eta_{STD}^2} \right)$$

In order to determine the fluorescence quantum yields of A^{pyr} , A^{mon} , and A^{phen} , the fluorescence standard's fluorescence quantum yield in the solvent of interest must be known. However, there were no established fluorescence quantum yields in the literature for some of the fluorescent standards in the solvents of interest. Thus, the fluorescence quantum yields of these standards were calculated manually, relative to a known fluorescence quantum yield of the same standard in a different solvent. This was done using the same procedure as for determining the fluorescence quantum yields of A^{pyr} , A^{mon} , and A^{phen} . The difference in solvent was accounted for by including a ratio of the refractive indices in the calculation, as seen in the above equation. The fluorescence quantum yields that were used for analysis are presented in Table 12.

Due to the low solubility of A^{pyr} , A^{mon} , and A^{phen} in H_2O , they were first dissolved in 0.20 mL of spectroscopic grade DMSO, prior to dilution with H_2O . However, considering the magnitude of dilution, the final concentration of DMSO in the analyzed samples is considered to be negligible. Similarly, due to insufficient solubility of quinine sulfate in H_2O , quinine sulfate in 0.5 M H_2SO_4 was used as the fluorescent standard for the

determination of the quantum yields of A^{pyr} , A^{mon} , and A^{phen} in H_2O . However, due to the low concentration of H_2SO_4 in the quinine sulfate samples analyzed, the effect of H_2SO_4 on the quantum yield is considered to be negligible.

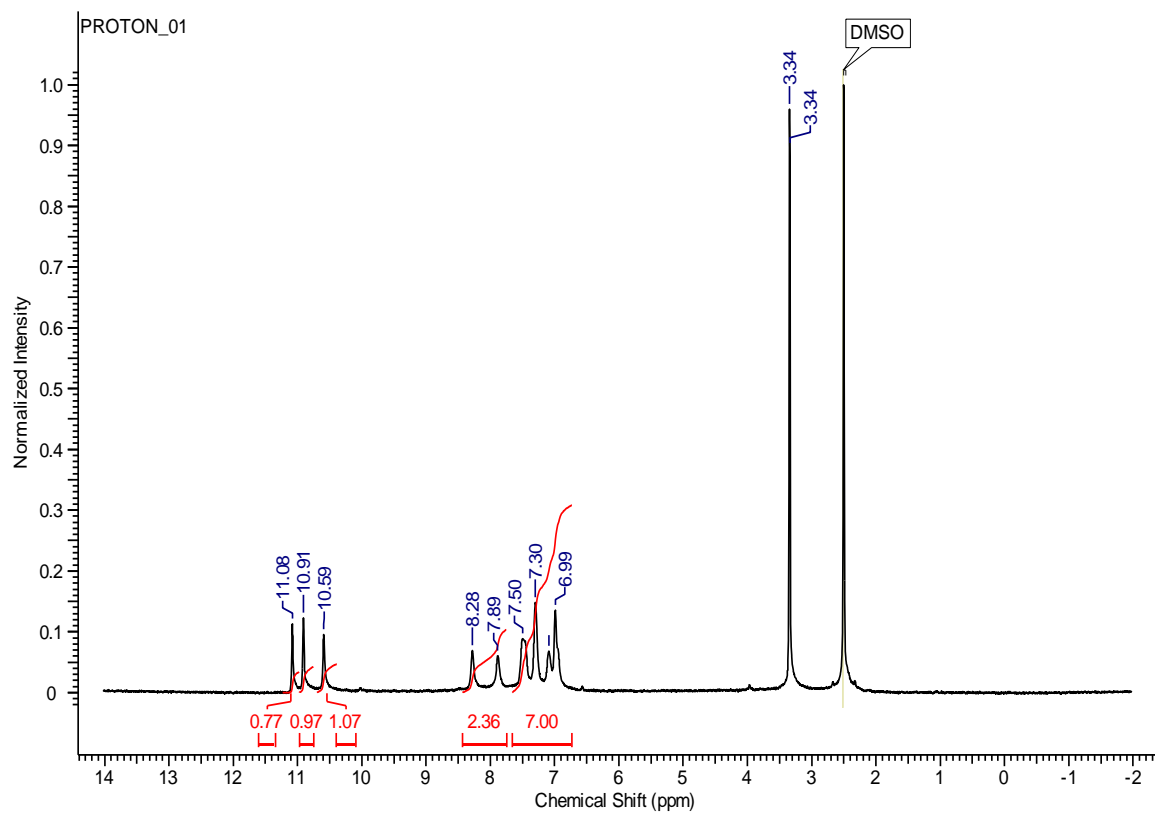
Nucleoside	Solvent	Fluorescence Standard	Lit. Φ_{F} ¹²	Calcd. Φ_{F}
A^{pyr}	EtOH	9,10-Diphenylanthracene	0.95	
	H_2O	Quinine Sulfate	0.55	
	Dioxane	9,10-Diphenylanthracene		0.83
A^{mon}	EtOH	Pyrene	0.65	
	H_2O	Quinine Sulfate	0.55	
	Dioxane	Pyrene		0.87
A^{phen}	EtOH	Pyrene	0.65	
	H_2O	Quinine Sulfate	0.55	
	Dioxane	Pyrene		0.87

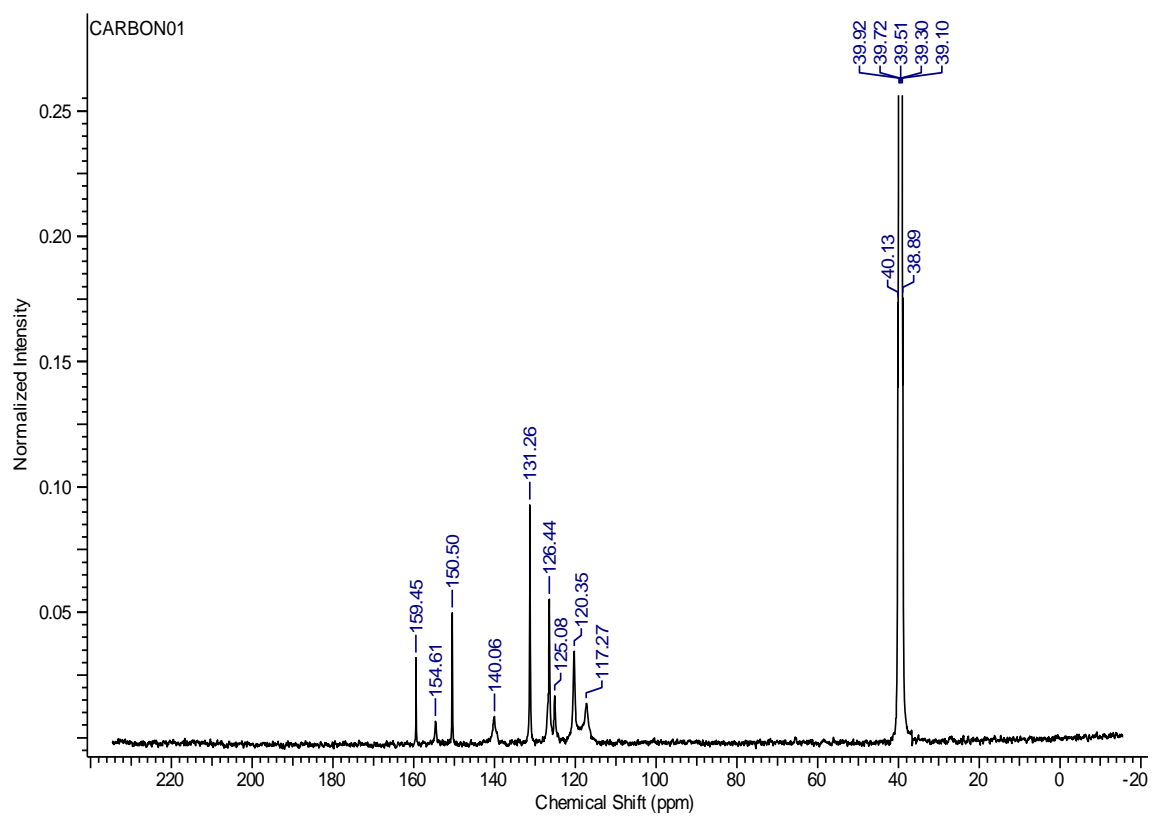
Table 12: Fluorescence standards and their corresponding quantum yields.

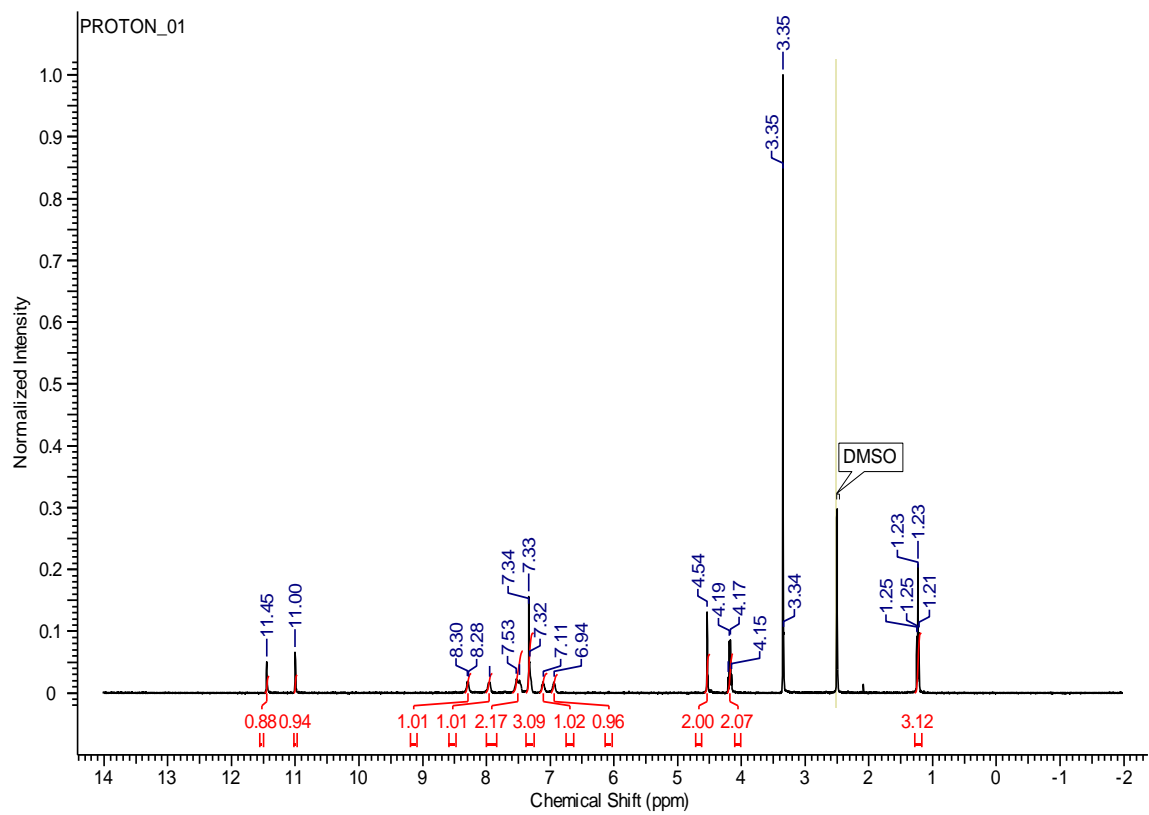
Appendix 4: Fluorescence quenching studies

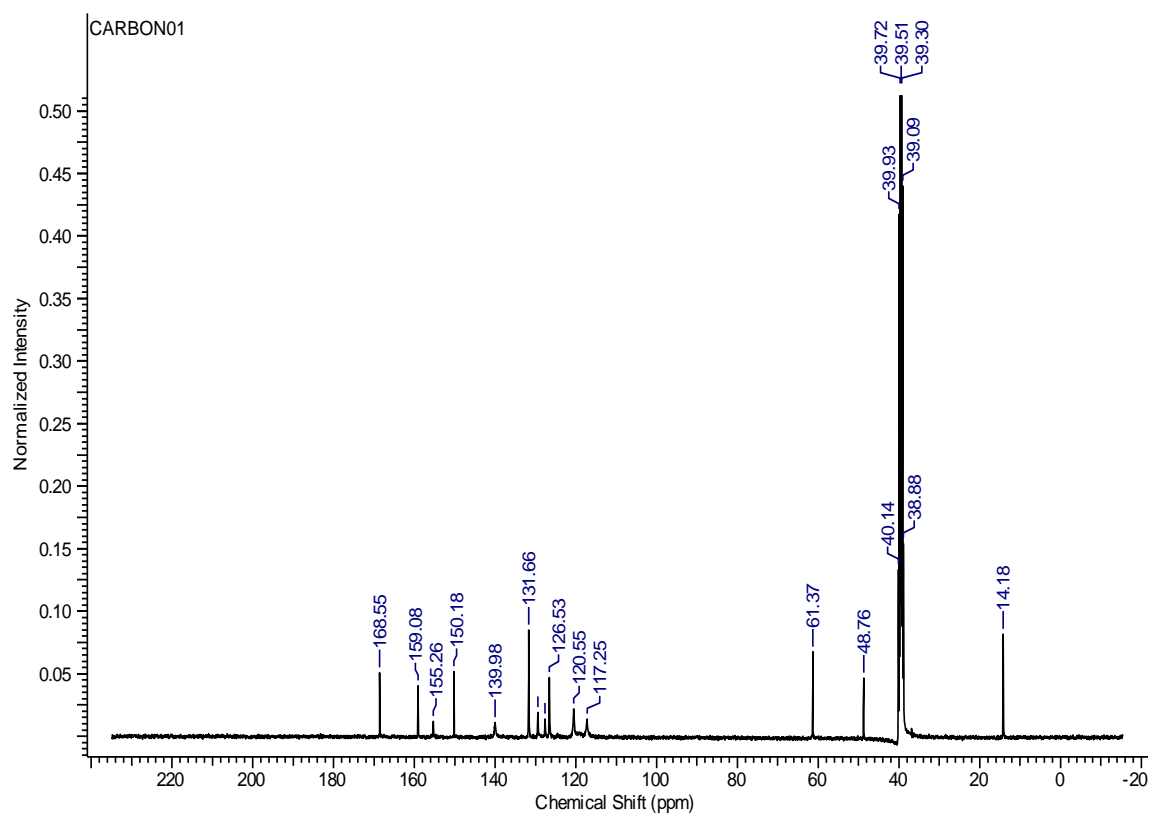
The fluorescence quenching studies were performed on a PTI fluorimeter. A 1 μM solution of pC was irradiated at 343 nm and the emission spectrum was obtained in the absence of quencher. Next compound **V-2** was added to the 1 μM solution of pC in 6 μL increments and the emission spectra were obtained to determine the amount of quenching. The UV-visible spectrum of each sample was obtained before and after the addition of quencher. The total concentration of quencher after each addition was determined and a Stern-Volmer plot was constructed to analyze the FRET pair.

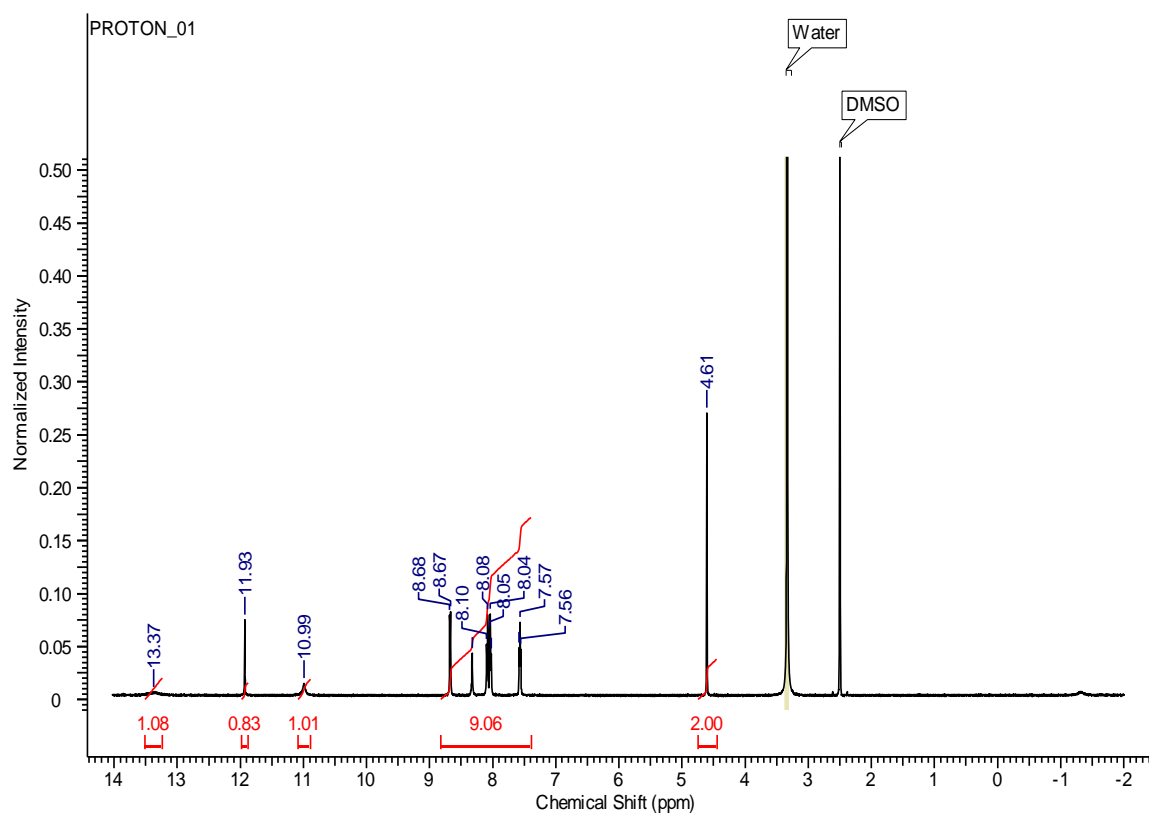
Similarly, a 1 μM solution of pyrene was irradiated at 336 nm and the emission spectrum was obtained in the absence of quencher. Compound **V-2** was then added to the 1 μM solution of pyrene in 6 μL increments and the emission spectra were obtained to determine the amount of quenching. The UV-visible spectrum of each sample was obtained before and after the addition of quencher. The total concentration of quencher after each addition was determined and a Stern-Volmer plot was constructed to analyze the FRET pair.

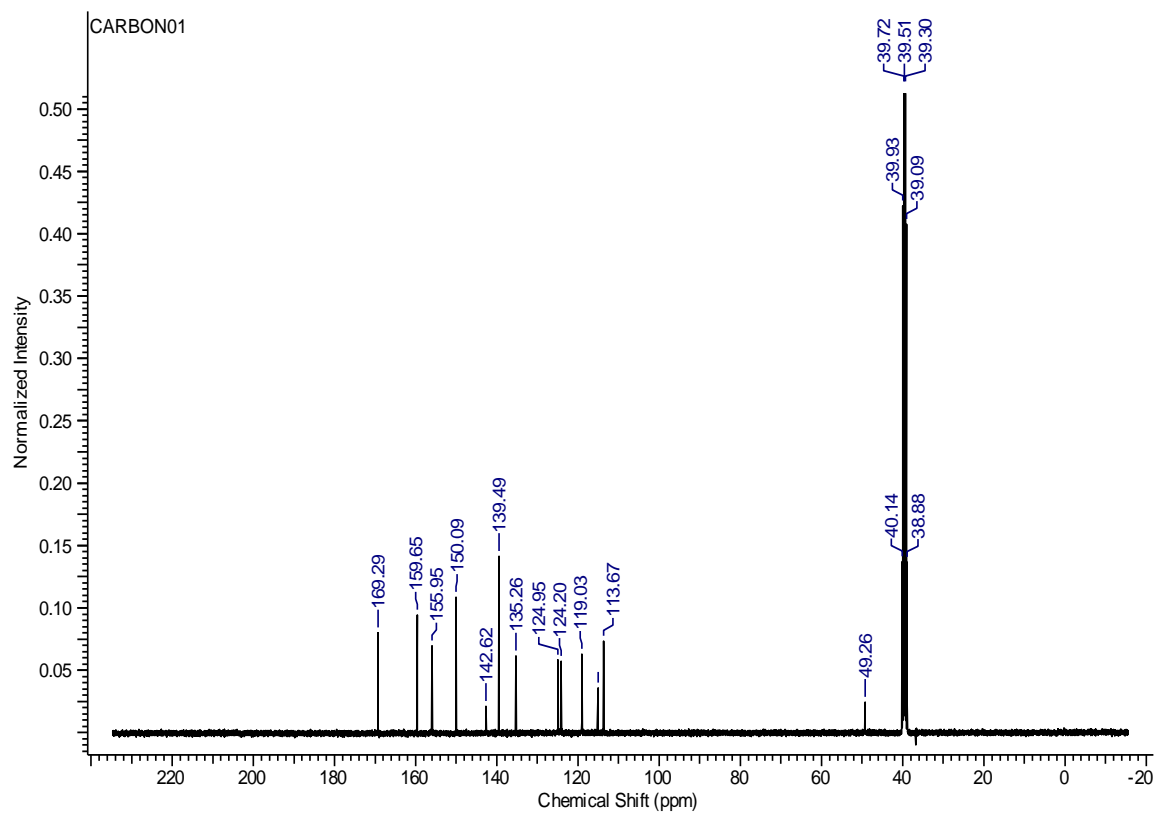
Appendix 5: ^1H -NMR spectrum of compound II-1.

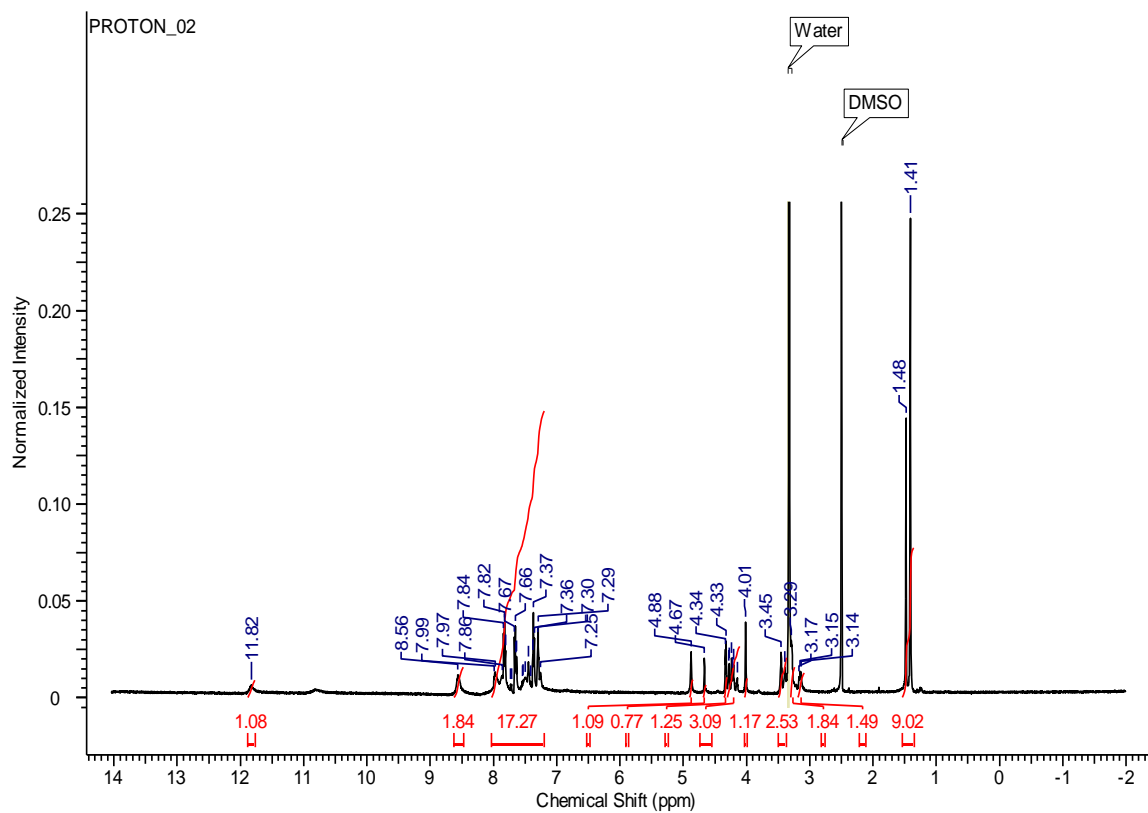
Appendix 6: ^{13}C -NMR spectrum of compound II-1.

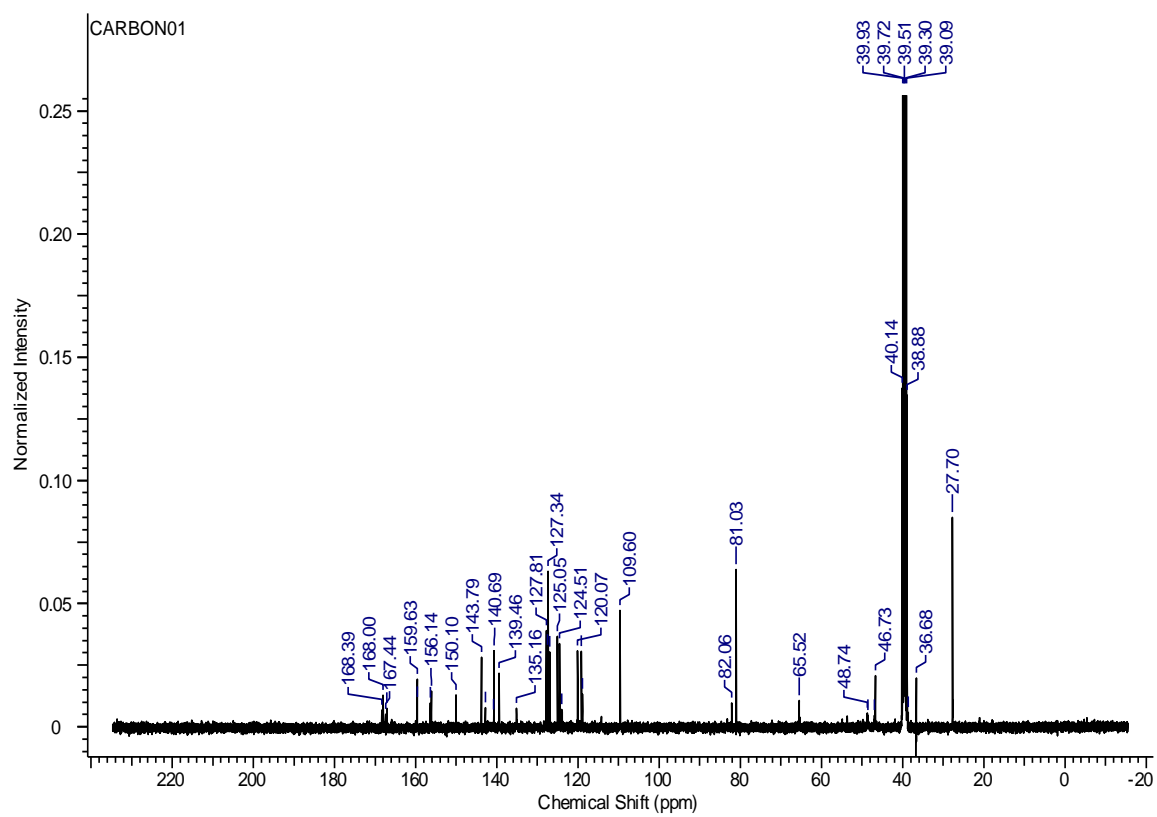
Appendix 7: ^1H -NMR spectrum of compound II-2.

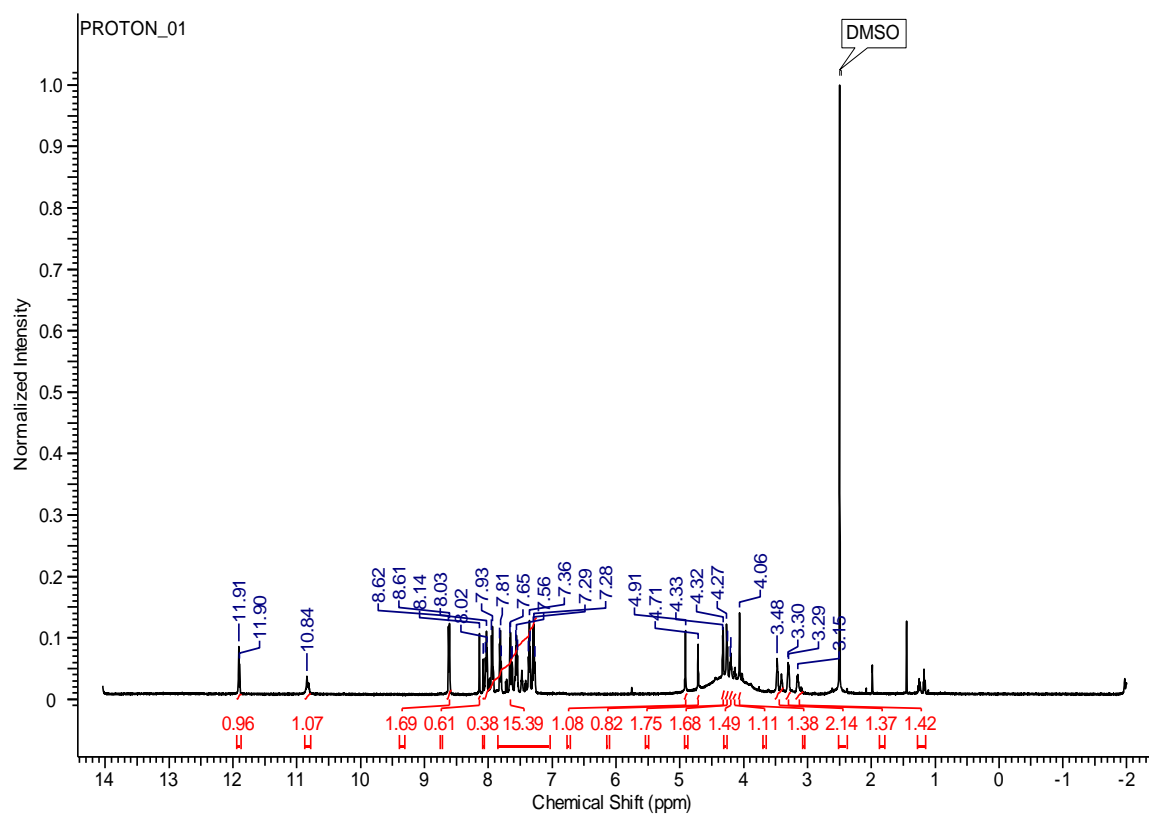
Appendix 8: ^{13}C -NMR spectrum of compound II-2.

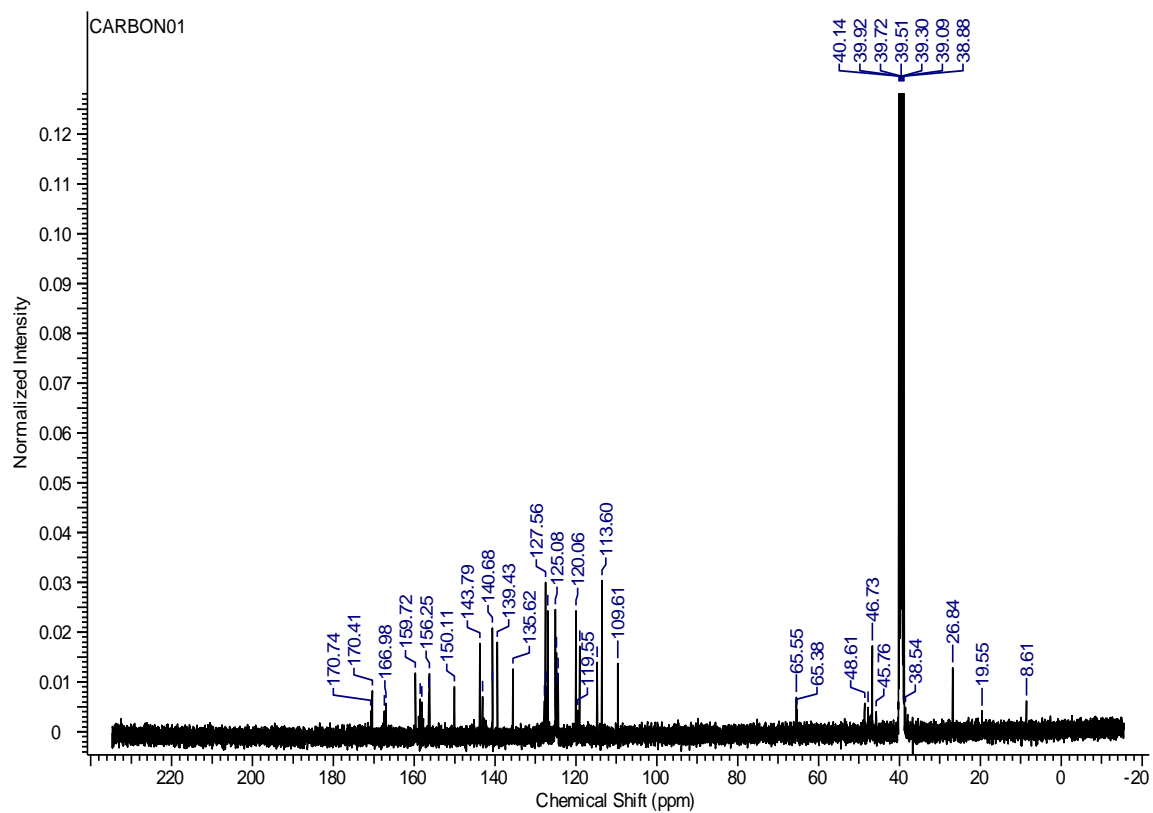
Appendix 9: ^1H -NMR spectrum of compound II-3.

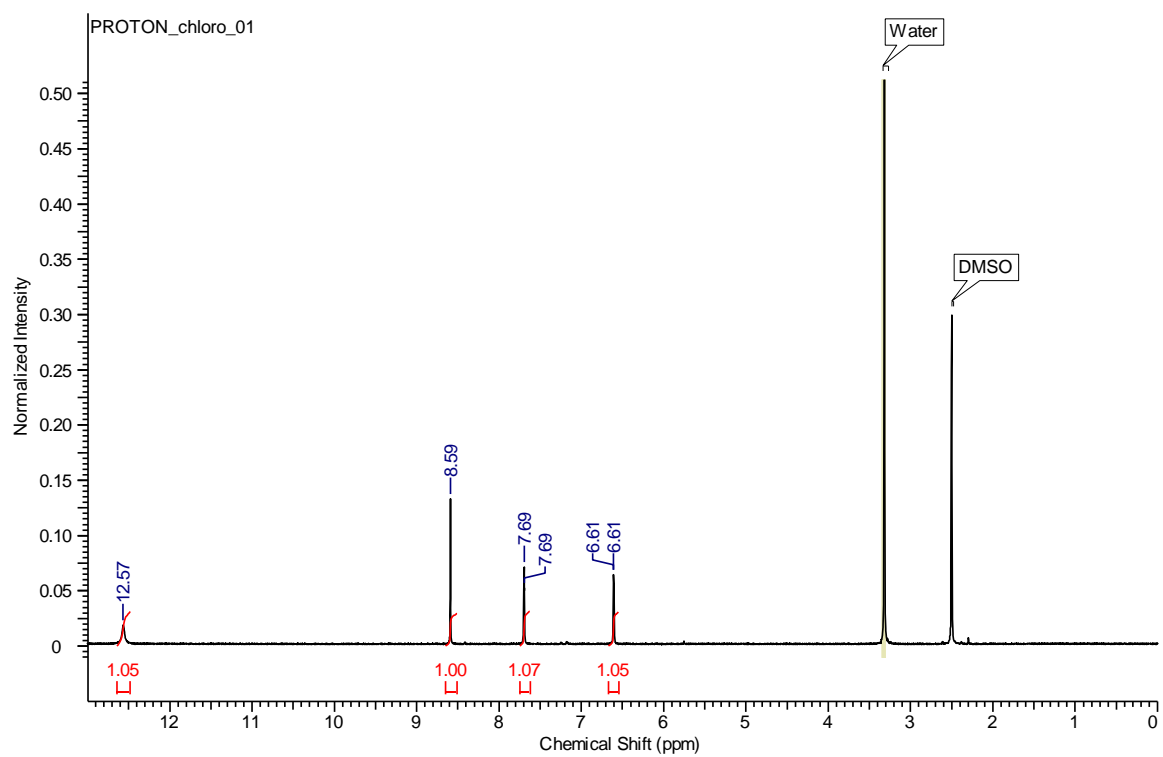
Appendix 10: ^{13}C -NMR spectrum of compound II-3.

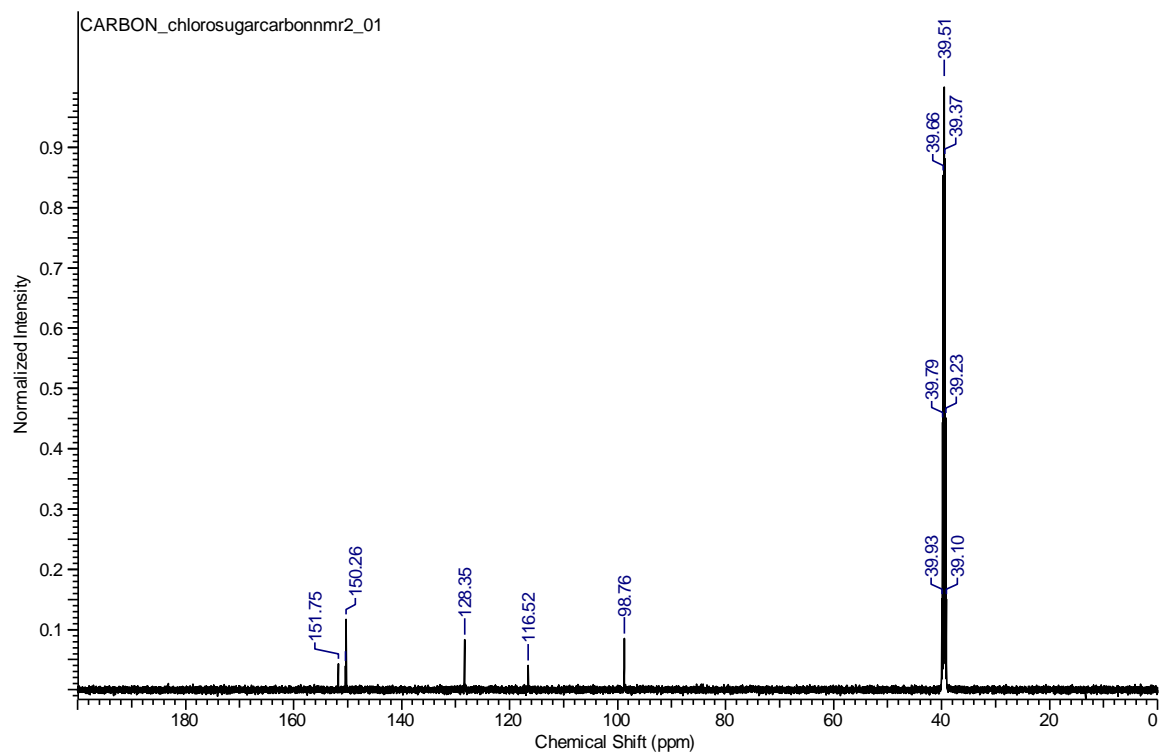
Appendix 11: $^1\text{H-NMR}$ spectrum of compound II-4.

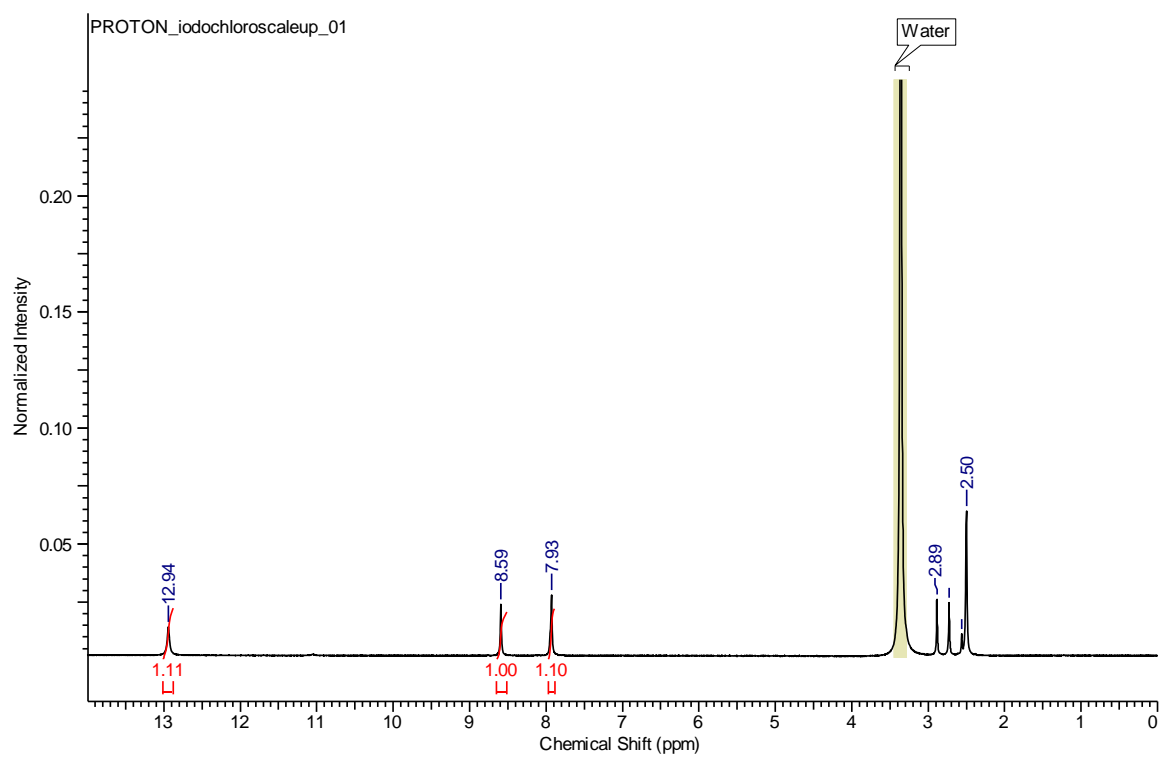
Appendix 12: ^{13}C -NMR spectrum of compound II-4.

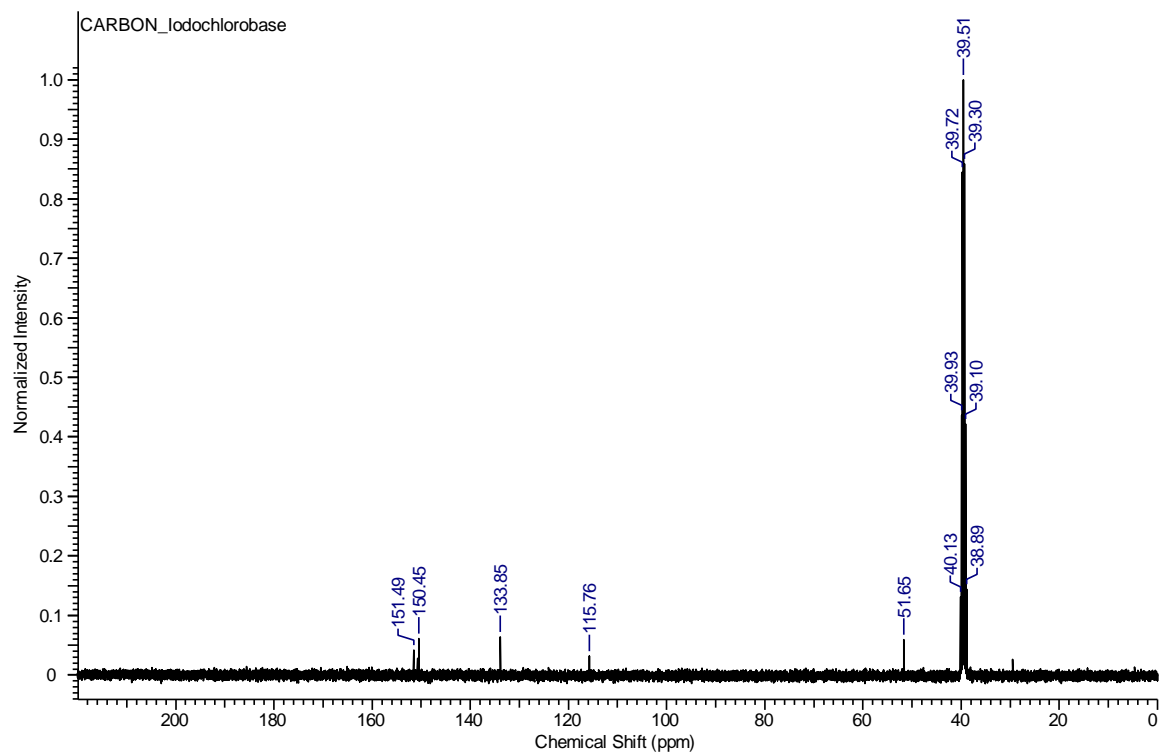
Appendix 13: $^1\text{H-NMR}$ spectrum of compound II-5.

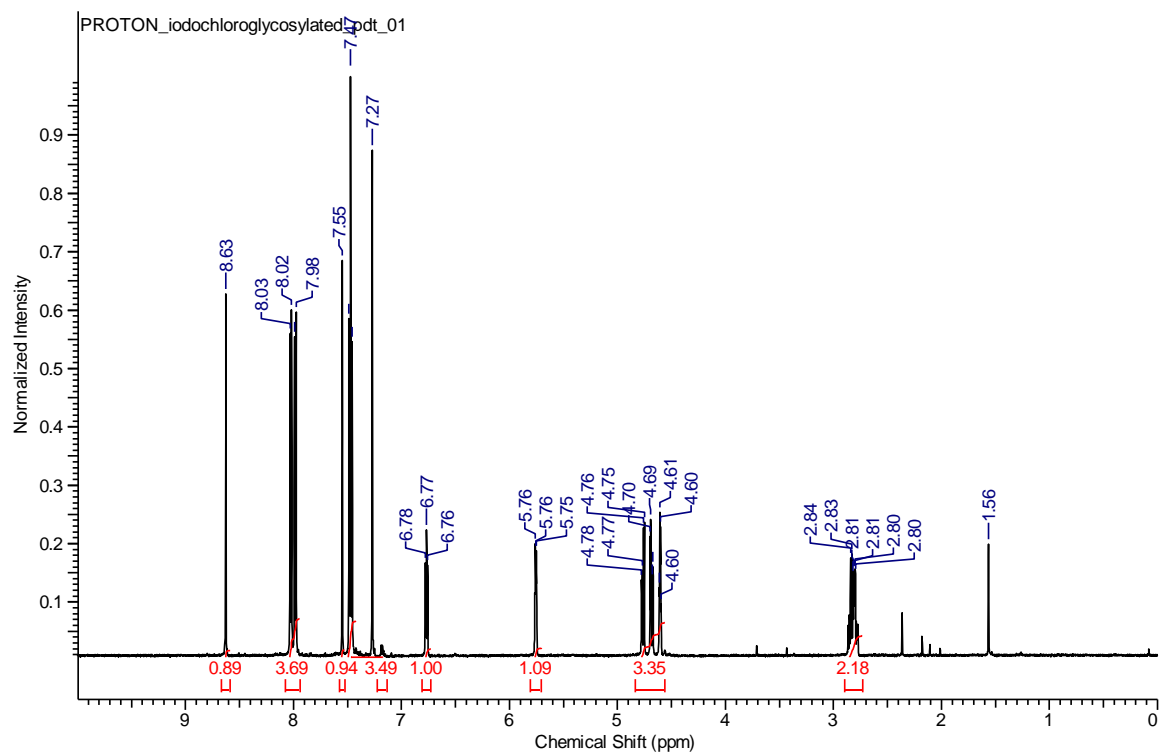
Appendix 14: ^{13}C -NMR spectrum of compound II-5.

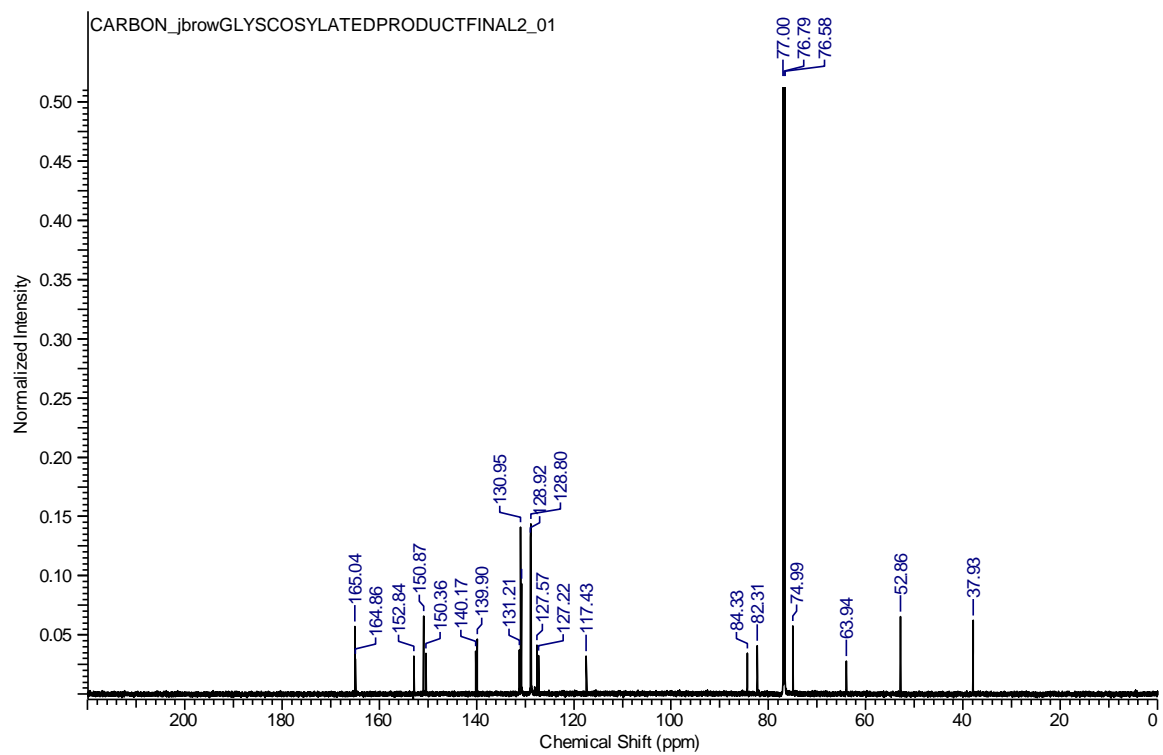
Appendix 15: ^1H -NMR spectrum of compound III-17.

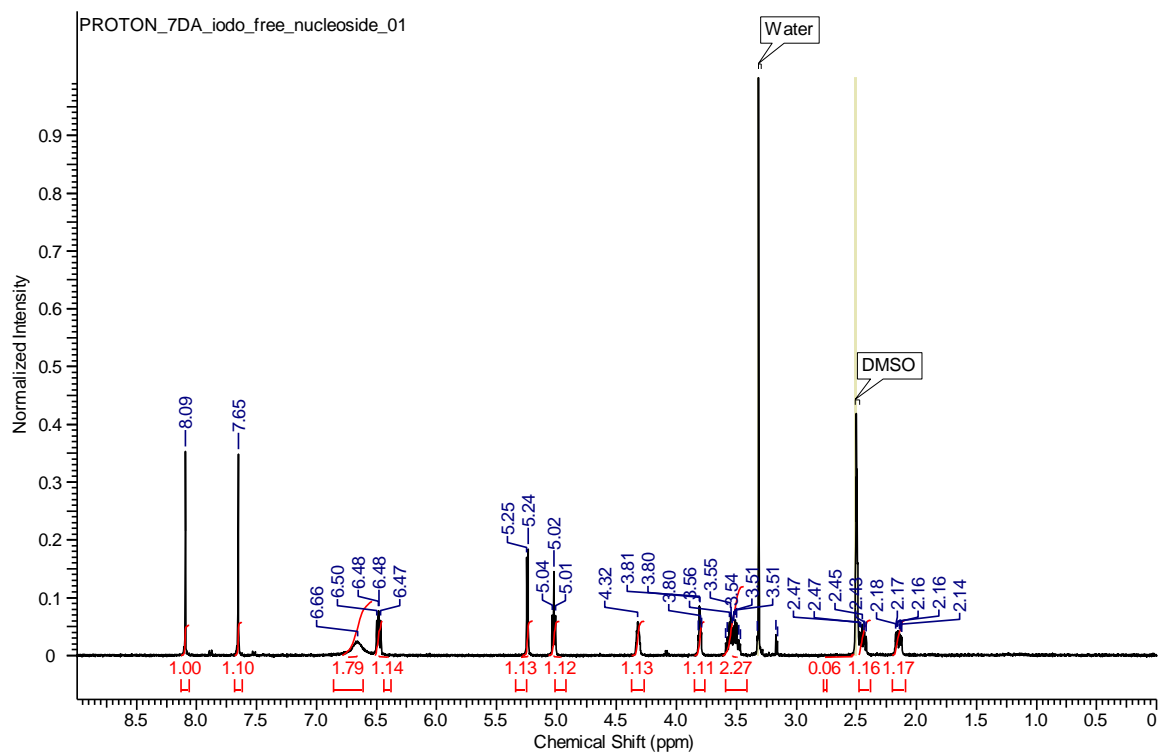
Appendix 16: ^{13}C -NMR spectrum of compound III-17.

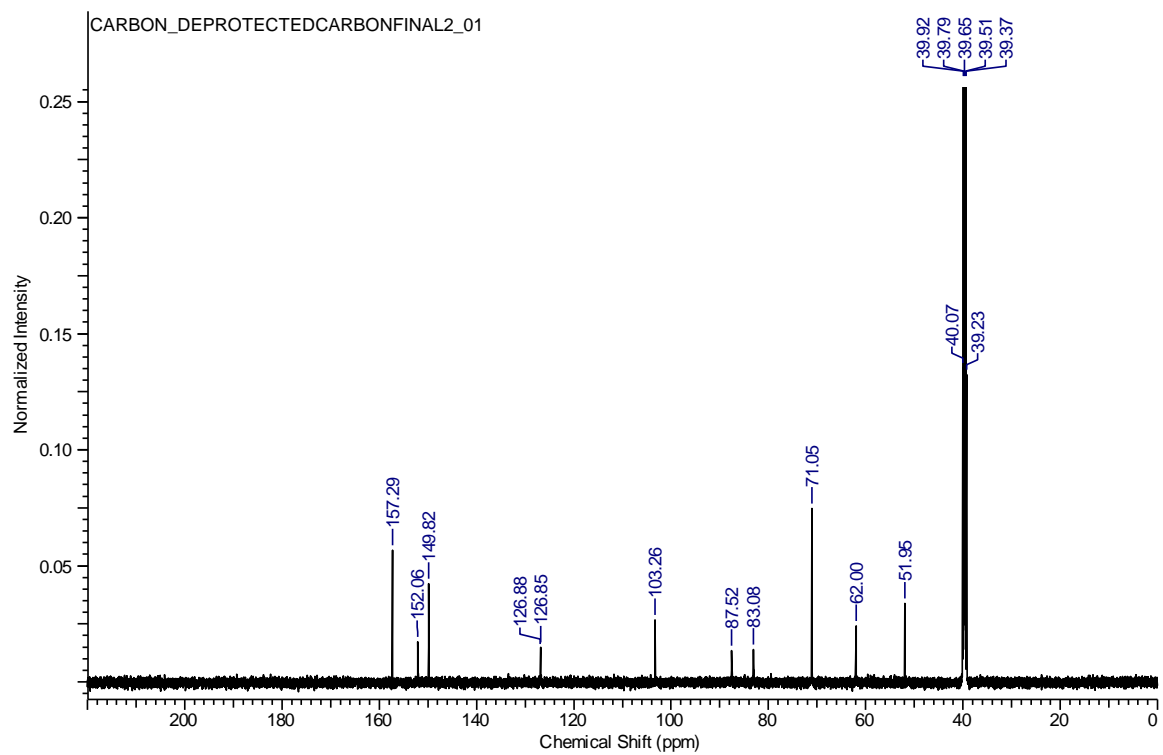
Appendix 17: ^1H -NMR spectrum of compound III-18.

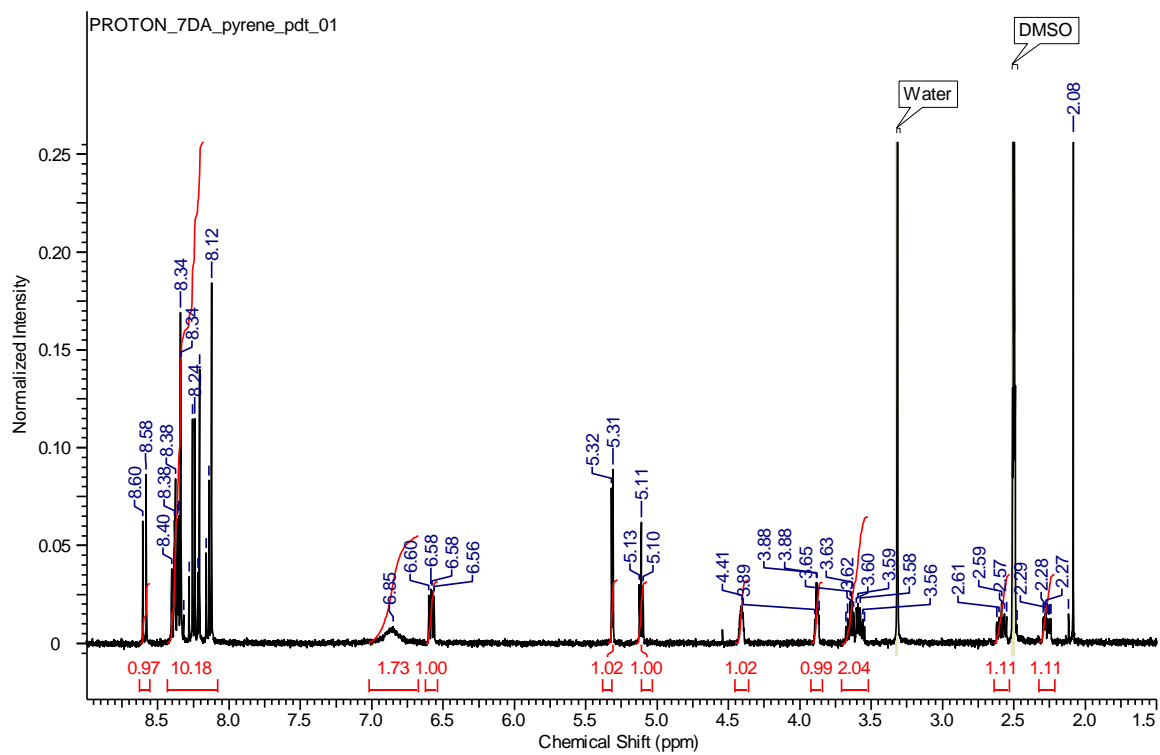
Appendix 18: ^{13}C -NMR spectrum of compound III-18.

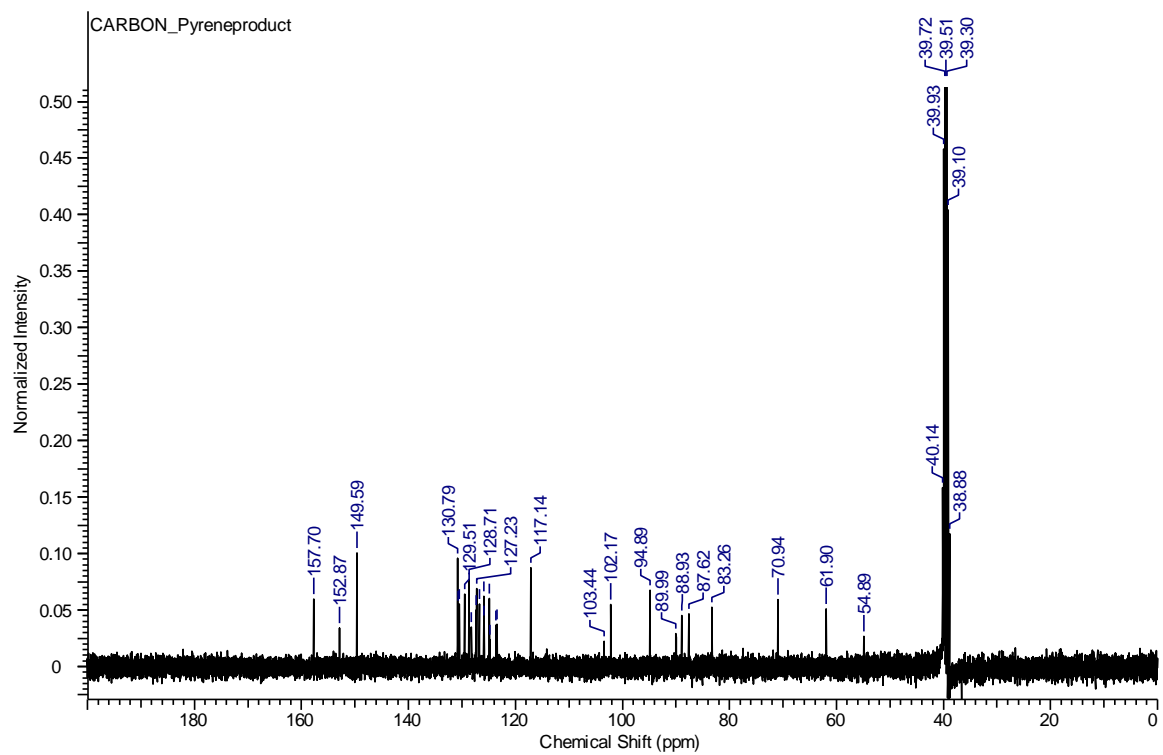
Appendix 19: $^1\text{H-NMR}$ spectrum of compound III-19.

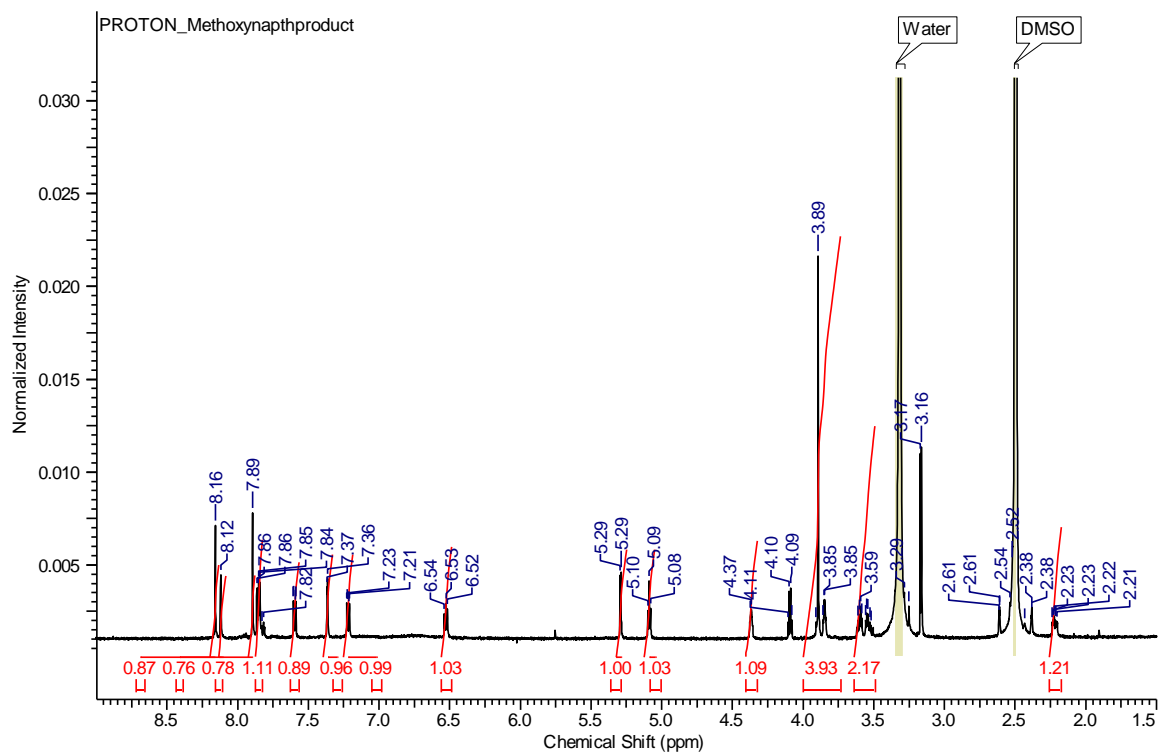
Appendix 20: ^{13}C -NMR spectrum of compound III-19.

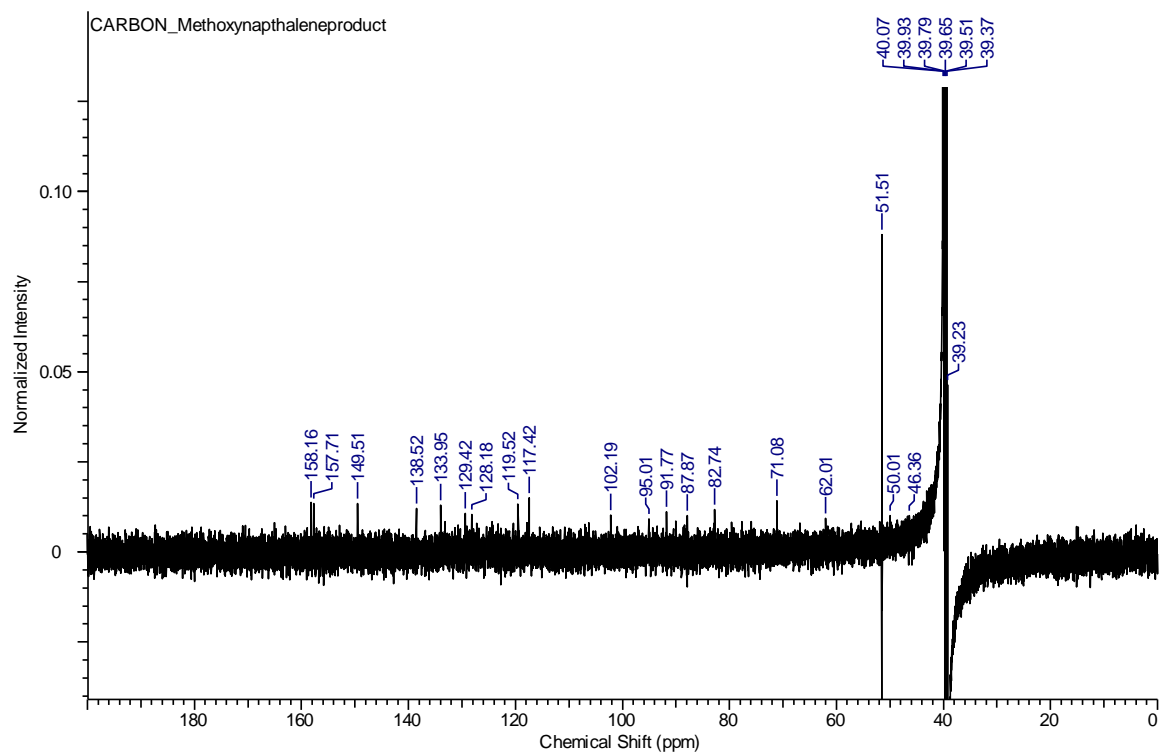
Appendix 21: $^1\text{H-NMR}$ spectrum of compound III-20.

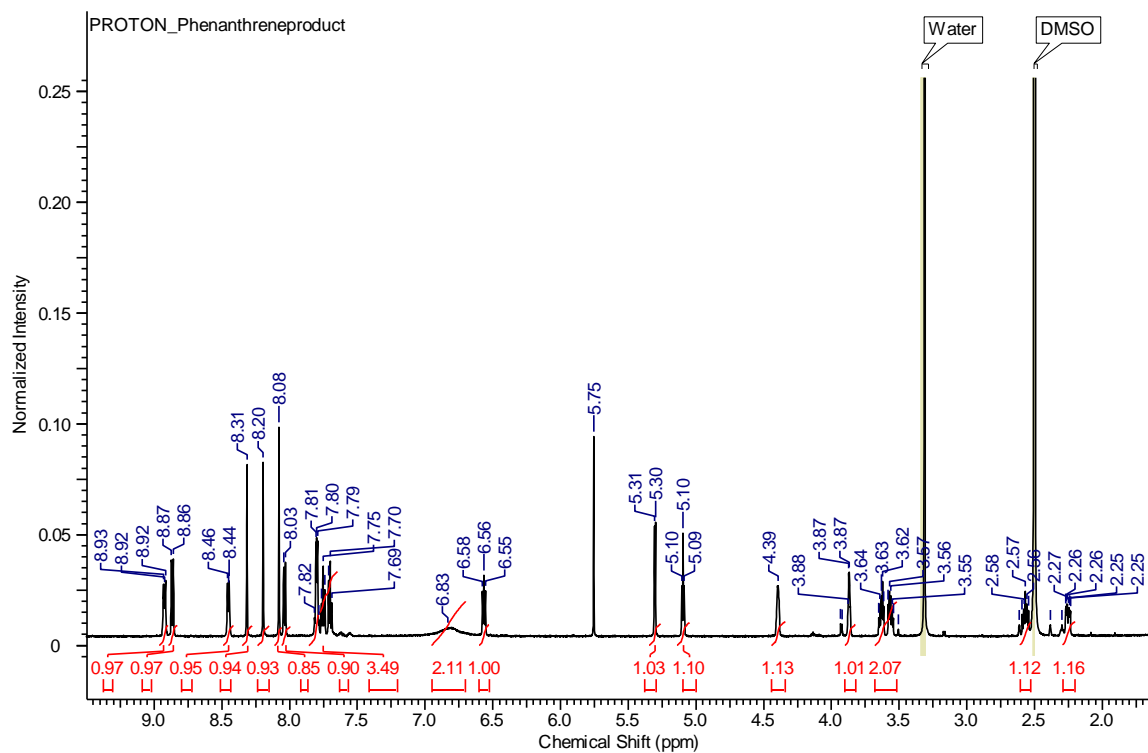
Appendix 22: ^{13}C -NMR spectrum of compound III-20.

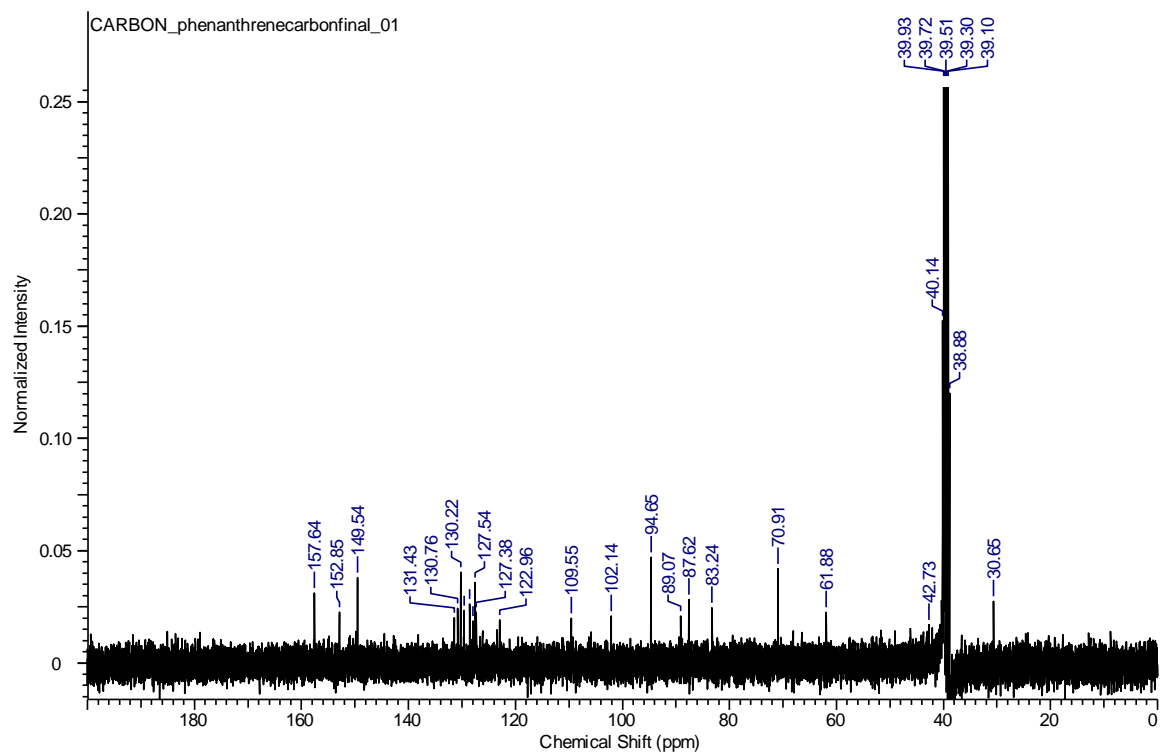
Appendix 23: $^1\text{H-NMR}$ spectrum of compound III-21.

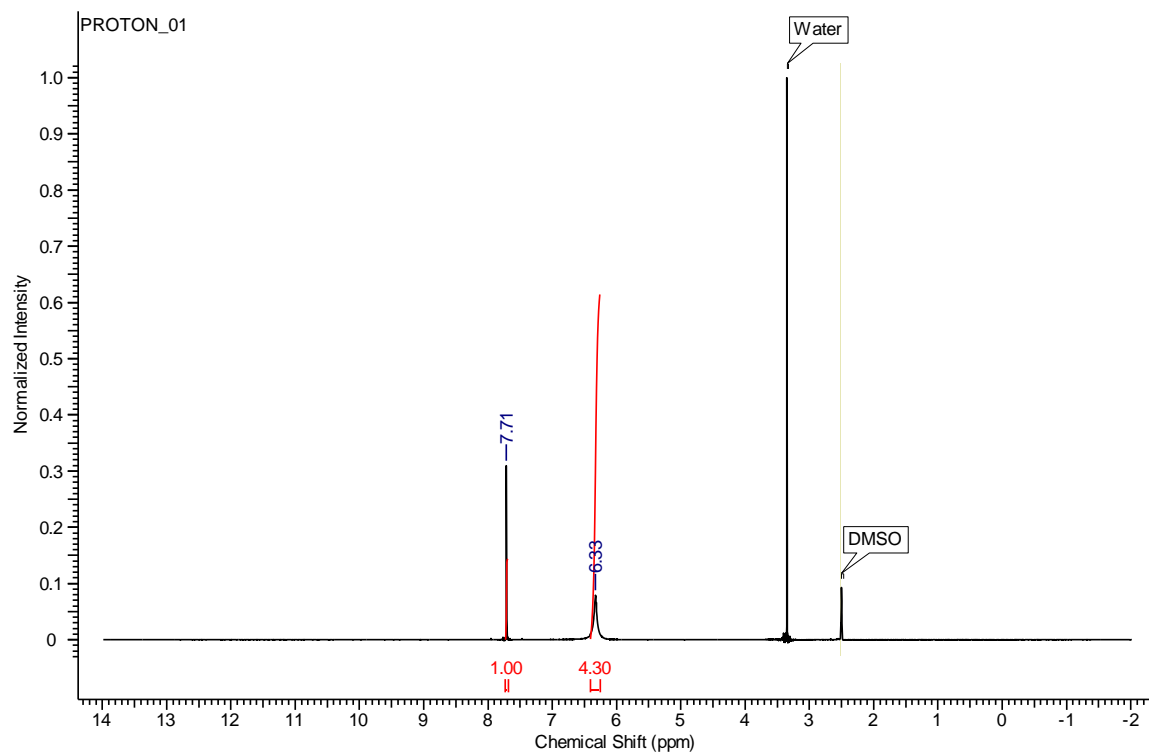
Appendix 24: ^{13}C -NMR spectrum of compound III-21.

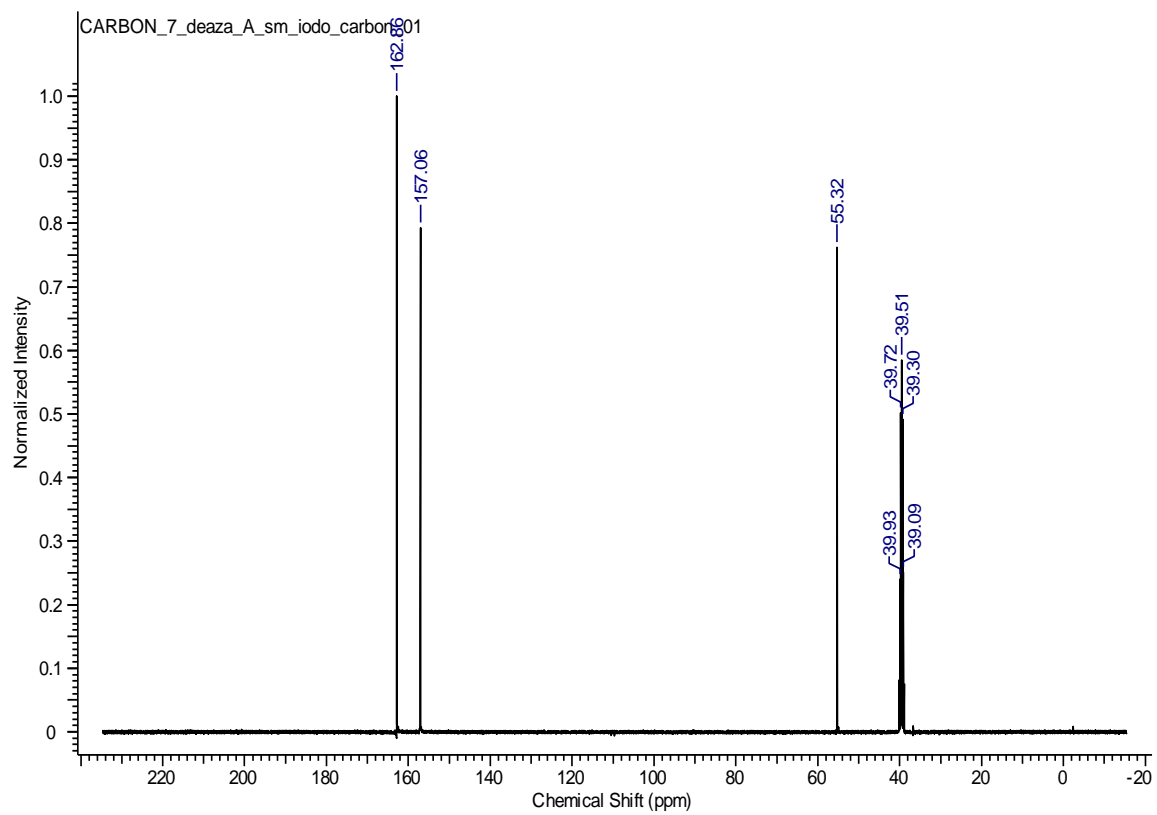
Appendix 25: $^1\text{H-NMR}$ spectrum of compound III-22.

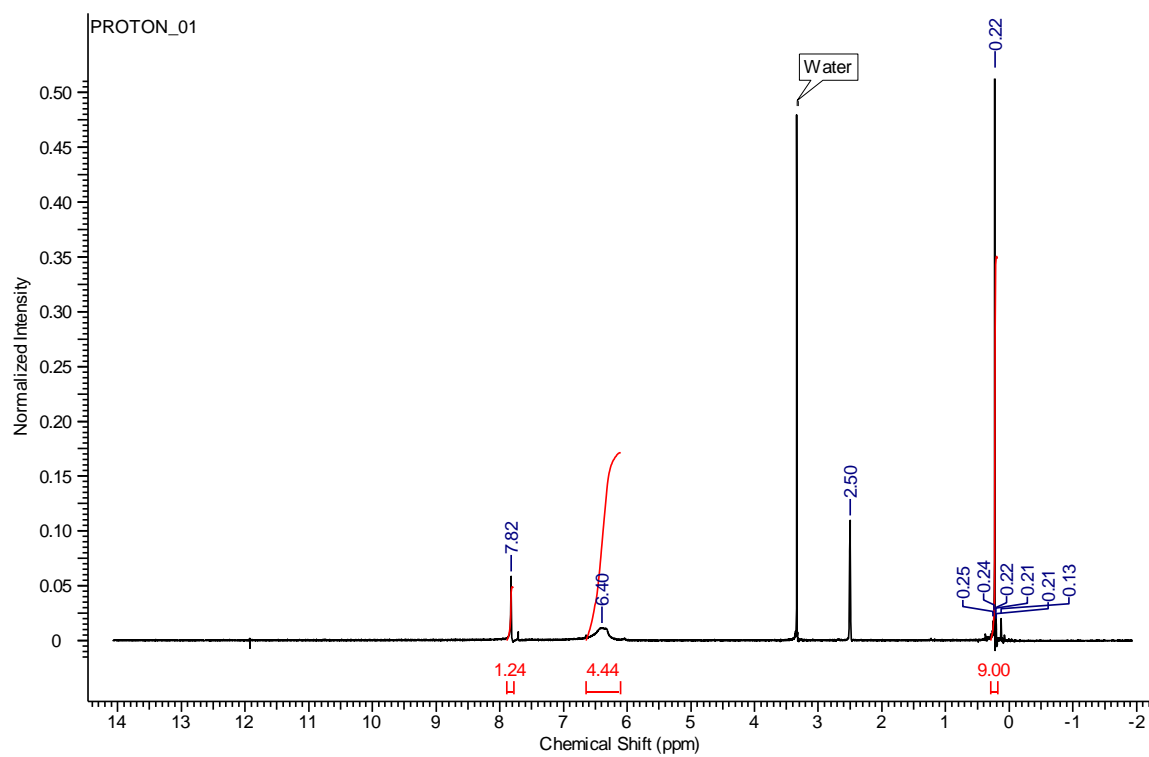
Appendix 26: ^{13}C -NMR spectrum of compound III-22.

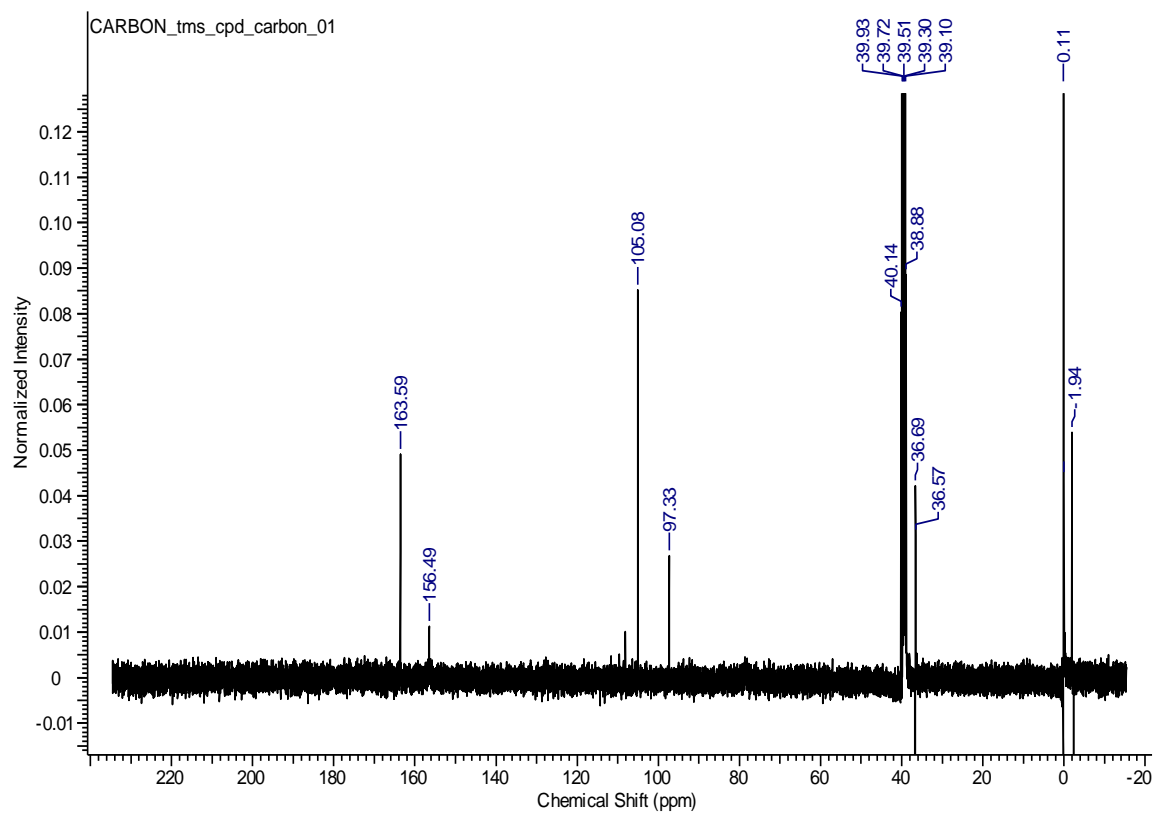
Appendix 27: $^1\text{H-NMR}$ spectrum of compound III-23.

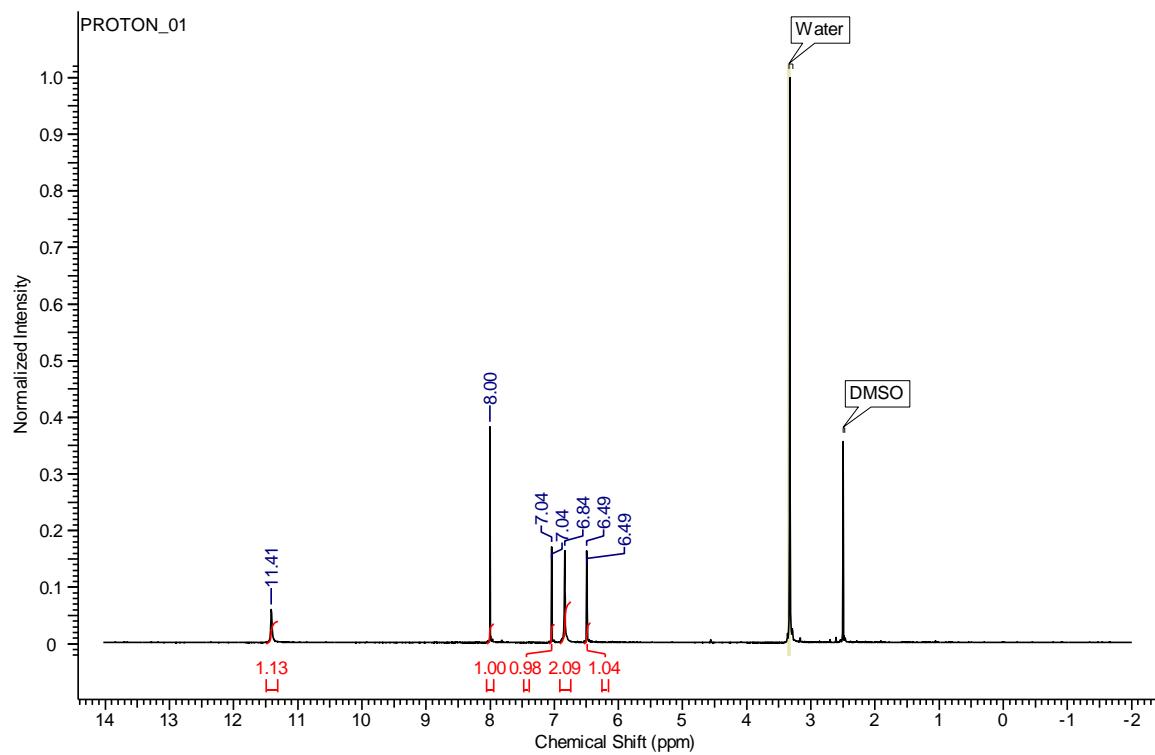
Appendix 28: ^{13}C -NMR spectrum of compound III-23.

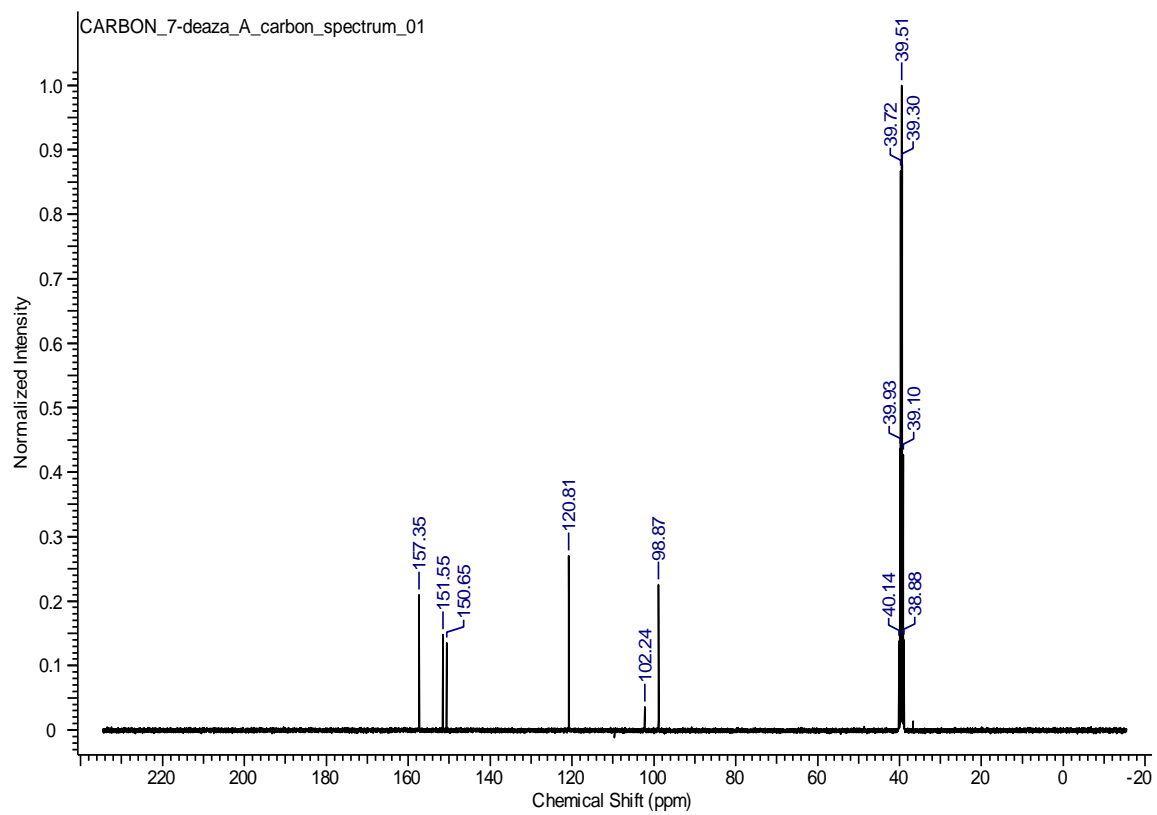
Appendix 29: ^1H -NMR spectrum of compound IV-7.

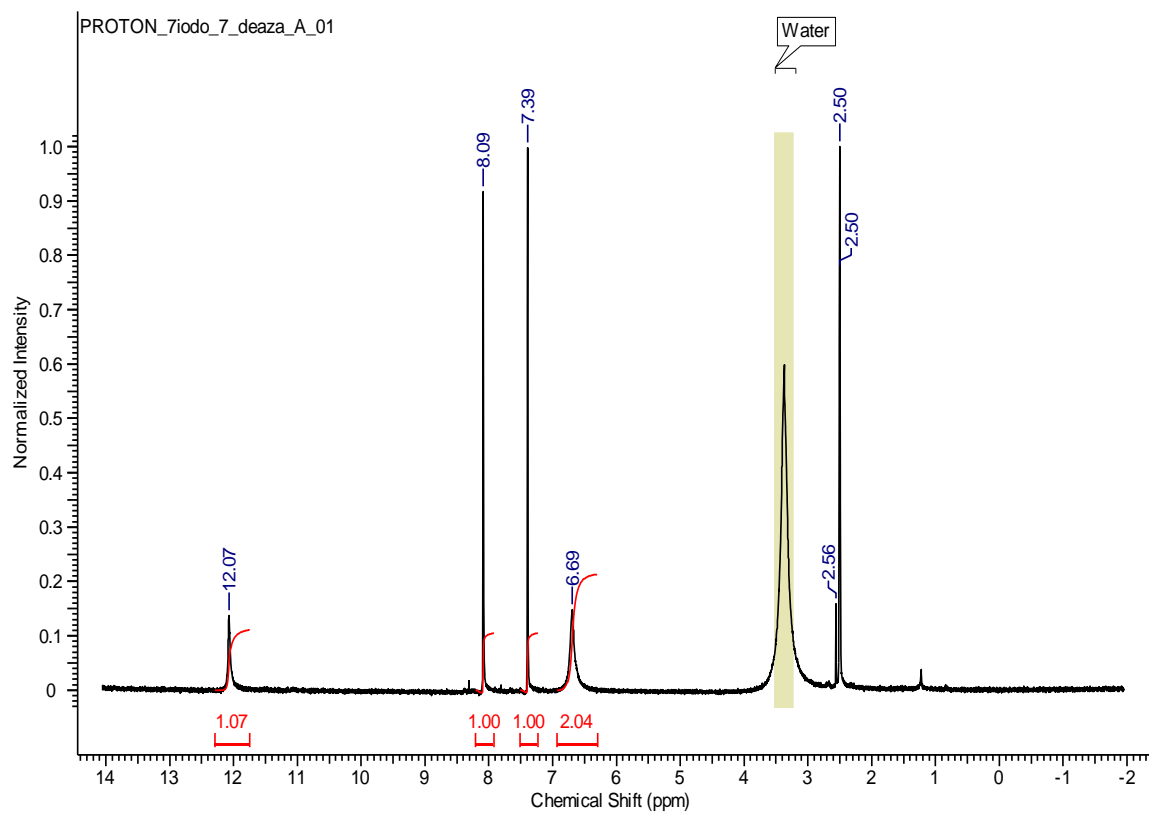
Appendix 30: ^{13}C -NMR spectrum of compound IV-7.

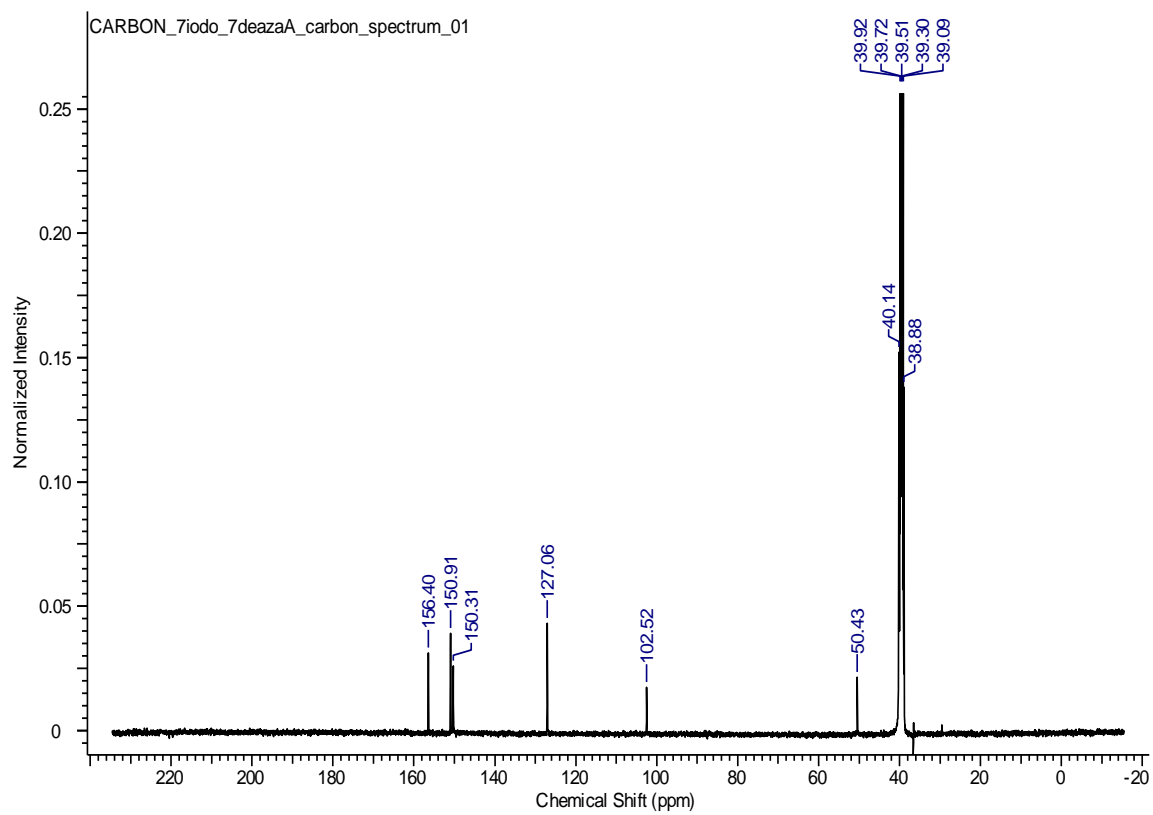
Appendix 31: ^1H -NMR spectrum of compound IV-8.

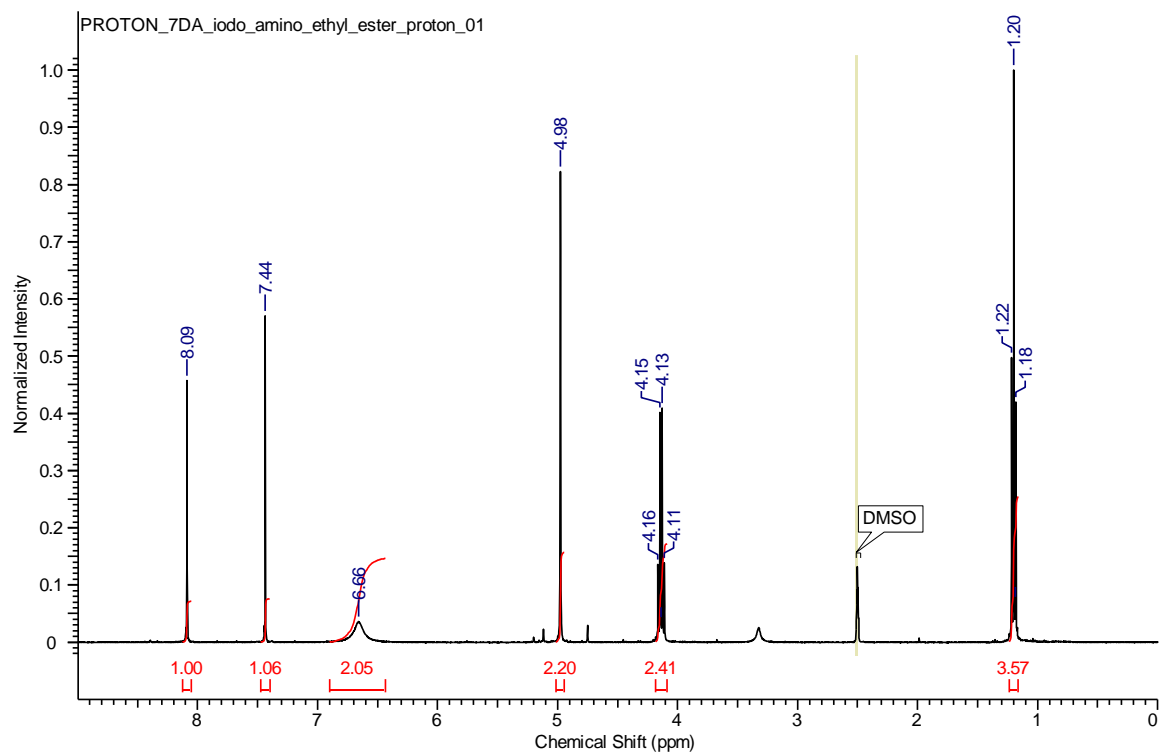
Appendix 32: ^{13}C -NMR spectrum of compound IV-8.

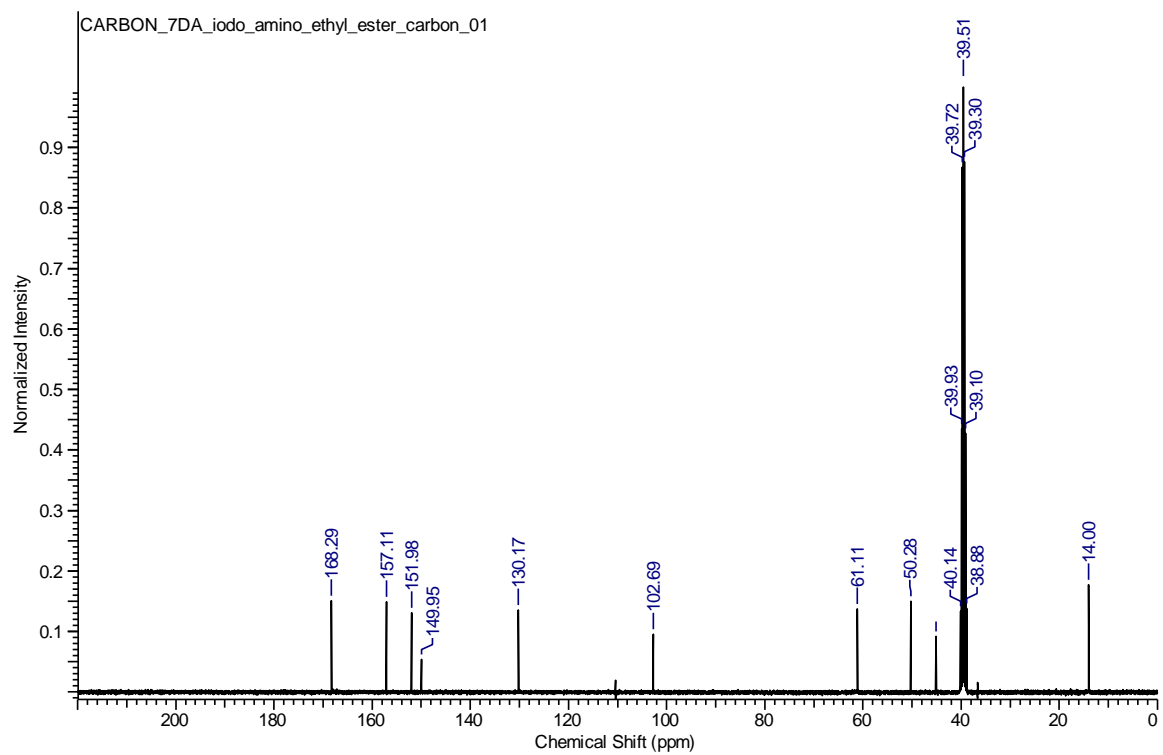
Appendix 33: ^1H -NMR spectrum of compound IV-9.

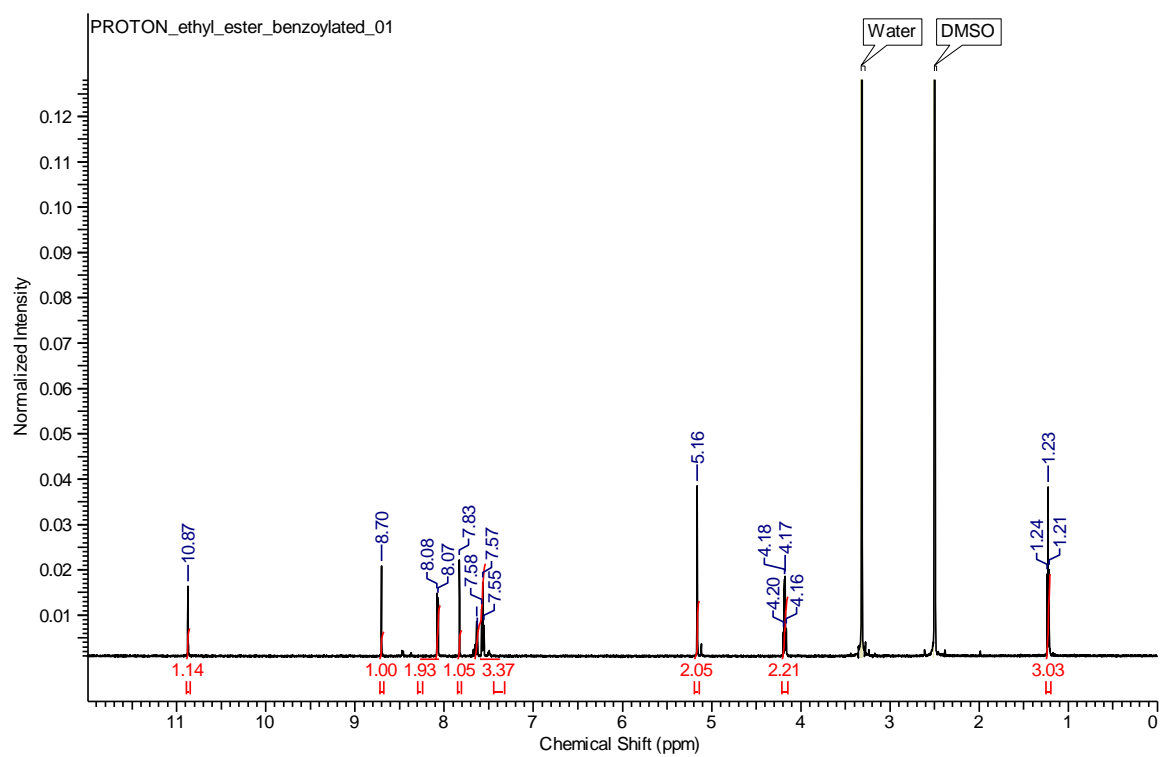
Appendix 34: ^{13}C -NMR spectrum of compound IV-9.

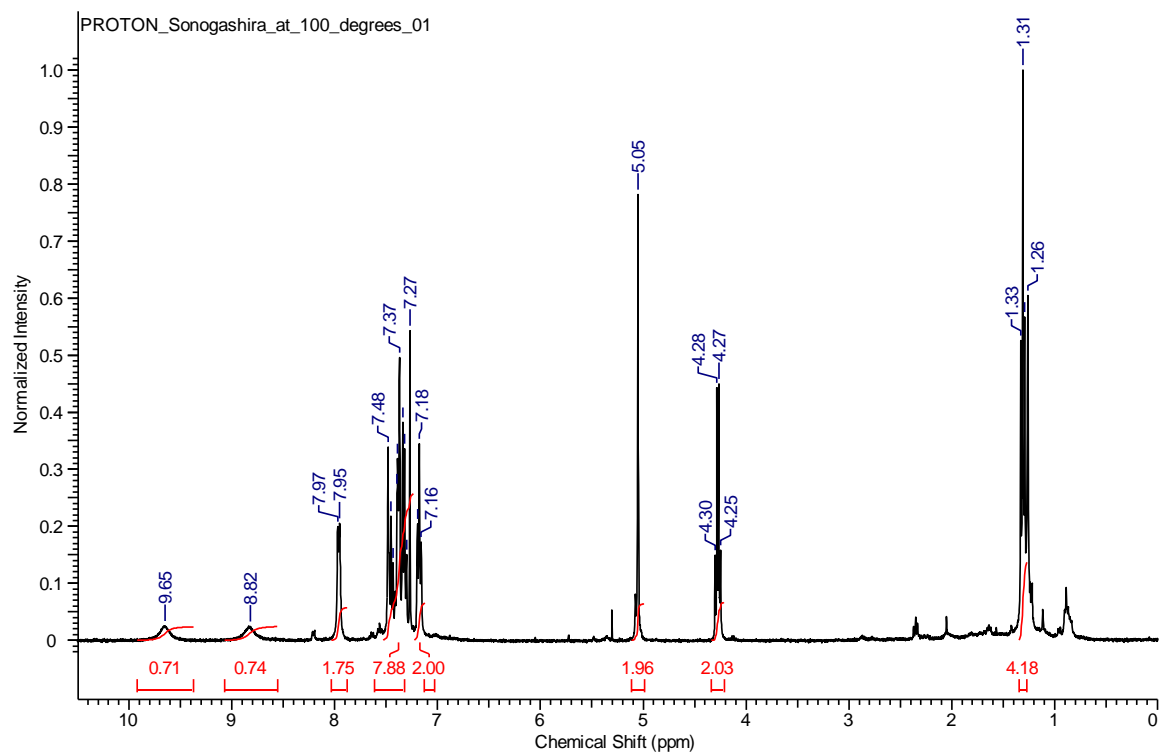
Appendix 35: ^1H -NMR spectrum of compound IV-10.

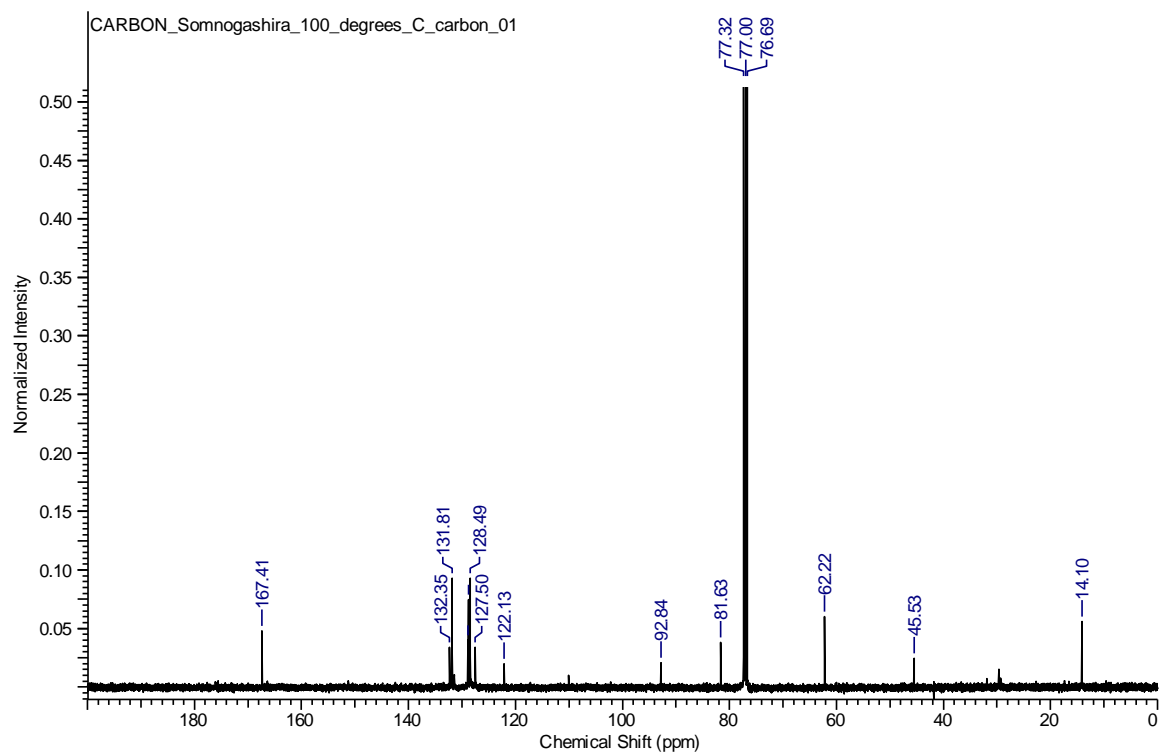
Appendix 36: ^{13}C -NMR spectrum of compound IV-10.

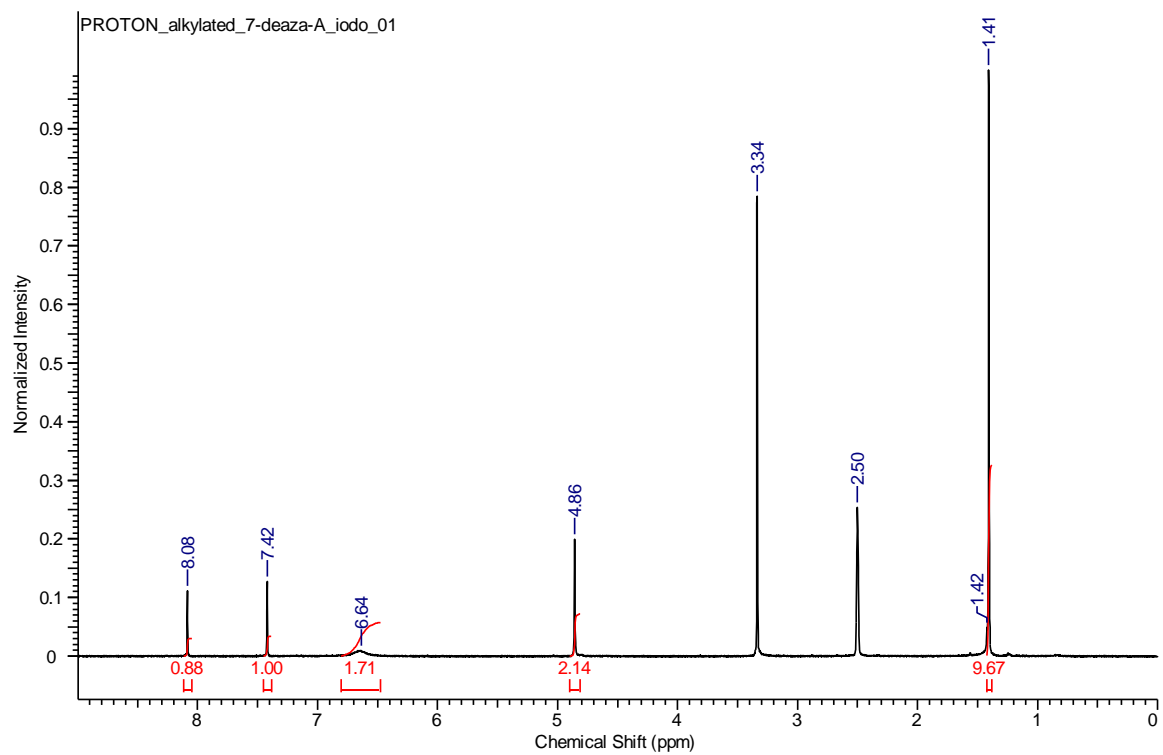
Appendix 37: $^1\text{H-NMR}$ spectrum of compound IV-11.

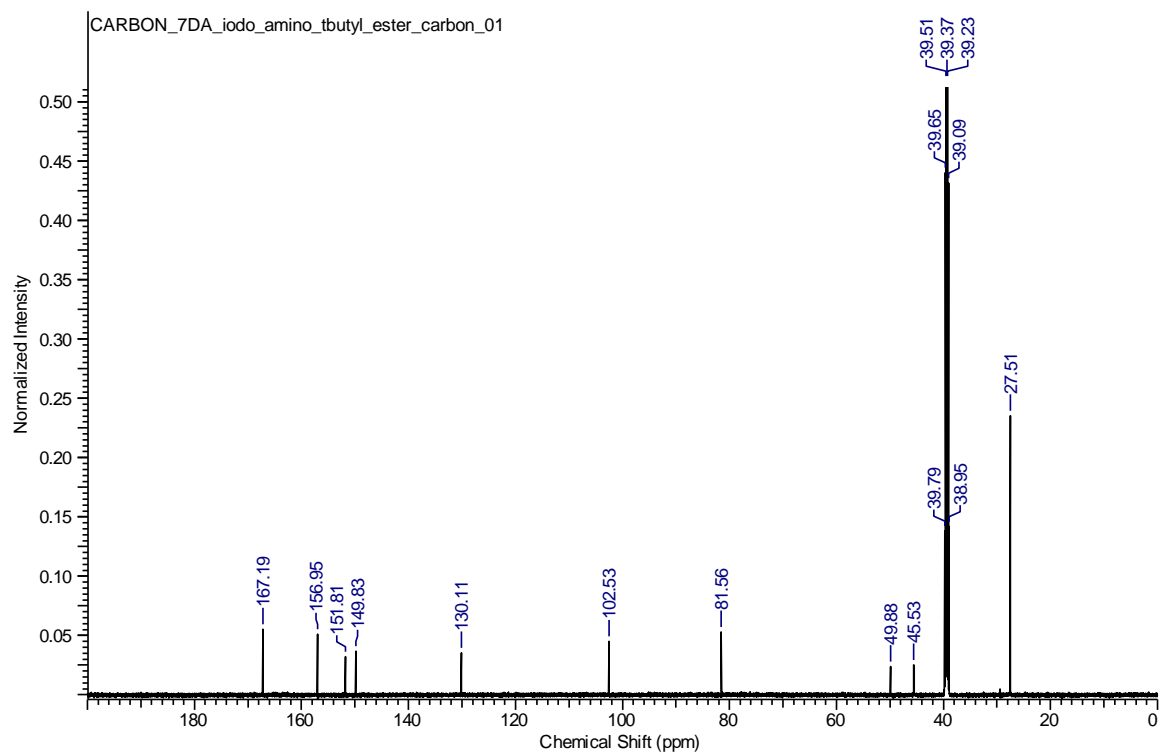
Appendix 38: ^{13}C -NMR spectrum of compound IV-11.

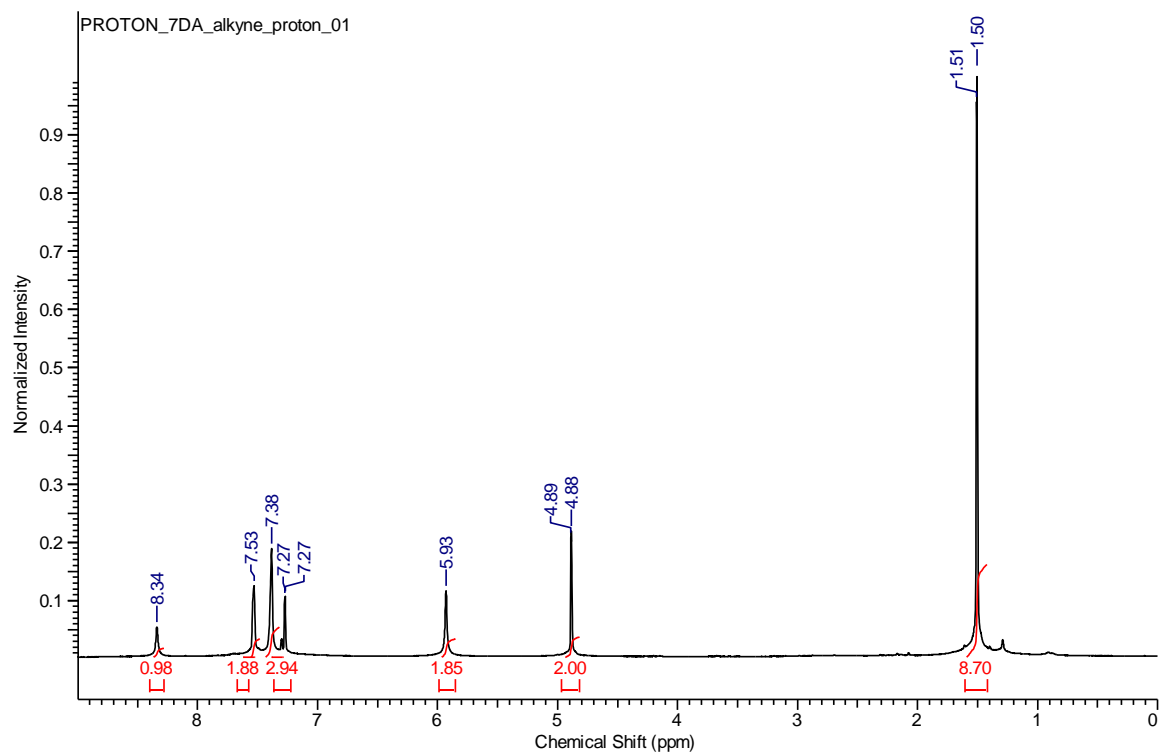
Appendix 39: ^1H -NMR spectrum of compound IV-12.

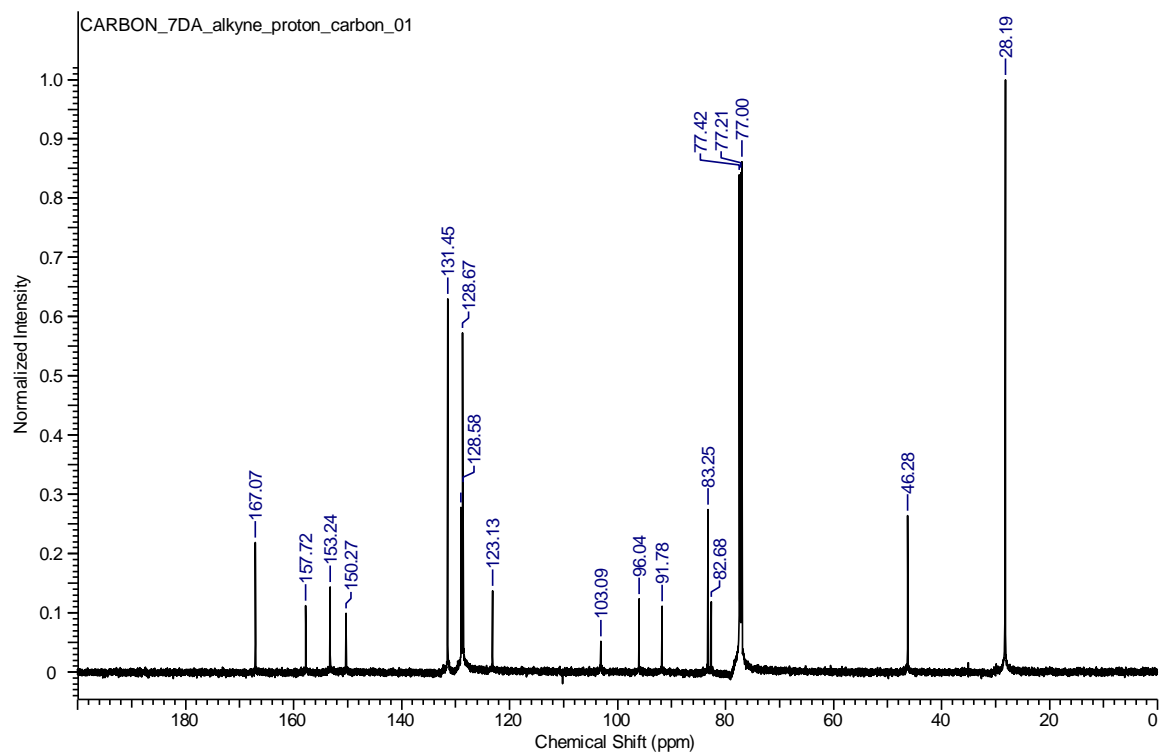
Appendix 40: $^1\text{H-NMR}$ spectrum of compound IV-13.

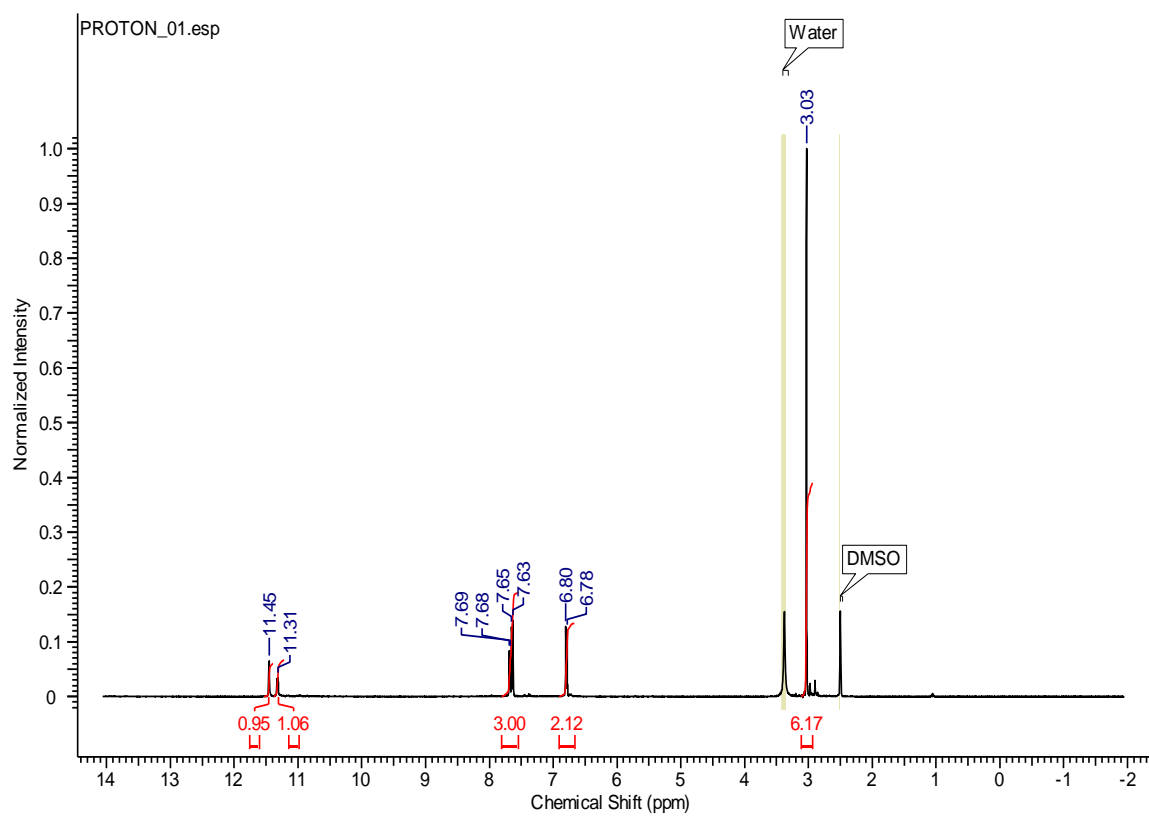
Appendix 41: ^{13}C -NMR spectrum of compound IV-13.

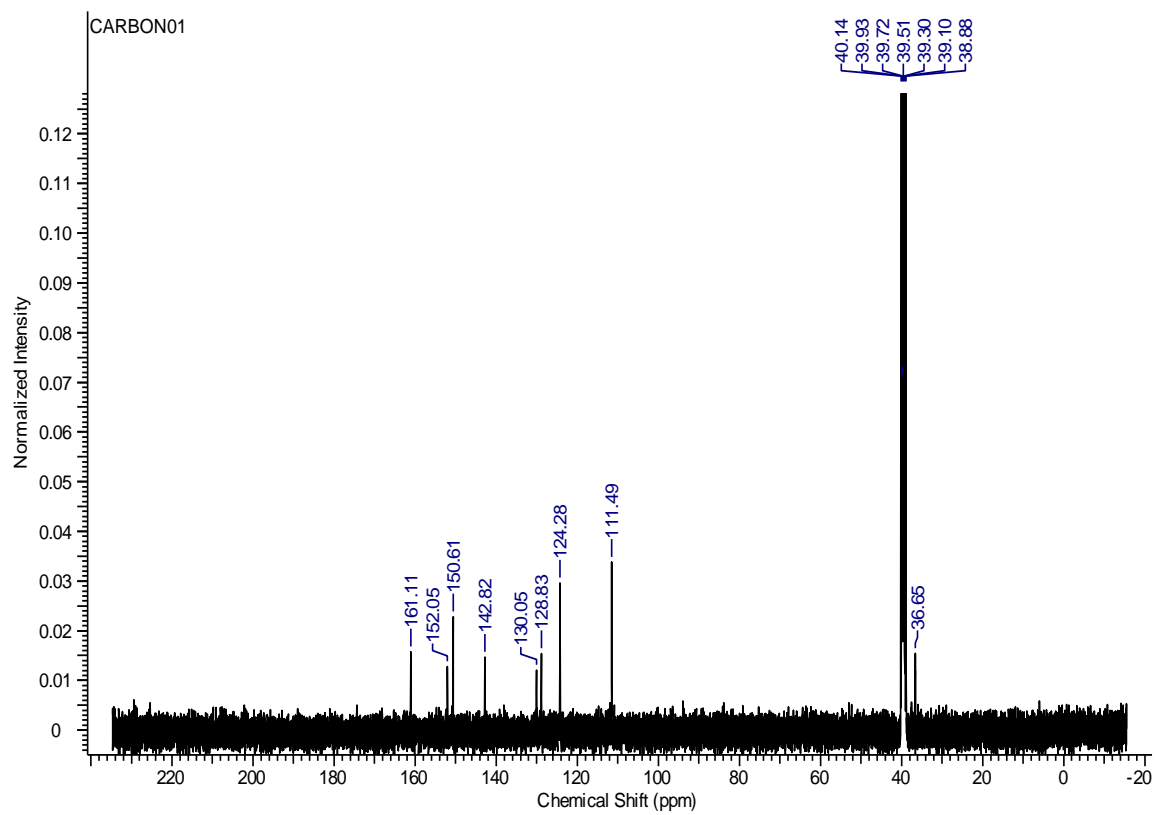
Appendix 42: $^1\text{H-NMR}$ spectrum of compound IV-15.

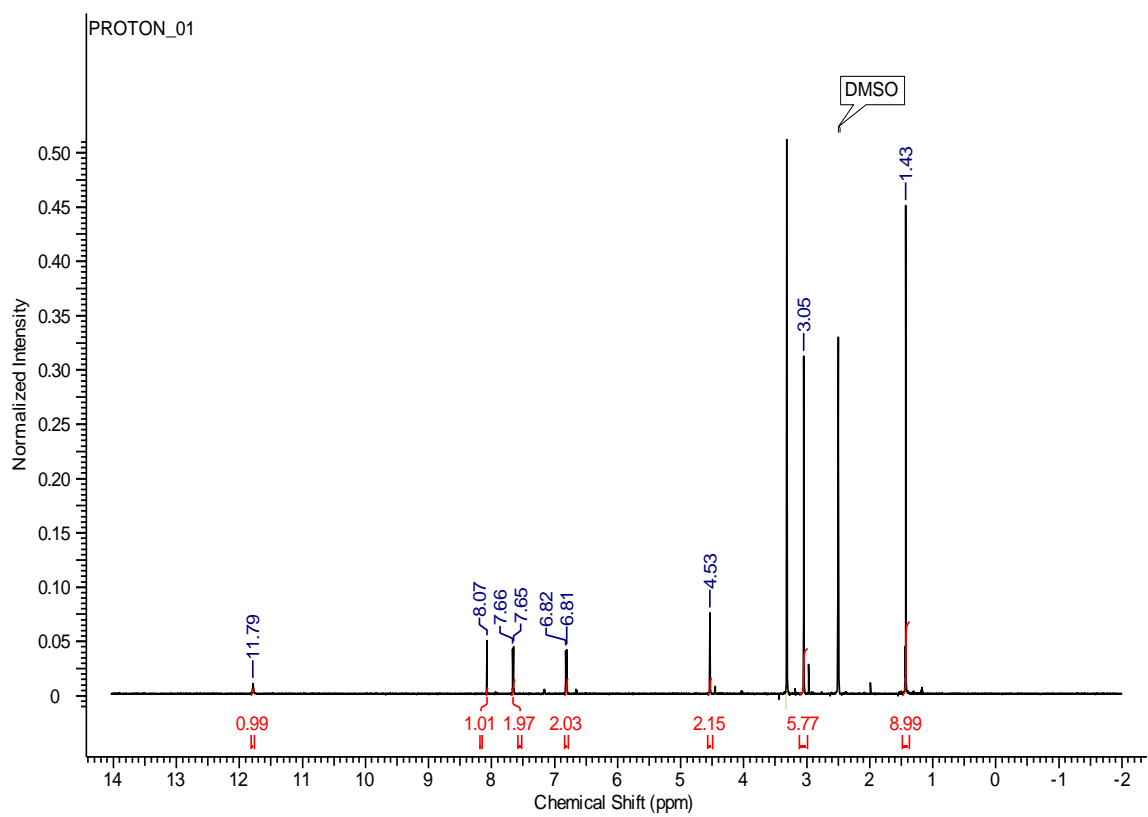
Appendix 43: ^{13}C -NMR spectrum of compound IV-15.

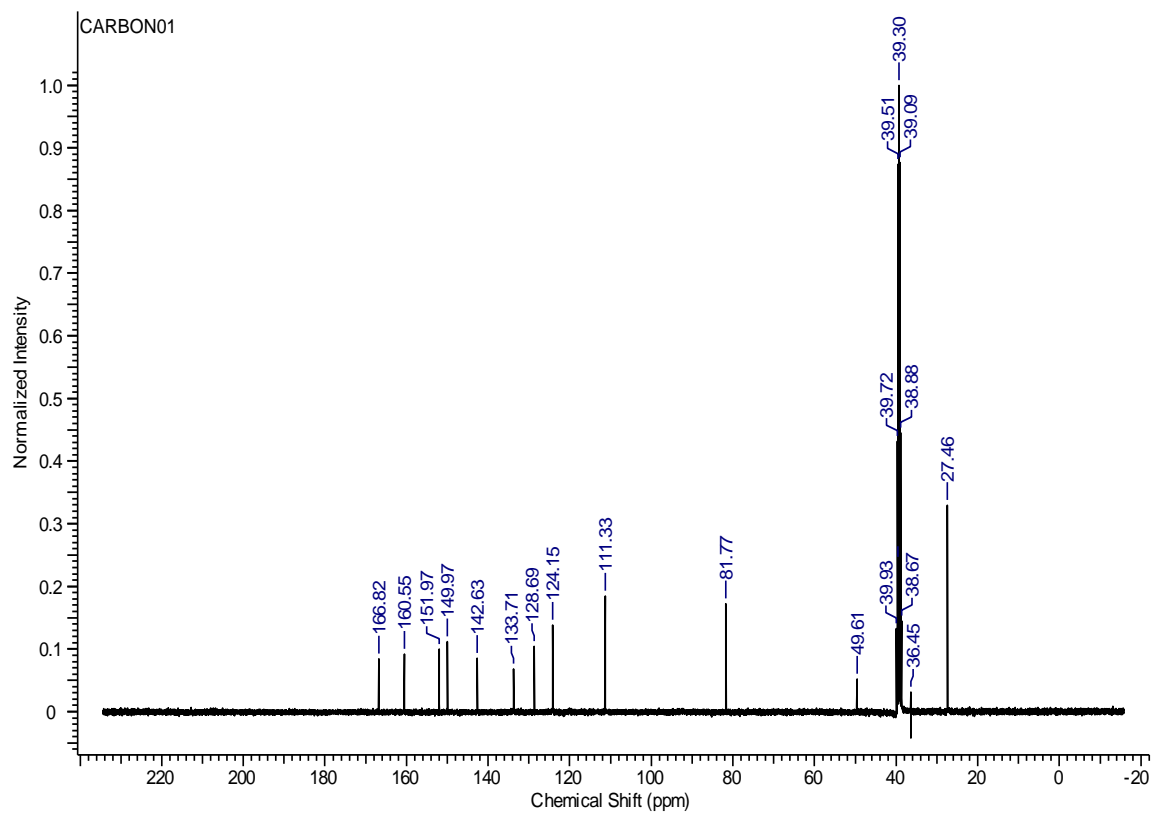
Appendix 44: ^1H -NMR spectrum of compound IV-16.

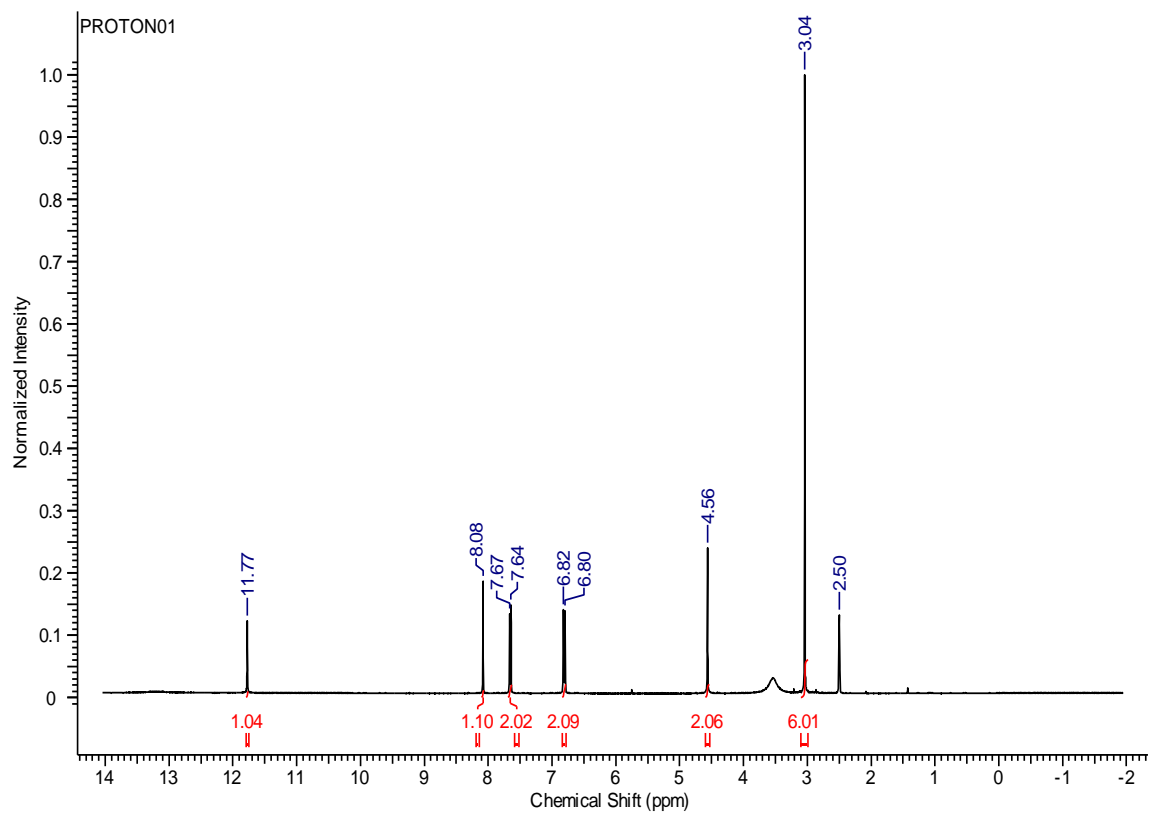
Appendix 45: ^{13}C -NMR spectrum of compound IV-16.

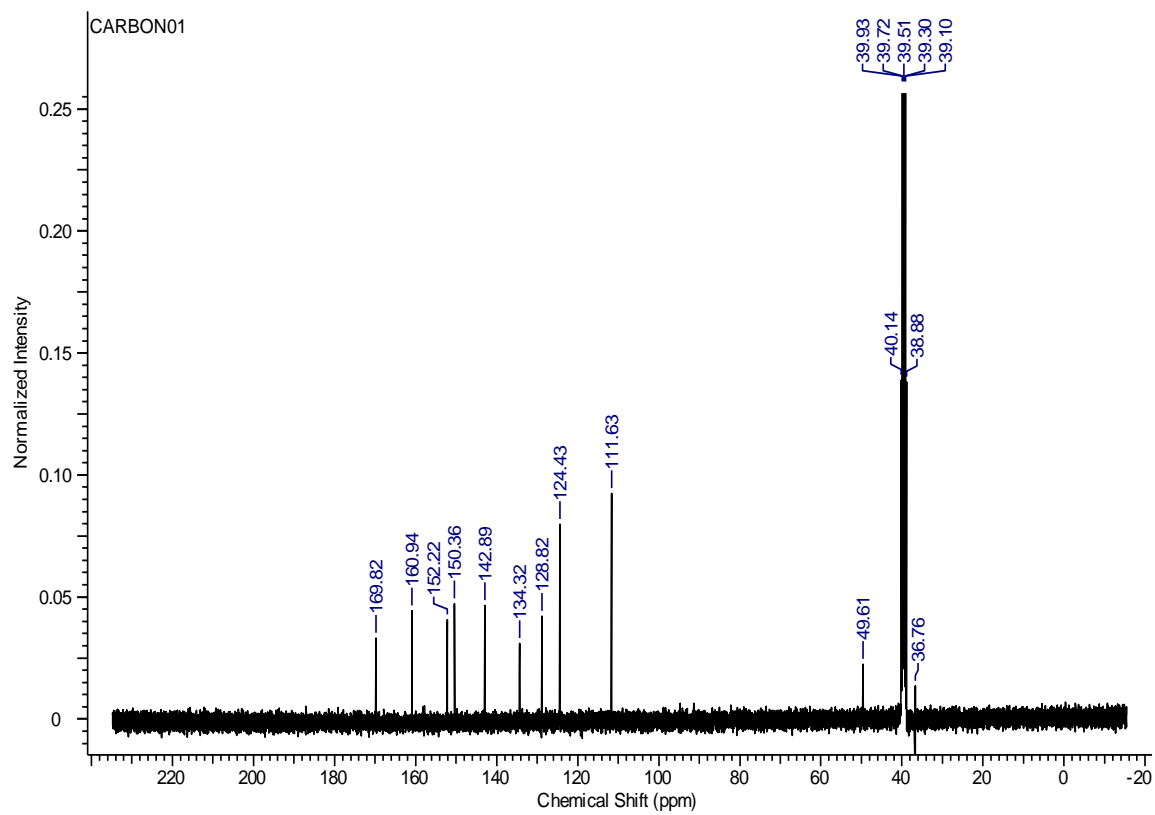
Appendix 46: $^1\text{H-NMR}$ spectrum of compound V-1.

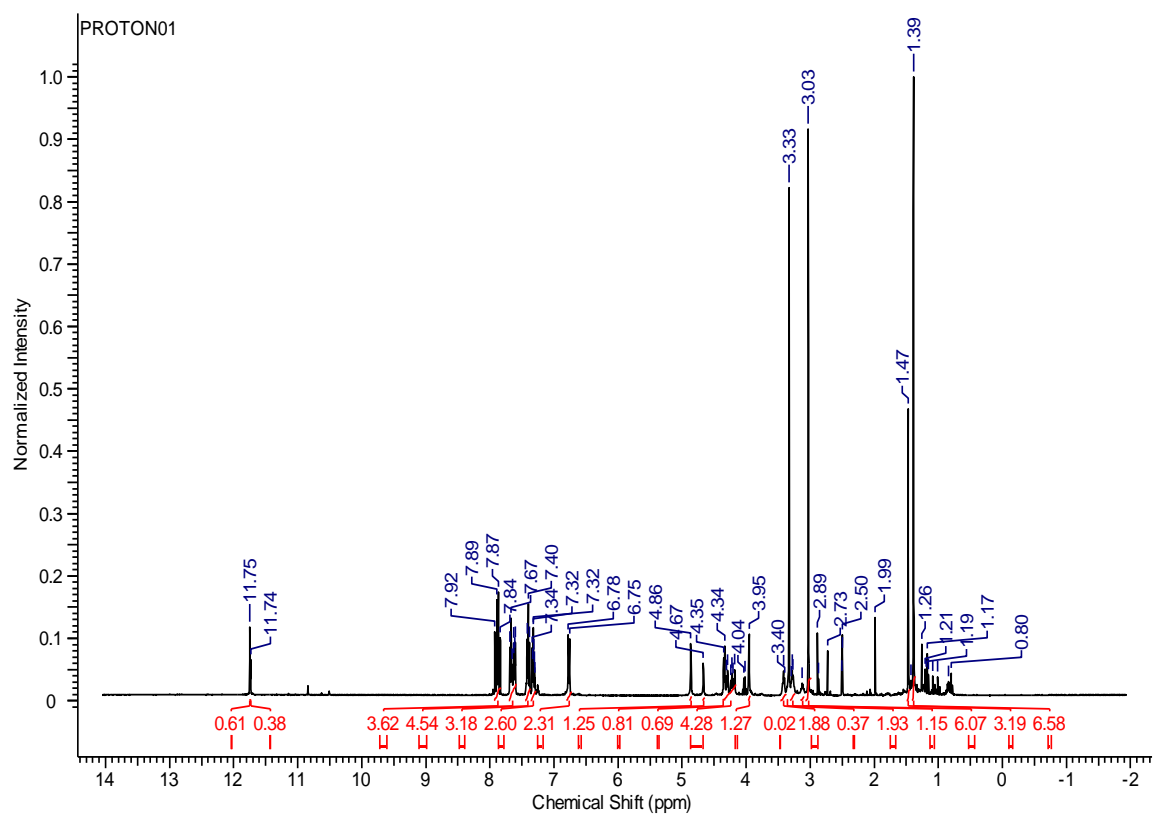
Appendix 47: ^{13}C -NMR spectrum of compound V-1.

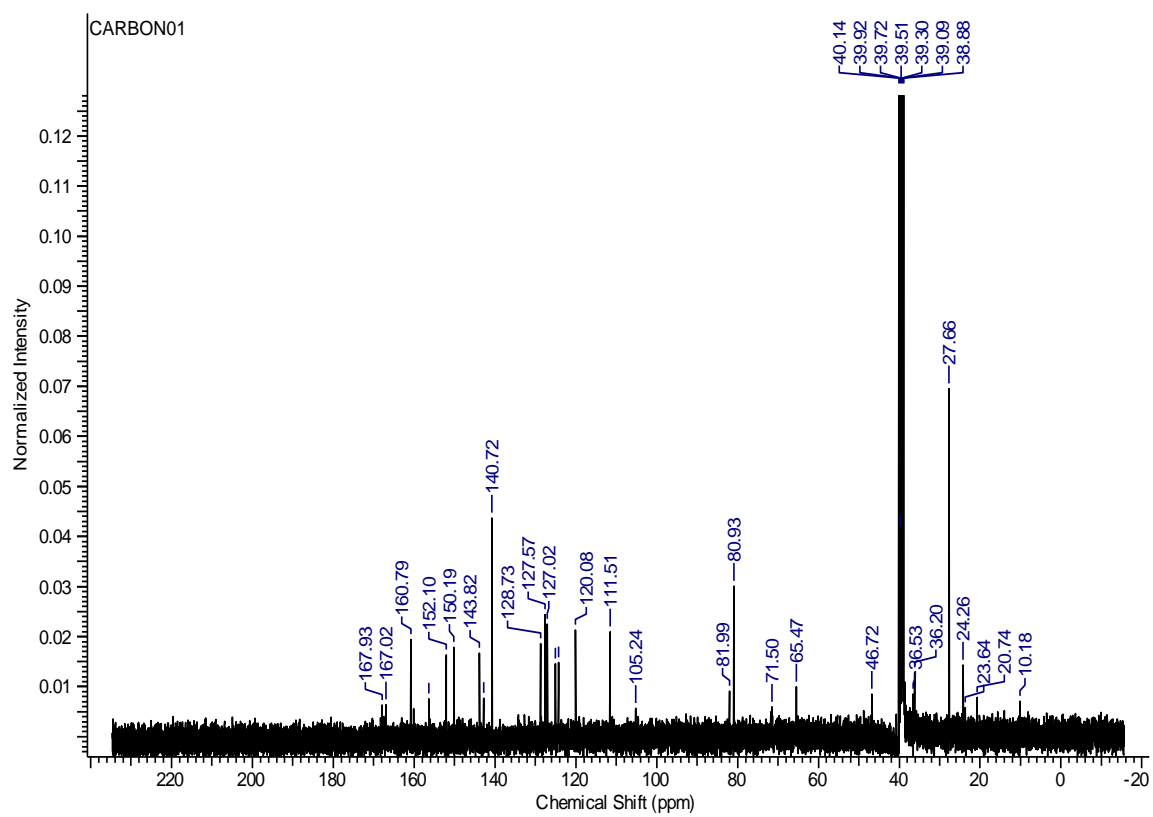
Appendix 48: $^1\text{H-NMR}$ spectrum of compound V-2.

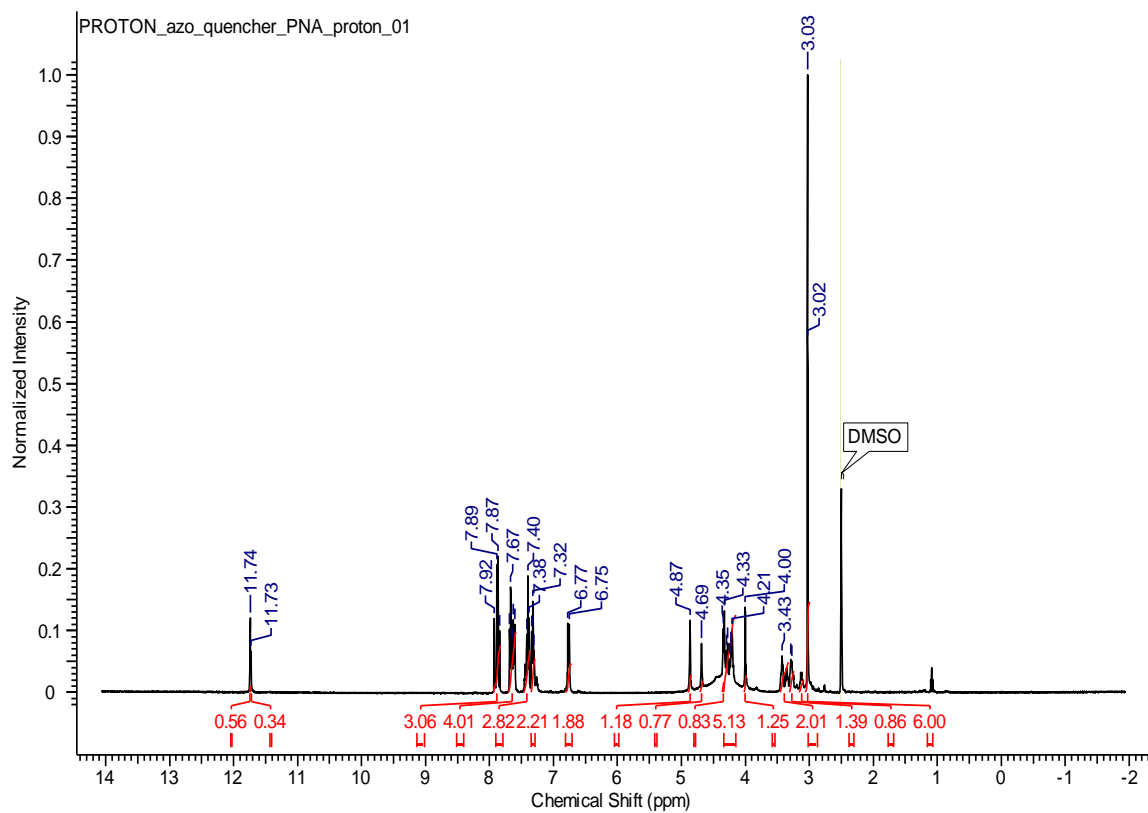
Appendix 49: ^{13}C -NMR spectrum of compound V-2.

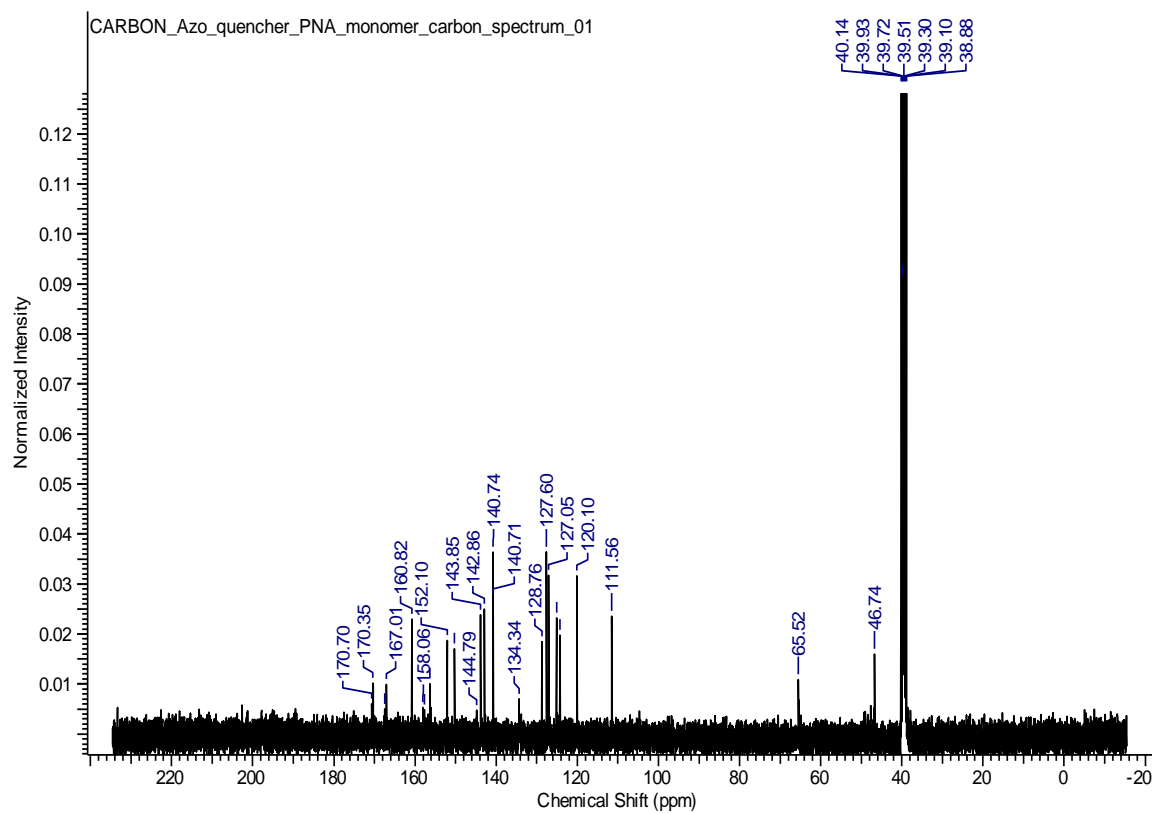
Appendix 50: ^1H -NMR spectrum of compound V-3.

Appendix 51: ^{13}C -NMR spectrum of compound V-3.

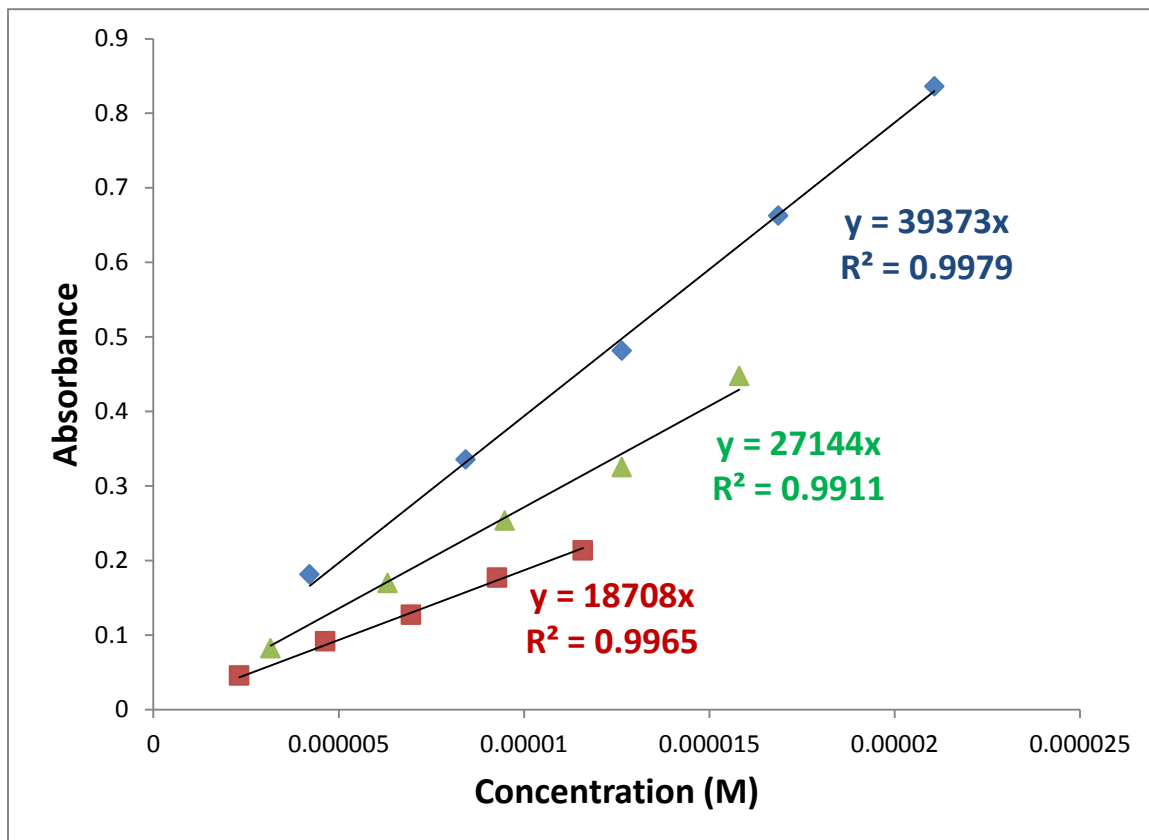
Appendix 52: $^1\text{H-NMR}$ spectrum of compound V-4.

Appendix 53: ^{13}C -NMR spectrum of compound V-4.

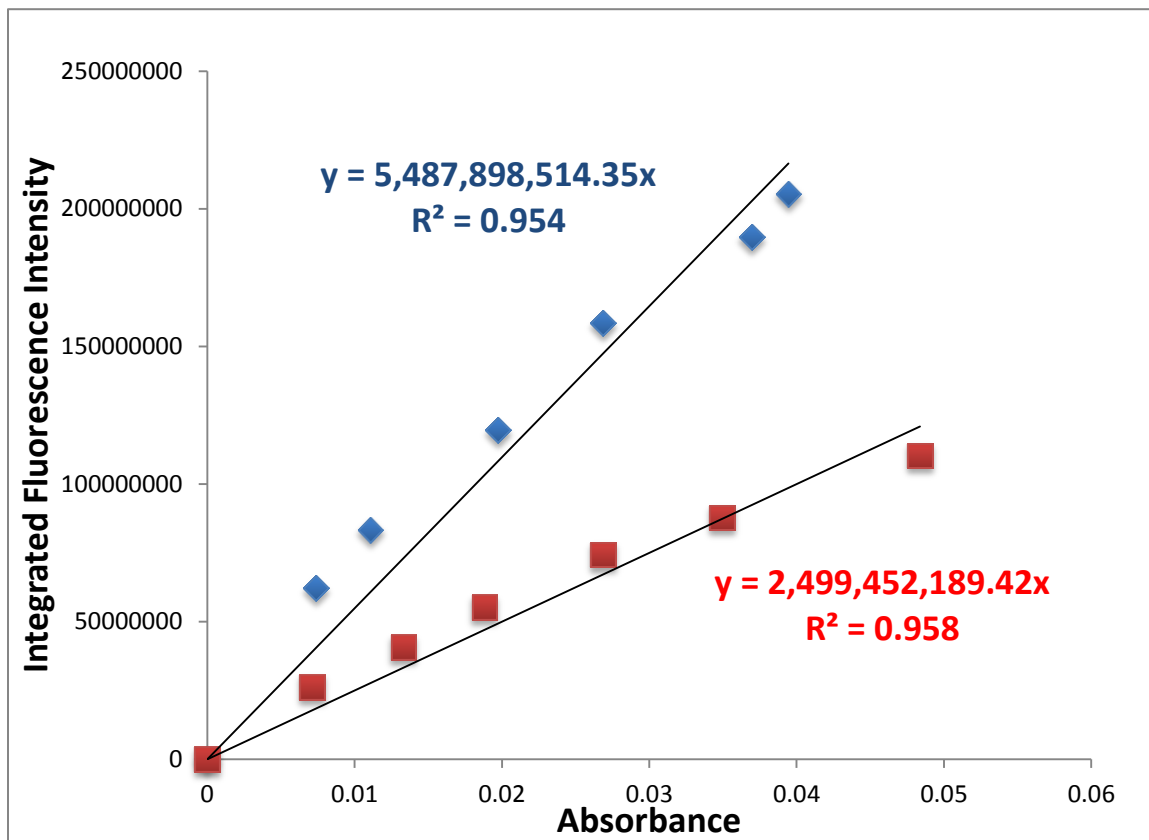
Appendix 54: $^1\text{H-NMR}$ spectrum of compound V-5.

Appendix 55: ^{13}C -NMR spectrum of compound V-5.

Appendix 56: Sample calculation: determination of molar extinction coefficients for compound III-21 (A^{pyr}) in EtOH at 366 nm (blue), dioxane at 367 nm (green) and H₂O at 364 nm (red).



Appendix 57: Sample calculation: data for the calculation of Φ_F for compound III-21 (A^{PYT}) in EtOH. A plot of the integrated fluorescence intensity at different absorbance values for 9,10-diphenylanthracene (blue) and compound III-21 (red).



Curriculum Vitae

Name: Augusto Matarazzo

Post-secondary Education and Degrees: Ryerson University
Toronto, Ontario, Canada
2005-2009 BSc. Chemistry

Ryerson University
Toronto, Ontario, Canada
2009-2011 MSc. Molecular Science

The University of Western Ontario
London, Ontario, Canada
2011-2015 Ph.D. Chemistry candidate

Honours and Awards: Dean's List, Ryerson University
2008-2009

Related Work Experience Teaching Assistant
The University of Western Ontario
2011-2015

Publications:

Fluorescent Adenine Analogues: A Comprehensive Survey. Matarazzo, A.; Hudson, R.H.E. *Tetrahedron* (2015) 71. 11. 1627-1657.

5-(Acridin-9-ylamino)uracil - A hydrolytically labile nucleobase modification in peptide nucleic acid. Matarazzo, A.; Moustafa, M.E.; Hudson, R.H.E. *Canadian Journal of Chemistry*. (2013) 91. 12. 1202-1206.